DEPTH PROFILING OF LOW ENERGY IONS IMPLANTED INTO METALS USING THE FIELD ION MICROSCOPE/IMAGING ATOM PROBE

By

SCOTT DOUGLAS WALCK

A DISSERTATION PRESENTED TO THE GRADUATE SCHOOL
OF THE UNIVERSITY OF FLORIDA IN PARTIAL FULFILLMENT OF
THE REQUIREMENTS FOR THE DEGREE OF DOCTOR OF PHILOSOPHY

UNIVERSITY OF FLORIDA

1986

To my wife and son, Karen and Adam Walck,

the "frog",

and my mother, Drucilla Linn

ACKNOWLEDGEMENTS

The author wishes to thank the members of his supervisory committee: Dr. Christopher D. Batich, Dr. Robert T. DeHoff, Dr. Paul H. Holloway, and Dr. Gary G. Ihas. This author is extremely grateful to his advisor and friend, Dr. John J. Hren, who furnished an atmosphere in which the author was allowed to find his own way and discover his full potential.

There are several members of the field-ion community without whose help and assistance the FIM/IAP at the University of Florida could not have been built. The author is deeply indebted to Dr. John A. Panitz of Sandia National Laboratories, whose generosity in terms of advice, aid, and criticisms to a struggling graduate student is nothing short of remarkable. The author also wishes to thank Dr. Gary G. Kellogg, also of Sandia Laboratories, for his advice and many stimulating discussions. Many thanks go to Gerry Fowler and Larry Karkeweitz, who shared with the author the knowledge of the details of the FIM/IAP instrumentation. Encouragement from Dr. Sidney S. Brenner of the University of Pittsburgh and the learning experience that he jammed into three months is greatly appreciated. Dr. Michael K. Miller of Oak Ridge National Laboratories is also thanked for his technical and scientific discussions.

Many technical and support groups at the University of Florida should also be thanked. Dr. Anthony Buonoquisti is thanked for the many fruitful discussions and scholarly advice he has given over the years.

Machinists Ralph Jones and Herman Bailor were indispensable with respect to designing and building the FIM/IAP. Many thanks go to Robert Owen whose late night discussions and help with electronics made impossible tasks a little easier. Mr. Don Sanford in the Department of Physics is thanked for his help in designing the new FIM/IAP specimen holder and TIG-welding the copper braid. The author wishes to extend thanks for the technical assistance given to him by Dan Steadham and Temel Buyuklimanli. He also expresses his gratitude to his fellow students who shared the same boat and helped to infuse into this degree some of the philosophy that goes with it. The author would like to thank the local chapters of the American Vacuum Society in Florida and New Mexico for the scholarships they have given him to attend meetings and short courses which were invaluable to him with respect to his research progress. Special thanks go to Norman Parsons of the Florida Chapter for his efforts to help the students

The author also would like to thank Tektronix employees: Dave Jackson, Bob Messer, John Loggee, and Richard Knapp for solving and helping to get the Tektronix equipment on-line as an integral part of the Imaging Atom Probe. They were invaluable in solving both software and hardware problems. These gentlemen not only stand behind their product, but represent the Tektronix motto, "Committed to Excellence."

The author wishes to thank the Department of Energy for funding of this effort. Gratitude is also extended to the University of Florida College of Engineering for the SEED money to start the project, the Major Analytical Instrumentation Center (MAIC) for technical and instrumental support, and the Department of Materials Science and Engineering for

supporting the author on the Center of Excellence program for an extended period of time.

TABLE OF CONTENTS

ACKNOWLEDGEMENTS iii

ABSTRACT x

CHAPTER I
LITERATURE SURVEY 1

Introduction 1
FIM Principles 4
    Field Ionization 4
    Field Evaporation 5
    Atom Probery 9
    Applications 10
    Field-Induced Stresses 11
Microstructure Of Implanted Metals 14
Hydrogen In Metals 18
    Hydrogen Embrittlement 21
    Trapping Of Deuterium 22
Nitrogen Implantation In Metals 24
    Tribological Studies 24
    Ion Beam Carburization 27
    Applicability Of FIM Techniques To Nitrogen In Metals . . 27

CHAPTER II
INSTRUMENTATION 30

Field Ion Microscope/Imaging Atom Probe (FIM/IAP) 30
FIM/IAP Description 31
    Chamber 31
    Sample Holder 37
    General Description Of The IAP 42
    TOF Mode 43
    Time-Gated Mode 47
    Computer And IEEE-488 Instrumentation 50
    7912AD 52
    Scientific Instruments 5500 54
    Bertan 205A-30R 55

IAP Data Collecting And Handling Programs 55
    Ion Gun 58
Mass Identification in the Colutron Ion Gun 65
Transmission Electron Microscopy 67
    FIM/IAP "Bulk" Holder 68
    FIM/TEM "Double-Tilt" Holder 70
    FIM/TEM "Field-Effect" Holder 72

CHAPTER III
EXPERIMENTAL CONSIDERATIONS 79

Depth Profiling Using The FIM/IAP 79
    Ring Counting Experiments 80
    Specimen Geometry 82
        IAP probed-volume considerations 84
        Volume calculation 85
        Determination of β 89
        Determination of K_D for nickel 91
        Experimental procedure 92
        Determination of geometric parameters 101
        Calculated curve 105
        Sample selection criteria 105
Effects Of Field Ionization Imaging And Evaporation 112
    Field Induced Stresses 112
    Field Evaporation Observations 118
        Dependency of evaporation field on imaging gas 118
        Implantation lowering of evaporation field 119
        Low field desorbed species 120
        He signal 122
Special Problems Associated With Hydrogen/Deuterium 123
    The Deuterium Background (D_1^+) 124
    Deuterium Implantation Conditions 129

CHAPTER IV
RESULTS OF IMPLANTATION EXPERIMENTS 132

Specimen Preparation 132
Nitrogen Implantation In Nickel 134
Nitrogen Implantation In Tungsten 148
Deuterium Implantation In Nickel 159
Carbon In Tungsten And Nickel 167

CHAPTER V
DISCUSSION OF RESULTS 172

Instrumentation 173
  FIM/IAP 173
  FIM/TEM Specimen Holders 175
Methods/Techniques 175
Discussion Of Experimental Results 177
  Control Experiments 177
    Field effects 178
    Ring counting experiments 179
    Automated data collection 179
    Background gases 180
    Deuterium background 181
  Nitrogen Implantation In Nickel 183
  Nitrogen Implantation In Tungsten 186
  Applicability Of The TRIMML Code To Low Energy Ions . . . 189
  Reproducibility Of Profile Results 189
    Curve shapes and total ions detected 189
    Error analysis of geometric model 191
  Deuterium Implantation In Nickel 192
  Carbon In Tungsten And Nickel 194

CHAPTER VI
CONCLUSIONS 196

Depth Profiling Techniques 197
Field-Induced Stresses 198
Nitrogen Implantation 200
  Nitrogen In Nickel 200
  Nitrogen In Tungsten 200
In Situ Implantation Results 201
Deuterium Embrittlement Of Nickel 202
FIM/IAP Observations 202

CHAPTER VII
SUGGESTED FUTURE WORK 204

Nitrogen In Nickel 204
Nitrogen In Tungsten 205
Carbon In Metals 205
Deuterium In Metals 206
  Deuterium Implanted Nickel Emitter Failure 206
  Deuterium Redistribution 208
    Cryogenic/room temperature experiments 208
    Temperature-controlled experiments 209

Field-Induced Stresses 210
Implantation Depths 211
Orthogonal Axis Implantation 212
Implantation Lowering Of Evaporation Field 213

APPENDIX A
IMPROVED FIM SPECIMEN HOLDER WITH TEMPERATURE CONTROL 215

APPENDIX B
ALIGNMENT OF THE COLUTRON ION GUN 218

APPENDIX C
MEASURED TIME DELAYS 222

APPENDIX D
FIM/IAP TEK BASIC PROGRAMS 225

IAPRING.HV 225
IAP2TAPE 246
PEAKPICKOFF.FAST 268
PEAKCUMULATOR 274
DATAREDUCER 275
CUMVSRING 280
FIMSUPPLY 286
TIPREDUCER 291
PROFILER 296

APPENDIX E
INDEXED FIM MICROGRAPH MONTAGE 305

RFERENCES 307

BIOGRAPHICAL SKETCH 313

Abstract of Dissertation Presented to the Graduate School
of the University of Florida in Partial Fulfillment of
the Requirements for the Degree of Doctor of Philosophy

DEPTH PROFILING OF LOW ENERGY IONS IMPLANTED INTO METALS USING THE FIELD ION MICROSCOPE/IMAGING ATOM PROBE

By

Scott Douglas Walck

August, 1986

Chairman: John J. Hren
Major Department: Materials Science and Engineering

The implantation depth is an important parameter if properties are to be modified in a controllable and reproducible fashion by ion implantation. The Field Ion Microscope/Imaging Atom Probe (FIM/IAP) is superb for depth profiling, having depth resolutions on the order of a crystal lattice spacing of the metal under investigation. This study involves the application of the FIM/IAP in obtaining depth profiles of low energy ions (<20 keV) implanted into metals.

Two technologically important ion species were used, nitrogen and deuterium. It was shown that the deuterium partial pressure was not a problem when a properly differentially pumped ion gun was used. Specific problems of applying FIM/IAP to these species were reported. The results of nitrogen implanted into nickel showed that the nitrogen resists field

evaporation even though the nickel was removed. Range and straggling values for nitrogen implanted into tungsten with energies of 2.5-9 keV were found and compared to Monte Carlo computer calculations.

Two special Transmission Electron Microscope (TEM) sample holders were developed for use with FIM specimens. Using these holders, it was shown that there was little or no influence of the high electric field on the implanted defect microstructure of the specimen. However, nickel was seen to be embrittled by deuterium implantation, but not by helium or nitrogen.

The use of TEM was critically important in obtaining the geometric parameters used to determine a depth scale from implanted emitters profiled under ultra-high vacuum conditions. The volume probed was related to the cumulative matrix signal. The geometric parameters were used to obtain the proportionality constant between the cumulative matrix signal and the probed volume (a function of depth).

Several critical observations for proper interpretation of FIM/IAP results were reported. Foremost of these was the lowered evaporation field of implanted emitters. This study established a methodology for applying the FIM/IAP to the depth profiling of ion implanted species into metals.

CHAPTER I
LITERATURE SURVEY

Introduction

In the field of materials science, there is a wide range of interest in the use of ion implantation. This interest extends from basic and applied research to commercial applications. Ion implantation has been used extensively in semiconductor processing for a number of years. Recently ion implantation is proving to be highly beneficial in the modification of surface properties of certain alloys. Reduced friction and wear and/or increased corrosion resistance have been reported in tool steels, cemented carbides, and titanium-based surgical prosthesis alloys. Radiation damage in alloys caused by the hostile environments of nuclear reactors has long been simulated by ion implantation. Ion implantation can cause amorphization of surface regions and impart special properties or created supersaturated concentrations of insoluble species not achievable by conventional methods. In fact, it can provide an almost limitless modification of surface composition, allowing the formation of phases and compositions without regard to thermodynamic stability.

The implantation depth is an extremely important parameter when ion beams interact with metals. Very little data are available for the ranges of light, low energy (<40 keV) ions into metals; conventional analytical techniques such as secondary ion mass spectrometry (SIMS), nuclear reaction analysis (NRA) and Rutherford backscattering (RBS) suffer from a limited spatial resolution for the shallow depths. Although it is not widely recognized outside the FIM community, the atom probe and imaging atom probe are superb for compositional depth profiling. With an imaging gas present, depth resolutions of one atomic plane are expected. The imaging atom probe (IAP) has several advantages over the conventional atom probe (AP) for profiling: 1) it offers a larger area of analysis (approximately 10^2-10^3 larger), 2) crystallographic effects are minimized, 3) a complete mass spectrum is collected with each pulse, and 4) all atoms within the probed volume will strike the detector. However, there are two disadvantages in using the IAP. The IAP employs an extremely short flight distance (≈.15m) as compared to the AP (≈1m) and mass resolution suffers accordingly. Because of this, material systems must be chosen such that the mass-to-charge ratios are sufficiently resolved temporally. The other disadvantage is the difficulty in the determination of ring collapses under ultra high vacuum (UHV) conditions (i.e. no imaging gas present). In the AP an increase in signal occurs when the edge of a ring sweeps by the probe hole [1,2]. (See below for a discussion of the AP.) This periodic increase corresponds to the collapse of a ring and can be used to assign the depth scale. In the IAP, distinguishing between an increase in signal and an increase due to a voltage increase is difficult to do because the signal from a single set of planes is small compared to that coming from the entire probed surface. This particular disadvantage will be discussed in detail and a solution put forth.

This study involves the application of the IAP toward the depth profiling of nitrogen and deuterium into field emitters. Specific instrumental problems will be addressed. These include those attributed directly to implantation into field emitters and those associated specifically with the implanted species. Deuterium and nitrogen are the primary implantation ions used in this study. The study of the interaction of hydrogen and its isotopes to defects in metals may well be one of the most important problems in materials science. A full understanding of the trapping of hydrogen at defects is essential for the operation of future fusion reactors. Essentially all of the energy sources of tomorrow will have hydrogen interacting in some way with the materials system. Nitrogen is now playing a major role in the surface modification of commercial alloys. Nitrogen, sometimes in conjunction with other elements such as boron and titanium, is the most widely used element for modifying surface properties by ion implantation. The advantages of ion implantation over conventional methods of surface treatment include relaxed heat treatment requirements, stability of final shape, controlled composition with depth, and the possibility of creating beneficial metastable phases.

Although the effects that deuterium has on materials may be deleterious and those of nitrogen may be beneficial, finding the range for low energies of these elements is a common problem. Each has particular instrumental difficulties which arise when the IAP is used to analyze for them. These difficulties will be discussed and solutions presented for overcoming them. A knowledge of the complexities for implanted nitrogen and deuterium in applying the IAP to studying them will be invaluable for its general use to other types of ions. Many of the problems for these interstitial-type species (i.e. nitrogen and deuterium) will not be present for substitutional-type elements, but it is essential that the experimentalist be aware of the potential problems when a new system is first investigated.

The rest of this chapter will be divided into four main sections: 1) a brief introduction to FIM principles, techniques, and terminology,2) the microstructure of implanted specimens, 3) a literature survey of hydrogen in metals, and 4) a literature survey of nitrogen implanted in metals.

FIM Principles

This section will be used to describe some of the fundamental aspects of FIM techniques for the reader who is not thoroughly familiar with them already. For a more complete discussion of FIM theory and practices, several excellent books are available. The three which this author recommends are: 1) Field Ion Microscopy edited by Hren and Ranganathan [3], 2) Field Ion Microscopy, Principles and Applications by Müller and Tsong [4], and 3) Field Ion Microscopy in Materials Science by Wagner [5], The last of these is the most recent and includes operating principles of both the atom-probe and imaging atom probe types of instruments.

Field Ionization

A basic FIM in comparison with today's sophisticated instruments is relatively simple. It employs no lenses, no primary beam, and requires no high power consumption. It consists of a vacuum chamber (usually

UHV), a cryogenically cooled specimen holder that can be biased to a high voltage (0-20 kV), and a leak valve which allows backfilling of the vacuum with an inert gas such as helium or neon to a pressure of approximately 1×10^{-5} Torr. Figure I-1 shows a schematic of a basic field ion microscope. The specimen is normally electrochemically polished to an emitter endform (having a radius of curvature of about 200 to 1000 Å) When a voltage is applied to it in the microscope, the shape of the emitter causes a high electric field that ionizes the gas molecules (field ionization) above the surface step sites where the planes of atoms emerge at the surface. The ionization process is due to quantum mechanical tunneling of an electron from the gas atom through a potential barrier between the metal surface and the atom. The ions are then repelled away from the positive tip and strike a phosphor screen assembly (a channel electron multiplier array (CEMA)/phosphor screen combination) where the image is photographically recorded. This process is illustrated in Figure I-2. Besides the apparent resolution of the image, crystallographic information can be obtained directly, i.e. without diffraction, but lattice parameter information cannot.

Field Evaporation

When the voltage is raised such that the fields exceed those normally used for imaging conditions, the atoms themselves can be positively ionized (termed field evaporation). This process can be considered to be the result of the electric field lowering the energy barrier for sublimation of the surface atoms. Because of this, field evaporation is a thermally activated process. Every metal has a characteristic field evaporation strength which is also a function of

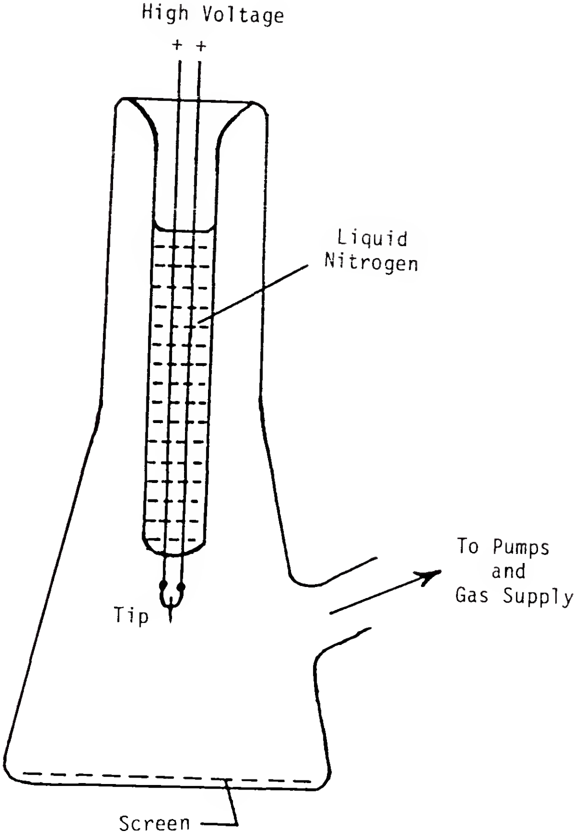

Figure I-1 Schematic diagram of a simplified field ion microscope.

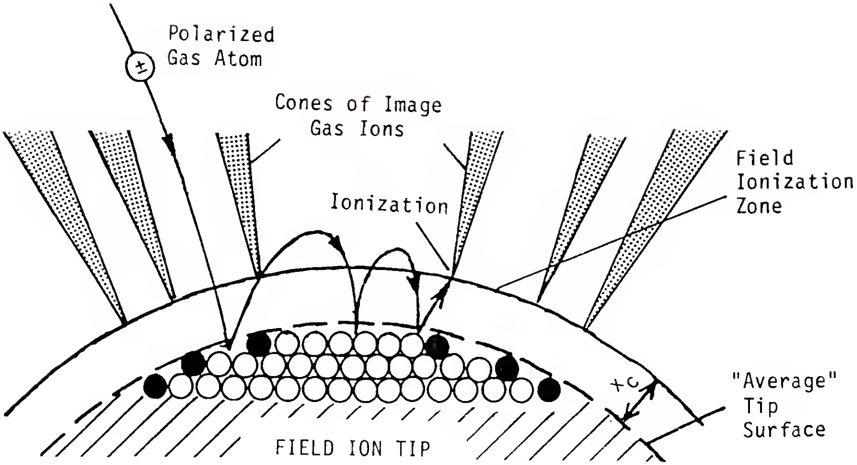

Figure I-2 Schematic diagram of the filed ionization process. The gas atom is polarized by the high electric field and is attracted towards the tip, strikes the cold surface several times, loosing some of its kinetic energy each time. At a critical distance above an ionizing site the gas atom looses an electron to the metal by a quantum mechanical tunneling process and is repelled from the tip towards the viewing screen where the image is photographically recorded.

temperature. The process of field evaporation can be controlled very precisely by varying either the applied field with the voltage or by changing the specimen temperature, and forms the basis for AP instruments. Atom probe instruments rely on one of these two methods to initiate field evaporation in a very short time in order for the ions to be measured temporally at a detector, thus forming a time-of-flight (TOF) mass spectrometer. A high voltage pulse with a subnanosecond risetime and 10-20 nsec width and having an amplitude of 1-3 kV is used in the conventional AP and imaging atom probe (IAP). The pulsed-laser atom probe (PLAP) is basically an IAP employing a nitrogen laser to instantaneously heat the surface of the emitter to cause field evaporation. The latter instrument enjoys the benefits of a reduced electric field and the capabilities of analyzing specimens with poor electrical conductivities, such as silicon, and glasses. Because the removal of atoms from the surface of the emitter is seen as a collapse of the characteristic rings which form the FIM image, depth resolutions of one atomic plane are expected.

It should be noted that field evaporation is the final step in the specimen preparation technique. When the voltage is applied for imaging in the FIM, local protuberances are field evaporated. The tip continues smoothing in this manner until the ring structure appears, and a stable image occurs. A particular radius of curvature can be "dialed-in" by continued field evaporation from the "as-polished" condition to a preset voltage which corresponds to that radius at the given temperature, providing, of course, that the initial radius is less than that of the desired radius.

Atom Probery

The conventional AP is designed with a 1-2m flight tube behind a CEMA/phosphor screen assembly that has a 4-6mm hole through it. Surface atoms which are aligned with and pass through this probe hole are then focussed with an einzel lens to strike the detector. Electronic timing circuits interfaced with a computer are used to determine the flight time which in turn is used to calculate the mass to charge ratios. The detector most often used is a Chevron assembly, constructed using two CEMA's. The mass resolution, $M/\Delta M$, of the AP is on the order of 200 [6]. The source of the poor resolution is due to energy deficits inherent in the field evaporation process [6]. The energy-compensated AP uses a Poschenreider lens [7] to increase the resolution to as high as 5000 [6]. In both instruments the apparent size of the probe can be changed by varying the tip to screen distance. Compositions of precipitates with dimensions on the order of 10 Å have been analyzed routinely. In addition, since the AP is a TOF instrument, all elements can be detected, including isotopes of hydrogen. It should be noted that the metallurgical applications of the AP did not advance at a rapid pace until the widespread use of fast electronics and computerized interfacing allowed the collection and reduction of large number of data. The early AP's employed a storage scope with the results of each trace needing to be analyzed by hand.

The IAP (and PLAP) are constructed with a Chevron assembly (which can be curved) mounted .1-.15m from the tip. The assembly is used as a detector and viewing screen. Since the IAP has such a short flight distance, extremely fast digitizing scopes are employed to capture the resulting waveforms. The IAP, although having poor mass resolution (≈50), does have the advantages of having a full spectrum result with each pulse and a large probe area (the entire imaging surface). The Chevron assembly can be gated to be turned "on" to coincide with the arrival a particular mass at the detector. In this mode of operation, the results of many pulses are integrated photographically to form a time-gated image. The resulting image can be compared with the FIM image in essentially the same way as an X-ray elemental map is compared to a SEM micrograph. The results can be very dramatic, for example showing the segregation of impurities to grain boundaries [8]. For metallurgical applications, the AP and IAP together in one instrument can be a powerful combination.

The FIM/IAP also suffers no problems of minimum detectability. In principle, it has single-atom detectability. Another important point to be made is that the IAP resolves deuterium from other low-mass peaks such as H^+ and He^+ very well, despite the flight distance being extremely short (.15 m).

Applications

The FIM and AP techniques are being applied to diverse areas of interest. The atomically clean surface of an emitter caused by field evaporation make them attractive techniques for surface science applications. Studies are being done in the areas of surface segregation, surface diffusion, adatom adsorption, precipitation, radiation damage, radiation-induced precipitation and catalysis. Segregation of elements to interfaces are the forte of the AP. Many different materials have been examined, including: steels, nickel-based superalloys, aluminum-copper alloys including those which develop Guinier-Preston zones, alloys which undergo order-disorder transformations, glasses, and semiconductors. The review by Wagner discusses in detail the fundamentals and applications of FIM techniques in materials science [5].

FIM techniques are by no means the solution to everyone's problems. Not all specimens that one would like to examine in the FIM can be prepared into the required shape. And if they can, it doesn't mean that they will withstand the effects of the high electric fields. One major disadvantage of FIM techniques is the extremely small volume of material which can be examined. The volume of a field emitter examined is on the order of 100 times smaller than that of a TEM specimen. This means that finding features of interest, even with the aid of TEM, can be quite difficult and care must be exercised when interpreting results from such a small sampling.

Field-Induced Stresses

Also of primary importance to the success of applying FIM techniques to the study of implanted species with defects is the influence that the high electric field has on them. Extremely high tensile and shear stresses are induced within the emitters due to electrostatic (coulomb) forces present at the surface of the emitters. These stresses can be visualized by imagining a sphere of the same radius of curvature as a field emitter to which the same voltage is applied (Figure I-3a). The stresses induced in this imaginary sphere are purely tensile and at the surface are equal to $F^2/8\pi$ where F is the electric field at the surface. The electric field is equal to V/r, where V is the applied voltage and r is the radius of the sphere. Within the volume of this sphere, there is

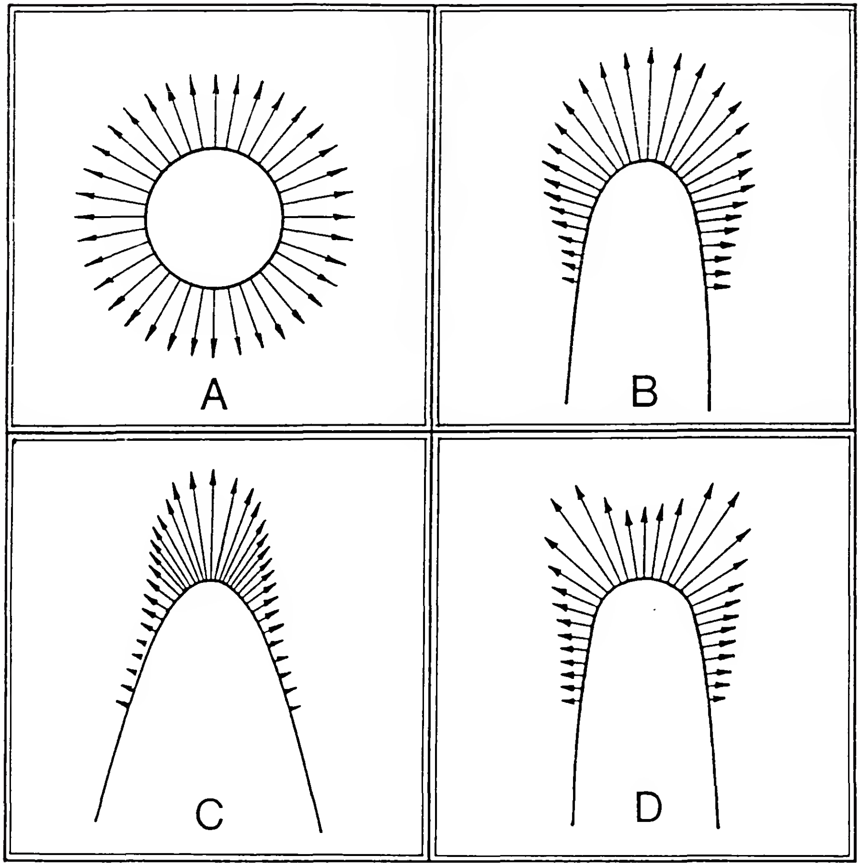

Figure I-3 Field distributions for various shaped emitters.
a) Idealized perfect sphere, b) spherical cap on cone shaped shank,
c) parabolic shaped tip, d) tungsten-like specimen with flattened apex.

no shear component of stress because of symmetry. Now imagine the model of an idealized field emitter (Figure I-3b), a spherical cap superimposed onto the apex of a cone. One can see that the field and hence the stresses taper off sharply down the shank where the local radius of curvature increases. Figures I-3c and I-3d show the added complexity of determining the electric field distribution and hence the stress distribution when samples deviate from this ideal model of Figure I-3b. This leads to significant stress gradients with both tensile and shear components. The large shear components can lead to massive plastic deformation and destruction of the specimen (known as flashing).

FIM samples are completely compatible with TEM when the proper holders are designed and used. In addition when wire samples are used having a preferred orientation, the crystallography becomes very simplified. TEM observations of tips are used routinely at many FIM locations for checking specimen quality.

Two especially designed transmission electron microscope (TEM) sample holders have been designed and constructed to be used to observe the influence of the applied field on FIM specimens containing defects. The first of these two is a "double-tilt" holder used for characterizing the defects using conventional TEM diffraction contrast. The second is a "field-effect" holder which is capable of having up to a 5 kV voltage applied to a FIM specimen in the TEM. The use of these holders is of considerable importance in understanding how the techniques developed in this study can be applied to studies of more general types of defects. These holders facilitate the search for a particular type of defect, and help to indicate whether it will be feasible to study such defects using

FIM techniques (i.e., is the defect stable under the field-induced stress?). The TEM has proven to be indispensible with in establishing a depth scale for specimens analyzed with the IAP.

Microstructure Of Implanted Metals

The microstructure of ion-irradiated metals is dependent on several variables. These include: ion species, energy, temperature, target composition, crystallographic orientation, and post-irradiation heat treatment. The combination of these experimentally controllable parameters determines the implantation depth, the amount of damage present in the lattice, the concentration profile, the size and type of defects, and the precipitation of second phases (if possible). A complete discussion of these parameters is outside the scope of this study. The discussion which follows will concentrate only on those aspects of ion implantation which relate to this study.

The most important parameter which determines the amount of damage in an irradiated target is the maximum energy, E_m, transferred to a lattice atom in a head on collision with the projectile ion. For non-relativistic particles, E_m is given by

$$E_m = 4Em_1m_2/(m_1+m_2)^2 \qquad \text{I-5}$$

where m_1 is the ion particle mass, m_2 is the lattice atom mass, and E is the kinetic energy of m_1. There are two critical values of E_m which separate implantation studies into three regimes. The first is E_d, which defines the minimum transferred energy which can produce a stable Frenkel pair with a probability of $\frac{1}{2}$. (A Frenkel pair is a self-interstitial atom (SIA) and its vacancy.) For values of $E_m < E_d$, no stable damage is produced. In this regime, the implanted species would be interstitial in nature (if diffusionally stable). The second critical energy, E_c, denotes the threshold energy required to form a displacement cascade (with probability of $\frac{1}{2}$) [9-12]. When $E_m > E_c$, the energy is transferred to a primary knock-on atom that creates the displacement cascade, characterized by a center depleted zone of high vacancy concentration. The interstitials are ejected from the zone by either a channeling process or a focussed replacement collision sequence [13,14]. In either case, the SIA's are found relatively far from the depleted zone.

Seidman and coworkers [14-24] have used the FIM to study depleted zones in tungsten which are produced by a single incident heavy ion. They photographically recorded each FIM image after a field evaporation pulse which removes on the average of one atom from a (222) plane. After the analysis of numerous frames (on the order of several hundred thousand), a three dimensional reconstruction of the depleted zone was accomplished with the aid of the computer. These depleted zones have a high fraction of clusters (approximately 83%) that are composed of more than six first-nearest neighbor vacancies, while only about 13% appear as monovacancies having no first-nearest neighbors [16]. The depth from the surface of the depleted zones depends on energy and mass. For 20 keV W^+ into tungsten it is about 20 Å [24]. Unfortunately, FIM results on the structure of depleted zones created by light elements such as hydrogen and helium have not been achieved to date.

For $E_d < E_m < E_c$, mainly isolated Frenkel pairs are created which may or may not agglomerate into defect clusters, depending on temperature, energy,fluence impurity content, etc. For E_m just over E_d only single Frenkel pairs are created. For high dosages, separate-event interstitials and vacancies can annihilate each other. For increasing transferred energies, both the number of Frenkel pairs per incident ion and the clustering of vacancies also increases.

The radiation induced point defects described above will not be able to be resolved with TEM unless they agglomerate by diffusional processes with sizes greater than a few nanometers. Here, size refers to either the physical geometrical size or the extent of the strain field of the defect. The types of defects which nucleate due to the migration of the point defects are both vacancy and interstitial dislocation loops, voids, gas bubbles, etc. In addition, pre-existing lattice imperfections can trap the point defects and hence change their local contrast. Any type of lattice inhomogeneity or defect that modifies the local diffraction conditions will result in contrast in the micrograph. The types of inhomogeneities which produce contrast include the following:

(1) A locally varying strain field.

(2) A planar defect, e.g., a stacking fault tetrahedron.

(3) A void or gas bubble within the volume observed.

(4) A local change in the extinction length, e.g., due to local variation in composition.

In general direct interstitial defects are difficult to find, because they are much more mobile than vacancies at low temperatures. On the other hand pure vacancy type defects can exist in equilibrium at relatively high temperatures. The image contrast from small dislocation loops which are visible in the TEM characteristically have a complex black-white contrast pattern. The contrast pattern depends on several factors, material, loop type (vacancy or interstitial), Burgers vector of the loop, beam direction, extinction distance, and relative position within the thin foil. The correct identification of small loops from TEM images therefore requires the aid of computer simulation. The computer simulation programs use a column approximation to the foil in which the intensity is found solely by the diffraction conditions within this volume. The various models used for the calculations for the volumes containing the defect and strain fields are reviewed by Wilkens [13] and Sykes [25]. Sykes et. al [26] have compiled a catalog of computer simulated TEM images of small dislocation loops in FCC and BCC metals. This catalog allows the microscopist to directly compare an experimental image for a loop with the catalog. The required parameters for the loop are the depth in the foil, foil thickness, and beam condition. It should be noted that all the loop contrast patterns are calculated under dynamical conditions, i.e., "two-beam" conditions. Therefore, all micrographs compared to simulated images should be made under identical conditions.

It must be emphasized that TEM observation of radiation induced defects is not feasible without an accumulation of the point defects and the formation of voids and/or loops of sufficient size (≥ 3 nm). Thorough discussions of the conditions required to identify such defect clusters are given by Wilkens [14], Rühle [27] Venables and Thomas [28], and Sykes [25]. As mentioned earlier, Seidman and coworkers [14-24] have used the FIM to study the distribution of clusters in the depleted zone of a displacement cascade. Their methods can also be used to determine both types of radiation induced point defects, vacancies and interstitials, and to map their spatial distributions within the emitter. The FIM is the only microscopic technique which can image point defects at a temperature at which no recovery occurs. Seidman and coworkers have utilized the FIM to its fullest in these studies and have contributed substantially to our present understanding of the spatial arrangement of point defects in irradiated metals.

Hydrogen In Metals

Most often, the presence of hydrogen in metals is deleterious. Since metals are frequently exposed to hydrogen, (e.g. containment) the harmful effects of hydrogen on metals are an important technological problem. As a result, interest in hydrogen in the field of materials science extends to both basic and applied research. Because hydrogen has relatively low-solubilities and extremely high diffusivities in most engineering alloys the study of the interactions of hydrogen with crystal defects is of basic importance. The term defect, as used here, means any microstructural feature differing from a perfect crystalline solid. Typical defects include: grain boundaries, dislocations, precipitates, interphase boundaries, vacancies, etc. The analysis of hydrogen associated with these defects cannot be studied by conventional electron probe techniques, such as analytical electron microscopy (AEM), energy dispersive x-ray spectroscopy (EDXS), electron energy loss spectroscopy (EELS), scanning electron microscopy (SEM), and Auger electron spectroscopy (AES), because these techniques are incapable of detecting it. Surface analytic techniques employing mass spectrometers for example, secondary ion mass spectrometry (SIMS) can detect hydrogen, but so far lack sufficient spatial resolutions. This spatial resolution includes both the lateral probe diameter and depth profiling resolution.

The quantity of hydrogen which can cause harmful effects to alloys can be extremely small and hydrogen defect interactions can be on extremely fine scale. Thus the techniques which can analyze hydrogen must have high sensitivity for it and adequate spatial resolution in order to study the mechanisms of degradation.

It has long been known that field ion techniques are extremely sensitive to the presence of hydrogen. In fact, this sensitivity has made it difficult to apply FIM and atom probe techniques to studies of hydrogen. In general all hydrogen studies using the FIM must overcome the same problems: 1) hydrogen's high diffusivity, even at low temperatures, 2) the apparently low solubility of hydrogen in the absence of defects, and 3) hydrogen is ever-present in the experimental background. Experimentally this means that hydrogen must be introduced into the metal, kept there for sufficiently long time to be analyzed, and confidently distinguished from pervasive background hydrogen.

Background hydrogen is always a consideration in mass spectrometric techniques because it is a major constituent in all normal vacuum systems, since it is difficult to pump. With FIM techniques the background hydrogen problem is further aggravated by the phenomenon of field adsorption. Field adsorption occurs because of the polarization of the hydrogen gas molecule under the influence of the applied field on the emitter. The rate of adsorption in the presence of a field and at a given partial pressure of hydrogen is several orders of magnitude higher than without the applied field. The consequence of this is that a hydrogen background desorption peak is present in all atom probe studies. To circumvent this problem, deuterium is used in this study instead of hydrogen. The deuterium and hydrogen signals are well differentiated in the IAP.

The introduction of hydrogen *ex situ* (with respect to the FIM/IAP chamber) requires very complex quenching and cryogenic/UHV transfer techniques. This difficulty is in addition to the elaborate control experiments required to determine the adsorption of hydrogen in all the steps preceding introduction into the FIM/IAP chamber. For these reasons *in situ* implantation of deuterium was chosen for the present study. This method offers major advantages since 1) both the deuterium and the defects can be reproducibly and controllably introduced into the lattice, 2) the background deuterium can be controlled by differential pumping and valving, 3) the number and complexity of the control experiments can be greatly reduced, and 4) the deuterium can be easily distinguished from the hydrogen background.

There are major questions which must be answered before the FIM/IAP can be applied to studies of general types of defects (i.e., those not induced by ion implantation). These questions will be addressed and answered in this study. The most important of these will be the feasibility of implementing a differentially-pumped ion gun for *in situ* implantation with respect to the deuterium field adsorption. Any ion gun coupled to the FIM/IAP and used for ion implantation of deuterium will contribute a deuterium partial pressure to the FIM/IAP chamber. The question arises, can the deuterium partial pressure be kept sufficiently low so as not to interfere with the implanted deuterium as detected with an IAP? This study will show that this question can be answered in the affirmative when special precautions are taken.

Hydrogen Embrittlement

A major impetus for studying hydrogen in metals is the phenomenon of hydrogen embrittlement in commercial alloys, especially steels. Because of hydrogen's extremely high diffusivity, even at low temperatures, failures involving hydrogen embrittled alloys usually occur catastrophically. Unfortunately, the mechanisms of hydrogen embrittlement are still little understood. In steel at least five different mechanisms for hydrogen embrittlement have been proposed. For example, Zapffe and Sims [29] developed a pressure-expansion theory in which very large gas pressures within internal micro-cracks and voids cause either plastic deformation or cleavage. This leads to a coalescence of the micro-voids and to eventual failure. However, this mechanism is inadequate to explain hydrogen embrittlement which occurs with hydrogen gas pressure of one atmosphere or less. Another proposed mechanism, by Petch and Stables [30,31], suggests that hydrogen adsorption lowers the energy of the surface created in crack propagation, which in turn lowers the work of fracture, according to Griffith's criterion. There are several criticisms of this mechanism as well [32-34] and it seems not to be generally applicable.

The decohesion theory proposes that high concentrations of hydrogen lower the intrinsic cohesive force between atoms [35,36-38]. It is postulated that the stresses developed at crack tips promote the accumulation of hydrogen to very high concentrations and thus substantially lower the cohesive forces. Unfortunately, the dependence of the maximum cohesive force on hydrogen concentration, interface structure, and alloy composition is not known. Still another theory proposed by Westlake [39] also centers on the processes occurring near a crack tip. It is postulated that hydrogen concentrates near the tips of cracks because of the hydrostatic stresses present there. A high enough hydrogen concentration, in turn, leads to hydride formation. Embrittlement then is thought to occur due to hydride cracking near the crack tip. In fact, Gahr et al. have shown that the hydrostatic stress field of a crack tip can stabilize hydrides in niobium which are otherwise unstable [40]. They also demonstrated embrittlement due to hydride cracking. For iron and steel, no hydride is stable up to 2 GPa [41] and Westlake's model is not considered applicable [32-42]. Nonetheless, calculations of the hydrogen atmosphere at a crack tip show that very high concentrations can occur there and that the hydride formation model could be appropriate [43,44].

Trapping Of Deuterium

Kellogg and Panitz [45] have directly observed the trapping of deuterium at a grain boundary in tungsten. In this study seven tungsten emitters were implanted with low energy (200 ev) deuterium ions. The specimens were imaged with the TEM and then transferred to a FIM/IAP and analyzed. The FIM/IAP can give a time gated image which can map the distribution of deuterium with depth. (The FIM/IAP and its modes of operation will be discussed further in Chapter II.) The only sample that retained any deuterium was one in which a grain boundary was present, the gated IAP image showing the deuterium associated with the grain boundary visible in the FIM micrograph. In a more recent set of atom probe experiments, Macrander and Seidman [46] have shown that 200 eV H_2^+ ions implanted into Tungsten emitters completely diffuse out of the samples at a temperature of 29°K. Their results indicate a diffusion coefficient at 29°K that is greater than 10^{-17} cm^2/sec. Since the implanted specimens in Kellogg's and Panitz's study were stored at room temperature for several days and were heated during imaging somewhat in the TEM, grain boundaries are apparently deep traps for deuterium.

In the second study, Panitz [47] demonstrated the importance of using control experiments to distinguish the difference between the implanted and the background deuterium signal in the IAP spectrum. Implantation was done in the specimen pre-chamber of the IAP and not *in situ*. Complex control experiments were required because the implantation was performed outside the IAP chamber. This suggests the possible benefits which could be derived if *in situ* implantation were performed.

The results of Panitz's study indicate that the 80 eV ions are implanted to a depth of 49 Å at 300°K and that adsorbed surface species selectively scatter some of the deuterium into preferred channels. These results are at odds with those of Macrander and Seidman [46] which indicate that the deuterium should have diffused out of the sample since no implantation damage can occur with 80 eV deuterium ions implanted into tungsten. The implantation was carried out at 300°K where the solubility of hydrogen is extremely small and the diffusivity is high. With these considerations the implanted deuterium should have diffused to the surface where it would have been field desorbed. A possible explanation for the discrepancy is that the background deuterium has not been accounted for adequately. There is the possibility of surface migration of deuterium up the shank during the profiling experiment. This deuterium would appear in the IAP spectra as an implanted ion. A change in evaporation rate due to a voltage increase during the analysis can change the arrival rate of the deuterium to the analyzed portion of the tip. Another factor which could affect a possible background signal is the time interval between field desorption pulses. These factors were not reported in this study [47].

Hren [48] confirmed the necessity for *in situ* studies when he performed several *ex situ* experiments preliminary to this dissertation using the facilities of Myers* and Panitz and Kellogg**. A discussion of the design requirements for coupling an ion gun to a FIM/IAP will be presented in Chapter II. The control experiments associated with *in situ* implantation of deuterium are relatively simpler than for *ex situ* implantation and will be presented in Chapter III.

Nitrogen Implantation In Metals

Tribological Studies

Nitrogen is by far the most widely used element for the modification of the surface properties of alloys to improve their wear resistance.

---

*Ion Implantation Facility, Sandia National Laboratories, Albuquerque, NM.

**Surface Physics Division, Sandia National Laboratories, Albuquerque, NM.

There is a great deal of research being done in the area of determining the mechanisms for the improvement of wear resistance in a variety of alloy systems. It should be noted that not only the wear characteristics are improved by implantation, but also often are such properties as fatigue, corrosion (both atmospheric and aqueous), toughness, strength, and high temperature oxidation. Wear resistance, however, is the common goal of applying ion implantation to alloy systems. Wear can be improved by increasing the surface hardness, by reducing the friction coefficient, by modifying the subsurface composition and structure to resist fracture and debris formation, and/or by increasing the wetability of the surface to lubricants. This lack of understanding of the basic mechanisms of wear improvement has not stopped the spread of industrial applications of ion implantation of nitrogen. The major thrust of commercial use of implantation involves tool steels and Co-cemented WC [49-52]. The area in which ion implantation is very attractive is where little or no dimensional changes and low processing temperatures are desired. It is also of interest where delamination of coatings applied by more conventional techniques may be a problem [51]. Basic research efforts are directed towards understanding the wear reduction mechanisms in technologically important alloy systems such as stainless steels [53-55], hard chromium plate [56], Ti-6Al-4V [57-60], and Co-cemented WC [61-63].

The increases in wear resistance are usually attributed to nitride formation and/or Cottrell atmosphere hardening. The nitride formation by implantation is usually in the form of finely dispersed, hard second-phase precipitates. The Cottrell atmospheres arise from nitrogen being attracted to dislocations and pinning them preventing them from being mobile and thus hardening the material. Depending on the material, one of these may be more predominant than the other. For example, mild steels without alloying elements having strong affinities for nitrogen such as Al, Cr, Mo, V, and Ti do not show dramatic increases in wear resistance upon nitrogen implantation [64]. One disadvantage to nitrogen implantation to improve the wear characteristics of an alloy is that the benefits are not retained at elevated temperatures. High operating temperatures must be avoided and this sometimes precludes its use in particular applications such as tools for chip forming. This is thought to be due to the instability of nitrogen-defect structures which are responsible for the improved wear characteristics [51,62]. This is supported by experiment. For example, Dose Santos et al. have seen nitride and carbo-nitride formation upon implantation and then subsequent dissolution at higher temperatures [65].

The understanding of the wear mechanisms are complicated by studies in which the nitrogen is seen to still be retained beyond the original implantation depth. The depths that the nitrogen is still modifying the surface behavior can be 10-50 times the implanted range [51]. Clearly this nitrogen retention is happening during the wearing of the material and microstructural changes must be occurring. There are several proposed ways for this to happen. During wear, the rubbing of asperities on the two surfaces causes localized heating. This thermal heating is thought to be responsible for the dissolution of the nitride phases and diffusion down the steep temperature gradient [66]. This mechanism would agree with the observations that nitrogen implantation does not give good results at high service temperatures. These local temperatures may be as high as 1000°K (e.g. Fe_2N has been shown to be stable in the electron microscope to 900°K [67]). This same local heating could also cause, the nitrogen, decorating dislocations to diffuse deeper into the material [68]. Another possibility for the retention of nitrogen is the continuous transfer of nitrogen back and forth between the surfaces as the wear front advances [51].

Ion Beam Carburization

Several investigators have reported improvements in properties in alloy systems with the implantation of inert elements such as neon, argon [51], and zirconium [59]. Others report that no effects are seen when elevated temperatures (500-600°C) are used during implantation [51]. The probable explanation of this is due to beam carburization of residual hydrocarbons in the vacuum system decomposing under the effects of the irradiation during implantation. Elements with high affinities for carbon tend to form carbides giving a characteristic improvement in surface hardness. It is more likely that at high temperatures the decomposed hydrocarbons are not stable and reform rather than the carbide phases being unstable. The resulting carbide phases would necessarily be quite small and finely dispersed.

Applicability Of FIM Techniques To Nitrogen In Metals

A variety of techniques have been applied to study the composition and morphology of implanted surfaces. These include secondary ion mass spectroscopy (SIMS), Auger electron Spectroscopy (AES), scanning electron microscopy (SEM) with energy dispersive analysis of X-rays (EDAX), Rutherford backscattering (RBS), nuclear reaction analysis (NRA), and TEM (and analytical electron microscopy, AEM). With the exception of TEM, all of these techniques have the ability to use the same samples which are used for the wear tests. Several of them can also analyze small particles within the wear tracks of the samples.

Field ion microscopy techniques offer some appealing features for studying nitrogen (and other elements) implanted into metals. It is a surface microscopic technique and the results can be directly compared with that of some of the above technique. It has the capability of resolving both the defect structure caused by implantation on an atomic scale and small precipitate phases which form. It has the ability to dissect these features as a function of depth with an accuracy of d-spacing of the material. The same method for determining the depth scale can be used with atom probe analysis, both AP and IAP, to give chemical information as a function of depth. Because the FIM samples are completely compatible with the TEM, the implanted samples do not require any further sample preparation to observe them there. In other words, the implanted structure is accessible to two high resolution microscopic and analytical techniques with no treatment to them after they have been implanted other than to introduce them into the specific instrument.

The delicate nature of a FIM specimen in terms of its geometry precludes it from also being used in wear test apparatus. However, the relationship between the microstructure and macroscopic properties of materials is one of the principal goals in materials science. The FIM sample lends itself to investigation by two microscopic techniques, FIM and TEM, without further specimen preparation after implantation. This study of the implantation depth of implanted nitrogen into tungsten and nickel in is the first step in applying the FIM/IAP to the future use in using it to observe and analyze the small nitride, carbides, and carbo-nitrides responsible for wear reductions in many ion-implanted samples. These types of precipitates in emitters have proven to be very amenable to FIM and AP analyses in the past.

CHAPTER II
INSTRUMENTATION

The instrumentation employed in the experimental work can be divided into three categories: FIM/IAP, ion gun, and transmission electron microscope. This chapter will describe the unique features or techniques which have been developed in utilizing these instruments for the present study, as well as document the instrumentation.

Field Ion Microscope/Imaging Atom Probe (FIM/IAP)

Until recently, no commercial FIM/IAP has been available and each instrument has been custom-built and usually designed with a specific purpose in mind. The FIM/IAP used in this study is no exception, and several unique features have been incorporated in it which will be discussed. It was designed to be a versatile instrument for metallurgical applications. The electronics and timing circuitries are based primarily on those of Panitz [69]. The vacuum chamber, specimen exchange mechanism, specimen holder/manipulator, and chevron/phosphor screen assembly have been designed primarily by this author. The construction of the FIM/IAP proceeded in stages. Each was a major design or developmental stage in the instrument leading to its present form. Most of the problems associated with each of these stages have been solved by this author. Several features have been included because of considerations to the present study or anticipated future studies involving hydrogen. Many of the design features or specifications within each stage are either common to both or intimately related. Figure II-1 is a diagram showing these major stages and the relationships between them. The arrows in this diagram indicate these relationships. A double-headed arrow represents the fact that the one stage is intimately related to the other and must be compatible. A single-headed arrow represents an independence, but that some of the same requirements in the one stage are also requirements in the other. The details of the design and interactions of the various stages represented in Figure II-1 will be described in each of the following sections. This chapter will provide the bulk of the documentation required for someone to learn to use this instrument.

FIM/IAP Description

Chamber

The FIM/IAP used in this study differs from other instruments in that the sample can be directed towards two, six-inch ports separated by 150° (Figure II-2). One of the six-inch ports is used as the FIM/IAP. It has a chevron assembly [70] mounted 15 cm from the chamber's axis. The assembly uses flat microchannel plates from Galileo Electro-Optics and was designed by this author. The other port is a utility port. Various options are available for use with this port which provides the versatility of this instrument. Originally, a conventional atom-probe [71] was planned to be attached to it after completion of the IAP. For the present study a Colutron Research Corp., model G-2-D ion gun was coupled to this port (Figure II-3). This gun was obtained as a kit, and

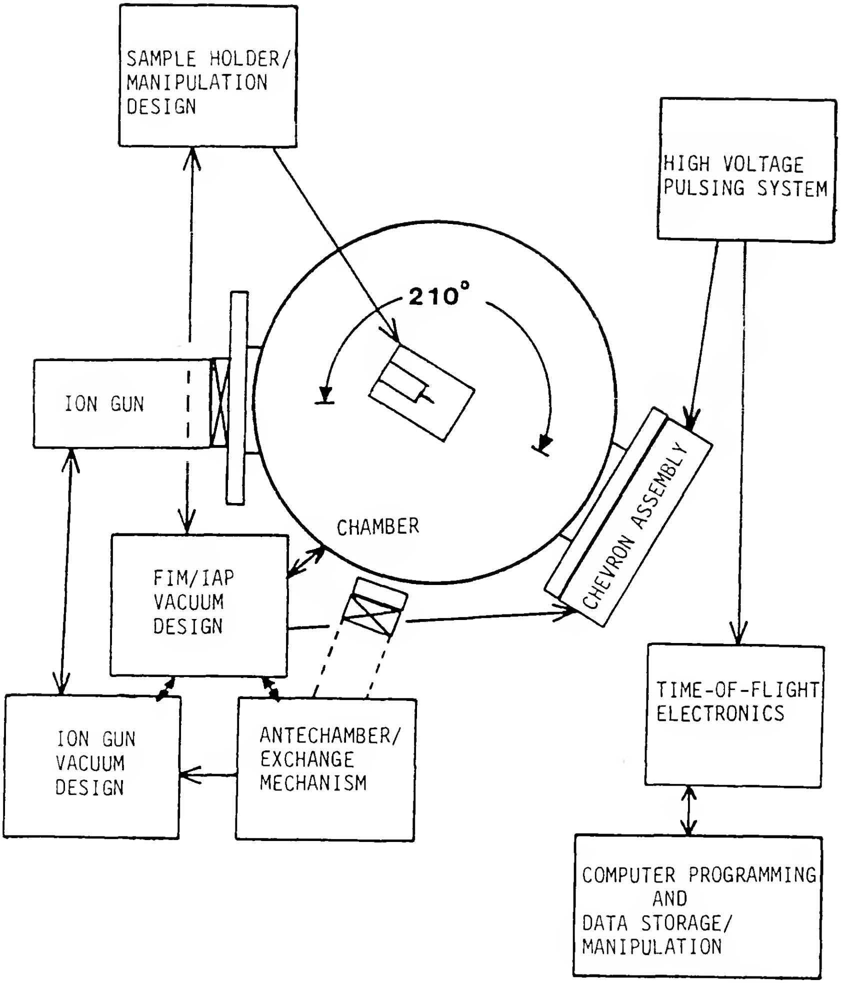

Figure II-1 Block representation of the major development stages of the FIM/IAP. The double-headed arrows indicate sections whose parts or design requirements must be compatible. The single-headed arrows indicate stages with sections having similar requirements as to those of the section of the arrow's origin.

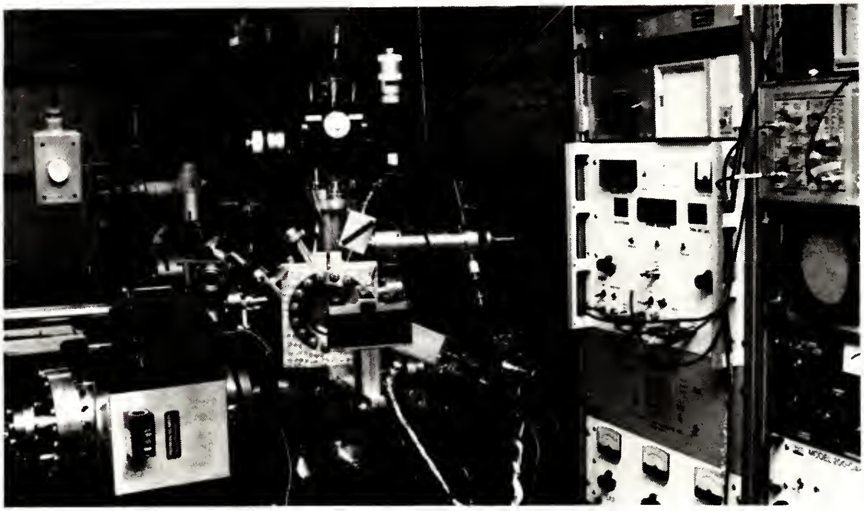

Figure II-2 View of the FIM/IAP shown from the IAP side. To the right is the associated electronics. The ion gun can be seen in the background.

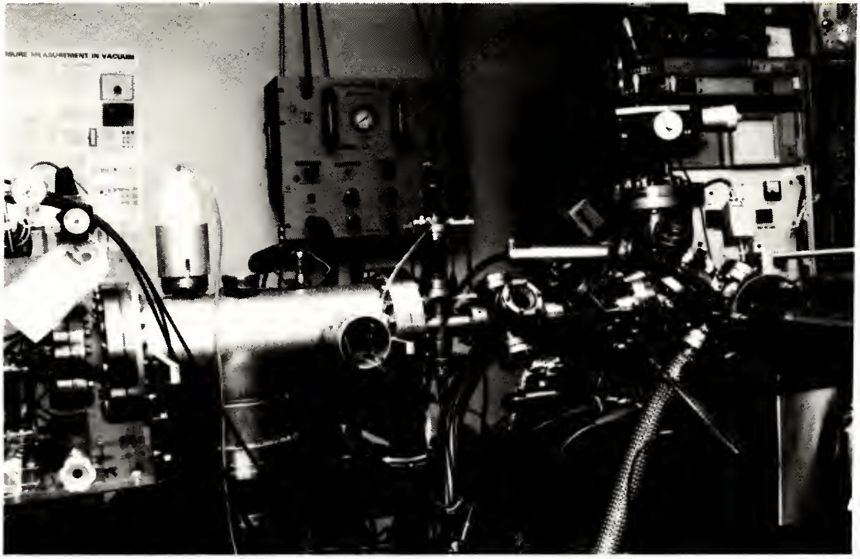

Figure II-3 Colutron ion gun coupled to the FIM/IAP.

then assembled, tested and made operational by the author. This port has also been used as a conventional FIM with a 7 cm tip-to-screen distance. Other uses for this port are anticipated, including an evaporation source and an electron gun for heating the sample.

Midway between the two ports described above is a mini-flange port (1.33 in. O.D.) used for the exchange of the specimen. Figure II-4 is a photograph of the exchange chamber. Huntington Mechanical Laboratories supplied the major hardware for the exchange system, including an MS-075 straight-through valve, a VF-169-10 magnetically-coupled linear/rotary drive, the special 6-way cross, and special 1.33 to 2.75 in., O.D. nipple. The minimum inner diameter is .625 in. which is that of the valve. A positioning device coupled to a bellows is used to align the insertion rod with the sample stage in the main chamber. A viton gasket is used for the blank flange used for the specimen exchange. A special clamp is used in lieu of bolts to seal this flange. A 170 l/s Balzers turbo-pump used on the ion gun is also shared with the exchange mechanism. An all-metal, bakeable valve separates the two volumes. An absorption pump first roughs the exchange valve to approximately 1×10^{-3} Torr. The valve is opened very slowly to the turbo-pump and an ultimate pressure of about 1×10^{-6} Torr is achieved in approximately 10 minutes.

The chamber is roughed by two absorption pumps used in series. A pressure of about 2×10^{-4} Torr can be achieved with these. A Perkin-Elmer 80 l/s ion pump is used as the primary pump to attain UHV pressures. This pump has special elements for higher pumping speeds for hydrogen. It is assisted by a Perkin-Elmer, liquid nitrogen cooled titanium sublimation pump. Additional pumping arises from the Air Products

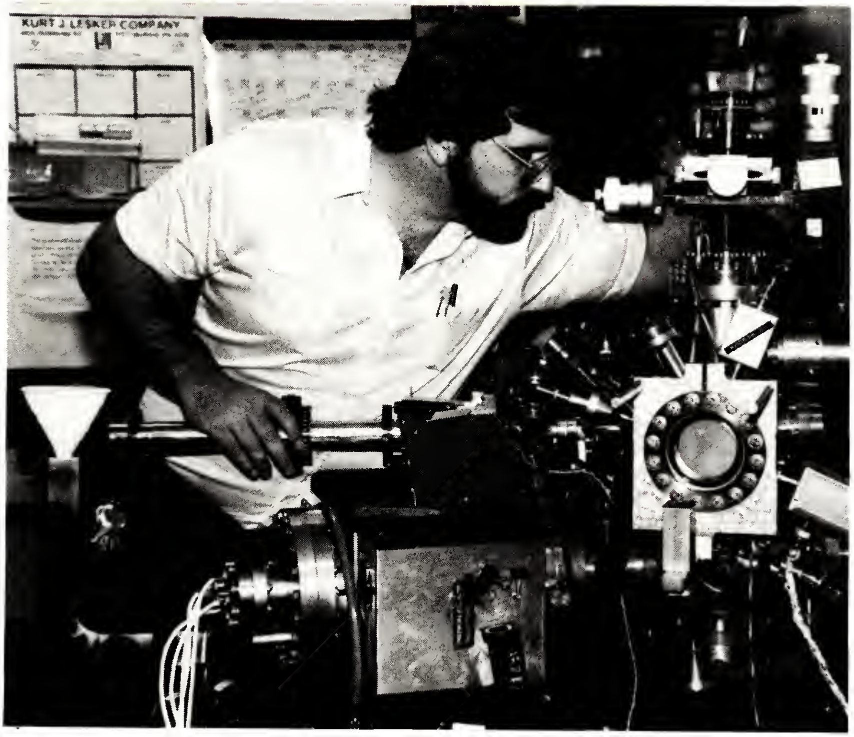

Figure II-4 Close-up photograph of the FIM/IAP showing the introduction of a sample into the chamber using the Huntington rotary-linear, magnetically coupled feedthrough.

Displex helium closed cycle refrigerator used for cooling the sample. A pressure of about $1x10^{-9}$ Torr can be achieved with the ion/Ti sublimation pump combination. The cryopumping usually brings the system pressure to about $5x10^{-10}$ Torr.

Although all the components in the vacuum chamber are bakeable to at least 300°C, this system has not been baked to achieve ultimate vacuum conditions. The system is, however, subjected to a procedure which does lower the pressure considerably. The conductance between the ion gun and FIM/IAP is approximately .01 l/s. Dry nitrogen from liquid nitrogen in a dewar flask is bled into the system through a leak valve. The valve between the ion gun and the main chamber is opened. The heater on the ion pump is turned on. By properly adjusting the leak valve, a pressure of about $1x10^{-1}$ Torr in the chamber and $9x10^{-4}$ Torr in the ion gun is achieved. These conditions lead to an intermediate flow regime for the nitrogen which helps drag difficult-to-pump gases such as He, Ne, and water vapor out of the main chamber. This is done for eight hours, after which the system is pumped down to $1x10^{-5}$ Torr by the turbo-pump, the valve closed, and the ion pumps started.

An imaging gas, either He or Ne, is admitted into the system by leak valves after the ion pump is turned off. The gas lines from the cylinders are carefully baked out when cylinders are changed. When He is admitted into the chamber, the pressure is monitored carefully until the desired pressure is achieved. The valve is immediately turned off. Helium is not pumped effectively by the cryopumping of the Displex refrigerator and the pressure is stable. The Ne is, however, pumped by this system and the valve must be opened very carefully to a set point to maintain a stable pressure. It was found that this set point is more easily achieved if the valve in the beam line to the ion gun is opened and a steady state condition is found. Furthermore, it was found that if the Ne leak valve is turned off, the turbo-pump will pump the main chamber to approximately $1\text{x}10^{-6}$ Torr. Closing the valve to the ion gun and turning the ion pump on achieves a lower ultimate pressure than if the ion pumps were used alone from the imaging pressure.

Sample Holder

There are extreme requirements imposed on the design of the FIM/IAP specimen stage. For a relatively simple holder with no manipulation, there are three major and somewhat conflicting requirements: i) the sample must be cooled to cryogenic temperatures, ii) a high voltage of up to 15 to 20 kV must be applied to the sample and iii) all materials must be UHV compatible, which includes being bakeable to at least 300°C. For good thermal conduction, OFHC copper is used. For poor thermal conduction, 304 stainless steel with a thin cross-sectional area is used. For electrical insulation with good thermal conduction, two materials can be used, either boron nitride or sapphire. Because sapphire is extremely difficult to machine, boron nitride was utilized for all holders designed for this instrument.

For metallurgical applications using the FIM/IAP, manipulation is also required further complicating the design. Two orthogonal tilt axes located at the specimen's apex allow the specimen to be examined thus, the disadvantages of the limited viewing area due to the increased tip-to-screen distance are overcome. This helps in crystallographic indexing of the sample and orienting a particular feature of interest for analysis. Linear motion in the X, Y, and Z directions is needed for alignment with the exchange rod and also with the ion gun. The two six-inch ports in the chamber, separated by 150°, add another complication in that both ports have the same degree of motion associated with them. A design requirement for this instrument was that the specimen should have a maximum of 30° in the extreme rotation position for each port, thus giving a total of a 210° rotation angle that the holder requires.

Figure II-5 shows a photograph of the specimen stage and manipulator. The stage consists of a cylindrical outer conductor of copper and stainless steel. The stainless part is attached to the manipulator so that the vertical rotation axis is in-line with the specimen. This connection also serves as the fulcrum for the up/down tilt supplied by a rod at the end of the cylinder. Copper braid (Beldon wire 5558) is silver-soldered to a collar on the copper portion of the outer cylinder. The other end of this braid is silver-soldered to a copper block (button) which is fastened to the end of the Displex refrigerator with a bolt. The silver-soldering of this braid proved to be the weak stage in this design. An improved braid/cold finger arrangement is described in Appendix A. There is an inner concentric copper rod into which a copper sample holder is screwed. This inner copper piece is held in place by two boron nitride insulators and tightening a copper nut on the threads of it. The boron nitride insulators are machined so that a high voltage breakdown path is not straight across the face of the insulator but is blocked by concentric ribs in them. When the system is cooled, the parts are contracted, making the fit even tighter. Since the heat path is from

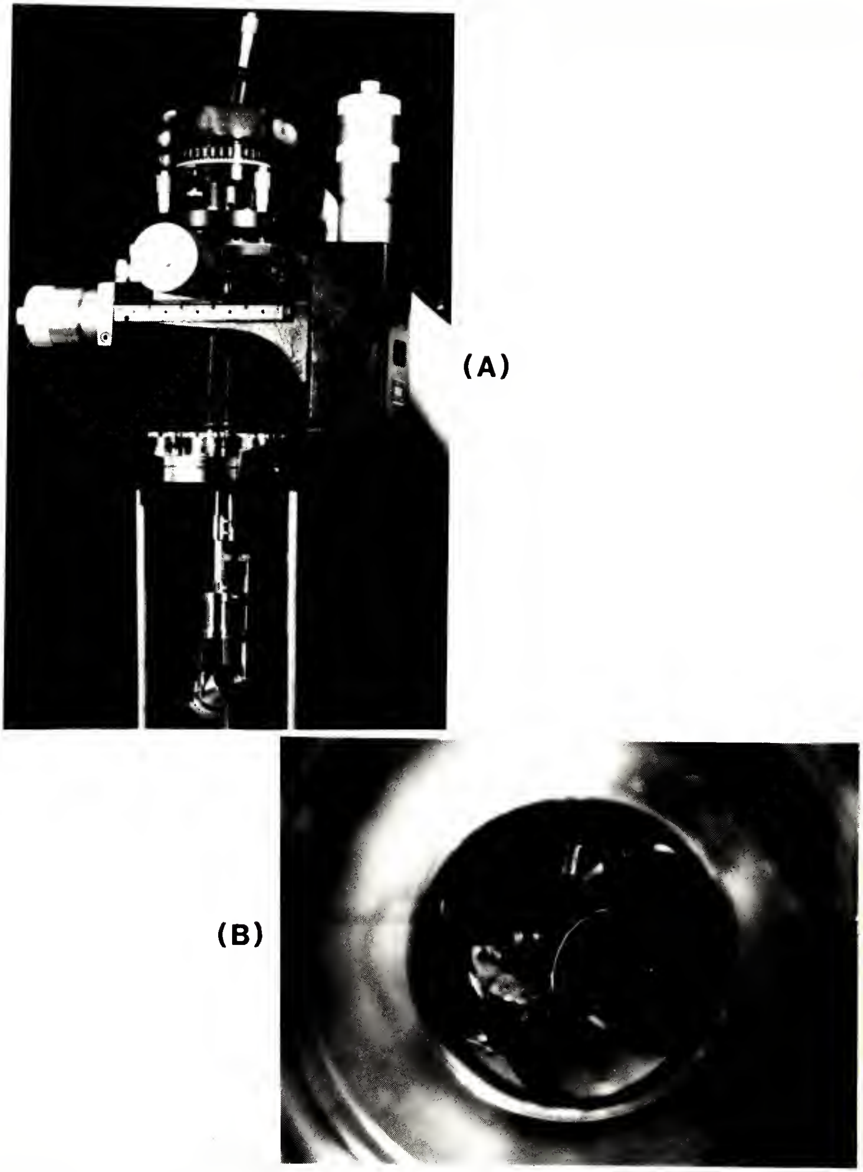

Figure II-5 Manipulator/Sample holder. a) is a photograph of the manipulator and sample holder outside of the FIM/IAP. Cooling braid is not attached. b) shows the holder in situ through one of the six-inch ports.

the sample, through the boron nitride, through the outer cylinder, through the braid, the outer cylinder will be colder than the specimen, providing some cryopumping directly around the tip. The stainless steel in the outer cylinder proved not to be the best design. An improved design (Appendix A) has an all copper outer cylinder. There is no radiation shield for this holder but one has been incorporated in the improved design.

The hardware attaching the manipulator to the cylinder provides the motion and the thermal insulation from room temperature. The vertical cylinder in Figure II-5 is 304 stainless steel. There is a .010 in. thick thin-walled section in this piece. This thin wall and the length of the prongs going down to the pivot points provides most of the poor thermal conduction. This section has been improved upon in the new design (Appendix A). The up/down tilt is provided by the coaxial-linear drive in the rotary feedthrough of the Huntington manipulator being coupled by a rod to the outer cylinder. The length of travel in this drive is approximately .5 in. At room temperature this provides about ±30° to the sample holder. At cryogenic temperatures, the increased stiffness of the copper braid resists the relaxation of a spring inside this manipulator and thus limits the upward motion of the specimen stage. A stiffer spring was tried but with little success.

The high voltage leads to the sample come down through this stainless steel cylinder. A thin-walled stainless steel tube is insulated with a glass tube and goes through a 210° crescent hole cut in the connecting flange between the large vertical cylinder and smaller diameter rod. A flexible, stainless steel, catheter guide connects this lead to a stainless steel pin screwed into the inner conductor for the sample stage. This electrical path is well insulated both electrically and thermally and is mechanically stable.

The following are the operating characteristics of this holder. The ultimate temperature is 65°K. The breakdown voltage of this stage is in excess of 20 kV. During operation breakdown first occurs in the external connection of the high voltage lines. A full 210° rotation is available which includes the 30° at the extreme positions. About +5° to -35° is available from second tilt axis. A new sample introduced through the sample exchange port is cooled within 30 min. Sufficient manipulation of the XYZ and tilt on the Huntington manipulator is present to center the sample in the beam of the ion gun. The alignment procedure for the ion gun with the sample holder is described in Appendix B.

A field-limiting aperture [69] is conspicuously absent from this specimen stage. Eaton and Gibson [72] have shown through finite-element calculations that the electric fields decrease rapidly away from the tip. In atom probes employing a field-limiting aperture, the mass-to-charge ration, m/n, is found by using the equation,

$$m/n = 1930\cdot(V_{dc} + \alpha\cdot V_p)t^2/D^2 \qquad \text{II-1}$$

where V_{dc} is the applied d.c. voltage in kV, V_p is the pulser charging voltage in kV, α is the fraction of this voltage which reaches the tip, D is the tip-to-screen distance in m, and t is the time-of-flight in microseconds [69]. Masses found with this equation and also by taking the ratios of the squares of a known and unknown mass agree quite well.

General Description Of The IAP

The physical appearance of an IAP is very similar to that of a simple FIM. The most obvious differences are the longer tip-to-screen distance and the increased number of cables and instrumentation attached to the electron multiplier channel plate/phosphor screen combination. The IAP's flight distance is usually between 10 and 45 cm. The channel plates, instead of a single plate, are incorporated into a chevron configuration, and have a maximum gain of approximately $1\text{x}10^7$ The IAP is a time-of-flight mass spectrometer with two operating modes. Ionization of the surface is initiated by high voltage pulses superimposed on the applied d.c. voltage to induce field evaporation. The detector of the system is the chevron assembly (including phosphor screen), which also serves as the imaging screen for the instrument in the FIM mode, but is operated at full gain. In the TOF mode, the instrument is essentially an atom probe with a very short flight distance and very large defining aperture. All atoms viewed in the FIM image will strike the detector in the IAP's TOF mode. The spectra obtained from the IAP are recorded with very fast storage scopes or transient waveform digitizers. The time-of-flight of the field evaporated ions are dependent on their specific mass-to-charge ratio, m/n, by equation II-1. The analysis of the TOF spectra is, therefore, straightforward. It should be noted that the mass resolution is extremely poor, approximately 20 to 50, because of the short flight distance.

The time-gated mode of the IAP is used to form an image using a selected mass in the TOF spectrum. The image formed is caused by the actual atoms from the tip striking the detector. These ions are selected by "switching on" the detector to coincide with the arrival time, and then the detector is "switched off" again. Only those ions arriving within this time window will result in an image. The gating on and off of the detector is accomplished by putting a high voltage pulse (formed in the same manner as the desorption pulse, except the high voltage switch employs a Krytron tube) onto the chevron assembly. The time window's duration is determined by the pulse width, which is determined by the charging cable length. In the instrument used in this study, the pulse width is 50 nsec. The selection of the particular mass is accomplished by delaying the triggering of this pulse to coincide with displayed TOF peak. Usually, several pulses are integrated into one micrograph by putting the camera in the "bulb" mode. The resulting micrographs, when compared with the FIM image, are capable of displaying with the same spatial resolution very sharp concentration gradients across interphase boundaries, and grain boundaries [73].

TOF Mode

The heart of the IAP is the Tektronix 7912AD transient waveform digitizer. It is extremely fast and has a digitizing rate of up to 100 GHz. The 7912AD is used primarily for collecting time-of-flight (TOF) data and setting up the proper conditions for the time-gated imaging mode. It also proved to be indispensable in determining cable and instrumental delays as well as system characteristics such as pulse shapes. The 7912AD can be operated in a limited way from the front panel, but is designed for operation via the General Purpose Interface Bus (GPIB or equivalently IEEE-488 interface). An important feature of the digitizer is that several waveforms can be added internally in a "signal average" mode. Three benefits are derived from this: i) the signal to noise ratio is improved, ii) collection of data can proceed at a much higher rate, and iii) the demand for computer storage of the waveforms is relaxed.

Figure II-6 is a block diagram of the electronics and computer system of the IAP in the TOF mode. All cables are terminated with 50 Ω impedances. There are two pulse pickoffs on the desorption pulse line. A Tektronix model CT-3 is the first in line on the desorption pulse line. It triggers the digitizer to sweep. The second pickoff is located just before the pulse line enters the vacuum system. The design of this pickoff was suggested by Miller*. It serves two purposes: i) it terminates the pulse with a 50 Ω impedance and ii) it picks off the pulse signal reduced by a factor of 21 to send to channel 1 of the digitizer. The coaxial cable leading from this pickoff to the digitizer is the same length as the one leading from the chevron plate detector to channel 2 on the digitizer. When the two channels are summed, the flight time is exactly that between the displayed pulse and the particular mass-to-charge species because all time delays due to cables have been considered. It should be noted that the time for conversion from the incident ion to the output in the chevron assembly is considered negligible [70].

Figure II-7 shows an analyzed spectrum from an Fe-Mo-N system previously studied by this author [74]. Several features of the spectrum should be discussed. The spectrum is the result of having the digitizer "signal-average" 16 waveforms. The lower left corner gives the d.c.

---

*Miller, M. K., private communication.

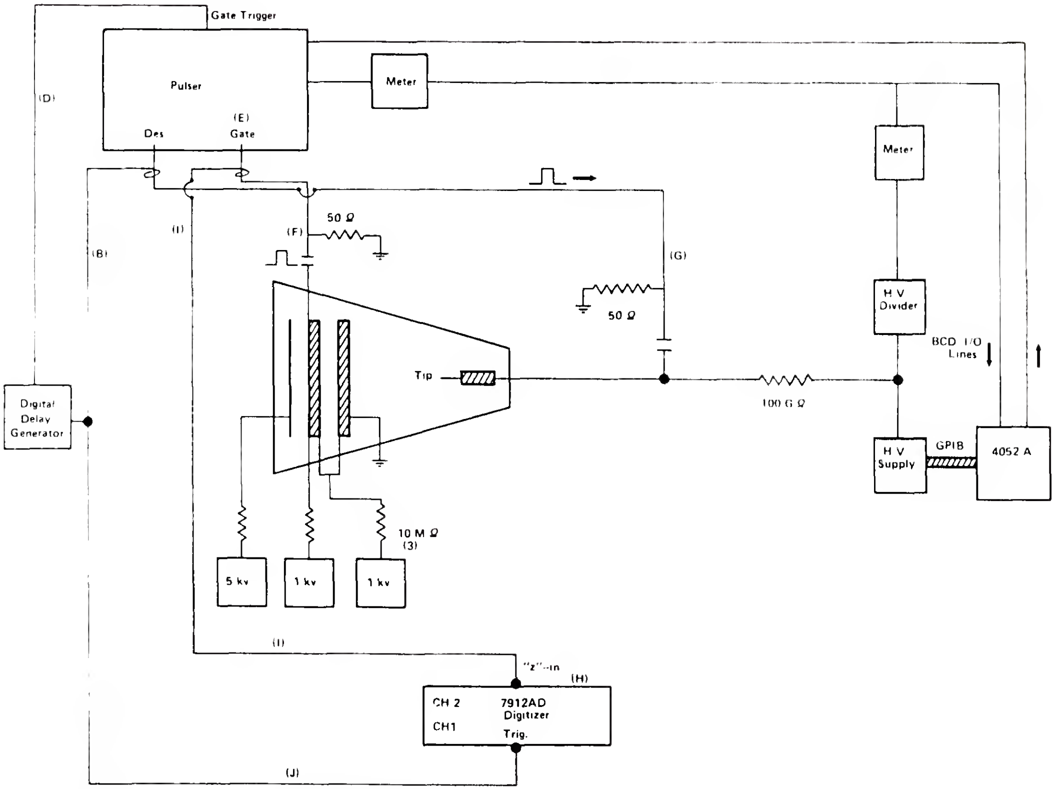

Figure II-6 Block diagram of the time-of-flight mode of operation of the FIM/IAP. See Appendix C for values of the delay times for the designated components.

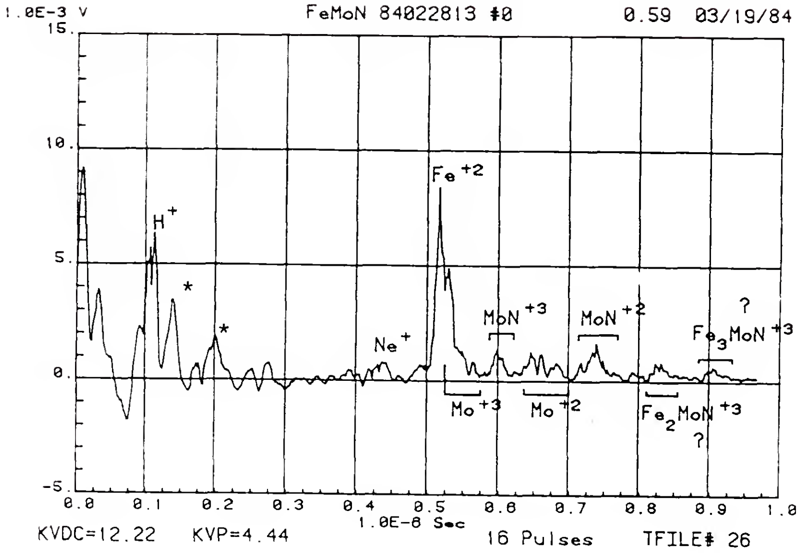

Figure II-7 Analyzed spectrum of an Fe-3at% Mo specimen which has been internally nitrided. The field evaporation voltage was 13.99 kV (12.22 d.c. + 0.4 x 4.44 pulse) at a temperature of 65°K.

voltage of 12.22 kV and the pulse charging voltage of 4.44 kV. With the pulse voltage being 40% of the charging voltage, the voltage for field evaporation was 13.99 kV. The time base of the digitizer was .1 sec/div, giving 1 sec full scale. The vertical amplifier was set at 5 mV/div, indicated by the step between solid vertical lines multiplied by the scale factor, $1\text{x}10^{-3}$ V. Note that the seven naturally occurring isotopes of Mo (A=92, 14.8% relative abundance; 94, 9.1%; 95, 15.9%; 96, 16.7%; 97, 9.5%; 98, 24.4%; and 100, 9.6%) are not resolved but their presence is reflected in the widths of the peaks. The two peaks indicated with the "*" are due to the combination of a ringing in the detector induced by the high voltage pulse and the truncation of the negative-going part of the ringing when the digitizer was used on the 5 mV scale. This condition has been remedied since this system has been studied and no longer interferes with the analysis of spectra.

Time-Gated Mode

The timing considerations for the time-gated mode of operation are rather more involved than the TOF mode. Figure II-8 is a block diagram of the IAP in the time-gated mode. In this mode all delays must be determined precisely. Once all the possible delays in the instrument are accounted for, the operation of the IAP in the time-gated mode is straightforward. To set it up in this mode, the cable from the CEMA output to channel 2 of the digitizer is disconnected and the voltage on the second plate is reduced to 1 kV. Since the voltage across this plate is zero, the gain of the chevron assembly is also zero. A Minolta XG-7 SLR 35 mm camera using Kodak 2475 Recording film is opened in the "Bulb" mode. The number of pulses for the integrated photograph is set on the

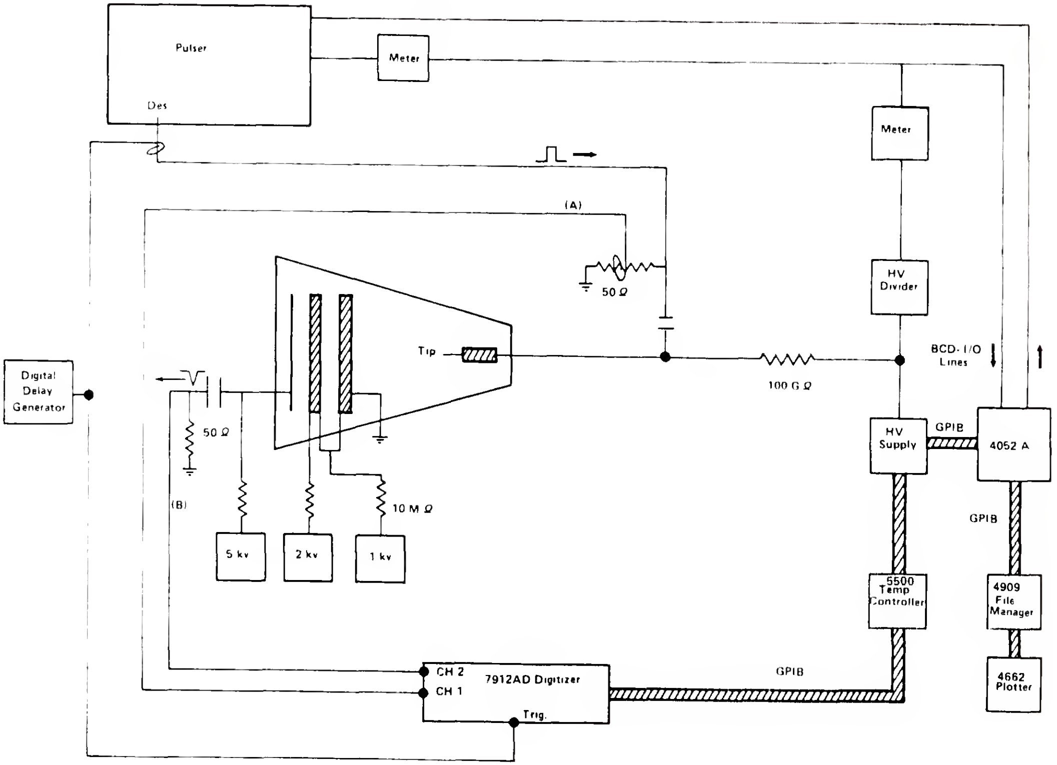

Figure II-8 Block diagram of the time-gated mode of operation of the FIM/IAP. See Appendix C for values of the delay times for the designated components.

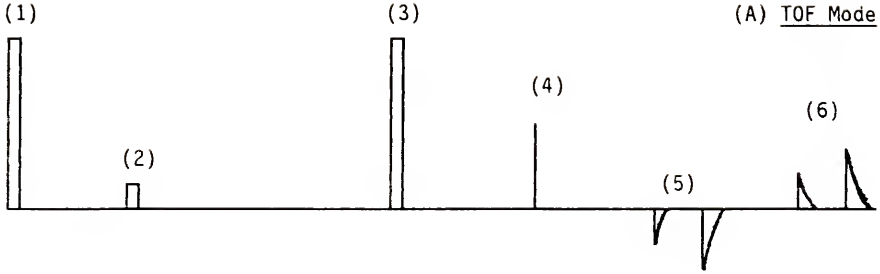

(1) Pulser fires. 1st pickoff pulse goes to trigger scope.
(2) 1st pickoff triggers scope. (delayed sweep with second time base)
(3) HV Pulse arrives at tip. 2nd pickoff pulse sent to channel 1 of scope.
(4) 2nd pickoff pulse displayed on scope.
(5) Ionic mass species strike detector.
(6) Mass signals inverted and displayed on scope.

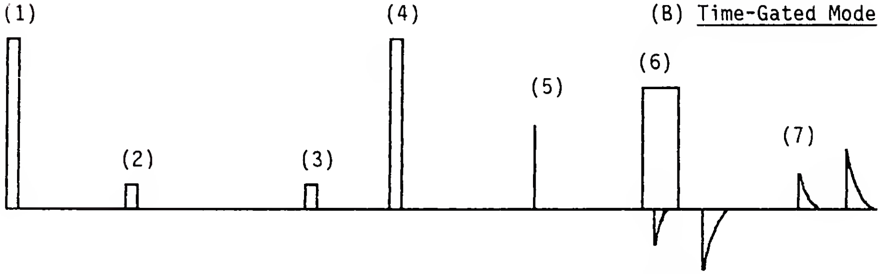

(1) Pulser fires. 1st pickoff goes to delay generator and to trigger scope.
(2) Pickoff pulse triggers delay generator and scope.
(3) Delay generator sends delayed pulse to gate pulser.
(4) HV pulse arrives at tip. 2nd pickoff pulse sent to scope.
(5) 2nd pickoff pulse displayed on scope.
(6) Gate HV pulse arrives at channel plates coinciding with the arrival of mass species. A gate pickoff was sent to "Z-in" on scope when gate pulser fired and is not shown for clarity.
(7) Trace on scope is intensified, outlining the portion of spectrum in which plates are active.

Figure II-9 Synchronization diagrams of the IAP in a) TOF mode and b) in time-gated mode. The larger pulses correspond to high voltage pulses, small pulses to 5v logic pulses, and exponentially decaying pulses to real and displayed signals.

control panel of the desorption pulser. The sequence of events for gating the channel plate is initiated by each desorption pulse. Figure II-9 shows the timing sequence and the instrumental and intentional compensating delays which occur in the IAP. Comparison of this sequence with Figure II-8 and the description which follows will help the reader follow what occurs during the operation in the time-gated mode. When the mercury-wetted reed switch of the desorption pulser fires, the pulse is sensed by a signal pick-off immediately. The high voltage pulse is intentionally delayed by a 53.2 m cable (Figure II-8, label G) to compensate for instrumental delays.

The pick-off pulse goes to the Berkeley Nucleonics Corp. Model 7050 digital delay generator through cable (B). The delay generator (C) supplies two pulses, an initial pulse and a delayed pulse. The initial pulse output triggers the digitizer trace through cable (J). The delayed pulse triggers the gate pulser through cable (D). The gate pulse is sent through cable (F) to the second channel plate in the chevron assembly. The channel plate is turned on for 50 nsec, the duration of the pulse. This cable is carefully terminated into 50 Ω. The delay generator is set to the time-of-flight of the desired mass specie. A cable (I) from the gate pick-off to the "Z"-intensification on the digitizer enables the mass to be visually selected. The delay generator is changed until the intensified portion of the trace overlaps the mass peak's position. The shutter of the camera is closed when the pulser stops.

Computer And IEEE-488 Instrumentation

The computer coupled to the IAP is a Tektronix model 4052A desktop computer. It uses an extended form of the BASIC programming language, especially designed for graphics and instrumentation control over the IEEE-488 interface bus. This is called the General Purpose Interface Bus (GPIB) by Tektronix. There are four instruments on the GPIB: i) Tektronix 7912AD transient waveform digitizer, ii) Scientific Instruments 5500 temperature indicator/controller, iii) Bertan 205A-30R D.C. high voltage supply, and iv) Tektronix 4662 Interactive digital plotter. The 7912AD and the SI 5500 are both microprocessor controlled and can operate independently of the 4052A, thus freeing the computer for other operations.

A Tektronix 4909 File Manager system is also on the GPIB. The 4909 is a hard disk storage drive with a total of 96 Mbytes of memory. Although it is on the GPIB, the interface is transparent to the user because it has no address and is controlled through a ROM pack inserted into the 4052A. The 4909 has been proven to be indispensable when the large number of waveforms in a depth profile are collected. During profiling, each waveform is stored while the digitizer is collecting the next waveform. This procedure minimizes the dead time between the collection of waveforms. Minimal data reduction is done to further increase this efficiency. Additional storage is provided by magnetic tape cartridges for the 4052A and an internal 256 Kbytes extended file manager. With the extended file manager is also a serial communications interface. There are four ROM slot positions. The third position must contain the 4052R10 advanced file manager ROM pack for the 4909. Two ROM packs are required for the operation of the IAP. The first is a TransEra 732-BCD I/O ROM pack. It has 40 lines, 32 of which are configured by software to be either input or output for binary coded decimal (BCD) information. Four digits each from the meters of the high voltage supply and the pulser's charging supply are read by the computer over these lines. Each of these meters has 4-1/2 digits. Since each meter has only 16 lines, the least significant digit is disregarded. This ROM pack has four control lines and four status lines, the latter not being utilized. Two control lines are used to start and stop the pulse control unit.

The second ROM pack required by the IAP control software is the Tektronix 4052R07. This ROM pack facilitates the handling of dimensioned arrays. Waveforms from the 7912AD are 512 point arrays. The ROM pack programs include MIN, MAX, CROSS, INT, DIF2, DIF3, and DISP. The MIN, MAX, and CROSS commands find the indices of the minimum, maximum, and where the waveform crosses a particular value. The INT command performs a numerical integration of the array while the DIF2 and DIF3 commands perform a two or three point numerical differentiation. The DISP displays the complete waveform on the 4052A's screen very fast.

7912AD

The Tektronix 7912AD is the fastest digitizer which exists. It can capture a single trace within a 5 nsec window into a 512 point array with full 9-bit resolution. It utilizes Tektronix 7000 series plug-in modules. The plug-in modules used in the IAP are the 7A24 dual time base and the 7B28 dual channel amplifier. The dual time base was chosen because a portion of the waveform can be expanded. The dual channel amplifier allows the pulse pickoff to be displayed in addition to the output from the chevron assembly. The 7912AD can be operated in a limited fashion from the front panel. In the non-storage or TV mode, the waveform is displayed on a monitor in real time. The monitor is used to set the beam intensity and to set the proper operating conditions such as time base and amplifier settings. When the digitizer is used from the front panel in the digitize mode, a dual parallel trace is displayed on a Tektronix 2213 oscilloscope. It is important to understand how the digitizer works and why the dual trace occurs because of the importance of setting the beam intensity properly. There are two electron beams in the digitizer, a "writing" and "reading" which face each other. The "reading" beam charges a solid state array chip and is scanned vertically from left to right. The "writing" beam discharges part of the array. When the slower reading beam scans these areas again, a current is sensed indicating the results of the writing beam. The two traces displayed are two arrays where the reading beam senses the change of state from written to non-written, i.e. the top and bottom of the trace. A command which is sent from the computer to the 7912AD is the "ATC" for average-to-center. This command causes the 7912AD to find the center value between the two arrays and fill in any missing points, and then store this new array in the digitizer's memory. It also displays it on the oscilloscope as a single trace. If the main intensity is too high, i.e. the trace is too thick, after the "ATC" command, the displayed peak will be smaller than it actually is. This means that in setting up the digitizer care must be taken in adjusting the intensity to make sure the digitized signal is the same as the monitored height. The pulse pickoff signal is used for this.

Another feature which the 7912AD has is the ability to average several traces together, thus increasing the signal to noise ratio. The signal averages 2,4,8,16,32 or 64 traces by adding each waveform to what is memory. Because each waveform has 9-bit resolution and each value is sent to the computer as a 2-byte word, no precision is lost in this averaging mode. This mode is important because both time and memory storage are saved by compressing the signal-averaged traces into one waveform. Care must be exercised in choosing the number of pulses per waveform because of the possibility of washing out the signal from a minor constituent in the sample.

Scientific Instruments 5500

The 5500 is a microprocessor-based, low temperature, indicator/controller. It is configured to use a chromel-gold w/.07% Fe thermocouple. The maximum heater output is 90 watts. All calibration and control can be done equivalently either from the front panel or over the computer interface. It has three modes: i) Stop, ii) Manual, and iii) Run. In the Stop mode, the heater power is shut off and the system will go to the lowest possible temperature. In the Manual mode the controller will try to maintain the set point temperature. In the Run mode, up to a 30-point temperature profile program stored in the 5500's memory is run. In all three modes, an actual temperature profile can be graphed on the screen and also output to the Tektronix plotter.

The 5500 was used with the specimen holder used in this study to determine the cool-down time and ultimate temperature. A heater was not used. The time required to reach this temperature of 65°K is approximately two hours. The thermocouple in this holder broke after a short time and was not repaired because of the need to disassemble the manipulator system. The new holder described in Appendix A has an improved cryogenic design and a heater is installed.

A program listed in Appendix D was written to input a program into the 5500, graph the temperature profile data, and change the set point temperature in the manual mode. The program name is "PROFILER" and it is stored in the public directory of the 4909 file manager.

Bertan 205A-30R

The Bertan 205A-30R is a 0-30 kV d.c. power supply. It can be controlled by the computer when used with the Bertan model 200-C488 interface controller. The controller accepts commands over the bus and converts them to a 0 to 5 volt output which is fed into the remote programming input for the 205A-30R. When the local/remote switch in the rear of the 205A-30R is put in remote, control is done over the interface. In the local mode, the output is the sum of the panel switch settings. Since the front panel settings on this supply are discrete and not continuous, a program was written to control the voltage with the user-definable keys of the computer. This program is also listed in Appendix D. The program is "FIMSUPPLY" in the public directory of the 4909. Because the supply is controlled by the computer, the IAP data-handling program had to be modified to include the voltage controls with the user-definable keys.

IAP Data Collecting And Handling Programs

The programs described in this section which collect and reduce the waveforms from the IAP are based on the Tektronix demo programs which were supplied with the 4052A and 7912AD. The programs evolved from having the waveform acquisition, storage on magnetic tape, and data manipulation done with single keystrokes of the user-definable keys to automatic data acquisition and storage on the 4909 file manager. The basic program used is "IAPINDEX_4909." This program stores waveforms on indexed files in the 4909. New indexed files can be created at any time. Single waveforms can be collected with one keystroke. Waveforms collected can be chosen to be automatically stored in the next available index within the file being used. The m/n ratios of peaks are calculated in two ways: 1) by taking the ratio of the squares of the flight times of an unknown and a known mass multiplied by the known mass; 2) by straight TOF calculation using the equation II-1, previously defined. The values obtained for the selected flight times are compared in table format. The best results are obtained when the largest mass-to-charge ratio known is used as the reference.

The "IAPINDEX_4909" program is written in independent sections, each section being a subroutine which can be addressed either from the user-definable keys or from within a controlling program. Two programs which utilize a control program using these subroutines are "IAPRING" and "PEAKPICKOFF." All control sections start at statement 60000. The "IAPRING" program collects and stores waveforms continuously. The "PEAKPICKOFF" program retrieves each waveform which was stored and finds the Ni signal peak height. "IAPINDEX_4909" is listed in Appendix D. The two controlling sections are also listed. The modified "IAPRING" program having the high voltage supply control sections is listed. Its name is "IAPRING.HV." In this program, all sections of "IAPRING" not required for data acquisition were removed and sections of "FIMSUPPLY" needed for controlling the high voltage supply were added. In addition all sections which are used most frequently are controlled by user-definable keys 1-10; the others required the shift key for 11-20. Table II-1 gives the

Table II-1
User-Defined Key Functions

User-defined key #		IAPINDEX_4909 & IAPRING	IAPRING.HV	FIMSUPPLY
Lower	1	Acq. waveform	(same)	Read V,I
	2	Move cursor left	Increase V by vinc	(same)
	3	Move cursor right	Reset power supply	not used
	4	Light cursor	Increase V 100v	(same)
	5	Read wfm. from file	(same)	Reset supply
	6	Graph wfm. @ plotter	Shutdown supply	Incr. inc 10%
	7	Calc. masses (eqn.)	Decrease V by vinc	(same)
	8	Graph @ screen	(same)	not used
	9	Calc. masses (ratio)	Decrease V 100v	(same)
	10	Mark TOF times	(same)	Shutdown
Upper	11	Change current file	(same)	Poll devices
	12	Set left marker	Move cursor left	not used
	13	Set right marker	Move cursor right	Limit current
	14	Marker's time dif.	Set V to 0v	not used
	15	Record wfm. on file	(same)	Set V to 0v
	16	Auto-store on/off	Volt. ramp on/off	Decr. inc 10%
	17	Graph@ plot. w/markers	Incr. vinc by 10%	not used
	18	Ground (DC offset)	(same)	Limit voltage
	19	Graph@ scrn. w/markers	Calc. masses(ratio)	not used
	20	Reset flight-times	(same)	not used

Note: Some of these functions can be used when the control sections (the portions of the IAP-series programs starting at statement number 60000), are running and looping. The result of pressing the key will not occur until an appropriate point in the program. These points are normally when the program is going from one subroutine to another. Non-critical subroutines can be interrupted, but the program returns to the point where it was interrupted and continues from there.

user-definable keys and their functions for the programs "IAPINDEX_4909", "IAPRING," "FIMSUPPLY," and "IAPRING.HV."

Ion Gun

The ion gun employed in this study is a model G-2-D system from Colutron Research Corp. This kit comes complete, assembled in a vacuum housing. It must be configured by the customer with ancillary equipment such as vacuum pumping system, power supplies and associated insulation housing, and cooling system for source and electromagnet. This gun was chosen for this study for several reasons, the most important being vacuum considerations. The *in situ* implantation of deuterium to overcome oxidation and cryogenic transfer problems presents a major difficulty with Field-Ion techniques, enhanced field adsorption of hydrogen. That is, during implantation with deuterium, the deuterium partial pressure in the FIM/IAP chamber must be kept sufficiently low in order that during subsequent IAP analysis field adsorbed deuterium does not interfere with the implanted deuterium signal. The ion gun system was designed in order to keep the FIM/IAP chamber pressure below 5×10^{-9} Torr during implantation. Figure II-10 shows the ion gun that is coupled to the FIM/IAP with associated hardware and electronics. With the experimentally determined operating parameters of this gun, the pressure in the chamber is approximately an order of magnitude better than the design limit.

The gun operates with a throughput of approximately 10^{-4} Torr-l/sec. With the Balzers TSU 170 l/sec turbopump, the pressure during operation is $5\text{-}8 \times 10^{-6}$ Torr in the gun and $4\text{-}6 \times 10^{-2}$ microns in the source. These values are typical with the gaseous charges used in the source. Although the gun is capable of using solid charges, for this study it has only

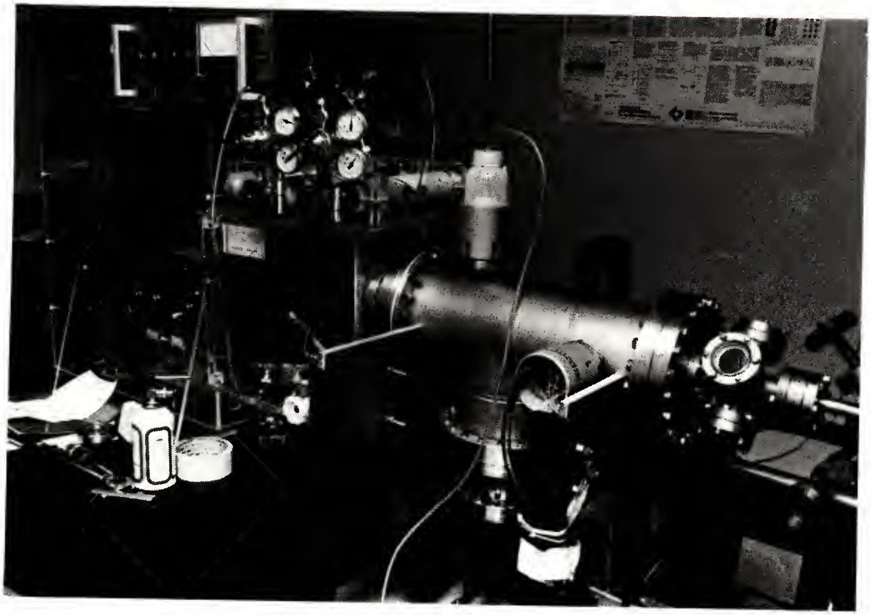

Figure II-10 Overall view of the Colutron ion gun and associated hardware, power supplies, and vacuum equipment. The anode and filament supplies, thermocouple gauge, and ion source float at high potential and must be isolated from ground. Cooling of the ion source and the velocity filter is accomplished with a 1/2 h.p. refrigeration system. Only the refrigerant lines can be seen in the photograph.

been configured for gases. The pressure loads for solid charges will be considerably higher and the beam currents will also be less. Additional differential pumping is done by a 20 l/sec Perkin-Elmer DI ion pump and titanium sublimation pump connected to the beam line with a flexible metal hose. Conduction limiting is also done with a 2 mm hole in a double-sided blank flange mounted before the straight-through valve which connects to the FIM/IAP chamber. Although the gun is capable of being baked-out, this is not done due to the difficulty involved with removing the freon cooling lines to the magnet and ion source.

Another important parameter of this gun which needed to be considered was current density. A reasonably short time is required for the implantation, again, because of the above arguments. For gaseous charges this gun produces ion currents up to about 10 uA. With the einzel lens in the system, current densities of 1-10 mA/cm^2 are easily achieved. The ion gun also incorporates vertical deflection plates and a velocity filter. The velocity filter is an $\underline{E}$x$\underline{B}$ type, or Wien filter, with a horizontal deflection plane. Normal operation for aligning and selecting an ion of a particular mass-to-charge ratio is done by changing the voltage on vertical deflection plates and varying the power to the magnet. The voltage on the horizontal plates are set at maximum supply output for maximum dispersion. The Colutron filter [75] differs from a simple $\underline{E}$x$\underline{B}$ velocity filter in that the electric field is shaped by electrically biased guard rings about the horizontal deflection plates. The reason they are needed is that the Wien filter is a strongly focussing lens and produces a line image with a very short focal length. This is due to the fringe field shapes of the finite sizes of the magnet

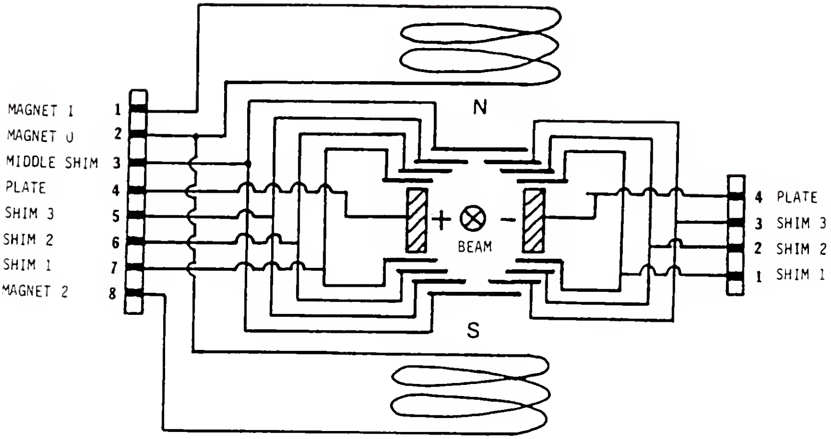

Figure II-11 Schematic diagram of Colutron velocity filter. A desired beam shape is obtained by carefully balancing the voltages on the shims. The guard ring control unit supplied with the filter is a set of parallel voltage dividers, each delivering a fraction of the deflection plate voltage to its respective ring.

and deflection plates. By carefully balancing the potentials on the various guard rings, the filter can operate in a non-focussing mode in which a circular beam is produced, or in a line mode with a very narrow line image. The resolution, M/ΔM, of this filter is approximately 400. Figure II-11 is a schematic of the velocity filter.

The use of this velocity filter provides several benefits to this study. Ions with different mass-to-charge ratios can be separated very easily. This allows less pure charges or mixtures to be used. In fact for the gases hydrogen, deuterium, and helium a mixture of 2% argon stabilizes the plasma and reduces the pressure in the source considerably. The filter separates the same species with different masses and charge states. For example, hydrogen can be ionized into H_1^+, H_2^+, and H_3^+ and argon can be ionized in two states, Ar^+ and Ar^{+2}. The choice of ion complex, of course, will affect the relative implantation depths. For example, the depth for H_2^+ would correspond to that of H_1^+ at half the energy.

The ion gun was mounted to the FIM/IAP in such a way that it can be decoupled and used independently. A special holder for FIM specimen is made from a MDC electrical feedthrough mounted on a Conflat flange. This holder, shown in Figure II-12, monitors the current density during implantation. The grounded shield has a .062" diameter hole in it so that the current measured multiplied by 50 (the reciprocal of the cross-sectional area in cm^2) is equal to the current density. When the gun is coupled to the FIM/IAP, the current is measured by disconnecting the high voltage lead and connecting it to an electrometer. It should be noted that the current measured at this point is not the actual ion

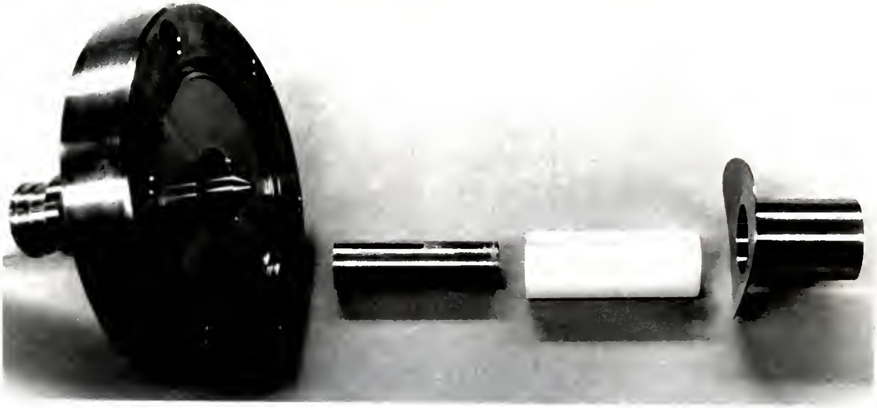

Figure II-12 Faraday Cup/Sample Holder. This holder is used on the ion gun when it is not coupled to the FIM/IAP. If the beam is larger than the grounded outer shield aperture (piece to right), the beam current density (A/cm^2) is obtained by multiplying the current by 100.

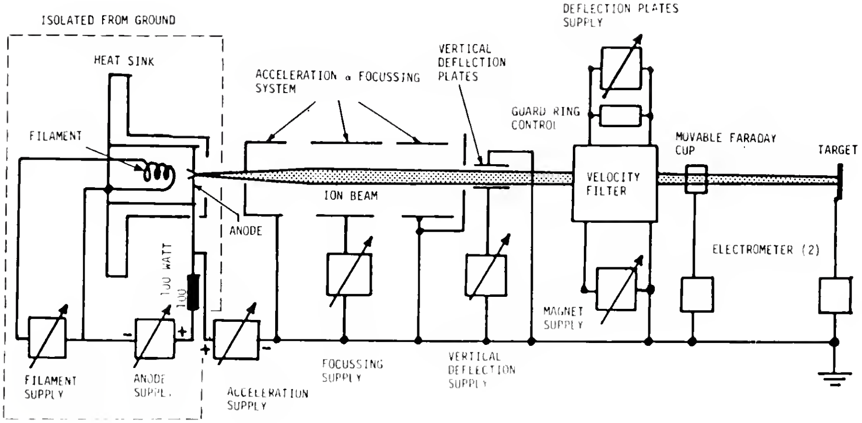

Figure II-13 Schematic diagram of the Colutron ion gun, beam line, and target.

current, but also includes secondary electron and ion currents. Both arrangements, ex situ and in situ, of the FIM/IAP can accommodate both FIM and TEM samples. SEM samples can also be used but there is a restriction on their physical size because of specimen transfer mechanisms.

The beam line has a transmission phosphor screen with a hole and a mirror for viewing, selecting and aligning the beam to be used. There is a Faraday cup which swings into the beam and can monitor the current and current density. The hole diameter of the tantalum grounding front shield is .140" such that if the beam is centered and larger than this, the current at the cup is multiplied by a factor of 10 to give the current density. This cup is used to optimize the beam conditions. The ion source pressure and anode voltage is adjusted for maximum beam current.

Figure II-13 shows a schematic diagram of the ion gun, beam line, and target. The filament and anode power supplies are Lambda model LK-351 and two LQ-524 (connected in series). These supplies together with the thermocouple gauge controller for the source are isolated from ground by a Colutron isolation transformer. This transformer is rated for 10 kV at 1 kVA. Field testing of this transformer has shown it to be capable of operation up to 22 kV. This value is the break-down voltage between the ion source flange and the ion gun body. Two Brandenburg 30kV power supplies provide the acceleration and einzel focussing voltage. A Colutron power supply contains three separate variable, regulated voltage supplies: a -100 to +100 V supply for the vertical deflection plates, a 0 to 300 V supply for horizontal plates, and a 30V-30A magnet supply.

For low Z ions with energies greater than 9 keV, an additional 45 V is required for the vertical plate voltage. A box containing five 9-volt transistor batteries in series is inserted in series with the above supply. The currents at the target and cup are measured by Keithley model 600B electrometers.

Mass Identification in the Colutron Ion Gun

A major advantage of the Colutron ion gun with the velocity filter is that gas mixtures may be present in the gun whether deliberately mixed for better performance or as the result of changing gases without prolonged purging of the lines. In selecting a beam with a particular mass to charge ratio by using the velocity filter, there sometimes is confusion as to the identity of the various beams. The low end masses are readily sorted out at a given energy by comparing the beams of the helium/argon and deuterium/argon mixtures. The He^+ and D_2^+ signals have the same mass to charge ratio and therefore the same magnet setting. Both gas mixtures have the Ar^+ and Ar^{+2} signals when hydrogen and deuterium are present in the ion source, four beams are present having $m/n = 1,2,3$ and 4 (H^+, H_2^+ or D^+, H_3^+ or HD^+, and D_2^+). In addition, the Ar^+ peak is always present when the gas mixtures are used, and the Ar^+ peak is usually the largest mass present, having the highest magnet setting.

The masses are tuned with the velocity filter by changing the magnetic field. The following expression holds true for determining the masses in the velocity filter,

$$B_2/B_1 = (m_2/m_1)^{1/2} \qquad \text{II-2}$$

where B_i is the magnetic field to balance the filter for mass, m_i. The magnetic field is proportional to the magnet current which in turn is proportional to the dial setting on the Colutron magnet power supply. Because of hysteresis effects, there is a constant offset current which needs to be added to the measured current. This setting which is the sum of the value read and the offset value is referred to as the true setting, S. Thus the following can be used in place of equation II-2,

$$S_2/S_1 = (m_2/m_1)^{1/2} \qquad \text{II-3}$$

It should be noted that the difference between two true settings and the measured settings is the same. Therefore rearranging equation II-3,

$$S_2/S_1 - S_1/S_1 = (m_2/m_1)^{1/2} - 1 \qquad \text{II-4}$$

or

$$\Delta S/S_1 = (m_2/m_1)^{1/2} - 1 \qquad \text{II-5}$$

By knowing two or more masses in the beam, a reference true setting for one of the masses can be found,

$$S_1 = \Delta S/(m_2/m_1)^{1/2}-1 \qquad \text{II-6}$$

The true setting for mass, m_1, can be found with two masses, or an averaged S_1 could also be found using other known masses. If m_1 is chosen as H_1^+ ($m_1 = 1$), then equation II-6 reduces to

$$S_H = R_{m2}-R_H/(m_2)^{1/2}-1, \qquad \text{II-7}$$

where R_{m2} and R_H are the measured settings of m_2 and H^+, respectively.

Once S_H is found, unknown masses are easily identified by rearranging equation II-7 and solving for m_x, leading to

$$m_x = [R_{mx}-R_H/S_H + 1]^2, \qquad \text{II-8}$$

where m_x refers to the unknown mass at the measured setting R_{mx}.

The program, "COLUMASS", is available on the Tektronix 4052A which will find both S_H for a given energy and an unknown mass for a particular setting. If more than two masses are known an averaged S_H value is found. Table II-2 gives the values of S_H at several energies and the differences between the mass setting values for the indicated ions and the setting for H^+.

Transmission Electron Microscopy

Three different holders have been designed and used for TEM imaging of field emitters in this study. The use of the TEM is indispensable for obtaining the geometric parameters required for the depth profiling programs which will be described in the next chapter. It also provides an independent means of checking the total depth which has been field evaporated during a profiling experiment. In addition, the TEM is unsurpassed in obtaining crystallographic information about defects on a fine scale with the use of diffraction contrast. In the following sections, each of the three different holders will be presented and their uses with respect to FIM studies will be discussed.

Table II-2
Hydrogen and Relative Magnet Settings for
Several Ions and Energies

			Difference Between Ion And H^+ Setting				
Energy (keV)	S_H	$S_H - H^+$	H_2^+, D^+	$(HD)^+$, H_3^+	D_2^+, He^+	N_2^+	Ar^+
5	50.1	24.1	22	36	48	---	198
6	45.6	22.5	19	35	43	---	184
7	44.1	25.1	18	35	41	---	176
8	39.4	24.9	14.5	30.5	41.5	---	159
9	30.0	26.0	13	22	30	126	156
10	31.3	18.3	12.6	22	32.5	---	133

FIM/IAP "Bulk" Holder

Figure II-14 shows a simple holder for use with the JEOL-SCSH bulk holder. This holder provides a single tilt axis about the specimen's

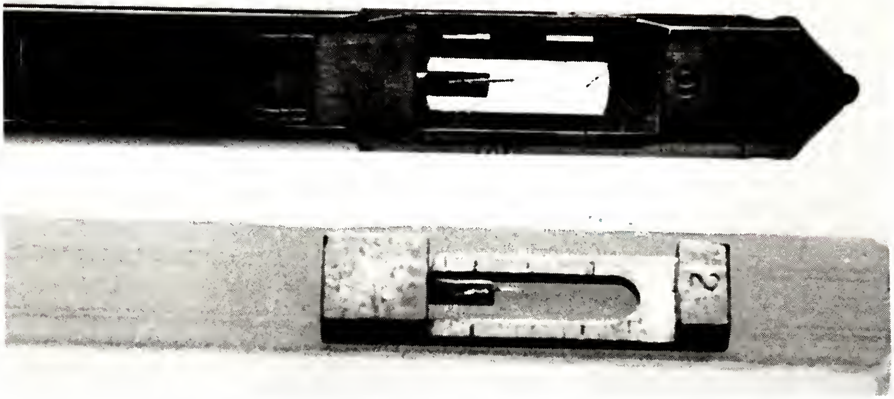

Figure II-14 FIM/TEM "BULK" specimen holder. This holder has only a single axis of rotation. Shown also is the sample insert which actually holds the specimen.

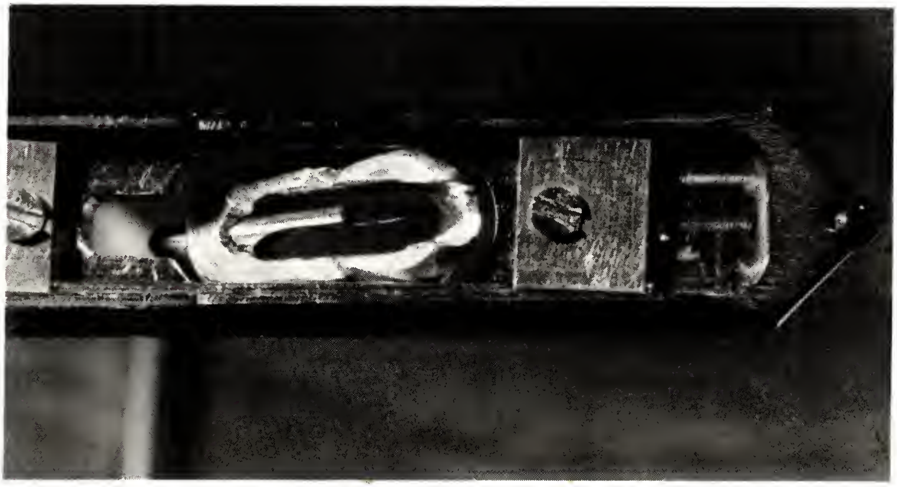

Figure II-15 FIM/TEM "Double-tilt" specimen holder. This holder has two orthogonal tilt axes and is required when specific crystallographic information is needed.

axis. This holder is useful when routine observation is desired, such as checking specimen quality after preparation or after implantation. When several of these holders are available, specimen throughput in terms of the cycle time required to obtain a two-beam imaging condition, record a micrograph, and insert a new sample is on the order of 15 to 20 minutes. A two-beam imaging condition is important when imaging FIM specimens because the penetration of the electrons is deeper due to dynamical conditions. The value of this holder is limited when crystallographic information is required. This is due to having only a single-tilt axis available. Because most FIM specimens are prepared from drawn wire, they have a preferred orientation along this axis. The orientation is a usually a low-index pole parallel to this axis. For example, nickel (FCC) has a (111) orientation, platinum (FCC) has a (001), and tungsten (BCC) has a (011). The attainment of a two-beam condition is relatively easy to achieve because of this, but the choice of the imaging condition is determined purely by chance. Studies such as the determination of defects are impossible with this type of holder because of the lack of a second, orthogonal, tilt axis.

FIM/TEM "Double-Tilt" Holder

The above problems with defect identification using diffraction contrast have been remedied by the construction of another TEM/FIM holder which incorporates the second tilt axis [76]. Figure II-15 shows this specimen holder. It is a modified standard JEOL-BST double-tilt holder. Both the original cups were removed and some machining of the rod was done to accommodate a single-elongated holder for FIM samples. The double-tilt is achieved by two rods applying friction to the cup as they

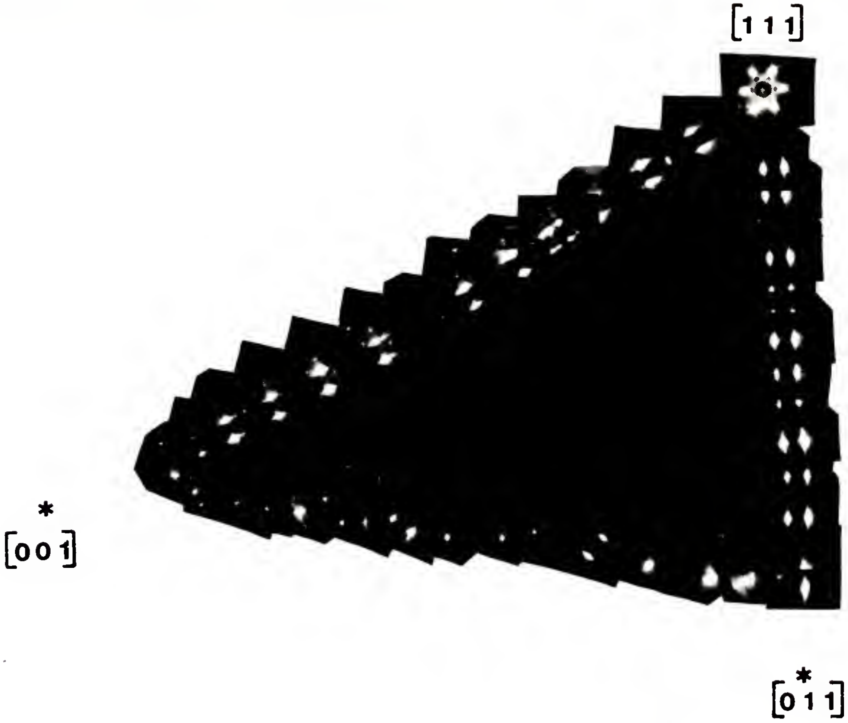

Figure II-16 Partial kikuchi map of a Ni specimen showing the extent of tilt available with the "Double-tilt" holder of Figure II-15.

move in and out thus tilting the cup. Figure II-16 is a portion of a Ni Kikuchi map illustrating the tilt capabilities of this holder. Approximately ±27° on the second axis is available with this holder. Two-beam conditions of various different orientations, can be obtained and defect characterization can be done by using the $\underline{g}\cdot\underline{b}=0$ criteria. This type of analysis was done on a dislocation found in a Ni specimen [77]. Figure II-17 shows two two-beam conditions, $\underline{g}=(11\underline{1})$ and $(\underline{1}1\underline{1})$ of this sample. In Figure II-17b, $\underline{g}\cdot\underline{b}=0$ and the dislocation is not visible. The $(11\underline{1})$ case was imaged close to the [112] zone axis while the $(\underline{1}1\underline{1})$ case was imaged close to the [011] zone axis. This illustrates the usefulness of this holder in obtaining the desired crystallographic information.

FIM/TEM "Field-Effect" Holder

The third TEM/FIM holder is shown in Figure II-18. This field-effect holder has only a single axis of tilt, but is capable of having up to approximately 5 kV applied to the sample *in situ* in the TEM. This holder was designed and constructed by Panitz*, but was first used by this author [77] to study the effect of field-induced stresses in emitters. This holder was found to have some peculiar operating characteristics. If the holder is used without a cable connecting the high voltage supply, the image would oscillate slowly. This was probably a charging effect because when a grounding connector was used on the end of it, the oscillations ceased. If the cable is attached and the power turned off, the image is again unstable and drifts. Turning the supply on and applying approximately 10 v stabilizes the image. Care must be

---

*Panitz, J. A., private communication.

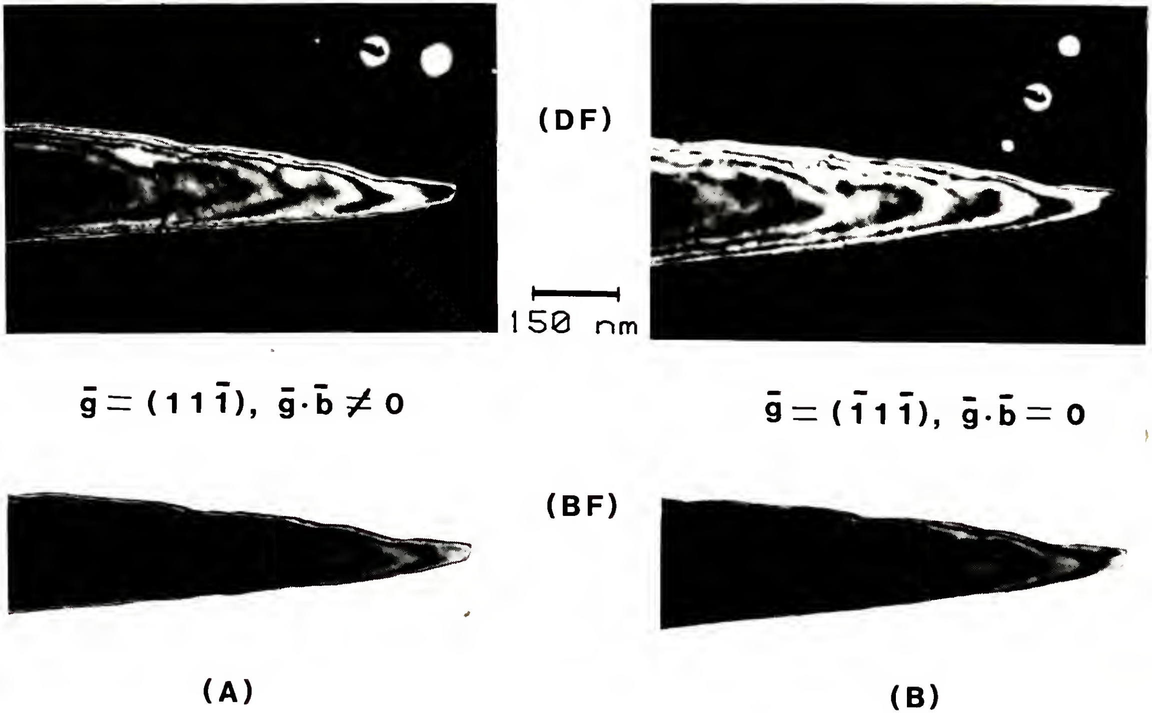
(DF)
150 nm
$\bar{g}=(11\bar{1}),\ \bar{g}\cdot\bar{b}\neq 0$
$\bar{g}=(\bar{1}1\bar{1}),\ \bar{g}\cdot\bar{b}=0$
(BF)
(A)
(B)

Figure II-17 Example of the use of the "Double-tilt" holder to image a dislocation in Ni using different "two-beam" conditions. a) Bright field (BF) and dark field (DF) images of tip using the $\underline{g}=(11\underline{1})$ reflection, $\underline{g}\cdot\underline{b}\neq 0$. b) BF and DF images of same tip using $\underline{g}=(\underline{1}1\underline{1})$ reflection, $\underline{g}\cdot\underline{b}=0$ causing the dislocation to vanish because of the lack of diffraction contrast.

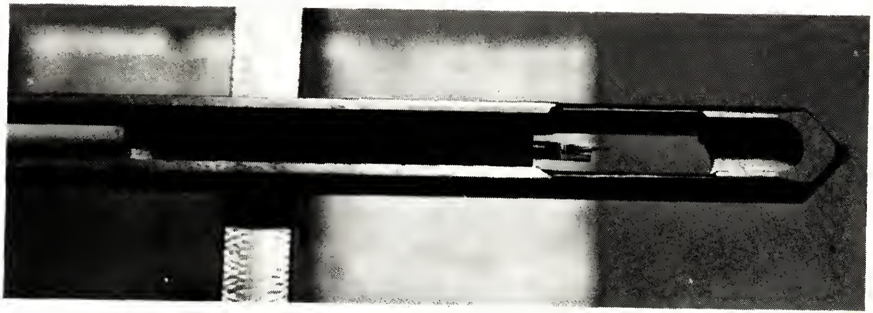

Figure II-18 FIM/TEM "Field-Effect" holder. Voltages between 0-5 kV can be applied to FIM specimens *in situ* TEM with this holder. Only a single rotation axis is available.

taken that the weight of the excess cable does not affect the mechanical stability of the stage. When applying relatively low voltages (up to 1.0 kV) to the emitter, the tip can still be imaged, but both mechanical and beam positioning must be done and extreme beam settings (e.g.,condenser and stigmater lens) must be done. Above approximately 1.1 kV an apparent "hole" forms at the apex of the specimen due to the electric field. As the field is increased, the "hole" gets larger and the specimens appear to disappear into it. Figure II-19 is a sequence of increasing voltage depicting this. Because of this, the results of applying the field to the sample in the TEM can not be seen while the voltage is on. Because field evaporation is a thermally activated process, the application of 3 kV to a specimen in this holder will result in a field evaporation voltage of about 13 kV if it would be returned to the FIM. For this reason, voltages above 3 kV should be avoided in the TEM. Figure II-20 is an example of the results of applying 3 kV to the Ni specimen containing the dislocation in Figure II-17. It is seen that the field-induced stresses have caused the dislocation to sweep through the sample. A faint slip trace can be seen in Figure II-20b and approximately 20 nm has been field evaporated.

The field effect holder will surely prove to be a valuable aid in future metallurgical applications of FIM techniques. Studies using this holder will be able to answer the most often asked question, what is the effect of the applied field to the sample?

Another major use for this holder will be to expose features of interest such as grain boundaries or precipitates to the surface for imaging in the FIM. This holder, in conjunction with back-polishing

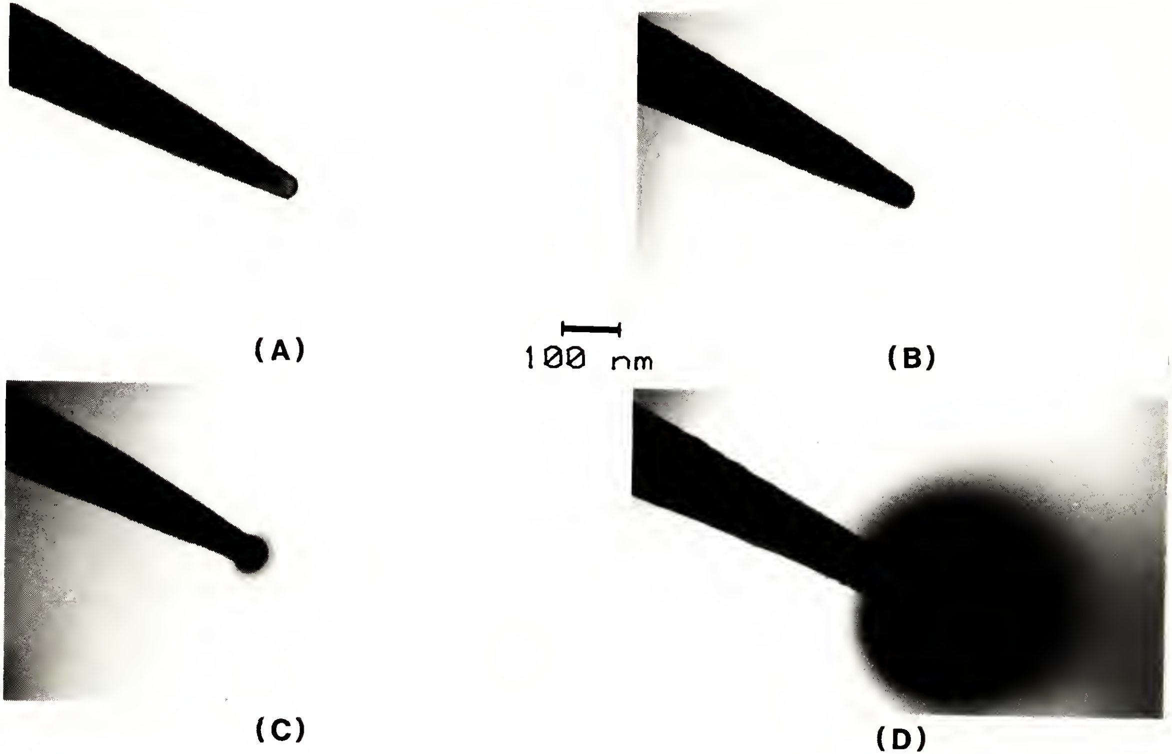

Figure II-19 Applied voltage sequence of a Ni specimen using the "Field-effect" holder of Figure II-18. a) applied voltage is 700 volts, image is same as zero volts, b) 900 volts, darkening of the tip is seen accompanied by an intensity change in the background, c) 1100 volts, "hole" appears at tip showing the effects of the field, d) 1300 volts, tip is completely obscured and "hole" is larger. At higher voltages, this area is larger and moves further down shank.

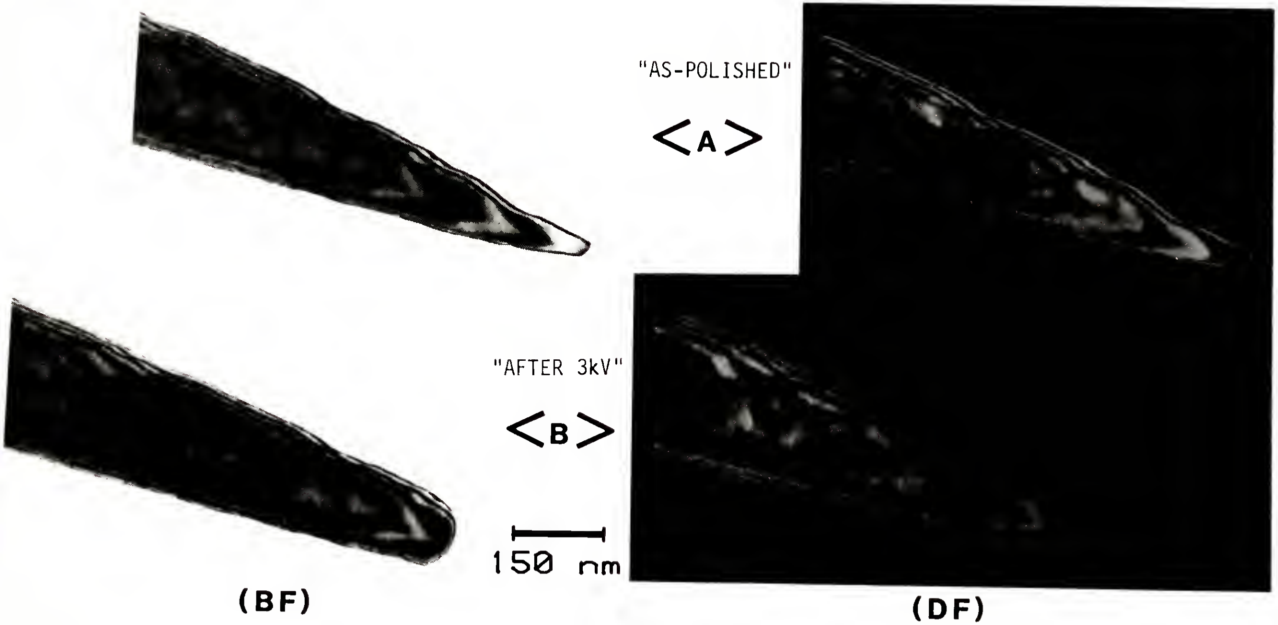

Figure II-20 Effect of field on the dislocation in Figure II-17. a) BF and DF images of an "As-polished" specimen before voltage applied. b) BF and DF images of same tip under the same imaging conditions after 3 kV was applied. The dislocation has swept through and approximately 150 nm has been field evaporated. A faint slip trace can be seen.

techniques developed by Nordén et al. [78,79], will help overcome one of the major disadvantages of FIM techniques, specimen size. Because of the extremely small volume accessible to analysis, features of interest are extremely difficult to find and, in general, many samples are required to be examined. This is true even when these features are present in large quantities, e.g., samples with high dislocation densities or extremely fine grain size for grain boundaries. In general, the geometry of FIM specimens is ideal for observation in the TEM. In addition, this field-effect holder can create experimentally controllable stress states which are similar to the conditions found in the volume just ahead of a crack tip in an embrittled alloy.

CHAPTER III
EXPERIMENTAL CONSIDERATIONS

Depth Profiling Using The FIM/IAP

This chapter deals with experiments designed to establish the validity of the procedures developed in this study. Without such experiments, a complete FIM/IAP study of the ion implantation into materials, especially the trapping of deuterium to implanted defects, would not be feasible or believable. In addition to these control experiments, the procedures for reducing the raw IAP data from implanted specimens will be presented. The actual results of implanted specimens will be given in Chapter IV.

This chapter will be divided into three main sections: 1) "Depth Profilng Using The FIM/IAP", 2) "Effects Of Field Ionization And Evaporation", and 3) "Special Problems Associated With Hydrogen/Deuterium." Each section is important with respect to the proper operation of the FIM/IAP and interpretation iterpretation of experimental results. The section on depth profiling in the FIM/IAP will demonstrate a method for establishing a depth scale for extended profiles when an imaging gas is not present. Such studies have not been possible to date and are critical for emitters with relatively low field evaporation fields. The section on the effects of high fields gives some of the answers to questions which are always raised about their effect on defect microstructures. There is reason for considerable optimism that some defects induced by implantation are unaffected by field induced stresses. The section on the special problems of hydrogen/deuterium will show that *in situ* implantation is indeed feasible. Field adsorbed D can be reliably distinguished from implanted D. This section will also present some observations of a more general interest to FIM studies but which also of importance to this study. Some of these are important to proper operation of the FIM/IAP and/or analyzing the data correctly. It should be born in mind that there are still fewer than twenty of these instruments worldwide, nearly all individually designed and built. Therfore, it is important that this type of information be disseminated.

Ring Counting Experiments

It is extremely important to be able to accurately depth profile implanted species. Depth profiling is the forte of FIM in conjunction with the atom probe. During evaporation, with an imaging gas present, each ring of atoms constituting an atomic plane, appears to collapse and disappear as evaporation proceeds. Each ring collapse of a particular set of planes denotes a precise distance probed equivalent to that d-spacing. This is the most accurate profiling method which exists, providing, of course, that one can observe these ring collapses implying that an imaging gas is present. In investigations which require UHV conditions during analysis (i.e. without an imaging gas), such as the present one, the rings can neither be seen nor directly counted. It was thus necessary to develop another method of ascertaining the depth.

Further complications arise with respect to the IAP spectra, since the signals vary in strength even when the voltages are held constant.

For shallow depth profiles a sudden increase in peak height indicates a ring collapse. Counting these gives the same accuracy as with counting the rings visually. This method is impractical for larger depths, such as those needed for ion implantation studies, typically 100 nm or more. This is because the voltages need to be raised many times in such a profiling experiment, and it is extremely difficult to differentiate reliably an increased pulse height due to a ring collapse or from an increased evaporation rate. Furthermore, up to 30 thousand pulses may be required to evaporate to the required depth on the order of 100 nm or so. It would be very tedious to sort through such a mountain of data in order to determine all the occurrences of ring collapses.

In Chapter II major requirements were cited for establishing a suitable procedure for extended depth profiles with the IAP. The first is that the method must be able to reduce the number of spectra to manageable levels. Consider a typical example: the amount of storage required if 30 thousand spectra are to be stored. (Because of the requirement for rapid pulsing the spectra must be collected and stored; analyzing them in real time requires too much time.) Each spectrum takes about 5 kbytes of disk storage. Thus for the 30 thousand spectra, over 100 Mbytes of storage is required! The signal-averaging mode of the Tektronix 7912AD alleviates this problem somewhat. The 7912AD can average 2,4,8,16,32 or 64 traces, thus reducing the storage requirement by the factor chosen. The second point, is that the method chosen for depth profiling must be insensitive to the field evaporation rate. During an extended profiling experiment the field evaporation rate will of course change widely, both while the voltage is being held constant (giving a decaying rate of field evaporation) and when the voltage is increased (leading to an increased rate of field evaporation).

In the remainder of this chapter the method chosen for the depth profiling requirements of this study are described in detail. It relies upon the geometry of field emitters observed by TEM, the basic principles of operation of the FIM, and a particular calibration procedure.

Specimen Geometry

The tip geometry assumed to apply for this study is a conical shank with a spherical cap at the apex. The spherical cap joins the shank tangentially, i.e. a radius vector from the center of curvature to this point is perpendicular to the shank. In the FIM only a portion of the specimen is imaged. Figure III-1 shows the assumed geometry of a specimen. The cross-hatched region represents the probed volume of our instrument with a subtended viewing half-angle of 20°. With this model, the radius of curvature is given as

$$R= (h+l_0)\cdot \sin\alpha/(1-\sin\alpha) \qquad \text{III-1}$$

where l_0 is the distance from the initial surface, α is the shank half-angle and h is the distance probed from the initial surface to the final surface. Figure III-2 is a montage of an evaporation sequence of a Ni specimen performed with the "field-effect" (FIM/TEM) holder. This figure illustrates two points, the geometric model is quite valid and the distance which the FIM/IAP is capable of probing is considerable (>1 um). The computer-generated figure was done using equation III-1. The parameter, α, was measured from the montage. Using the Tektronix 4662

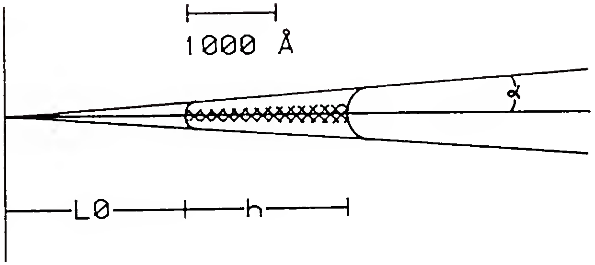

Figure III-1 Assumed geometry of emitter. Cross-hatched region indicates volume probed by IAP. The distance h is the depth probed from the initial surface to the second surface.

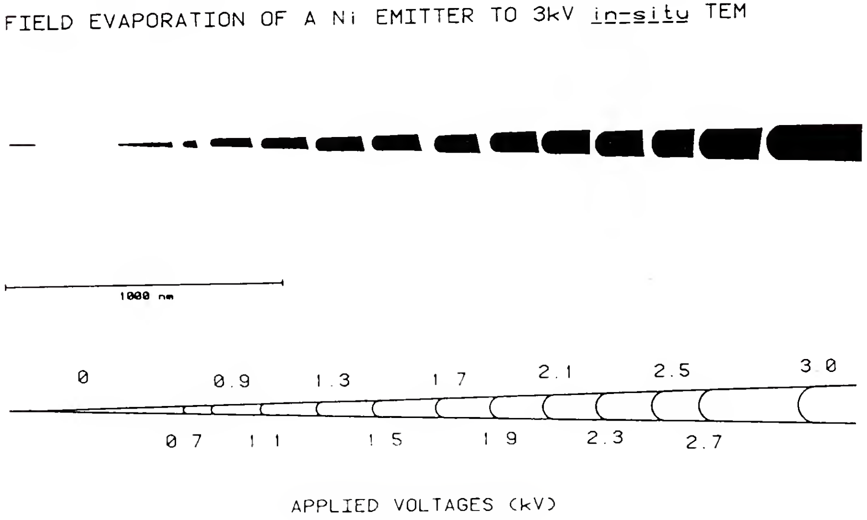

Figure III-2 Montage of TEM micrographs field evaporated in situ TEM in the FIM/TEM "Field-Effect" holder. Also shown for comparison is a computer-generated sequence using the model for the tip geometry discussed in text.

plotter, each radius was drawn at the measured distance from the apex of the cone (equal to l_0 in equation III-1). The computed radii at the various voltages in Figure III-2 are all very close to the actual radii from the micrographs except one, the radius drawn at the indicated voltage of 3 kV. This radius was measured from the micrograph and drawn at the distance given by equation III-1. When it was drawn by the computer, it did not match the location in the montage. After examining the montage more carefully, it was found that one micrograph, taken at 2.9 kV was missing. The last micrograph in the sequence had been positioned a little too far to the left. The offset between the surface drawn and the one in the montage is approximately the displacement due to this error. It should be pointed out that this error was not found until after the application of equation III-1 in generating the figure. This suggests a precision of better than 10 nm.

IAP probed-volume considerations

For the Chevron plates used as the detector in the IAP, it has already been shown that the detector efficiency and gain is constant over the energy range and for the types of ions employed here [70]. Furthermore, it is the detector which limits the width of the area probed indicated in Figure III-1. If all the atoms within that volume strike the detector and the detector efficiency is constant, the integrated signal should be proportional to the number of atoms contained within the probed volume. The number of atoms within this volume is simply related to the volume by the density of the specimen. This model is the foundation for the method used to determine depths in this study. That is, it is assumed that the integrated bulk signal from the Chevron detector is proportional to the volume probed. The integrated signal is easy to measure, since it is just the cumulative matrix signal from the spectra collected. The accumulation of spectra approximates an integration very closely because of the small step involved with a ring collapse, and that it can take many pulses to evaporate one layer. The one assumption made with this method is that the concentration of the element used for the accumulation process is constant and is proportional to the probed volume. There may be situations for which this assumption is not valid, e.g. ion implantation of massive ions or the presence of precipitates, but for ion implanted deuterium into nickel, this assumption is certainly reasonable.

The problem of depth profiling using the model just described is reduced to finding the functional dependence of the volume with depth and geometrical parameters of the specimen. Then to compare these with a calibration experiment in which the rings are counted and the cumulative signal is found from the spectra.

Volume calculation

The calculation of the probed volume is straight-forward. Figure III-3 shows a representation of the cross-hatched volume in Figure III-1. The volume of interest is the shaded region bounded by the two spherical caps representing the initial and final surfaces, and the sides of the cone representing the limit of the area of the emitter surface projected onto the detector. The bases for the spherical caps are indicated by dotted lines. This volume can be seen to be

$$V = V_1 + V_2 - V_3 \qquad \text{III-2}$$

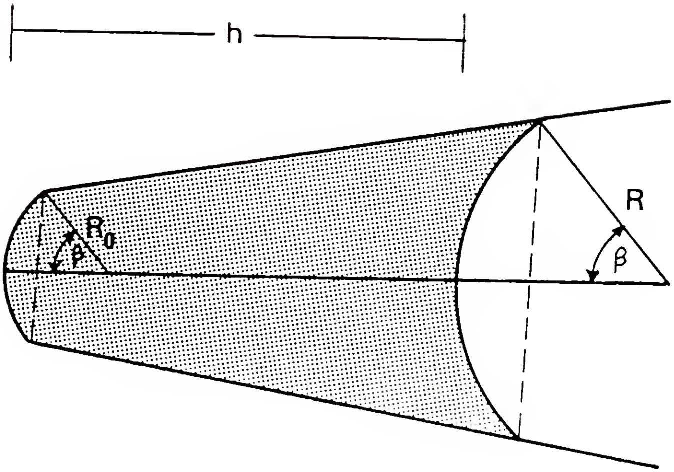

Figure III-3 Representation of the volume probed by the FIM/IAP in an emitter. The shaded area corresponds to the cross-hatched area in Figure III-1.

where V_1 is the volume of the frustrum of the cone bounded top and bottom by the dotted lines, V_2 is the spherical cap of radius R_0, and V_3 is the spherical cap of radius R. The value h is equal to the number of planes evaporated normal to the emitter's axis, (N d_{hkl}). Using equation III-1, the radii of curvature can be expressed as

$$R_0 = l_0 \cdot \sin\alpha/(1-\sin\alpha) \tag{III-3a}$$

and

$$R = (h+l_0) \cdot \sin\alpha/(1-\sin\alpha) \tag{III-3b}$$

The equation for the volume of a spherical cap subtended by an angle, β, and radius, R_c is

$$V_{s.c.} = \frac{\pi}{3} \cdot R_c^3 \cdot (2-3\cos\beta + \cos^3\beta) \tag{III-4}$$

Using this formula, V_2 and V_3 are given as

$$V_2 = \frac{\pi}{3} \cdot K_\alpha^3 \cdot l_0^3 \cdot (2-3\cos\beta + \cos^3\beta) \tag{III-5a}$$

and

$$V_3 = \frac{\pi}{3} \cdot K_\alpha^3 \cdot [h^3 + 3h^2 l_0 + 3h l_0^2 + l_0^3] \cdot (2-3\cos\beta + \cos^3\beta) \tag{III-5b}$$

where $K_\alpha = \sin\alpha/(1-\sin\alpha)$, and l_0 is defined above. Using equations III-5a and III-5b,

$$V_2 - V_3 = -\frac{\pi}{3} \cdot K_\alpha^3 \cdot [h^3 + 3h^2 l_0 + 3h l_0^2] \cdot (2-3\cos\beta + \cos^3\beta) \tag{III-6}$$

The volume of a frustrum of a cone is given as

$$V_F = \frac{\pi}{3} \cdot Z \cdot (R_T^2 + R_B^2 + R_T R_B) \qquad \text{III-7}$$

where R_T and R_B are the radii of the top and bottom areas, and Z is the height of it. For V_1, $R_T = R_0 \sin\beta$, and for V_3, $R_B = R\sin\beta$. Using equations III-3 and substituting into equation III-7 and doing a little algebra, V_1 is given as

$$V_1 = \frac{\pi}{3} \cdot [K_\alpha^2 \sin^2\beta + K_\alpha^3 (1-\cos\beta)\sin^2\beta] \cdot [h^3 + 3h^2 l_0 + 3h l_0^2] \qquad \text{III-8}$$

Substituting III-8 and III-6 into III-2, and simplifying the coefficient terms,

$$V = \frac{\pi}{3} \cdot [K_\alpha^2 \sin^2\beta - K_\alpha^3 \cdot (1-\cos\beta)^2] \cdot [h^3 + 3h^2 l_0 + 3h l_0^2] \qquad \text{III-9}$$

This is the probed volume to which the cumulated matrix signal is proportional. The parameters needed for each specimen to be found are the shank half-angle, α, and l_0, the initial surface to apex of the cone made by extending the sides of the emitter to their point of convergence. The system parameters to be determined are the detector viewing half-angle, β, and the proportionality constant between the volume and the accumulated signal. This constant, K_D, has several other constants within: the emitter density, the efficiency of the detector, the gain of the detector, the gain of the amplifier, etc. Determination of K_D will be discussed in a later section.

Determination of β

For the depth evaporated in an IAP experiment the viewing half-angle, β, is assumed constant. The reason for this can be explained by considering the FIM image. The image is a projection of the surface of the tip onto the screen. This projection is similar to a stereographic projection in that the projection point is close to that used in a stereographic projection [80]. With this pseudo-stereographic projection, the angular positions between poles of crystal planes are still approximately constant at all radii. This is true even though the radius of curvature is increasing as the emitter is field evaporated since the radius of the emitter is much smaller than the radius of the sphere of projection. It can be understood by considering the distance the projection point changes with depth (on the order of 1 um) as compared to the projection distance (on the order of 10 cm). The only difference between low and high voltage images of the same tip is the appearance of higher-indexed planes as the radius increases. The invariance of the motion of the relative positions of the major poles present at all radii can be observed by d.c. field evaporation. The value of β can be determined in the same manner as FIM micrographs are indexed [80]. Figure III-4 shows an indexed micrograph of a Ni emitter. The viewing screen angle can be found from the following relationship,

$$2\beta = (D_{screen}/D_{(111),(113)})\cdot\Theta_{(111),(113)} \qquad \text{III-10}$$

where D_{screen} is the measured diameter of the total viewing area of the micrograph, $D_{(111),(113)}$ is the measured distance and $\Theta_{(111),(113)}$ the

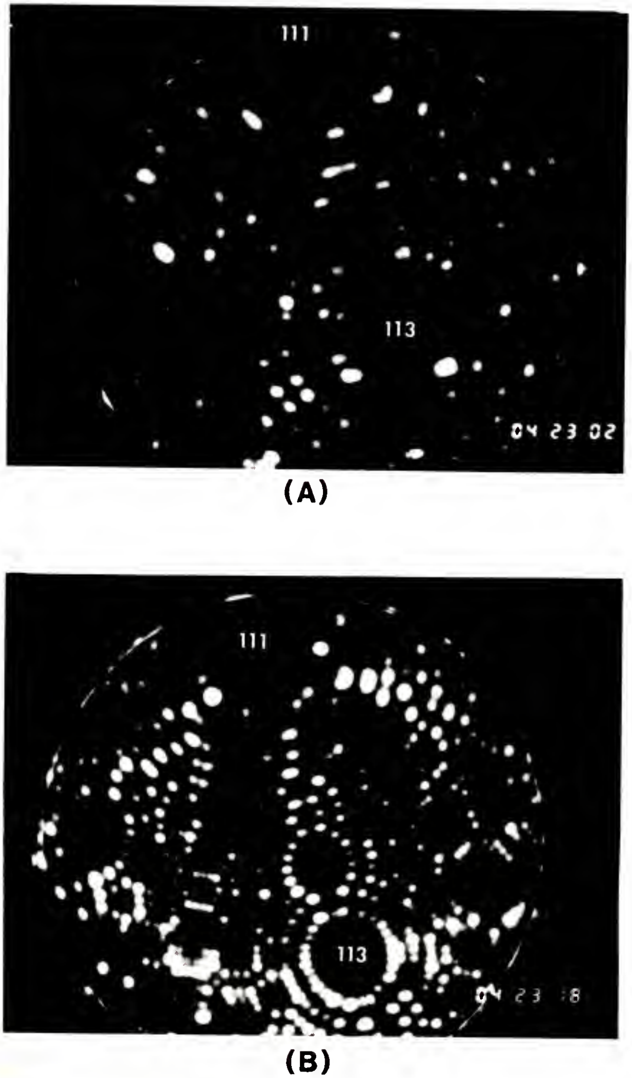

Figure III-4 Indexed FIM micrograph of a Ni emitter at two different voltages. a) Ne image at 5.82 kV. b) Same specimen after IAP analysis, imaged at 9.49 kV. The specimen has been physically moved between a) and b), but note that the distance from the (111) plane and (113) is the same in both. The angular distance between the two poles is 25.2°.

known angle, 25.2°, between the (111) and (113) planes. Using this method, β is found to be 20°.

Determination of K_D for nickel

This section will describe the procedures involved in the determination of K_D, the proportionality constant between the cumulative Ni signal and the volume (equation III-9). With the value of K_D and the geometric parameters of an emitter, a depth scale can be ascribed to the cumulative Ni signal data. This is done by graphing a calculated curve versus the depth probed, h in equation III-9, for that emitter. The depth scale is given as the number of rings collapsed; the total depth given as N d_{hkl}, where d_{hkl} is the d-spacing of the set of planes used for the determination of K_D and N is the total number of planes evaporated. The experimental data collection and handling procedures will be described together with a brief description of the programs used. TEM data are also used, for both collecting the required geometric parameters of the specimen, and to check the depth scale in the ring-counting experiment. It is relatively easy to find K_D by collecting data with an imaging gas present, noting the number of rings collapsed, adding the signals of all the spectra, substituting this value into the relationship and solving for K_D. However, the ring-counting control experiment which will be described also checks the validity of the model used for the volume probed by the use of a curve matching procedure. The selection criteria for specimens used for implantation and subsequent analysis will also be discussed.

Experimental procedure

The experimental procedure used in obtaining the cumulative Ni signal versus the ring count data is described in this section. The number of steps involved in getting the data in final form is rather large, but it is straightforward. It may seem a little confusing because of the number of different instruments utilized and the different programs used to reduce and manipulate the data into the desired form. Figure III-5 is a flowchart of the procedure in finding K_D, the experimental curve, and the calculated curve, and will help in following the text.

The calculated curve will be the information which can be used to establish a depth profile which does not use the imaging gas to establish the depth scale. The only difference in the flow chart for an actual depth profile experiment is that this experimental curve and K_D will not be output from the program. The reason of course is that the ring counting is not performed and the "pulsenum" information in the flow chart is not collected.

The experimental procedure begins with the imaging of an "as-polished" specimen. Nickel specimens are polished with a taper angle as sharp as possible in order for them to first image well below 5.5 kV. The reason for this is that the specimen is field evaporated up to a voltage of 6.0 kV, at which voltage the selection criterion for a tip is that the portion of the specimen imaged is larger than the detector area. Satisfying this criterion usually assures that the hemispherical surface meets the shank tangentially as the model prescribes. Another selection criterion for Ni is that the specimen have a [111] orientation which is

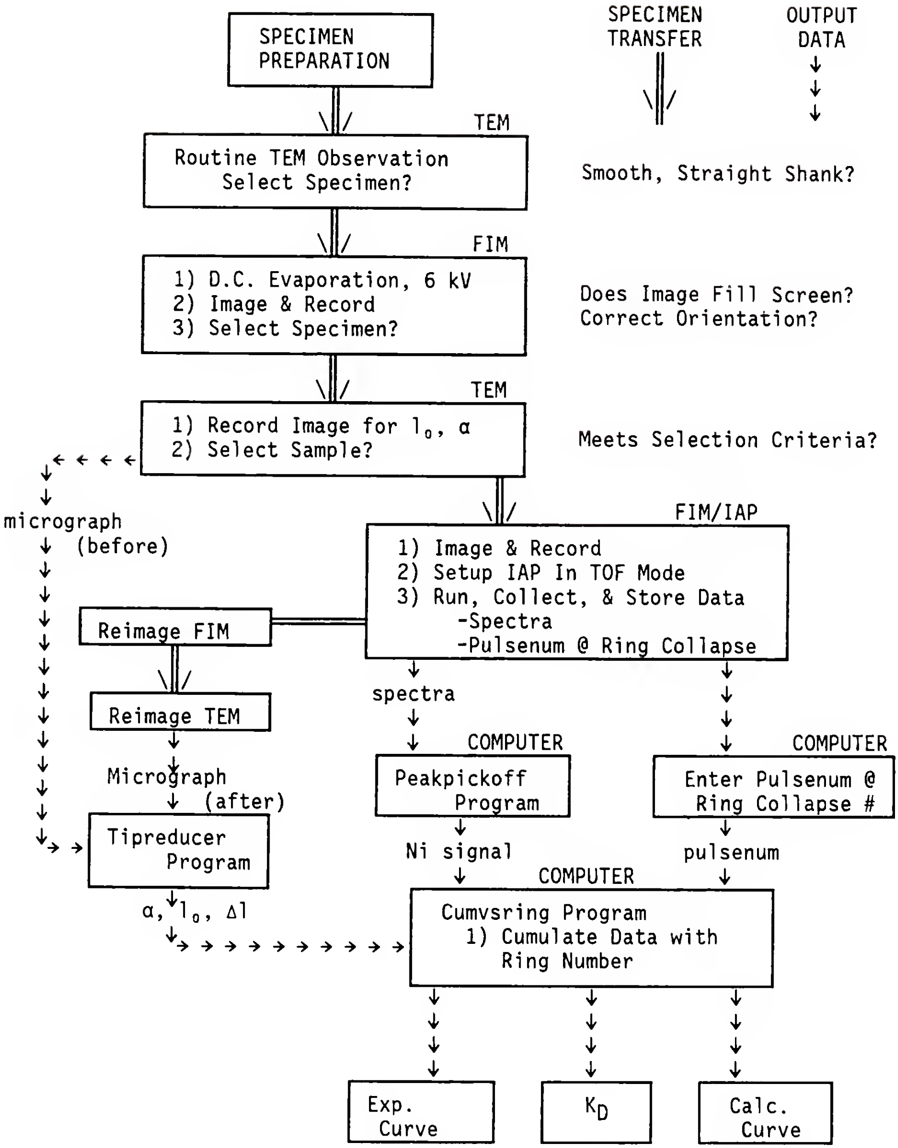

Figure III-5 Flowchart of the procedures involved with finding the cumulative matrix signal as a function of depth. The arrows indicate the transfer of the sample or data between instruments or programs.

the most common orientation found for the samples in this study. The reason for this is that the calibration curve used to obtain K_D has been collected using this orientation.

After the specimen is evaporated to 6 kV in the FIM, it is transferred to the TEM for imaging. The FIM/TEM "Bulk" holder is used (see Chapter II). The position of the stainless steel specimen mount is noted because the specimen will be re-imaged again under approximately the same imaging conditions. The image is recorded using a particular reflection in a "two-beam" condition; for Ni emitters, it is usually a (111) type reflection. The (111) type reflections are very distinctive when in the diffraction mode and because of the wire texture, easily found using the FIM/TEM "Bulk" holder which has only a single rotation axis. This allows for ease of comparison between two micrographs of the same specimen taken at different times. The micrograph obtained will be used to determine α and l_0 using the program, "TIPREDUCER," described in a later section. (This program is also described and listed in Appendix D.) The specimen is also examined for its suitability at this point. It must have a smooth, straight shank and the surface must meet the shank tangentially as discussed above.

After TEM imaging, the specimen is transferred back to the FIM/IAP where the voltage is raised to the imaging voltage again. FIM micrographs are recorded over the complete imageable area of the tip in order to determine the crystallographic orientation and radius. (The micrographs are recorded in the same manner as was done in constructing the montage of Appendix E.) The specimen is then oriented toward the detector with the (111) pole in the center of the screen. The imaging gas pressure is lowered to approximately $5x10^{-6}$ Torr and the Chevron gain is increased to maximum (approximately 10^7). The d.c. voltage is lowered in anticipation of using the pulse at its charging voltage of 5 kV. (At 5 kV, the pulse voltage is approximately 2 kV.) This value remains constant throughout the experiment.

The digitizer is now prepared for collecting spectra and the pulse counter is reset to zero. The first spectrum is taken with a d.c. voltage low enough such that no field evaporation occurs. This is done to establish the d.c. offset of the digitizer. This offset is subtracted for all subsequent spectra collected. The file name and number of waveforms per spectrum to be averaged are also selected at this time. This number (with the program variable name of NUMAVG) should not be too small for two reasons: 1) the number of spectra stored probably would be too large for the available memory and 2) problems can arise while storing the spectra and the digitizer is collecting its next waveform. Initially, it takes about 4 seconds to store a single spectrum. As the number of records in a file increases, it takes longer. For example, if NUMAVG is eight and the time interval is 0.6 sec, it takes longer to store a waveform on the file manager than it does to collect the next spectrum when the number of records in the file manager exceeds six hundred. It is important that this condition is avoided because extra pulses will occur, the number of which also increases as the number of records in a file increases. The reason the extra pulses occur is that the computer sends a "stop" signal to the pulser after it reads the waveform. If the 4909 is still storing the previous spectrum, the 7912AD cannot send the data, which means the computer does not send the "stop" signal to the pulser. The signals due to the extra pulses are lost, and thus, the cumulative values obtained are in error, being less than the actual conditions. For this reason the program, "IAPRING.HV" has been modified. It "clamps" the number of records within the file to 500 and then creates a new file with the same generic name but with the next sequential filename modifier. The best value for NUMAVG is 8 for a balance between storage requirements, background averaging, and the assumption that the result of each pulse within a spectrum has the same results. This latter point is important with respect to the method in which the peak heights are cumulated.

To start the ring-count experiment, the command, "RUN 60000" is typed. Automatic looping of the data acquisition and storage sections of the program will occur. When a ring collapse is seen at the screen, the pulse number from the pulser is noted. Manual control of the high voltage supply can be accomplished through the user-definable keys, even though the program is running. A key's action is delayed until the digitizer completes the current operation. The "VOLT.RAMP ON/OFF" user-key will toggle a voltage ramp on/off. When on, the voltage ramp will increase the voltage by the variable "VINC" every 5 minutes. Spectra are not automatically displayed at the computer's screen because it takes approximately 3 seconds to output it and it would be redundant since they are automatically displayed on the digitizer's storage display monitor. A spectrum can be displayed at the screen, by simply pressing the "Redraw @ Screen" key. The experiment is continued until a predetermined number of rings have collapsed. The last waveform must be saved manually because they are only saved automatically when a new waveform is being collected. Interruption of the program is accomplished by pressing the "Redraw @ Screen" key and then using the "Break" key before the graph is completed. The program can be recontinued by starting the program at statement number 60000 again.

It is important to note the large amount of data which would be collected to this point. For 650 (111) rings of one particular Ni specimen, 3366 spectra were collected, requiring 26,920 pulses in a typical experiment. For this number of rings, the time required to perform the experiment was longer than seven hours; with data being taken continuously during this period. At the end of this experiment, the specimen is re-imaged in the FIM mode (open large area in Flow chart of Figure III-5).

After the spectra are collected, the pulse numbers corresponding to the occurrence of a ring collapse must be entered into the computer. The number of values being entered is the number of predetermined ring collapses for the experiment. These values are most easily entered using the Tektronix Editor ROM pack. They can be listed and corrected while they are being entered. The editor can only store these values on magnetic tape, but they are easily transferred to the file manager. The entered values can be checked for errors by using the ROM subroutine, "DIF2." The values are read into an array and "Diff2" used. Any negative values of the differentiated array or any very large values indicate errors in the entered values and must be corrected.

The Ni signals must be located on the stored spectra. The program "PEAKPICKOFF.FAST" is used to find these values. (See Appendix D). This program is a general routine for "picking-off" up to eight mass peaks from spectra stored on the file manager. It will create a new file for each mass peak and one file for information pertaining to the number of peaks, the mass-to-charge ratios of each peak, and the number of spectra collected. When using this program, a time window for each peak must be defined using the marker section of the program. The program calculates the time of flight for the mass peak and also shifts the window with respect to the previous position of the peak in the previous spectrum. If the two do not agree, the calculated value takes priority. For 3366 spectra, it takes about 6 hours to run this program.

While the program "PEAKPICKOFF.FAST" is running, the specimen is transferred to the TEM and imaged with as close to identical conditions as possible from those previously used. As was noted above the specimen is inserted into the FIM/TEM "Bulk" holder with the stainless steel mount positioned as close as possible to the position used initially. This allows the use of the TEM "X"-rotation scale to more easily find the previous tilt conditions. It is imperative that when specimens are imaged at different times and are to be compared, that the TEM be set up in an identical (or standard) mode of operation. This includes aligning the microscope, making the sample eucentric, and focussing the diffraction and intermediate lenses such that the diffraction pattern is formed in the plane of the objective aperture and the image is formed in the plane of the diffraction aperture. With the certainty that the two images have been taken with the same magnification, the distance probed can be checked between the two micrographs. (Of course, the TEM magnification must be calibrated for this.) It is also important to check that nothing abnormal has happened to the specimen in the process of collecting the data (e.g. mechanical damage, electrostatic discharge, etc.)

After the Ni peak values are stored in the file manager, they need to be summed with respect to the pulse numbers recorded during the ring counting experiment. The values are accumulated using the "CUMVSRING" program. This program will create a file into which the accumulated Ni signal array will be put. The program works in the following manner: It reads the first pulse number from the file in which these values were stored. It divides this number by the value NUMAVG used in collecting the spectra. The integer value of this result is the spectrum number in which that ring collapsed. The Ni peak values are summed to this point. The fractional part of the result gives the multiplier for the spectrum to be added to the cumulated value. The result of this is stored as the first value in the cumulation file. The next pulse number is read and the process repeated, the value at each ring collapse being put into the cumulation file. The index of the position of each cumulative Ni value corresponds to the ring collapse number at that value. These are the experimental data which are used to graph the curve which should be proportional to the volume curve given by equation III-9. Figure III-6 shows an experimental curve found using this procedure. It can be seen that it is monotonically increasing and is smooth. This curve is insensitive to the fluctuations in the original data. Figure III-7 shows the range of values for the Ni signals used to generate the curve in Figure III-6. It can be seen that the evaporation rate does not affect this curve. This is true for relatively high, low or decaying evaporation rates. One of the prerequisites for finding a method for

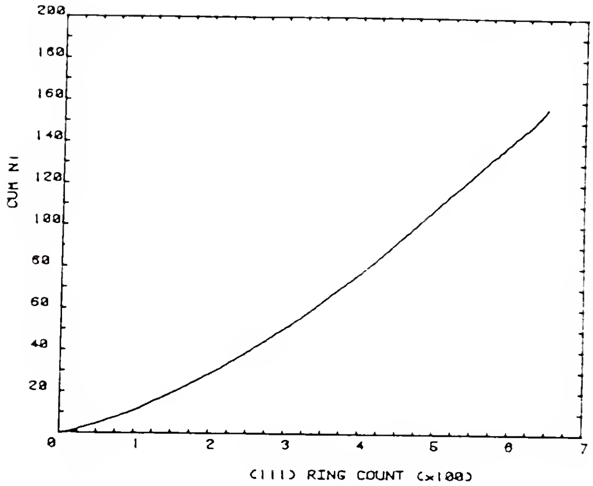

Figure III-6 Experimental cumulative Ni vs. (111) ring count curve. Each data point represents the cumulative signal at a ring-collapse number. The depth scale is found by multiplying the ring number by 2.03 Å (d_{111} for Ni).

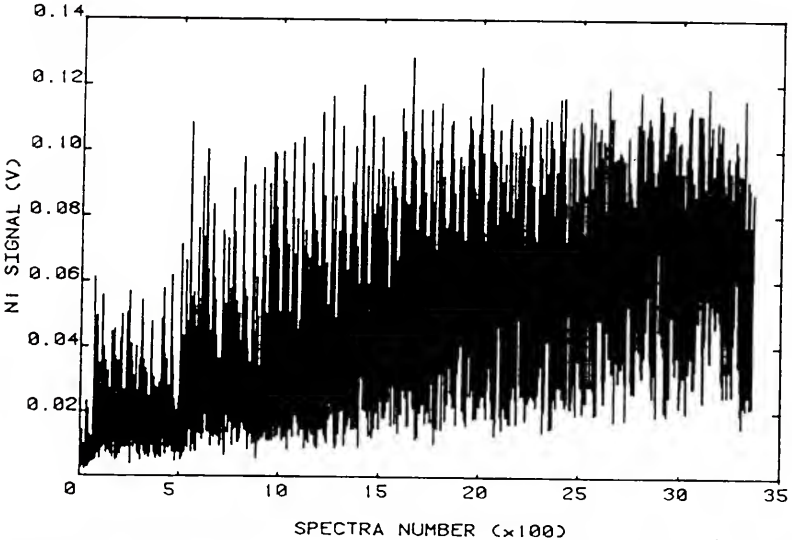

Figure III-7 Ni peak values for the spectra which generated the curve in Figure III-6.

assigning a depth scale to the data was that it be independent of evaporation rate, and this seems to be the case. TEM and FIM micrographs of before and after the ring count experiment are shown in Figure III-7.

Determination of geometric parameters

To fit the experimental curve in Figure III-6 the parameters, α, and l_0 must be determined from the TEM micrographs in Figure III-8. This is done using the program, "TIPREDUCER" (Appendix D). The TEM micrograph in Figure III-8a is put on the Tektronix 4662 Interactive plotter. Several points are digitized along each side of the shank. A "least-squares" straight line is found for each line and the intersection of the two lines gives the apex of the cone. The shank half-angle is simply half of the angle between these two lines. A point along the center line of the emitter and at the surface is also digitized. The distance between this center point and the apex of the cone gives the value l_0. These values are used in equation III-9. Figure III-9 shows an example of the graphic output from this program using the tip in Figure III-8b. (The tip in Figure III-8a was also digitized, but will be discussed in a subsequent section with respect to a problem it had with finding l_0.) The output is given in mm and must be corrected by the magnification of the micrographs. To be used in the "CUMVSRING" program, l_0 is divided by d_{hkl}. This gives l_0 in the number (hkl) planes from the surface to the apex. For Ni, d_{111} is 2.03 Å. This program can also be used to find the distance evaporated. The same procedure is used on the micrograph before evaporation and after. The difference in the output of the two different l_0 values is the distance evaporated.

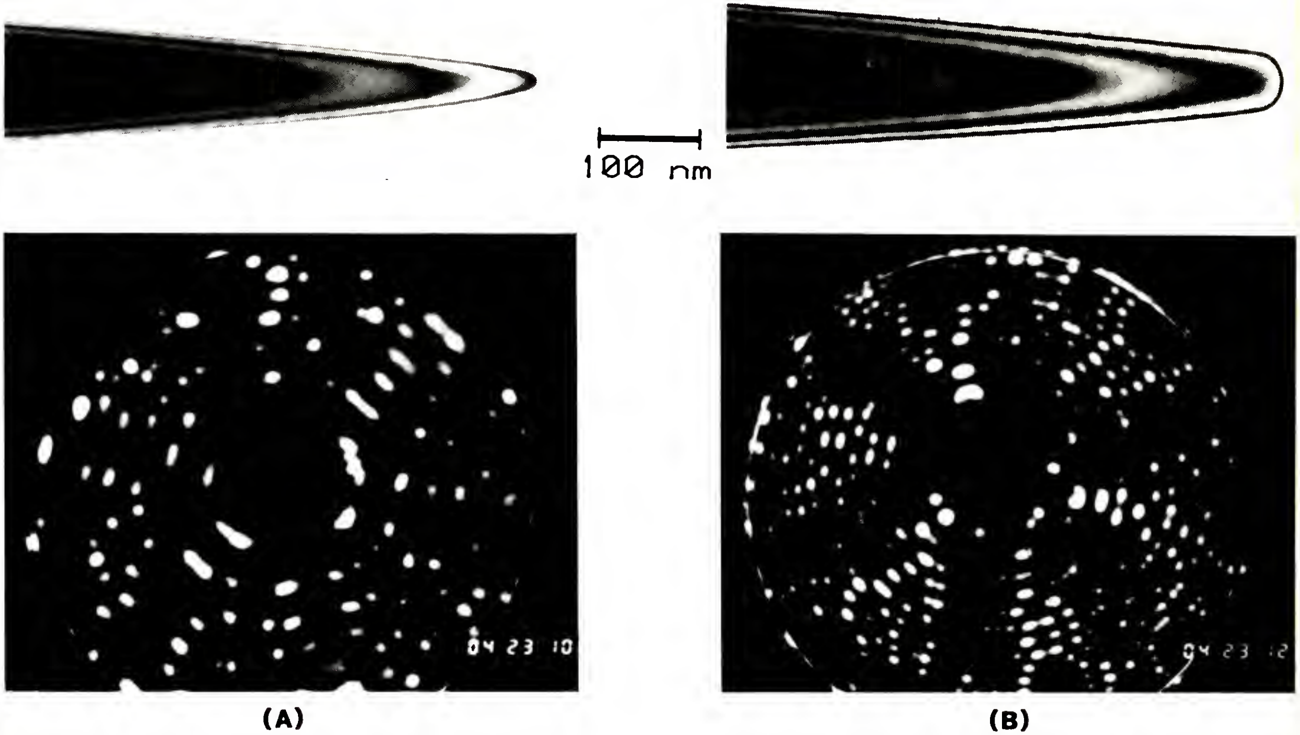

Figure III-8 TEM and FIM micrographs a) before and b) after ring count calibration experiment. The FIM image in a) was imaged at 5.82 kV and b) at 9.49 kV. Manipulator was in same position in both cases.

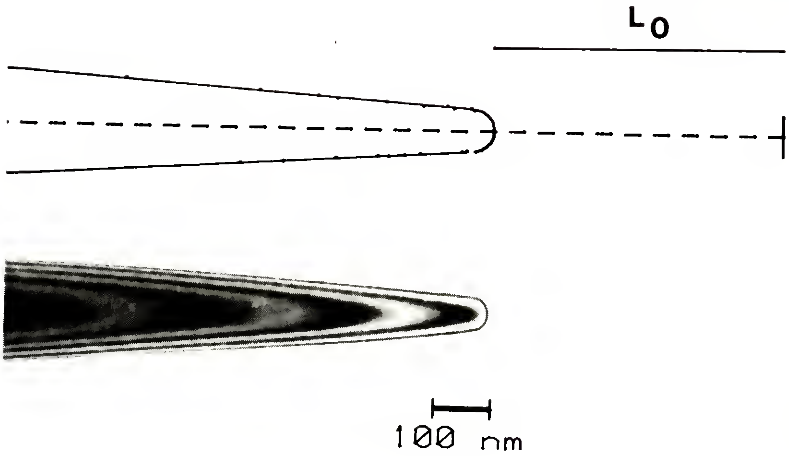

Figure III-9 Graphic output from the program "TIPREDUCER." Specimen is same as that in Figure III-8b. The shank and the point on the surface along the tip's axis is digitized. The program then finds the values α, l_0, and R_0 using equation III-3a.

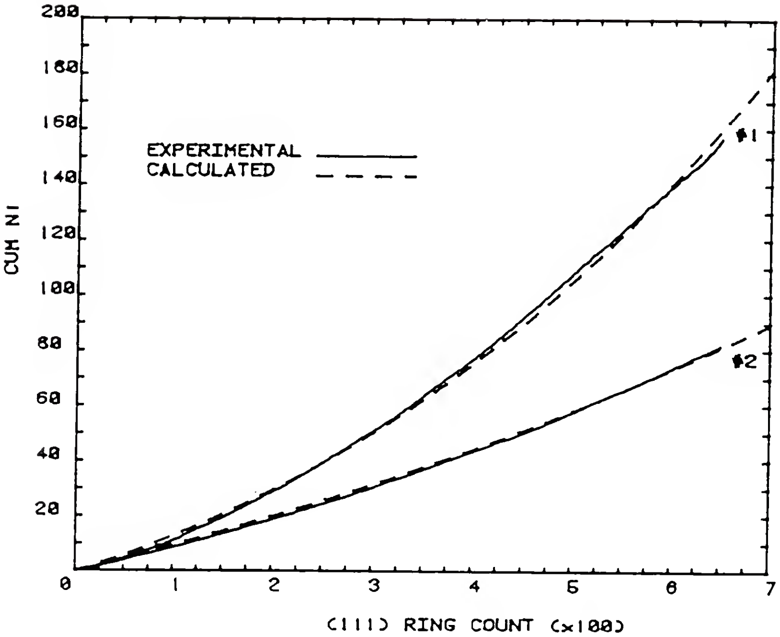

Figure III-10 Cumulative Ni signal versus Ni (111) ring count for two specimens. Curve #1 is the specimen shown in Figure III-8. The data in the experimental curve were used to generate K_D for the calculated curve. ($K_D=5.16\times10^{-5}$). This value was then used along with the appropriate α and l_0 to generate the calculated curve #2. It is compared to the experimental curve.

Calculated curve

The value of K_D was found as described above. Figure III-10 shows two examples of the calculated curves compared to the experimental curves. Curve labeled #1 was used to determine K_D. This value was used along with the measured geometric parameters to find curve #2. This result shows the validity of using this method to determine the depth scale.

The procedure for establishing the depth scale for an implanted tip is straightforward. The geometric parameters are measured with the TEM and the cumulative curve versus ring count is generated. The steps in this procedure would be essentially the same as those attained in the flow chart of Figure II-5, except that the implantation occurs just prior to analyzing in the IAP. No ring counting is performed, so that the "pulsenum" data are not collected. The indices of the calculated curve array give the depth at that point in N d_{hkl} units. For the profiled tip, an array of cumulated values are found. The indices of this array are the spectra number taken during the profile. The ROM pack routine "CROSS" can be used for each value in this array as the argument of the crossing value, and the calculated curve array is used as the array argument. The output from this routine gives the index. This gives the depth at each spectra for the profiled specimen.

Sample selection criteria

At this point it would be beneficial to summarize the selection criteria discussed in the various sections above. Most of the specimens which are rejected are done so on the basis of TEM observations. Figure III-11 shows four specimens which for obvious reasons are not

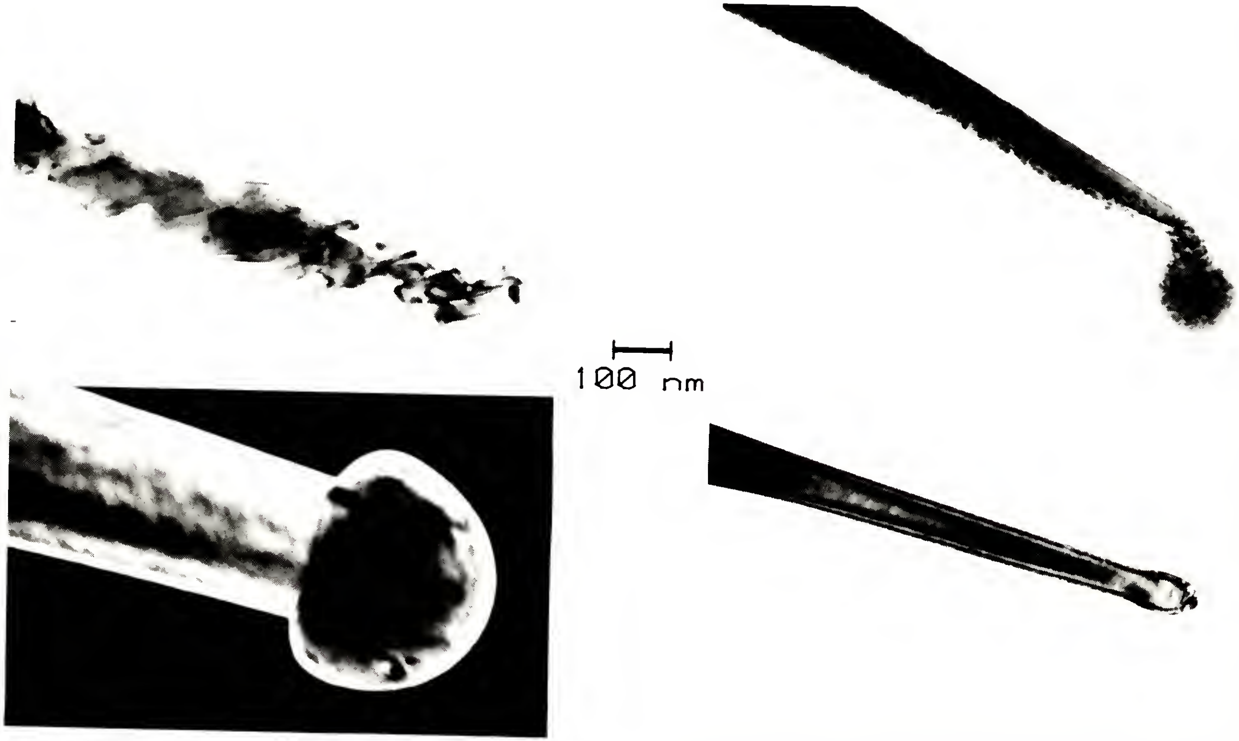

Figure III-11 Four examples of Ni specimens which for obvious reasons are not suitable for use with the method discused in text.

suitable for applying the geometric model used to reduce the data. ed in the 4909 file manager when they were collected. All of the files related to a particular profile have the same file name (which will be referred to as the generic filename) except for the file extensions. The original spectra are stored on files restricted to 500 records in length and having the extension, ".Fn", where n refers to the n^{th} file of the profile. The peak values are stored in files with the extension, ".PFn", where n refers to the n^{th} peak of interest except when n = 0. Specific experimental data are stored in the file, generic.PF0, including the number of spectra collected the number of peaks examined with "PEAKPICKOFF.FAST" and their masses, etc. The file generic.PF1 contains the data for the reference peak. This peak is the primary matrix peak for the specimen. For example, for tungsten tips it is W^{+3} and for nickel it is Ni^{+2}. After the generic.PFn files are generated, the original spectra files, generic.Fn, can be deleted. This is done because they require a large amount of storage space on the file manager and must be erased for further profiles to be performed. The generic.PFn files are then used to find the cumulation files. There are two problems with using the signals as found by "PEAKPICKOFF.FAST" which will be discussed below.

The first problem deals with the d.c. offset associated with the digitizer. The digitizer normally operates with an offset and this offset must be subtracted from the waveform. There is no value of the d.c. offset that can be read from the digitizer and therefore it must be found through software. This is done by using a single value in the first waveform collected and subtracting it from all subsequent spectra.

The use of this single value can lead to a slightly non-zero d.c. offset. When the peak values from several hundred spectra are summed, there is a significant component which will be included. The second problem is that there is always a certain amount of noise in the waveform. This is alleviated somewhat with the signal averaging which is done with the digitizer. The typical peak-to-peak levels in a waveform signal-averaged with eight traces are approximately 0.5mV. Once the d.c. offset level and discriminator level are found, the offset level is first subtracted from each peak value and that value is tested to see if it is above the discriminator level. If it is not, the value is set equal to zero. This also prevents negative values from occurring.

The program, "DATAREDUCER", is used to find the cumulative peak values from the generic.PFn files and it is also used to determine the d.c. offset and the discriminator values. It produces two file types, generic.CUMn and generic.CUMDISCn. The first file type is simply the cumulative file of the corresponding generic.PFn file. The first graphic output from this program is a plot of the cumulative peak of interest versus the cumulative reference peak. An example of this is shown in Figure III-13a for a nickel specimen implanted with nitrogen. After observing all the spectra in this profile (≈1200), it is asserted that between the two indicated points on this curve the N^+ peak is no longer appearing. The positive non-zero value of the slope of this portion of the curve is a consequence of the d.c. offset in the peak values. The d.c. offset is found by marking the two indicated points on the curve with a cursor and averaging the peak values between them. Using this value and a discriminator level of .5mV, the second file type,

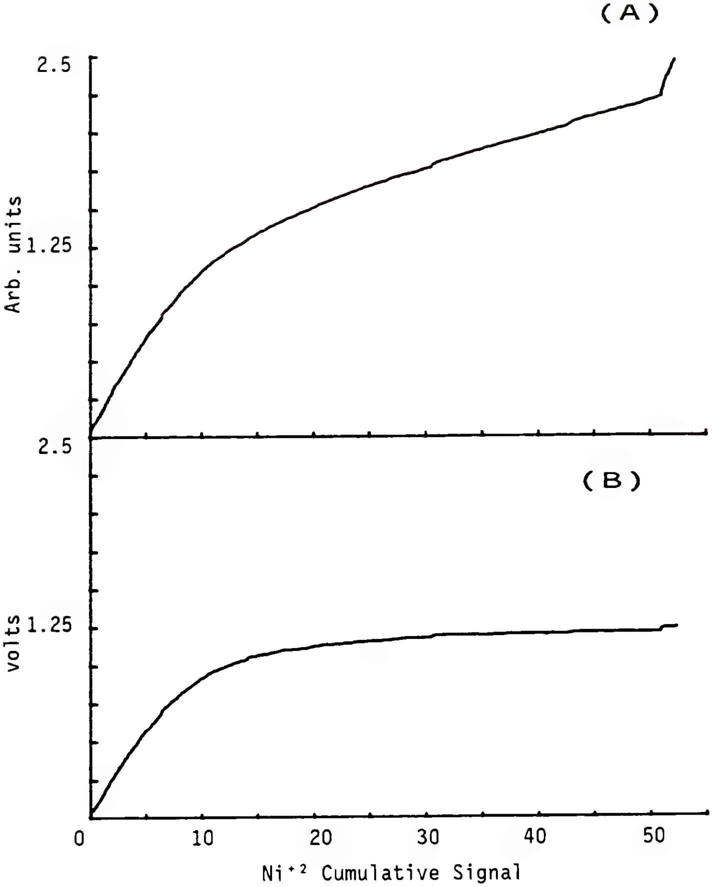

Figure III-13 Unprocessed and processed cumulative N^{+} signal versus cumulative Ni^{+2} signal. a) Unprocessed cumulative N^{+} from the program, "DATAREDUCER." b) Output from program after d.c. level has been stripped subtracted and discriminated.

generic.CUMDISCn, is created. Figure III-13b is the second graphic output of this program showing the result of this procedure applied to the curve in Figure III-13a. Ideally the minimum value of the d.c. offset is found which just makes the curve flat in order that no signal is lost in the process.

The two methods for obtaining the cumulative curve versus depth, ring counting and geometric calculation, both require that the data are processed through "DATAREDUCER" to obtain the d.c. offset levels. When the depth scale is to be calculated from geometric parameters, "DATAREDUCER" will prompt for the values of α and l_0 and the program will continue in order to generate the cumulative peak signal versus depth. The output from this section of the program is saved in the file, generic.CUMVSRINGn. If, on the other hand, the profile was done by ring counting, then "DATAREDUCER" is stopped when the question for geometric parameters is printed on the screen and the cumulative peak signal versus depth will be found using the program, "CUMVSRING." The only information from "DATAREDUCER" which needs to be passed to this program is the d.c. offset level. It also requires that the file, generic.CNT, has already been created and contains the pulse number corresponding to each ring collapse. The output from this program will create the file, generic.CUMVSRINGn.*

Figure III-14 shows a comparison of the steps involved in reducing the IAP data to give the cumulative peak signal versus depth for the two methods. It also serves as a summary for the different files created for

---

* This file has the same name as the output from "DATAREDUCER" with no distinction made about the method of data collection. This file name can only be produced by one of the programs, not both.

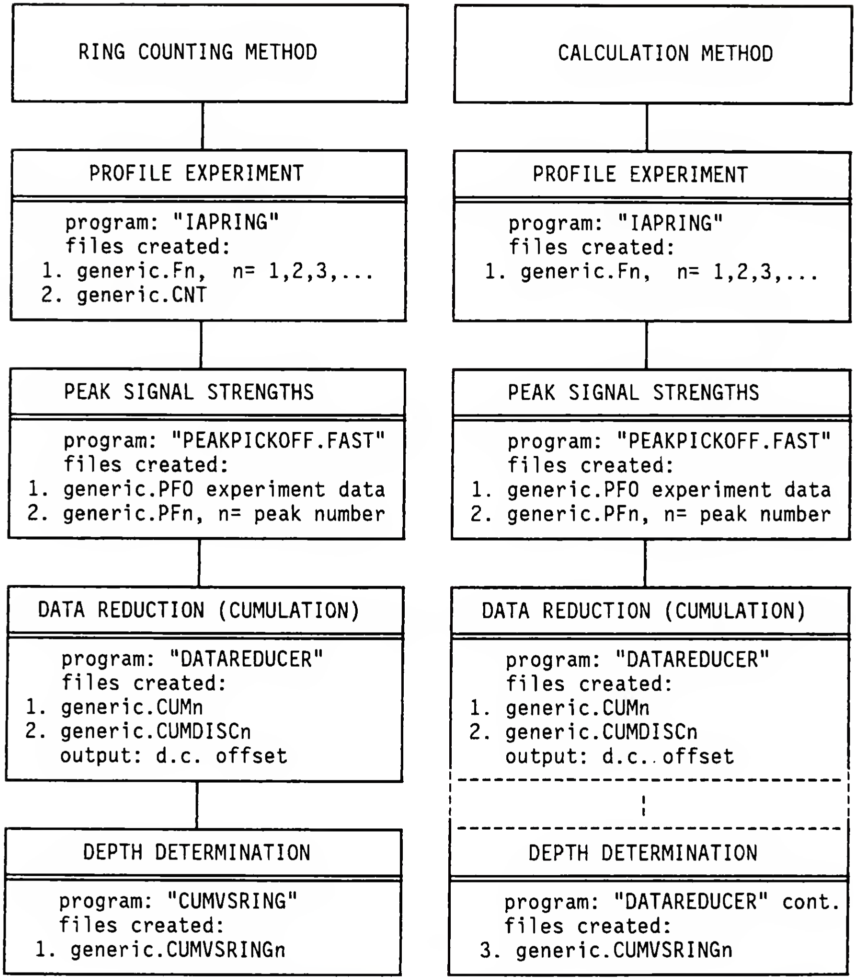

Figure III-14 Direct comparison of the data processing steps of the two IAP profiling methods, ring counting and calculation. The word, generic, applies to the part of the file name common to all the files created with respect to a particular profiling experiment. All of the output files are stored as singly-indexed arrays and the values can be input into the Tektronix 4052A graphic system easily. Only a few commands are then needed to produce a desired graph.

each method. After these files are generated, the program, "IAP2TAPE", is used to save specific spectra on magnetic tape prior to deleting the generic.Fn files from the 4909 file manager.

Effects Of Field Ionization Imaging And Evaporation

This section has two goals. The first is to discuss the results of a set of experiments designed to understand the effects of the high electric field on the implanted defect structure. The second is to point out interesting observations related to the application of the field which may affect experiments performed in the FIM/IAP.

Field Induced Stresses

A major problem associated with all FIM based studies is a lack of experimental knowledge on the influence of field-induced stresses within emitters on microstructure at the atomic level. For example, how does the electric field generated stresses affect the defect structure, the distribution of implanted species, or the value of the evaporation field compared to an unimplanted tip. As discussed in Chapters I and II, very high stresses are present in the emitter due to the presence of the electric field. It was shown that these stresses are sufficiently high to cause dislocations in the emitter's shank to sweep out of the specimen (see Chapter II, Figures II-17 and II-20). The purpose of the present work was to establish the procedures for using the FIM/IAP to profile ion-implanted species into materials. The question first arises as to what effect the field has on the implanted defect structure. The most direct way to determine the effects of field induced stresses on the implanted structure is 1) to image the implanted specimen in the

TEM, 2) then transfer it back to the FIM for imaging, and finally 3) transfer it back to the TEM and re-image using exactly the same imaging conditions as in step 1). The major difficulty with this procedure is obtaining exactly the same TEM imaging conditions in steps 1) and 3). A very small angular difference (i.e. a fraction of a degree) in beam orientation can significantly change the TEM image that arises from diffraction contrast. This is illustrated in Figure III-15. The Ni specimen in Figure III-16 was first field evaporated at 10 kV in the FIM/IAP (T=65°K) and then implanted with 8 keV He^+ ions. The specimen was then transferred to the TEM and imaged using a (111) "two-beam" imaging condition (Figure III-16a). Next, the specimen was taken out of the holder and stored in a desiccator for three days. This step approximated a typical experiment and allowed for the randomization of the microscope parameters: alignment, focus, eucentricity, astigmatism, etc.--controls normally altered in a multi-user, TEM facility. Figure III-16b shows the same specimen after re-imaging in the TEM; using as closely as possible, the same imaging conditions previously employed (including exposure time). This sample was then transferred to the FIM/IAP and a voltage of 5 kv was applied without imaging. This somewhat low voltage was chosen because implanted samples were found independently to have a significantly reduced field evaporation voltage. Since spectra are collected while the d.c. voltage is slowly raised during the usual analysis in the FIM/IAP, the choice of 5 kV approximates the point where adsorbed surface species would start to field desorb and be collected in the TOF imaged under the same imaging conditions (Figure III-16c). The conclusions from the above experiment

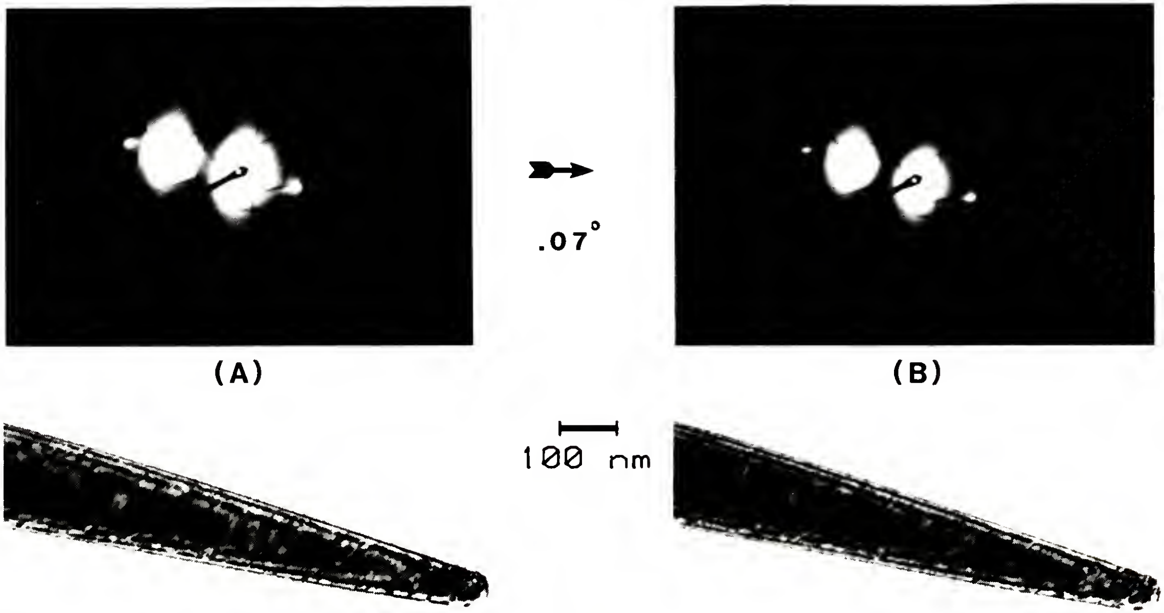

Figure III-15 Effect of TEM image with a slight rotation. a) This shows the diffraction pattern and bright field image of a He^+ implanted Ni specimen as seen in the TEM (image rotation with respect to diffraction pattern is not corrected). b) Same specimen as in a) rotated in a counter-clockwise sense about the emitter's axis. The diffraction contrast of the defects does change.

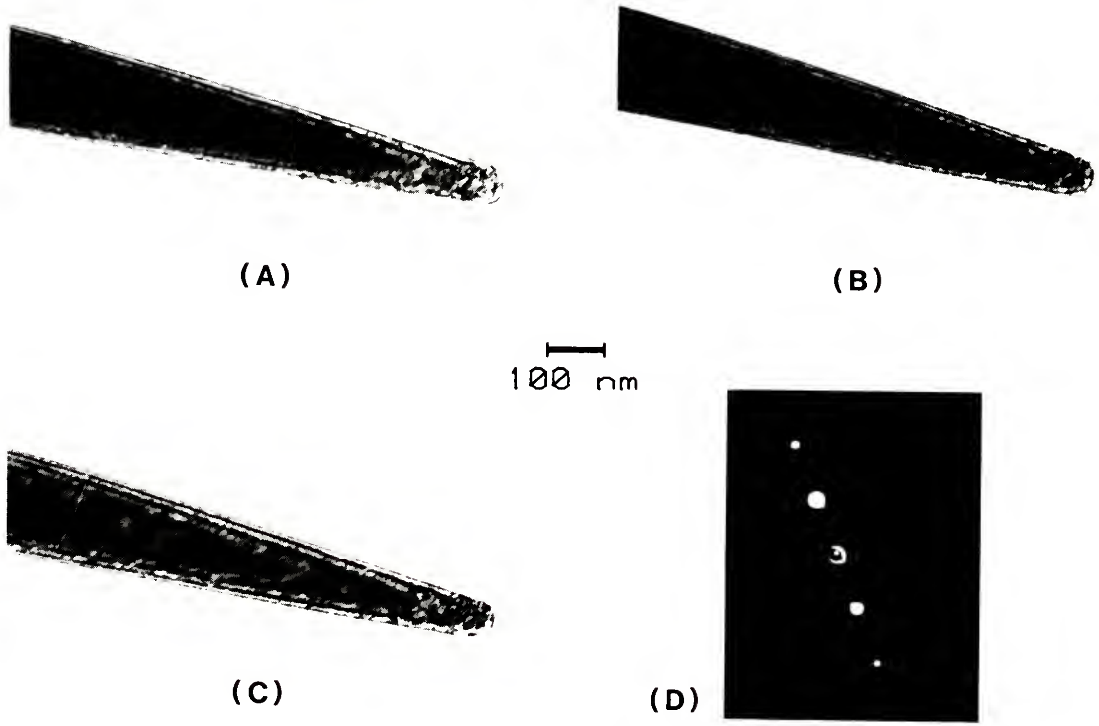

Figure III-16 Effects of the field applied in the FIM observed by TEM. a) Initial He^+ implanted Ni specimen. b) Same specimen after three day storage, same imaging condition as in a). c) Same specimen after applying 5 kV to it in the FIM under cryogenic conditions. d) Diffraction condition common to all micrographs. It can be seen that the defect density is essentially unaffected.

were ambiguous. The implanted defect structure density is apparently the same; however, it can not be said for certain whether the defect structure had been rearranged slightly. The ambiguity is in large part due to the extreme sensitivity of these TEM images to the precise diffracting conditions. The question still remains as to what the effect is of the field-induced stresses on the implanted defect structure.

Another experiment using the "field-effect" TEM holder can yield a little additional information on the influence of field induced stresses on defect microstructure. A nickel specimen was first field evaporated at 3 kV in the TEM (at room temperature). It was then removed and implanted with 8 kev He^+ ions. TEM images were recorded before and after the application of 2.5 kV at room temperature, without changing any imaging conditions in the TEM. (The lower voltage was chosen to assure that no field evaporation occurred as a result of He^+ ion implantation lowering the field evaporation voltage.) Figure III-17 shows the results. There are essentially no differences between the two micrographs. Although this is an encouraging result, it must be viewed judiciously. Because field evaporation is a thermal process, the applied field was limited to the evaporation field at room temperature for Ni. This is only approximately 30% of the field the sample "sees" in the FIM at cryogenic temperatures. In addition, the flow stress of the Ni specimen is also temperature dependent. Until a cryogenic "field-effect" holder is designed and constructed, the answer to the persistent question of field induced stresses influencing defect microstructure will remain only partially answered.

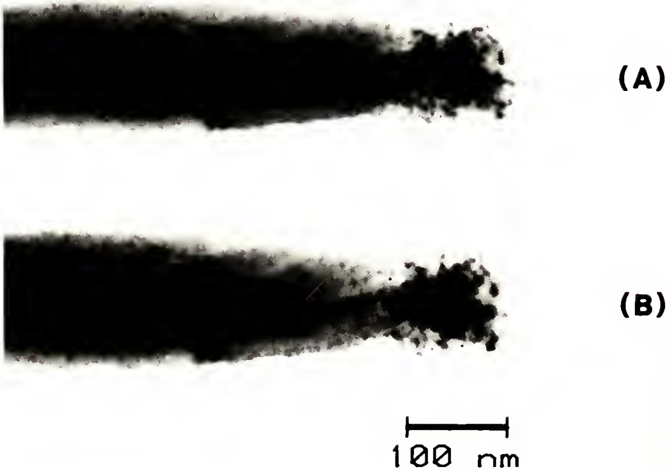

Figure III-17 Field-Effects of He^+ implanted Ni observed *in situ* TEM using the FIM/TEM "Field-Effect" holder. a) He^+ implanted Ni emitter imaged prior to application of voltage. b) After 2.5 kV applied. No differences between the micrographs are observed.

Field Evaporation Observations

During the course of this study, several interesting observations were made with respect to field evaporation and features in the IAP spectra. Some are of obvious importance in interpreting the data, others are only reported. They are summarized in this section.

Dependency of evaporation field on imaging gas

It has long been known that the presence of an imaging gas affects the evaporation field. Nishikawa and Müller showed the dependency of evaporation field of W on the He and Ne pressure in the range 1×10^{-4} to 2×10^{-3} Torr [81]. The presence of He or Ne lowered the evaporation field of W by approximately 1.5% and 10%, respectively in this pressure range. During the course of the present study, W was analyzed and the field dependencies at He and Ne of somewhat lower pressures (1×10^{-6} Torr range) were investigated. The voltage required for field evaporation of W in the presence of He was found to be 2-3% less than under UHV conditions (5×10^{-10} Torr). Field evaporation of W with a partial pressure of 1×10^{-6} Torr Ne was approximately 8% less than under UHV. When this experiment was repeated with Ni, the reverse effect was found! With Ne present at pressures between 2×10^{-6} and 1×10^{-5} Torr the evaporation voltage was found to be about 5% higher than for field evaporation under UHV. There is as yet no satisfactory explanation of this difference, but it is often important that an investigator be aware of such effects. For example, if the IAP is operated with an imaging gas present and used as a known mass, if the gas is removed, the d.c. voltage would need to be changed accordingly. In the case of Ni this would be especially important because of the possibility of losing the sample by "flashing", (see next section) since the voltage would be substantially higher than needed under UHV conditions.

Implantation lowering of evaporation field

Part of the specimen preparation procedure for all the Ni specimens used in the present study is to field evaporate them to a d.c. voltage of 6.00 kV. There are several reasons for doing this. Although most of the samples start to image from 2-5 kV, better than 90% of them will have an imageable area larger than that projected on the screen when evaporated to 6 kV. This is a critical selection criteria for specimens, the reason will become clear in the section on specimen geometry. There is another convenience in choosing this starting voltage. With the combination of d.c. and pulse voltages equivalent for field evaporation at 6 kV, the flight time for the Ni^{+2} signal is about 0.9 usec with full scale being 1.0 usec. This means that the time base need not be changed as the voltage is increased.

In the early stages of this study, specimens were prepared as above and then implanted with He and/or D. The d.c. voltage was raised relatively quickly to the d.c. value required prior to implantation, the pulse voltage remaining fixed for all spectra. Most specimens "flashed" very early [82]. Flashing refers to a term used to describe the fracture of the specimen due to the field. When such an event occurs, one sees a sudden flash on the phosphor screen, hence the term "flashing." In an IAP spectrum, a flash can be recognized by a d.c. offset in the waveform part-way through the trace. It was first thought that the implanted species were embrittling the specimens and the high stresses were causing them to flash. After some trial and error, the d.c. voltage was finally started at zero, and spectra collected as it was slowly raised. At approximately 96% of the voltage previously used (with or without imaging gas), equivalent signal levels appeared. Ion implantation appears to lower the field required for field evaporation. In Ni, this decrease in field strength has been observed so far for the ions, H^+, D^+, He^+, and N^+ .

This effect was also seen in the FIM/TEM "Field-Effect" holder used in the TEM (Chapter II). A sample was field-evaporated in this holder with a voltage of 3 kV. The specimen was implanted and then transferred back to the TEM. The image was recorded and a voltage of 3 kV applied again. The image was recorded again. Upon comparing the two images, approximately 23 nm of the specimen was field evaporated. Subsequent experiments of this type used 2.5 kV for the second applied voltage and prevented removal of material after the implantation [82].

Low field desorbed species

Panitz and Hren have seen the low field desorption of CO^+ from the surface of Pt, Fe, and W in the IAP*. There is a range of field values far below the value for the evaporation of the emitter in which the CO^+ signal appears. In fact, this phenomenon can be used as a means of desorption imaging at low field strengths. During the experiment with Ni under UHV conditions (5×10^{-10}Torr) the CO^+ signal also appears in a small voltage range, also well below the evaporation voltage, when the voltage is raised from zero volts. Figure III-18 shows two examples of a spectra showing this peak, one at lower voltages in this range,and one at a higher voltage. Above this voltage range, the CO^+ peak does not

---

*Panitz, J. A., and Hren, J. J., private communication.

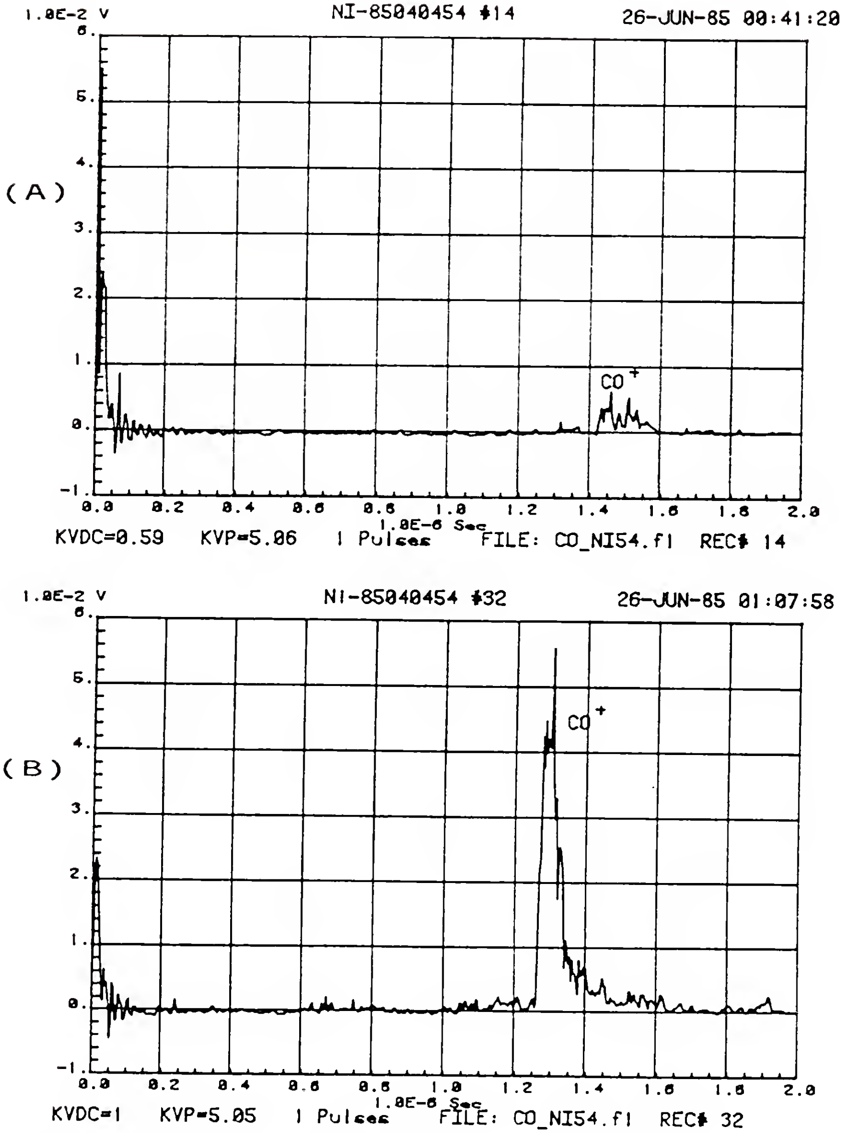

Figure III-18 Low-field spectra of CO^+ on Ni. Ni starts to field evaporate at KVDC=4.3. CO is not present above KVDC=2.

appear in any spectra. With the pulse value used in Figure III-18, Ni^{+2} signal appeared at approximately 4.5 kV d.c.

In addition to the CO^+ peak appearing when the voltage is raised, an H_2^+ peak also appears at approximately 85% of the voltage which causes field evaporation of the matrix. This peak disappears before the field evaporation voltage is reached, agreeing with the results of Kellogg and Tsong, discussed above [83].

He signal

Nickel and ion implantation were selected for the present study because of the previous work of Myers et al. on metal foils (See Chapter I.) They used implantation of He ions to create additional trap types for deuterium. A parameter used in their model to match the experimental curve with a theoretical curve was the number of deuterium atoms associated with a He bubble (trap). It was originally thought that IAP spectra could provide a correlation between He and D atoms from the respective signals in the spectra. He^+ implanted Ni samples failed to show any He^+ peaks in any IAP spectra. To check to see if He would show up in Ni spectra, it was backfilled into the chamber to various pressures while data collection was done. Helium peaks did not appear in any spectra. The difficulty is that the field evaporation field of Ni is less than the ionization field of He on Ni. It is evident that if the correlation of He and D experiment is to be performed, a refractory metal such as W must be used where the evaporation field is higher than the ionization field for He. This explanation is also consistent with results obtained by Kellogg using Mo and the Pulsed Laser Atom Probe (PLAP) [84].

Special Problems Associated With Hydrogen/Deuterium

There are only a few analytical instruments that can be used to analyze hydrogen. Among these, only the spatial resolution of the ion microprobe is close to the scale at which hydrogen interacts with crystal defects. However, even the ion microprobe (or microscope) has insufficient sensitivity to unfold hydrogen atmospheres at dislocations, grain boundaries or small dislocation loops, precipitates, or bubbles. A conventional atom-probe would have the desired small probe and sensitivity to study such problems, but it suffers from the poor statistics inherent with its use. That is, in the "probed volume" in a atom probe sample, only a small fraction (10^{-3}-10^{-4}) of the accessible imaging points is detected. Fortunately, the Imaging Atom Probe (IAP) has the same spatial resolution and sensitivity as a conventional atom probe, but it does not suffer from the statistical problem. It can be used to analyze a volume 10^2-10^3 larger than the atom probe. One objective of this study is to establish a reliable methodology for studying deuterium and its interactions with general types of crystalline defects using the FIM/IAP.

Although the IAP seems ideal for studying deuterium implanted into metals, there have only been two studies reported so far. [45,47]. (See Chapter I.) Both of these have used low implantation energies (80 and 250 eV) so that implantation depths were extremely shallow (10-40 Å). One study reported the observation of deuterium trapping to a grain boundary in tungsten and used *in situ* implantation. The other study required a series of rather relatively complicated control experiments to assist with the interpretation of results, because the deuterium implantation was carried out _ex situ_. There have also been doubts within the field-ion community about the feasibility of conducting representative _in situ_ implantation experiments because it would be so difficult to distinguish the implanted D from that field adsorbed from the UHV background. It is important that _in situ_ implantation be the means of introducing deuterium because this method eliminates the complex control experiments referred to earlier [47]. This section will show that it is possible to do _in situ_ deuterium implantation, when certain conditions are met.

The Deuterium Background (D_1^+)

It is well known that field-ion microscopic techniques are very sensitive to the presence of hydrogen. In fact this has been the single most important drawback to studying hydrogen with FIM techniques. In an IAP spectrum taken under UHV conditions, an H_1^+ peak is nearly always present. This is due to two primary reasons: 1) hydrogen is the most difficult residual gas to pump and is always a major constituent in any UHV system and 2) hydrogen is continuously field adsorbed on emitters, i.e., the rate of adsorption on the surface of the emitter is increased under the influence of the field itself. For both these reasons, deuterium and not hydrogen is used for atom probe studies. In addition many of the problems encountered and the controls required when implantation is carried out in a separate chamber can be overcome by _in situ_ implantation. The major remaining concern is whether the partial pressure of deuterium will increase sufficiently to be ever-present in the background spectra afterwards.

The vacuum history of the present FIM/IAP is completely known since this author was its primary designer and builder. It was known, for example, that the chamber had never been exposed to deuterium so there could be no D adsorption of consequence on the chamber walls. (The relative abundance of naturally occurring deuterium is 0.01%.) A very simple but extremely important experiment was done to demonstrate the feasibility of _in situ_ implantation of deuterium in controlling background pressure. Spectra from a nickel emitter were recorded prior to the opening the valve between the ion gun and the FIM/IAP chamber. The introduction of deuterium into the FIM/IAP was done by implanting into the side of the specimen holder. Beam conditions were D_2^+ at 40 μA/cm² with an approximate spot size of 2 mm in diameter for 4 minutes. The background pressure in the ion gun and the FIM/IAP prior to opening the valve for implantation for the first time was 6×10^{-6} Torr and 5×10^{-10} Torr, respectively. The pressure in the FIM/IAP increased to 8×10^{-10} Torr during implantation under the differential pumping conditions and remained constant until the valve was closed. The pressure dropped to 5×10^{-10} Torr in less than 5 minutes thereafter. A small D_2^+ peak appeared on a residual gas analyzer with an approximate 10% increase on the $H_2(D_1)^+$ peak. The first IAP time-of-flight spectra of the Ni taken after deuterium was introduced showed a large D_1^+ peak, comparable to the H_1^+ peak (Figure III-19). Subsequent spectra showed somewhat smaller peaks.

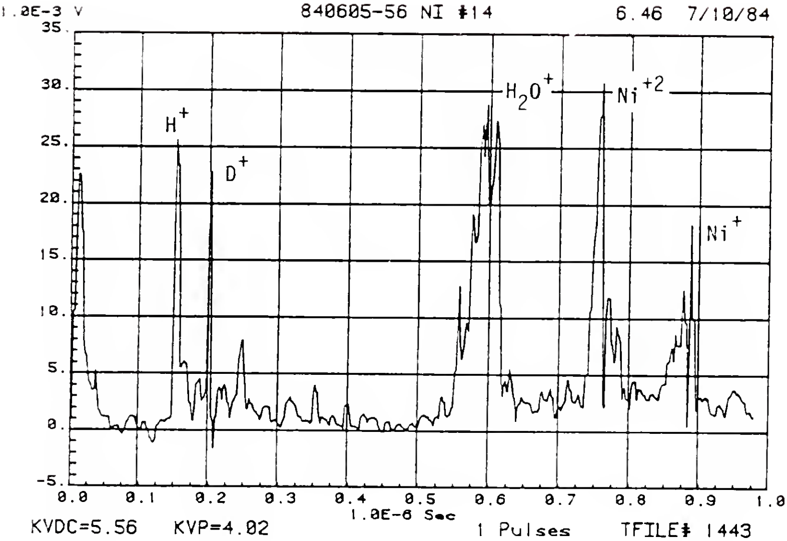

Figure III-19 First spectrum of a Ni specimen after deuterium admitted into the FIM/IAP chamber by implantation into the side of the specimen holder, simulating actual implantation conditions. The H_1^+ peak occurs at 0.15 μsec and D_1^+ at 0.2 μsec.

At first glance, this result could be quite discouraging. However, previous experience with the IAP showed that the ever-present H_1^+ signal is dependent on the time interval between desorption pulses under UHV conditions. At small intervals, the H_1^+ signal is reduced considerably. The D_1^+ signal can be eliminated completely by pulsing rapidly enough. Figure III-20 shows two spectra, one with pulsing occurring at 2.5 sec intervals prior to collection of the spectrum and the other without. The D_1^+ shows up only in the spectrum taken without the "pre-pulse." These results indicate that there should be a maximum time interval below which no D_1^+ will be present. The time interval between pulses was varied and spectra collected. With an interval of 20 sec, D_1^+ shows up in approximately 50% of the spectra; at 30 sec, it is present greater than 90% of the time. Since data collection is done with intervals of less than one second, any D_1^+ signal appearing in the analysis will come from implanted and not background deuterium.

It was thought after the above results were found that the quantity of deuterium in the background would increase with time and that this maximum time interval between pulses would eventually decrease to a point where background deuterium would be present in all spectra. However, a few days after the first experiments, it became necessary to bring the FIM/IAP chamber up to atmosphere. After the vacuum was re-established the D_1^+ peak was not detectable. Apparently, the deuterium was flushed out of the chamber or its partial pressure reduced to levels undetectable with the IAP. Thus, the build-up of deuterium can be prevented simply by bringing the chamber up to air or by flushing with a suitable gas (e.g. N_2, see Chapter II).

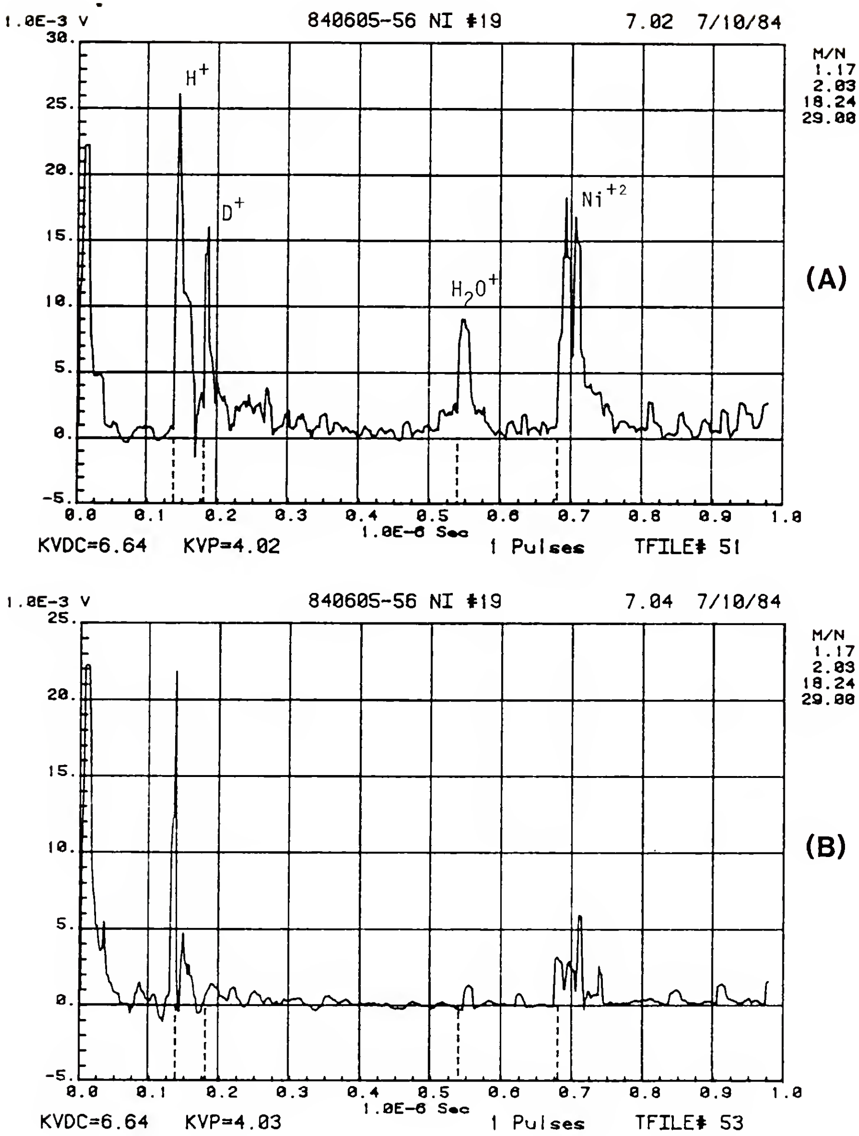

Figure III-20 Influence of pulse interval on D_1^+ signal. a)First spectrum of Ni after deuterium introduced into chamber, no "pre-pulsing." b) Pulsing occurring every 2.5 sec between pulses prior to collection of spectrum. No D peak is seen.

Another related problem with respect to the D_1^+ background signal is the ratio of the H_2^+ to H_1^+ signal. Kellogg and Tsong have shown that the ratio, H_2^+/H_1^+, field desorbing from an Rh surface is dependent on field strength [83]. This ratio goes to zero for the fields required for evaporation when the specimen is held at cryogenic temperatures. No spectrum acquired prior to the introduction of deuterium into the main chamber had an H_2^+ peak. To date this includes spectra taken from specimens of tungsten, platinum, iron, nickel, and an Fe-3at.%Mo alloy. Although this is true for specimens held at cryogenic temperatures during analysis, it will need to be taken into account when specimens are heated. (See Appendix A and the program, "PROFILER" in Appendix D.)

Deuterium Implantation Conditions

After the ion gun is set up and stable beam conditions are found, the valve is opened between the FIM/IAP and the ion gun, the faraday cup in the beam line is swung out of the way, and the current at the target is optimized with the horizontal and vertical deflection controls. The beam current, various pressures, anode voltage, emission current, magnet setting, acceleration voltage, and time of implantation are all recorded. The valve between the two chambers is closed as soon as the implantation is complete in order to minimize the increase in deuterium partial pressure in the FIM/IAP. The pressure in the FIM/IAP during implantation is always less than 1×10^{-9} Torr. The beam current for D_2^+ varies between 0.1 and 0.5 μA with a spot size at the target approximately 2 mm in diameter. The IAP background signal is assumed to be negligible when spectra are collected with short intervals between pulses. Figure III-21 shows the results of a background experiment performed to monitor the build-up of deuterium in the IAP chamber. The spectra from an un-implanted specimen were collected after several Ni emitters had been implanted with deuterium. The cumulative time that the valve was open for these implantations was approximately 26 minutes. The time interval between pulses was varied between 1 and 50 seconds with 5 second steps. At each pulse interval chosen, ten spectra were collected with one pulse per spectrum. The peak value of the D^+ peak was found, with a discriminator level of 0.3×10^{-2} volts. Figure III-21a shows the results. There are ten points per interval, values which are less than the discriminator level are set to zero. Figure III-21b shows a sample spectrum from this experiment in order to compare the voltage values of Figure III-21a with the relative signals seen in the raw experimental data. Figure III-21b corresponds to one of the values at the 15 sec interval, and it can be seen that the discriminator level is too low, because there is no D^+ signal in this spectrum. It is, however, better to have this value too low than too high in order that no signal is missed. As was discussed in the depth profiling section of this chapter, the difference can be handled after the data are processed.

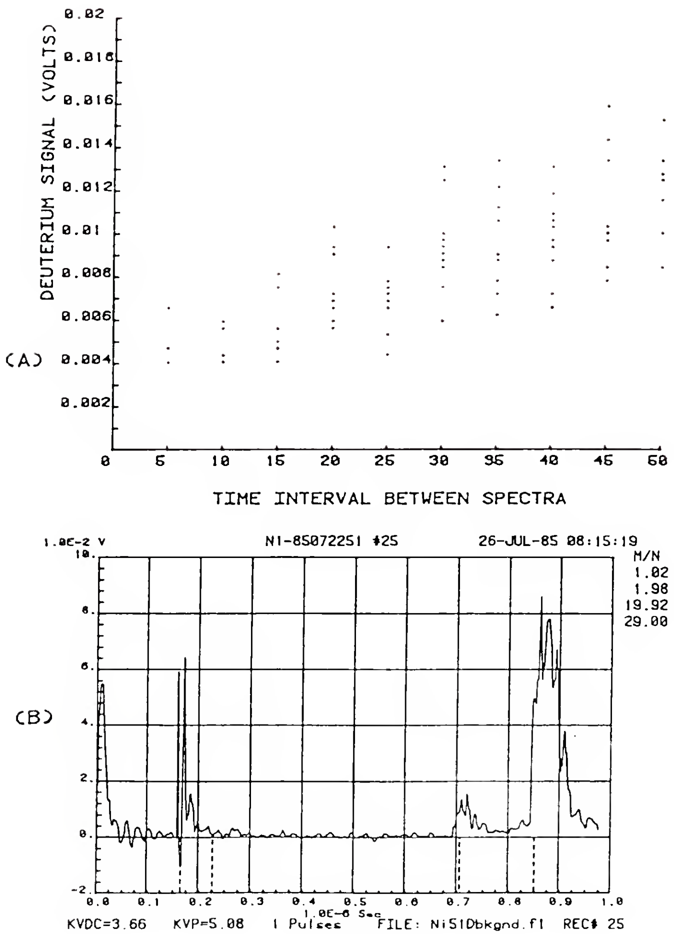

Figure III-21 Background D^+ signal after a total cumulative D_2^+ implantation time of 26 minutes. a) D^+ signal values were found with the use of the program "PEAKPICKOFF.FAST" using a discriminator level of $.3\times10^{-2}$ volts. The horizontal axis corresponds to the time interval between pulses for the spectra collected. Ten spectra were collected at each interval. b) Sample spectrum of the D^+ background experiment in (a). The interval for this spectrum is 15 sec and no D^+ is present.

CHAPTER IV
RESULTS OF IMPLANTATION EXPERIMENTS

This chapter is divided into four main sections: 1) "Nitrogen Implantation In Nickel", 2) "Nitrogen Implantation In Tungsten", 3) "Deuterium Implantation in Nickel", and 4) "Carbon In Nickel and Tungsten." Each section will give the results of the experiments performed with respect to the particular ion used. These results will include those of both in situ and ex situ implantation. In the next section, there is also included a brief description of the preparation and handling of the specimens used in these studies.

Specimen Preparation

The nickel specimens used for the profiling experiments in this study have been well-annealed (900°C for 4½ hrs.). The specimens were first put into the FIM/IAP where they were d.c. field evaporated to 6 kV and then imaged. They were then transferred to the TEM where the images and diffraction conditions are recorded in order to compare with post-profile images. There were no defects apparent in the TEM images, either in the near-apex region (where micrographs are recorded) or in the shank (where micrographs are not recorded, but visual observations are made). In the case of ex situ implantation, the emitters were transferred to the ion gun for implantation and then returned to the FIM/IAP for analysis. Prior to in situ implantation the voltage on the specimens was again raised to 6 kV where slight evaporation still occurs, and they were re-imaged at the BIV (Best Image Voltage). There were two reasons for doing this: 1) the field evaporation "cleans" the specimen surface of adsorbed gases, the slight oxidation formed during exposure to atmosphere, and any contamination layers which form during electron irradiation in the TEM; 2) the crystallographic orientation of the specimen can be determined and positioned with respect to the screen. The implantation of the specimen was carried out as quickly as possible after the FIM imaging.

After imaging and prior to implantation the titanium sublimation pumps, both on the beam line and the FIM/IAP chamber (for in situ implantation), were activated to insure the highest possible pumping speed for deuterium during implantation. The specimen was then oriented towards the ion gun port and the manipulator settings were adjusted with those found by the ion gun alignment procedure (see Appendix B). The high voltage cable to the FIM/IAP was replaced with a cable leading to an electrometer used for monitoring the beam current.

Only slight variations of these procedures were required for samples in the other experiments described in this chapter. The basic goal was to provide a clean, well-defined tip (i.e. sample geometry) for the ion implantation and have the specimens characterized in the TEM. In the case of nickel, this characterization was principally for sample selection criteria and obtaining geometric parameters. In the case of nitrogen in tungsten, where the implanted specimens could be viewed while profiling, the need for TEM was relaxed since samples can be adequately characterized in the FIM.

Nitrogen Implantation In Nickel

The profiling of nitrogen implanted into nickel was done using the calculation method as opposed to the ring counting method for determining the depth scale. (See Chapter III for a complete description of both methods.) The image could not be viewed during field evaporation when using the calculation method because: 1) the damage produced by the energetic nitrogen ions is so great that ring collapse of the planes is extremely difficult to discern and 2) the neon used as the imaging gas for nickel suppresses the detection of the N^+ signal. (This point will be discussed further in a later section of this chapter.) The most important parameter determining the amount of damage resulting from implantation is the energy deposited into the substrate. As was discussed in the section "Microstructure Of Implanted Metals" in Chapter I, this is determined by the primary energy and the relative masses of the ions and target atoms. The maximum energy transferred to a nickel atom from an incident nitrogen ion is 60% of the primary energy. This was the reason for the lack of ring definition in the FIM image, even for the relatively low energies used in this study (2.5-9 keV). In comparison, the light elements, helium, deuterium and hydrogen transfer a maximum of approximately 24%, 13%, and 7% of their energies to nickel atoms, respectively, and are low enough for the ring structures to be discerned. Since the image could not be viewed, profiles were determined under UHV conditions and TEM micrographs were taken before and after profiling in order to determine the geometric parameters needed to calculate depths as discussed Chapter III.

The resulting profiles for nitrogen implanted into nickel were quite surprising. None of the profiles show a distinct implantation peak (i.e. a distinct range). Rather, they showed a general falloff of nitrogen signal from the surface with occasional bursts of signal at depths greater than the theoretically calculated range. (See Figures IV-1 and IV-2 as examples.) These results will be discussed below. Implantation was accomplished using both *in situ* and *ex situ* conditions, with respect to the FIM/IAP chamber, with no apparent differences in the experimental profiles except those pertaining to the presence of carbon in specimens implanted *ex situ*. This last point will be covered separately in this chapter.

Figure IV-1 shows the result of a profile from a Ni tip implanted with 10 keV N_2^+ to a fluence of $\approx 1.0\text{x}10^{16}$ N^+/cm^2. Figure IV-1b is the cumulative peak signal versus the depth in (111) planes. The d-spacing for Ni_{111} planes is 2.03 Å. Figure IV-1a is a numerical 3-point derivative of the curve in Figure IV-1b computed by using the Tektronix 4052A's ROM routine, "DIF3"[*], on both the y-axis array (cumulative N^+ array) and the x-axis array (ring count array), and then dividing the result of the y-axis array by the result of the x-axis array[**], and finally plotting versus the original x-axis array. This apparently complex manipulation of data is actually a simplified way of obtaining a curve which closely approximates the derivative of the original cumulative profile. It is accomplished with only three simple BASIC statements. The resulting curve reflects the composition profile that one is normally accustomed to seeing with other techniques. Figure IV-1 is compared with Figure IV-2 which was implanted with 5 keV N_2^+ ions to a fluence of = $2x10^{16}$ N^+/cm^2. Note that the two N^+ profiles have approximately the same shape and depth distribution. In general, this is true for all the nitrogen profiles in nickel regardless of implantation energy or whether in situ or ex situ conditions are used. However, there are some slight differences between profiles as will be discussed below. Note that the profiles have a relatively large surface peak (within the first 1-2 atom layers) followed by a distribution which falls to zero over about 20-25 atom layers.

---

[*] The BASIC calling statement for "DIF3" is 'Call"DIF3",A1,A2', where A1 is the original array and A2 is the differentiated output array, with the assignments: A2(1)= [-3·A1(1)+ 4·A1(2)- A1(3)]/2, A2(N)= [A1(N-2)- 4·A1(N-1)+ 3·A1(N-1)]/2, and A2(i)= [A1(i+1)- 3·A1(i-1)]/2 for i = 2,3,..., N-1.

[**] Array division is done element by element, i.e. A=A1/A2 is defined as A(i)= A1(i)/A2(i).

The curves in Figures IV-1 and IV-2 are missing features that are common to many of the profiles, sudden and unexpected "bursts" of N^+ (Figure IV-3). Such "bursts" of N^+ signal during the profiling experiment occurred during periods of gentle (slow) field evaporation, and were not associated with sudden increases in the d.c. voltage level. Although, rapid evaporation was more likely to induce the occurrences of these "bursts." In addition, they often occurred during long intervals between spectra during which the N^+ signal was not detected at all and from depths well beyond expected values. A typical "burst" manifested itself as a sudden jump in the cumulative peak versus depth curves as seen in Figure IV-3. These "burst" events could also be detected during profiling. Differing from a flash in a which specimen fractures, a large signal flash could also be seen at the screen corresponding to the pulse producing the "burst." There was no precursor to these events and there

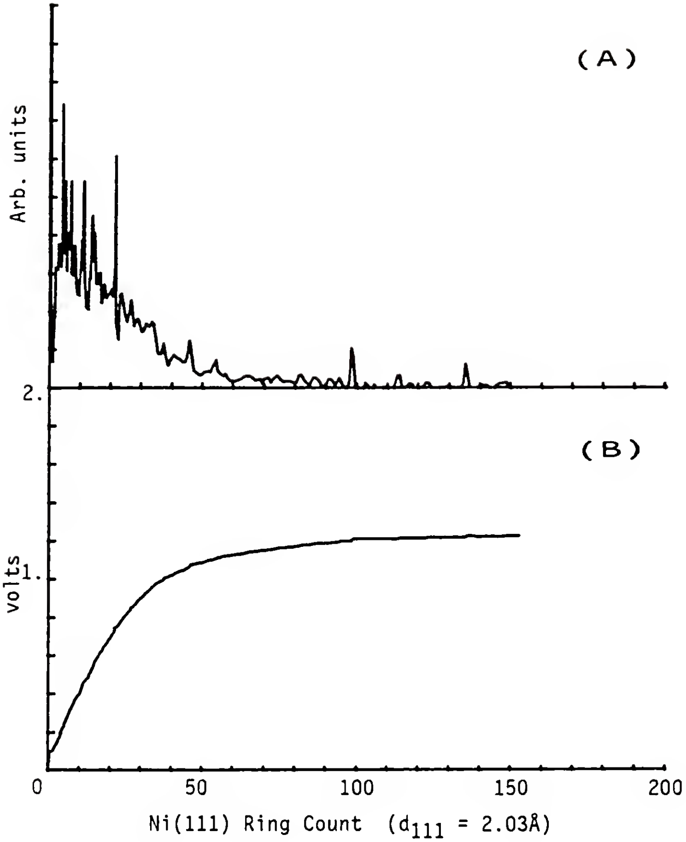

Figure IV-1 Profile of 10 keV N_2^+ implanted Ni specimen to a fluence of $1\text{x}10^{16}$ N^+/cm^2. a) Three-point derivative of b) cumulative N^+ signal versus calculated ring count.

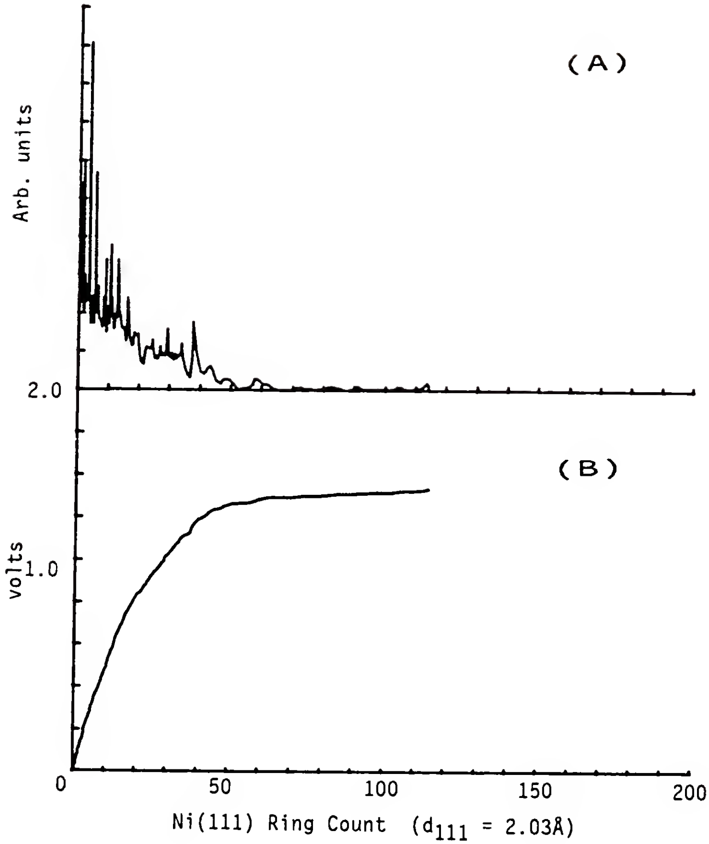

Figure IV-2 Profile of 5 keV N_2^+ implanted Ni specimen to a fluence of 2×10^{16} N^+/cm^2. a) Three-point derivative of b) cumulative N^+ signal versus calculated ring count.

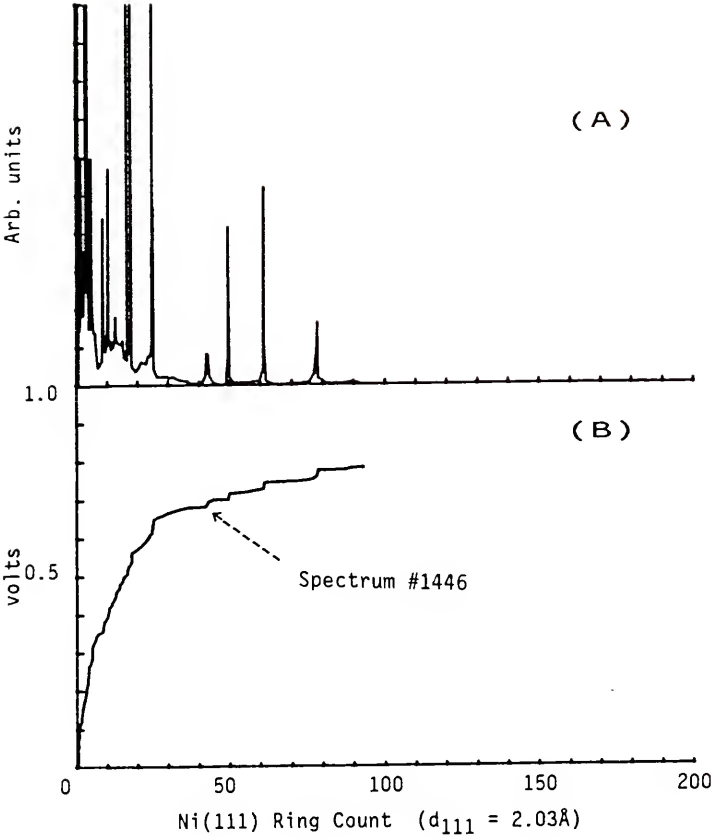

Figure IV-3 Profile of 10 keV N_2^+ implanted Ni specimen to a fluence of 1.4×10^{16} N^+/cm^2 showing the sudden "bursts" during data collection. a) Three-point derivative of b) cumulative N^+ signal versus calculated ring count. A sequence of spectra associated with the indicated point are given in Figure IV-4.

Figure IV-4 Spectra associated with N^+ release in Figure IV-3. a) Spectrum prior to the indicated "burst" in the profile in Figure IV-3, b) "Burst", c) next spectrum after "burst". Note that rate of field evaporation was moderate and that the "burst" was not due to a voltage increase.

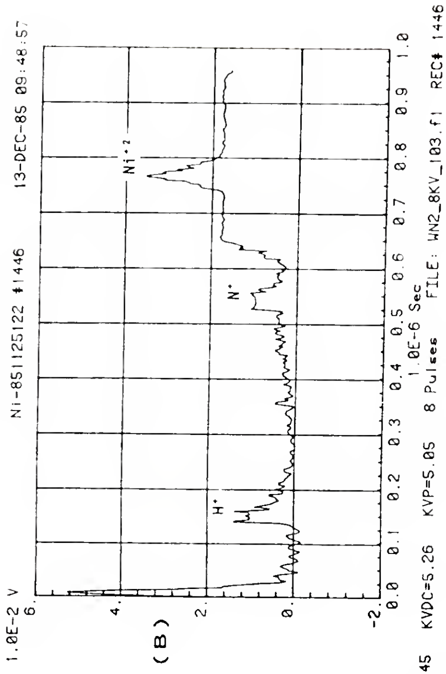
(B)
Ni-851125122 #1446 13-DEC-85 09:48:57
1.0E-2 V
6.
4.
2.
0.
-2.
H⁺
N⁺
Ni⁺²
0.0 0.1 0.2 0.3 0.4 0.5 0.6 0.7 0.8 0.9 1.0
1.0E-6 Sec
KVDC=5.26 KVP=5.05 8 Pulses FILE: WN2_8KV_103.f1 REC# 1446

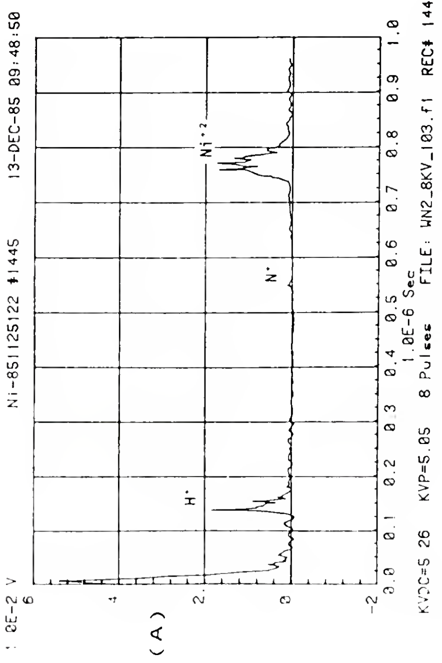
(A)
Ni-851125122 #1445 13-DEC-85 09:48:50
1.0E-2 V
6
4
2
0
-2
H⁺
N⁺
Ni⁺²
0.0 0.1 0.2 0.3 0.4 0.5 0.6 0.7 0.8 0.9 1.0
1.0E-6 Sec
KVDC=5.26 KVP=5.05 8 Pulses FILE: WN2_8KV_103.f1 REC# 1445

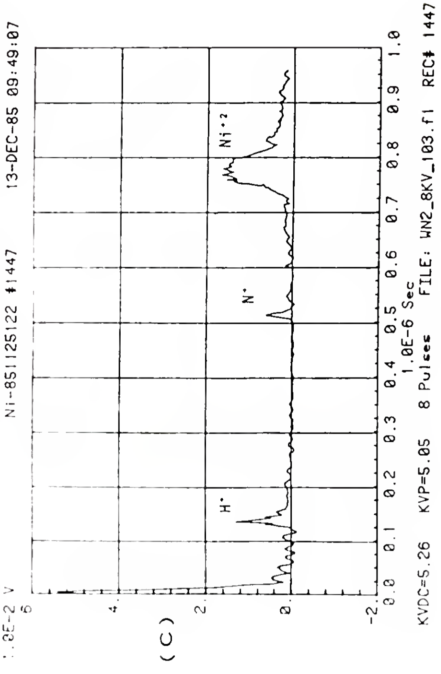
(C)
Ni-851125122 #1447 13-DEC-85 09:49:07
1.0E-2 V
6
4.
2.
0.
-2.
H⁺
N⁺
Ni⁺²
0.0 0.1 0.2 0.3 0.4 0.5 0.6 0.7 0.8 0.9 1.0
1.0E-6 Sec
KVDC=5.26 KVP=5.05 8 Pulses FILE: WN2_8KV_103.f1 REC# 1447

were indications that they were dependent on the evaporation rate. Often a large Ni^{+2} peak also occurred during a "burst". Figure IV-4 shows a sequence of three spectra with the middle one corresponding to the indicated "burst" in Figure IV-3. As can be seen in the spectra prior to and after the event, each have approximately the same Ni^{+2} and zero N^{+} signal levels.

These "bursts" should also be differentiated from the other types of spikes observed in the derivative profile curves. These are the result of a large N^{+} occurring during normal profiling. All atom probe work is subject to normal statistical fluctuations of this type and smooth output data as in other analytical techniques are not expected. Primarily the reason for this is that the probe is averaging over such an extremely small volume as compared to these other techniques. In addition, there also is the tendency for these larger peaks to occur when the d.c. voltage is raised to increase the evaporation rate. The frequency of these peaks correspond roughly with the frequency of voltage increases. It should be stated, however, that not every voltage increase produces one of these spikes. They are more likely to occur when the voltage increase produces rapid field evaporation over several spectra and it does not result in a "burst."

The lack of a well defined implantation maximum for nitrogen, the invariance of the profiling curve with respect to implantation energy, and the occurrences of the N^{+} "bursts" can be explained by a mechanism in which the nitrogen resists field desorption and tends to remain on the surface during field evaporation while the bulk nickel is removed. Such a mechanism has been seen before by Hren and Kellogg [85] in studying sulfur adsorption on the surface of nickel. Sulfur atoms deposited onto a nickel emitter were observed to resist field desorption over many layers before their removal even though the substrate was evaporated. The sulfur atoms could be seen as bright spots on the ledges of the nickel rings (evaporation was done in the presence of an imaging gas) and "clung" to the nearest ledge as atoms were removed. When the ring finally collapsed, the sulfur atoms would immediately migrate along the surface to the next ledge site. Only very vigorous field evaporation could desorb the sulfur from the surface. It seems very likely that nitrogen on nickel acts in the same manner as sulfur on nickel except that nitrogen is not as tenacious in binding to the nickel ledges as sulfur. In the present study the images could not be viewed during field evaporation for the reasons discussed above. Given such a sticking action, the true depth distribution of nitrogen implanted into nickel could not be measured. This mechanism also explains the "bursts" of N^+ at depths greater than that expected from the implantation parameters. It is well established among catalytic chemists that both sulfur and nitrogen poison the effectiveness of nickel substrates, sulfur more effectively than nitrogen. The present results and those of Hren and Kellogg may well be the atomic observation of the mechanism by which such poisoning occurs.

One extra piece of data supports the model just described. During the automatic profiling of one nitrogen implanted tip, the closed-cycle helium refrigerator stopped. Data were still being collected inadvertently as the specimen warmed. Since the evaporation field is so sensitive to temperature, the evaporation rate increased dramatically.

Figure IV-5 shows the resulting profile of this specimen. In addition to the Ni^{+2} signal increasing, the N^{+} signal also increased very rapidly. Note that even though the Ni^{+2} signal stayed high, the N^{+} signal fell to zero. This can be seen in the sequence of spectra in Figure IV-6. Each spectrum is referenced to a point on the profile in Figure IV-5. When compared to other specimen profiles of approximately the same geometry and fluence, the total cumulative signal indicated by the top level portion of the curve is about the same value. A subsequent experiment showed that there was no d.c. field evaporation occurring between pulses. This result implied that it took much longer than seven minutes (the timed length of the test) for d.c. field evaporation to occur. This length of time is approximately four times the length from when the refrigerator stopped to the time when the N^{+} signal stopped completely. The conclusions to be drawn are the following: 1) all of the implanted nitrogen not detected to the point when the refrigerator stopped was on or just below the surface of the emitter, 2) the field evaporation in the collected spectra was initiated only by the voltage pulses, not by the increase in temperature, and 3) the high evaporation rate caused all of the nitrogen to come out.

Further experiments were attempted in which very high evaporation rates were induced by a combination of d.c and pulse voltages, but field evaporation of implanted specimens did not proceed in a smooth manner. Bright flashes at the viewing screen indicated that large amounts of material came off suddenly. The resulting spectra had peaks well off-scale while subsequent spectra showed no peaks or only very small peaks until the voltage was again increased considerably.

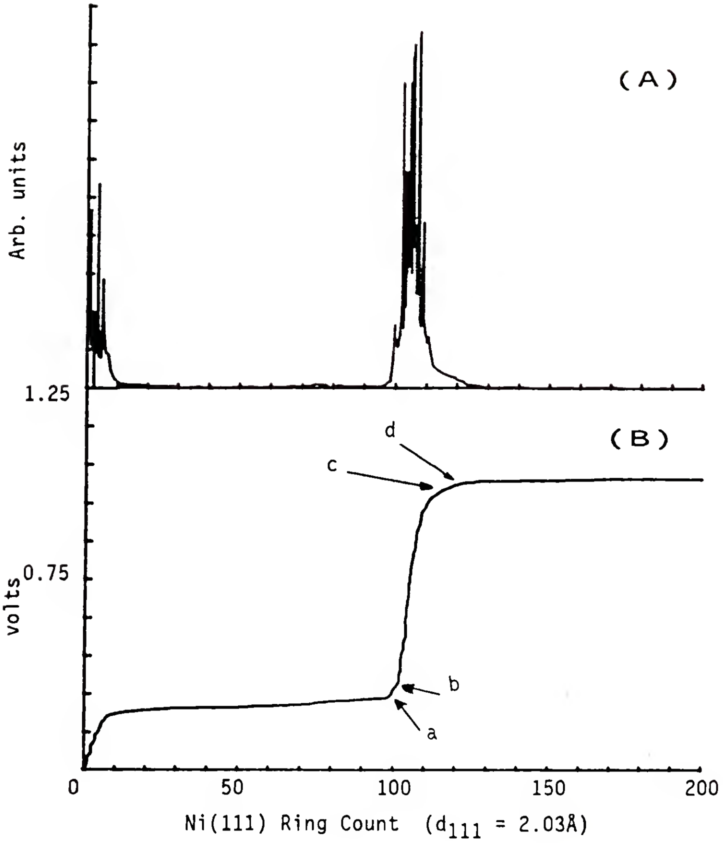

Figure IV-5 Profile of 10 keV N_2^+ implanted Ni specimen to a fluence of $1x10^{16}$ N^+/cm^2 in which cryogenic refrigerator stopped during profiling. a) Three-point derivative of b) cumulative N^+ signal versus calculated ring count. The associated spectra for the indicated are seen in Figure IV-6.

Figure IV-6 Several spectra associated with the profile in Figure IV-5 in which refrigerator went off and evaporation rate increased because of warming of the tip. The labels a) through d) also refer to the indicated points on the profile in Figure IV-5. a) Spectrum showing large N^+ peak a few minutes after cryogenic refrigerator turned off. The Ni^{+2} peak is offscale and is approximately 40% larger than what is seen. b) Ni^{+2} peak is just slightly offscale. Subsequent spectra are all within range. c) Ni^{+2} signal still high, but N^+ signal is dying. d) N^+ signal is gone and not detected in subsequent spectra, but Ni^{+2} signal remains high.

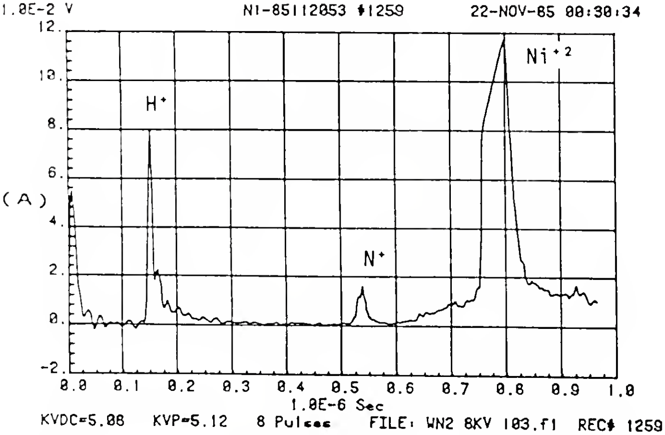
(A)
1.0E-2 V
NI-85112053 #1259
22-NOV-85 00:30:34
12.
10.
8.
6.
4.
2.
0.
-2.
H⁺
N⁺
Ni⁺²
0.0
0.1
0.2
0.3
0.4
0.5
0.6
0.7
0.8
0.9
1.0
1.0E-6 Sec
KVDC=5.08
KVP=5.12
8 Pulses
FILE: WN2 8KV 103.f1
REC# 1259

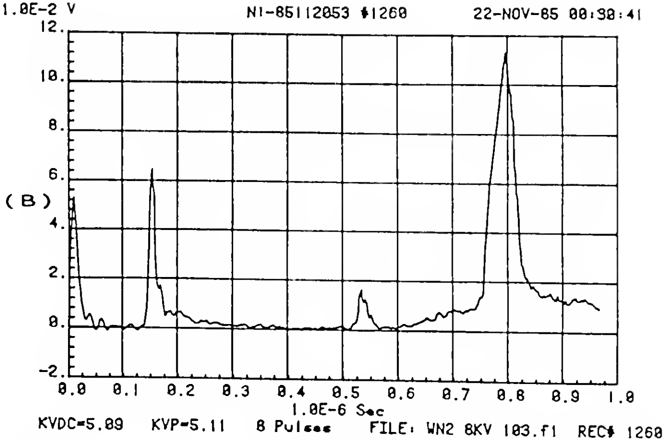
(B)
1.0E-2 V
NI-85112053 #1260
22-NOV-85 00:30:41
12.
10.
8.
6.
4.
2.
0.
-2.
0.0
0.1
0.2
0.3
0.4
0.5
0.6
0.7
0.8
0.9
1.0
1.0E-6 Sec
KVDC=5.09
KVP=5.11
8 Pulses
FILE: WN2 8KV 103.f1
REC# 1260

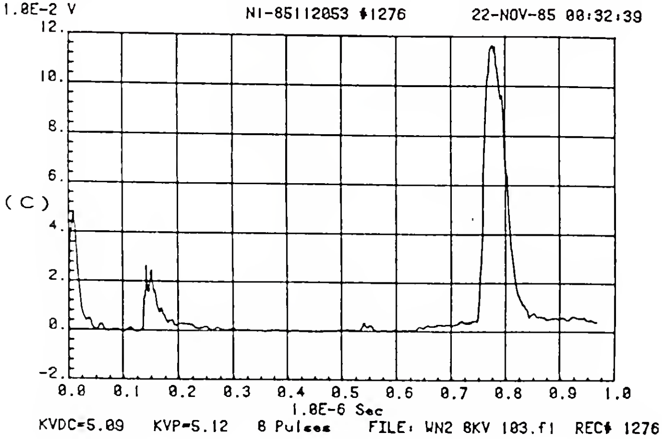
(C)
1.0E-2 V
NI-85112053 #1276
22-NOV-85 00:32:39
12.
10.
8.
6.
4.
2.
0.
-2.
0.0
0.1
0.2
0.3
0.4
0.5
0.6
0.7
0.8
0.9
1.0
1.0E-6 Sec
KVDC=5.09
KVP=5.12
8 Pulses
FILE: WN2 8KV 103.f1
REC# 1276

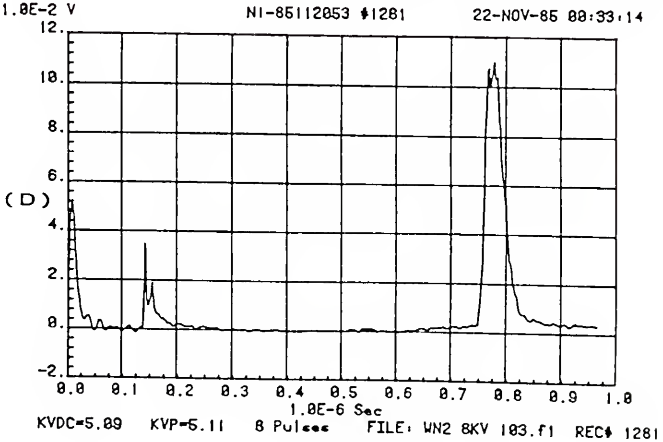
(D)
1.0E-2 V
NI-85112053 #1281
22-NOV-85 00:33:14
12.
10.
8.
6.
4.
2.
0.
-2.
0.0
0.1
0.2
0.3
0.4
0.5
0.6
0.7
0.8
0.9
1.0
1.0E-6 Sec
KVDC=5.09
KVP=5.11
8 Pulses
FILE: WN2 8KV 103.f1
REC# 1281

It appears that implantation depth profiles of nitrogen into nickel cannot be obtained by the methods just described. The results of the above experiments in which the refrigerator shut down indicate that varying the evaporation rate with temperature instead of voltage levels may lead to a successful profiling technique for nitrogen in nickel. There are two possible means for profiling implanted or diffused nitrogen with the techniques developed in this study. First it is essential to be able to control the temperature of the sample in order to be able to control the evaporation rate in a way other than with voltage levels alone. The other way is to use the pulsed laser atom probe (PLAP) instead of the IAP. The PLAP uses a laser to initiate the evaporation process (i.e. applying a thermal pulse to the tip). Such an instrument also provides a lower field environment, but suffers from the disadvantage of permitting short-range migration prior to field evaporation. We are not presently equipped to perform either experiment.

Nitrogen Implantation In Tungsten

It was possible to profile nitrogen implanted into tungsten by the ring counting method. During profiling, a helium imaging pressure of approximately $4\text{x}10^{-6}$ Torr was used in all of the tungsten analyses. With the gain of the channel plates at maximum, this gave quite acceptable images for viewing the collapse of (011) rings of tungsten at reduced imaging pressures ($\approx 1\text{x}10^{-6}$ Torr). The maximum energy transferred to a tungsten atom from an incident nitrogen ion is only about 27% of the primary energy (compared with 60% for N_2^+ into nickel). This value coupled with the energies used in this study is sufficiently low enough to permit the ring counting technique to be performed. It should be noted that this value is comparable to that for helium into nickel and the damage, as seen with the FIM, is similar to that for nitrogen into tungsten.

The distribution of the damage in the specimen can be qualitatively seen in the FIM image during analysis in two ways. The first is in the quality of the FIM image itself. The rings of an implanted specimen are not smooth and continuous as in an unimplanted specimen. They show an irregular pattern with breaks of a few atoms in length around the rings. Figure IV-7 compares FIM images between an un-implanted tungsten tip and one implanted with 10 keV N_2^+ to a fluence of $5\text{x}10^{16}$ N^+/cm^2. This micrograph was taken during profiling and after about 8 (011) planes have collapsed (17 Å). The second way of seeing the damage distribution is also qualitative. In images of specimens viewed before implantation the rings collapse inwardly in almost a symmetrical fashion. In an implanted specimen, the rings collapse in a jerky manner and are unsymmetrical. As the tip is profiled through the implanted region, this irregular behavior evolves into that of an un-implanted tip and the operator can distinguish this transition quite clearly. This visual observation coincides nicely with the results of the IAP profiles just as the implanted nitrogen signal is no longer detected.

Since the FIM technique has long been used to image single vacancies, it was natural during ring counting to qualitatively observe the type and size of the defects produced during implantation (see Microstructure section in Chapter I). However, these experiments were

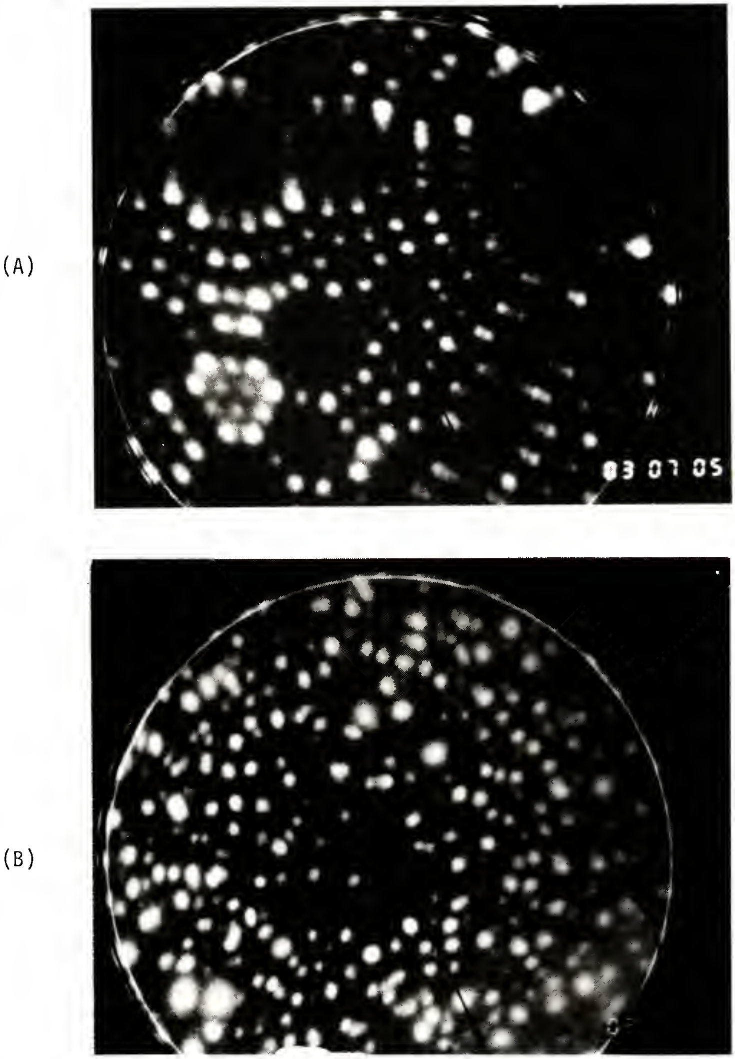

Figure IV-7 Comparison between a) un-implanted tungsten specimen and b) one implanted with 10 keV N_2^+ to a fluence of 5×10^{16} N^+/cm^2. The micrograph in b) was taken during profiling with reduced imaging pressure and full gain on channel plates after approximately 8 (011) layers have been removed.

not directed specifically towards defect identification and were not optimum for this purpose. In several experiments ,a spiral would suddenly emerge on the (011) pole of tungsten (the pole used for counting), persist for several ring collapses, and then disappear. The visibility criteria for dislocations and the rules for defect identification in the FIM image has long been deduced [86-88]. The basic rule is that $\underline{g}\cdot\underline{b} = n$, where $\underline{g}$ is the pole in which the spiral forms, $\underline{b}$ is the Burger's vector of the dislocation, and n is an integer. The interpretation of the present appearance and disappearance of spirals during profiling is that they are the result from small dislocation loops with the Burger's vector oriented in the proper direction to satisfy the above conditions. However, an unambiguous identification cannot be made without data from another crystallographic plane and this is nearly impossible since the size of the loops are on the same order of the number of rings collapsed. All of the loops observed in this study have been between 10 and 20 Å in size. Figure IV-8 shows a typical sequence of one loop observed during a particular profiling experiment. The spiral was observed to last approximately 10 rings.

To observe individual vacancies with the FIM, all of the atoms on the plane in which the vacancy exists on the surface must be visible. For tungsten the only planes for which this condition is met is the (111) and its near-neighbors. Because of the limitations of the manipulator and the tip-to-screen distance inherent to the FIM/IAP used in this study, only one (111) pole is normally imaged. Since the (011) pole is used for counting during the profiling, the (111) pole is off the screen

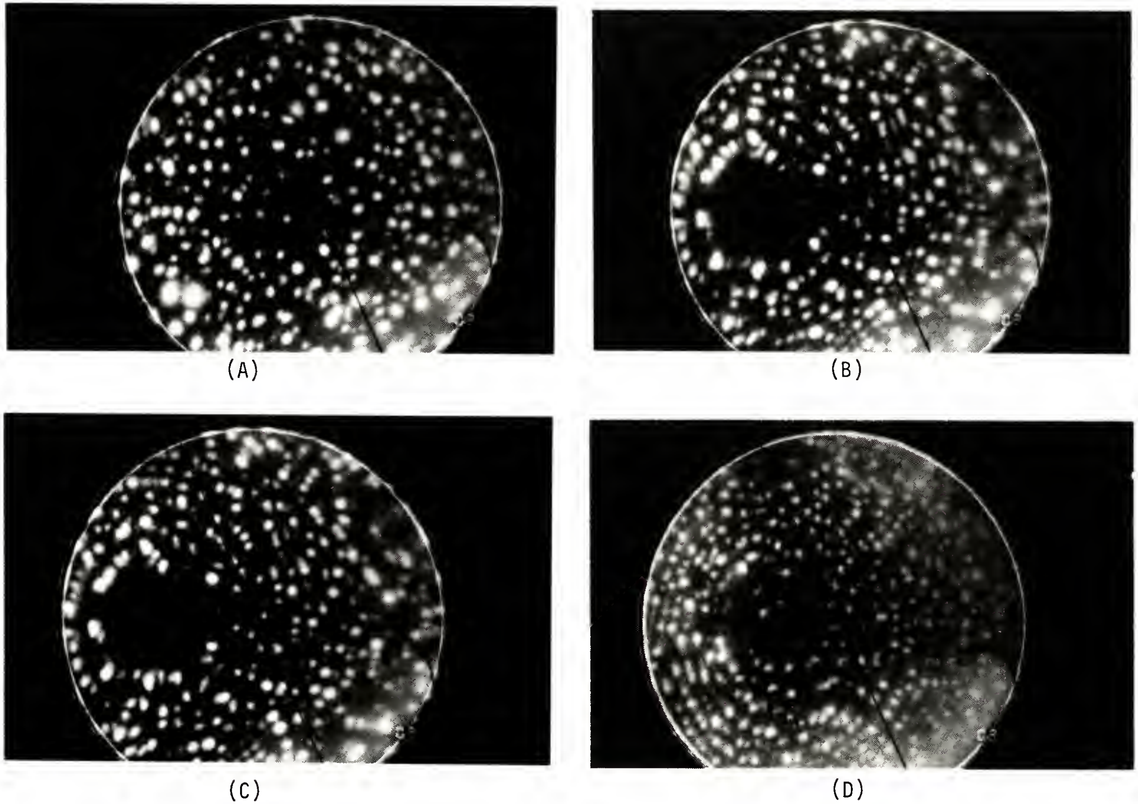

(A) (B) (C) (D)

Figure IV-8 Four FIM micrographs taken during profiling sequence, a) through d), of a 10 keV N_2^+ implanted tungsten emitter showing the presence of a spiral due to dislocation loop. The spiral was seen to last approximately 10 ring collapses.

during an experiment. Furthermore, the (111) region in tungsten blurs during analysis because of local variations in the radius of curvature of the tip (and hence the local field strengths). For these reasons the (111) regions are not used to observe the damage or used for determining the depth scale. The best way to resolve the atoms in the region around a (111) pole is to reduce the d.c. voltage well below that for optimum overall imaging (BIV for best imaging voltage). In this case only those poles on the zone axes associated with those poles are clearly visible. Figure IV-9 shows two examples of the images obtained in this way. Figure IV-9a is a specimen showing no damage around the (111) while Figure IV-9b is one showing a dislocation loop which has formed on it. It can be seen that the size of this loop is also 10-15 Å.

A further reason that the ring counting method can be employed for nitrogen-implanted tungsten is that, unlike the nitrogen-nickel-neon system the N^+ signal is not suppressed by the background helium pressure. A word of caution, if there is a significant neon partial pressure present in the imaging gas, the N^+ signal will be suppressed in this system also. Therefore, care must be taken to minimize the neon pressure during profiling. In addition, neon is known to considerably reduce the evaporation field for tungsten. The reason for the lack of a N^+ signal with neon present is that the nitrogen is probably being field desorbed by the d.c. field between voltage pulses. This limitation has not proven to be a major problem because if neon is present in appreciable quantities it can be easily seen in the IAP spectrum and steps can be taken to eliminate it.

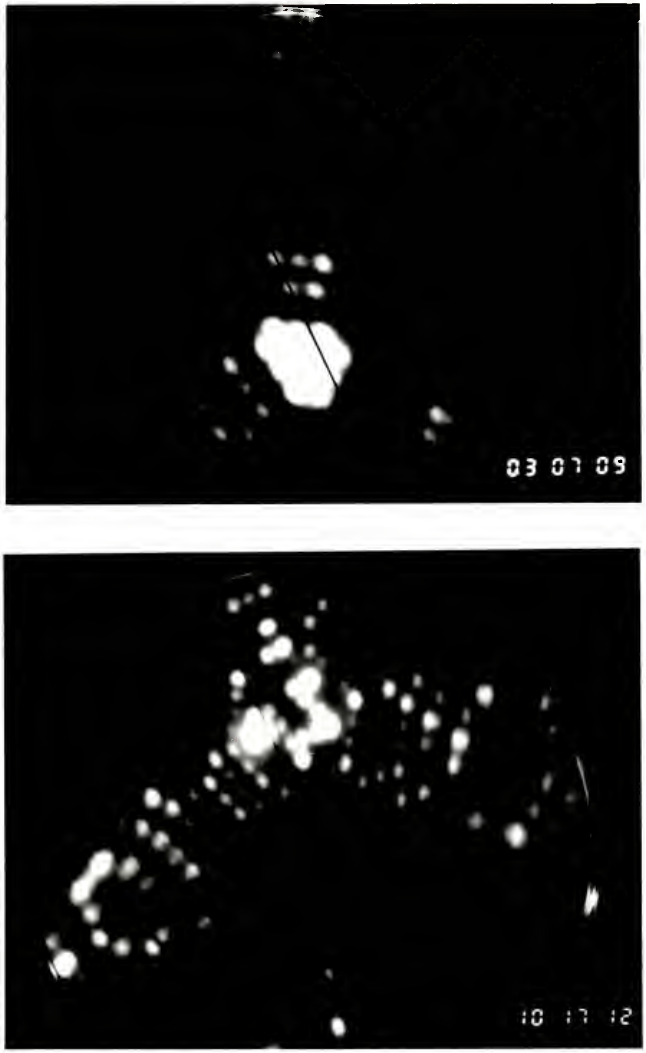

Figure IV-9 Two examples of imaging the (222) region of Tungsten by lowering the voltage to approximately 70% of BIV. a) un-implanted specimen. b) implanted with 10 keV N_2^+ showing a dislocation loop collapsed onto the (222) plane. The size is approximately 10-15 Å.

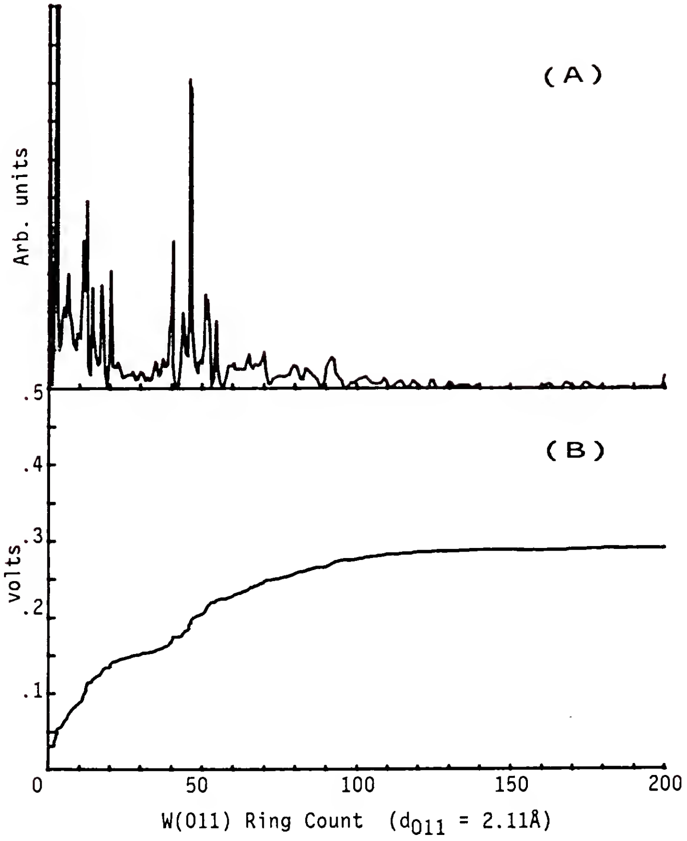

Figure IV-10 Profile of 10 keV N_2^+ implanted W specimen to a fluence of 1.86×10^{16} N^+/cm^2. a) Three-point derivative of b) cumulative N^+ signal versus experimental ring count.

The implantation profiles of the nitrogen implanted into tungsten are more along the lines of those expected for an implanted species from classical theory. That is, the profiles show "S"-type curves when the cumulative N^+ signal is plotted as a function of depth or the cumulative W^{+3} signal. Figure IV-10 shows the IAP profile of a 10 keV N_2^+ implanted tungsten with a fluence of 1.86×10^{16} N^+/cm^2. Note that there are three parts to the curve which can be easily distinguished. The surface peak within the first 1-2 layers is similar to that which is seen in the nitrogen/nickel system. It corresponds to nitrogen detected prior to any rings collapsing. The peak at about ring number 50 (105 Å) corresponds well with the calculated value of 101 ± 58 Å predicted by the TRIMML program*. The near surface peak which extends from just below the surface to approximately 40 Å is a new feature not well understood. Indeed, FIM seems able to study this feature better than any other now known method. This peak is of similar shape and size (i.e. depth) to peaks found in all of the profiles of tungsten in this study at various energies, except one which was at the highest implantation energy available, 18 keV. Conceivably, such surface peaks are only present at low energies and these have not been extensively studied to date. In the profile shown in Figure III-11, this sub-surface peak is absent, but there is a distinct smaller peak found at approximately 49 Å. It is suggested that the sub-surface peak is related to the backscattering of incident particles inside the material not having sufficient energy to

---

*TRIMML stands for TRansport In Materials, MultiLayer and is a Monte Carlo calculation program for the distribution of the trajectories of energetic particles [89].

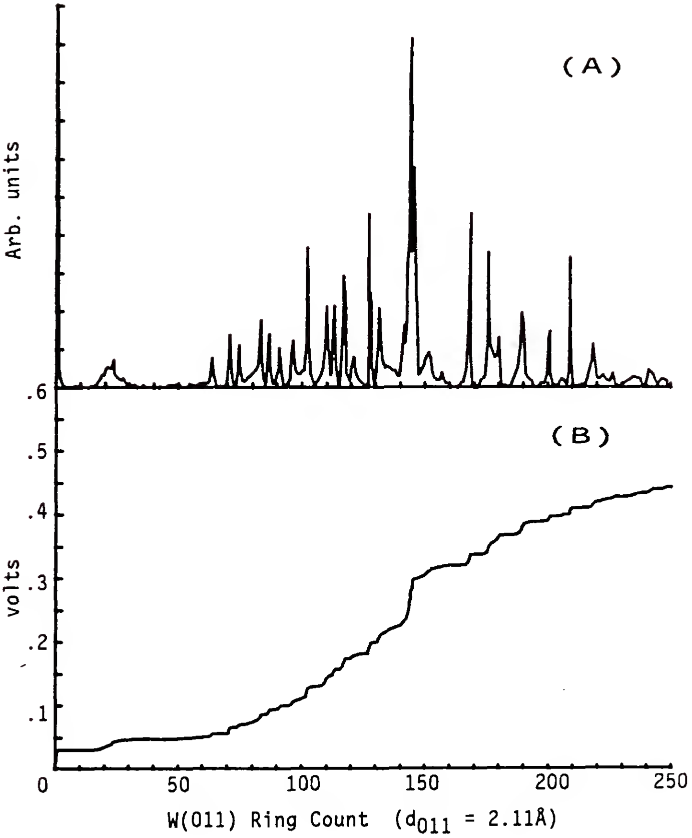

Figure IV-11 Profile of 18 keV N_2^+ implanted W specimen to a fluence of $1\text{x}10^{16}$ N^+/cm^2. a) Three point derivative of b) cumulative N^+ signal versus experimental ring count.

escape. There may also be a barrier for the escape due to the surface damage. Higher energies would have the damage distributed deeper and the particles would have better chances of escaping. When the energy is small, calculated profiles from the TRIMML program show a Gaussian profile in which the leading edge is truncated at the surface. The number of particles in this truncated portion are considered to be backscattered from the sample. In other words, the program agrees with the experimental ranges found, but it does not predict the sub-surface peak seen in the profiles. Table IV-1 shows a comparison values of range and straggling found with the IAP and the calculated values form the TRIMML program and the number of experiments performed for each implanted energy. The range and straggling (half width at half maximum) values are found by "eyeballing" an approximate Gaussian curve about the peak in the derivative curve.

The general applicability of this program to low energy ions to both nitrogen and tungsten will be discussed in Chapter V.

Table IV-1
Experimental and Calculated Range and
Straggling Values of Nitrogen in Tungsten

Trials	E (keV)	IAP Range(Å)	Straggling(Å)	TRIMML[†] Range(Å)	Straggling(Å)
3	2.5	19	5	46	28
2	4.0	85	42	86	50
4	5.0	105	42	101	58
1	9.0	295	116	253	136

[†] The factor used to modify the Linhard-Scharff-Schiott constant was 1.0. The factor used to modify the screening length of the scattering potential was 0.75.

Deuterium Implantation In Nickel

There were two main accelerating voltages chosen for the D_2^+ implantations, 5 and 3 keV. With the corresponding implantation energies of 2.5 and 1.5 keV, the mean projected ranges in nickel are 160 ± 160 Å and 80 ± 120 Å [90]. These energies were chosen because the ranges would limit the number of spectra that needed to be taken and simultaneously the length of time per profiling experiment. As was seen in Chapter III with respect to the nickel depth calibration specimens, profiling distances on this order are easily achieved. The nickel specimens were implanted with deuterium *in situ* in the FIM/IAP chamber and at cryogenic temperatures. This was done in order to control the gases to which the surface was exposed and to keep the sample below the release stage (temperature) for deuterium. Specimens were first field evaporated and imaged in the FIM and taken to the TEM in order to obtain micrographs for measuring the geometric parameters. They were then reimaged in the FIM to clean the surface prior to implantation. The voltages were removed and the specimen pointed toward the ion gun port. After implantation the samples were immediately analyzed.

The results of the deuterium implantation into nickel were disappointing, since no complete profiles were obtained from any implanted specimen. Essentially all of the specimens implanted with deuterium and subsequently profiled flashed during IAP profiling. Since the maximum energy transferred was very low, radiation damage is unlikely to be the cause of this difficulty. It seems almost certain that some form of hydrogen (deuterium) embrittlement is the fundamental cause of the difficulty, as shall emerge.

The moderate fluences used in this study were between $1\text{x}10^{16}$ and $5\text{x}10^{16}$ D^+/cm^2. A cumulative D^+ signal comparable to a cumulative Ni^{+2} signal of several monolayers was expected at the projected range. The implanted deuterium in nickel system acts as if the nickel is being embrittled by the deuterium. Although the deuterium profiles were not obtained, the results will be presented for completeness and because nickel is not ordinarily thought to be embrittled by hydrogen. Furthermore, future studies can rely upon the experience gained here and suitable experimental changes can be made. The proven ability of the IAP to profile through the nitrogen-implanted region of nickel emitters quite clearly demonstrates that the nickel is not embrittled due to the damage caused by the implantation process but is inherent in the hydrogen-nickel system.

Before implantation, nickel emitters are able to be field evaporated at extremely high rates. In fact this author found it very difficult to intentionally fracture nickel specimens with extreme overvoltages during d.c. evaporation. After implantation with deuterium, these same emitters are very sensitive to field evaporation and almost always fracture during attempts at profiling. Even after implantation with nitrogen, nickel emitters are still capable of very high rates of evaporation, consistent with the hypothesis that radiation damage per se is unimportant. Furthermore, when deuterium-implanted specimens flash, they do so in an un-foreseen manner.

Figure IV-12 shows examples of three deuterium implanted nickel specimens which flashed during profiling in the IAP. The micrographs to the right are the specimen prior to implantation in the FIM/IAP. Out of

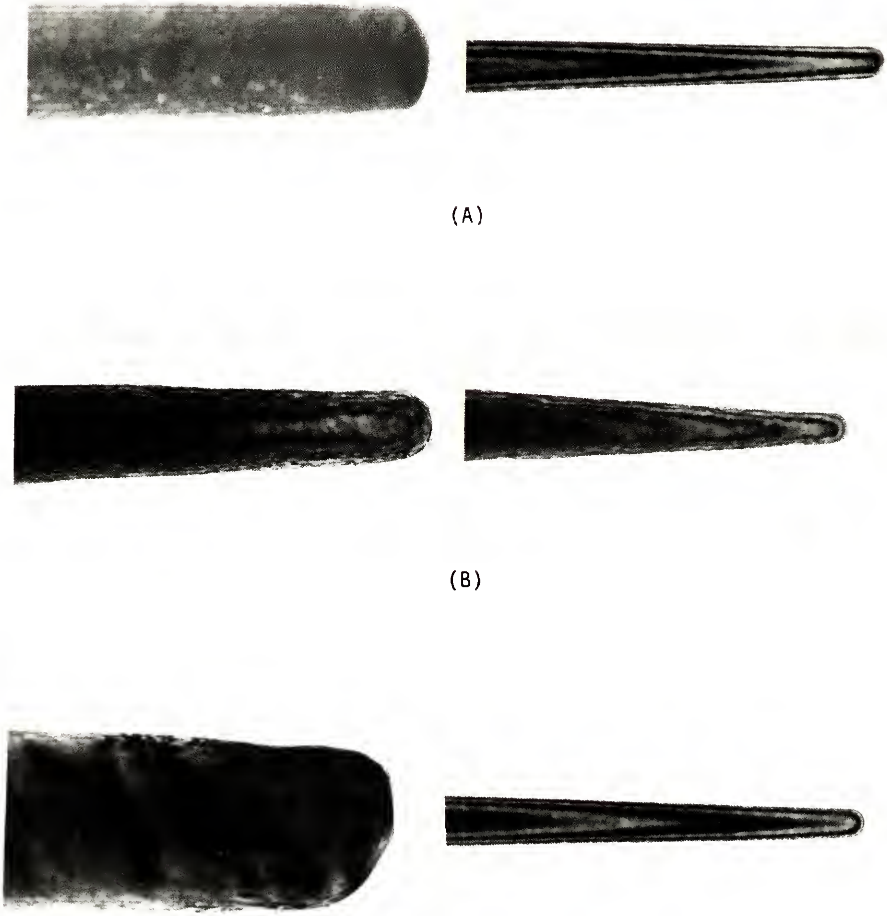

Figure IV-12 TEM micrographs of three samples before (on right) and after (on left) implantation and profiling in the FIM/IAP and which fractured. Implantation conditions for a), b), and c) are given in Figure IV-13.

the field of vision in these micrographs are the shank regions of the tip. However, when the specimens are examined in the TEM prior to imaging in the FIM, all of the electron transparent volume is viewed including the shank. In fact, the thicker part of the shank is usually used to orient the tip so as to obtain specific diffracting conditions because the Kikuchi lines are more pronounced there than in the thinner regions near the tip. Since the emitters were all examined in this way, it is very unlikely that pre-existing defects of any kind (dislocation, grain boundary, etc.) were located in the shank of these emitters within 2-3 μm.

The micrographs to the left in Figure IV-12 are from the same three specimens after they had fractured during the profiling experiments. All the specimens have a [111] tip orientation and have been imaged using a {111} reflection. All the micrographs show distinct facets on the fracture surface. This observation plus the absence of grain boundaries in any nearby region prior to profiling, indicates the mechanism of embrittlement is intragranular in nature. The nucleation and growth of hydrides (deuterides) is not precluded as a possibility.

When the samples flash during the profiling experiments, all of the spectra show a marked increase in H^+ and D^+ peaks in addition to a characteristic sudden step in the d.c. level somewhere in the waveform. This abrupt step in the d.c. is an artifact caused by the method by which the digitizer accounts for missing points in a waveform. The internal microprocessor of the digitizer interpolates all the points missing between two detected points. If a large portion of the waveform goes off-scale, a straight line is generated between the points where it

Figure IV-13 Spectra showing the fracture of the three specimens in Figure IV-12. Implantation conditions: a) 0.5 μA, 150 sec, 5 keV and 0.25 μA, 300 sec, 3 keV; b) .35 μA, 300 sec, 5 keV; c) 0.4 μA, 60 sec, 5 keV. The masses are identified by the dotted lines in the spectra and the calculated mass-to-charge ratios to the right of each spectra, increasing mass going from left to right. The mass identities are: 1.00 for H^+, 2.00 for D^+, 20.00 for Ne^+, and 29.00 for Ni^{+2}.

(A)

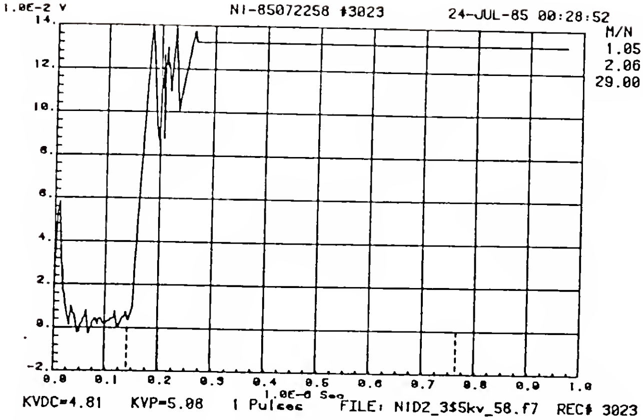
1.0E-2 V
NI-85072258 #3023
24-JUL-85 00:28:52
M/N
1.05
2.06
29.00
14.
12.
10.
8.
6.
4.
2.
0.
-2.
0.0
0.1
0.2
0.3
0.4
0.5
0.6
0.7
0.8
0.9
1.0
1.0E-6 Sec
KVDC=4.81
KVP=5.08
1 Pulses
FILE: NID2_3$5kv_58.f7
REC# 3023

(B)

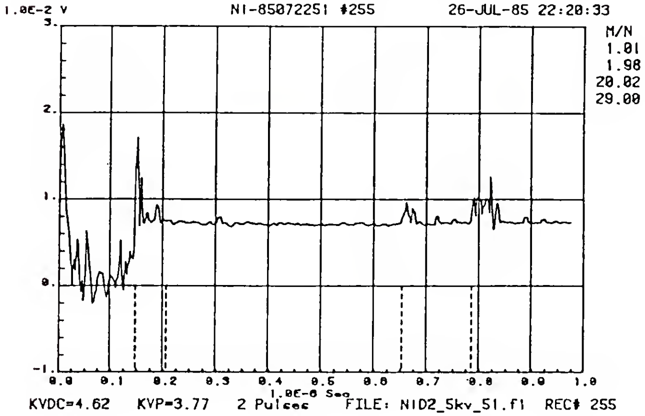
1.0E-2 V
NI-85072251 #255
26-JUL-85 22:20:33
M/N
1.01
1.98
20.02
29.00
3.
2.
1.
0.
-1.
0.0
0.1
0.2
0.3
0.4
0.5
0.6
0.7
0.8
0.9
1.0
1.0E-6 Sec
KVDC=4.62
KVP=3.77
2 Pulses
FILE: NID2_5kv_51.f1
REC# 255

(C)

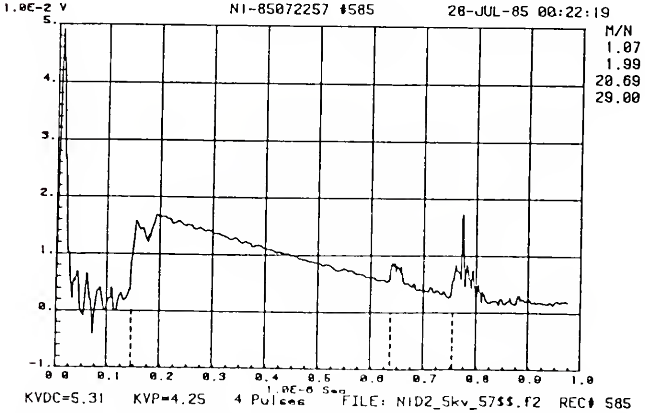
1.0E-2 V
NI-85072257 #585
28-JUL-85 00:22:19
M/N
1.07
1.99
20.69
29.00
5.
4.
3.
2.
1.
0.
-1.
0.0
0.1
0.2
0.3
0.4
0.5
0.6
0.7
0.8
0.9
1.0
1.0E-6 Sec
KVDC=5.31
KVP=4.25
4 Pulses
FILE: NID2_5kv_57$$.f2
REC# 585

goes off-scale and where it comes back on. Signal-averaged waveforms are added within the digitizer with the output a superposition of all the traces. Thus, the point at which the waveforms go off-scale can be estimated from the waveform.

Figure IV-13 shows the spectra at those points in the experiments where the specimens in Figure IV-12 flashed. Note that each spectrum has a different value of the number of pulses per spectrum. Various values of this parameter were attempted for two reasons: 1) to determine whether the signal averaging of multiple traces would mask a D^+ signal coming from only one trace, and 2) to try to capture the details of the very spectrum at which the fracture occurs. As can be seen from the three spectra in Figure IV-13b and c, signal averaging can mask the spectral details when a tip flashes, but that the location where the trace goes off-scale corresponds to the expected flight time for H^+. Figure IV-13a shows an example of a spectrum from a single pulse and the off-scale H^+ and D^+ can be seen. In each instance there is some evidence of a release of deuterium at the instant a specimen flashes.

There is another experiment which further supports this generalization. A specimen was first implanted with 5 keV D_2^+ and then with 3 keV D_2^+ to a fluence of 1.5×10^{16} D^+/cm^2 for each of the energies. During profiling there were two flashes seen in the spectra, (the second being fatal). For the first flash, only the Ni^{+2} signal went off-scale. Figure IV-14 shows a sequence of spectra which includes this first flash. The tip was being field evaporated rather slowly and small amounts of deuterium were detected as evidenced by the Ni^{+2} and D^+ peaks in Figure IV-14a. When the spectrum in Figure IV-14b was taken, a flash of light

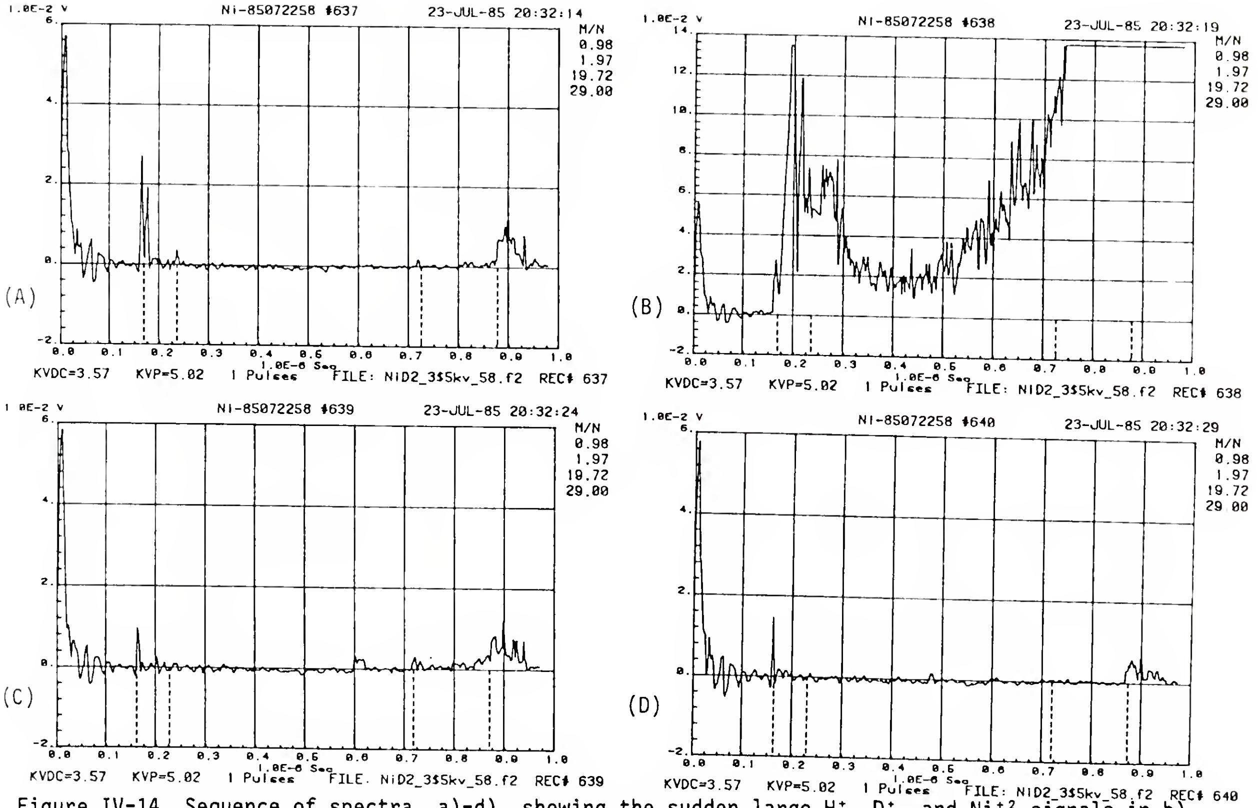

Figure IV-14 Sequence of spectra, a)-d), showing the sudden large H^+, D^+, and Ni^{+2} signals in b). Voltages were constant and the evaporation rate was relatively mild.

was seen at the viewing screen and the spectrum looked as if the specimen had fractured, however, continued pulsing showed that the tip was still intact and producing a Ni^{+2} peak as seen in Figure IV-14c and d. Figure IV-14b shows quit clearly the large D^{+} peak, completely on-scale, coming from the sample. Profiling of this sample continued until it flashed for the second time. The spectrum showing this flash was seen previously in Figure IV-13a and the TEM micrographs of this tip is in Figure IV-12a. Figure IV-15 shows the as-collected cumulative D^{+} signal versus the cumulative Ni^{+2} signal. The indicated points correspond to the two flashes and have depths of 10 and 96 Å calculated from the cumulative Ni^{+2} signal. The two releases of deuterium are at two distinct depths and probably correspond somehow to the two implantation energies used for this sample, 1.5 and 2.5 keV although these depths do not agree with the values given at the beginning of this section.

Carbon In Tungsten And Nickel

As was indicated above, there were no measurable differences in the nitrogen profiles of specimens implanted in situ or ex situ. However, there was an observable difference in the presence of another element, carbon, for ex situ experiments. When specimens were implanted in situ, no C^{+2} or C^{+} peaks were ever detected. When ex situ conditions were used, the carbon peaks were always present, even though the ion beam used was carefully mass filtered. Another feature of the carbon peaks was that they were only present at shallow depths from the surface ($\leq$ 30 Å), indicating that they were not implanted at the implantation energy, but were probably the result of knock-on events with the primary beam at the

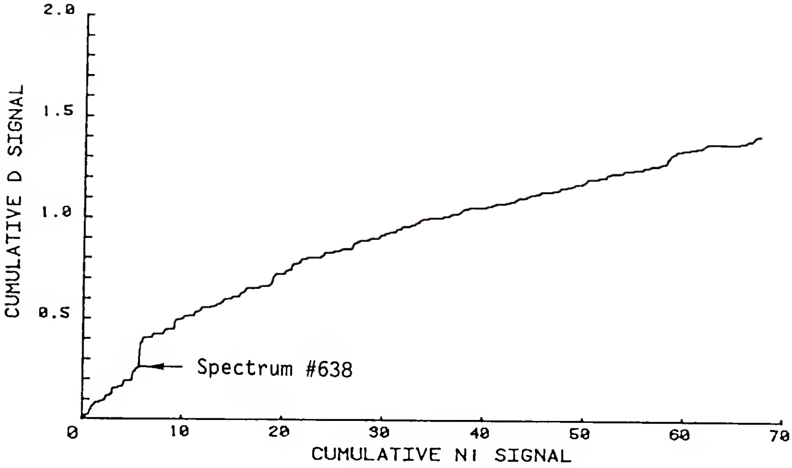

Figure IV-15 Cumulative D^+ signal versus the cumulative Ni^{+2} signal for the same sample shown in Figure IV-12a. The arrow indicates spectrum number 638 shown in Figure IV-14b. Specimen failure occurred in the next spectrum after the last spectrum from which this data is taken, presumably due to the deuterium implanted at 5 keV.

surface. Figure IV-16 shows a spectra which contains C^{+2}, N^{+2}, and N^{+}, from a 10 keV N_2^+ implanted tungsten tip. The depth at which this spectra was taken corresponded to 12 (011) layers or about 24 Å. Profiles of the carbon are not given because of the interference with the background level from the He^{+} signal. There is also a difference with relative signal strength for the C^{+2} and C^{+} peaks with depth. The C^{+} peak seems more prevalent near the surface (≤ 10 Å) and is usually not seen as far as the C^{+2} peak is seen. For example the C^{+2} peak is not seen in Figure IV-16.

It should be stated from the outset that the difference in carbon concentration does not arise due to transport of ex situ implanted tips through atmosphere since in situ nickel tips were also transported to the TEM both before and after implantation in the FIM/IAP and thus were also exposed to atmosphere. There are two other environmental parameters which are different between in situ and ex situ implantation. First, when samples were being implanted in situ, UHV conditions were always maintained in the FIM/IAP chamber. The pressure in the ion gun for ex situ implantation was nominally 5×10^{-6} Torr. Typically a monolayer per second may be deposited from the gas phase at 1×10^{-5} Torr, a reasonable proportion of which could be CO. The time for a monolayer to form increases by about an order of magnitude for each decade decrease in pressure. The second difference between the two implantation conditions is the sample temperature. In situ specimens were implanted at cryogenic (≈65°K) temperatures while ex situ tips were implanted at room temperature. It is well known that electron beam contamination occurs more rapidly at room temperature than when the sample is cold [91]. The

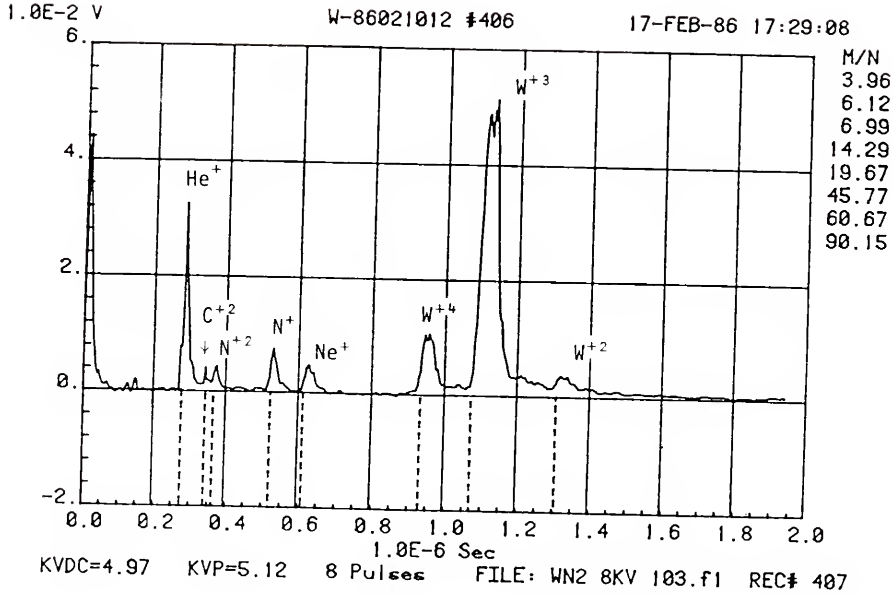

Figure IV-16 Spectrum of a 10 keV N_2^+ implanted tungsten emitter taken at a depth of approximately 24 Å showing the presence of carbon.

beam essentially polymerizes contaminants diffusing across the surface. Cryogenic temperatures reduce the diffusion rate of the contaminants and are used to minimize contamination rates in the TEM. It is likely that the same mechanism operates during ion implantation in the present studies. The lower tip temperature and better vacuum conditions together easily account for the lack of carbon in the *in situ* profiling experiments. The reverse conditions, of course, account for its presence in the *ex situ* experiments.

CHAPTER V
DISCUSSION OF RESULTS

The results of this study can be divided into four main categories: 1) instrumentation design, 2) methods and techniques, 3) experimental results, and 4) FIM observations. The section on Instrumentation, of course, includes the design and construction of the FIM/IAP, but also involves the Colutron ion gun, two special FIM/TEM holders, and a variety of computer programming and interfacing. All in all, research in this category resulted in the publication of seven notes or publications and consumed about one-half of the total research effort. The Methods And Techniques section included the characterization of field-induced stress effects, depth determination for profiling studies without an imaging gas, *in situ* ion implantation techniques, and the handling and reduction of data. The section, Discussion Of Experimental Results, includes the control experiments described in Chapter III and the implantation experiments detailed in Chapter IV. The FIM observations are those described in Chapter III and are those critical to utilizing the FIM/IAP so that meaningful data rather than experimental artifacts are obtained. These observations include a determination of the dependency of the evaporation field with imaging gas, pressure and type, lowering of the evaporation field by the act of implantation, the absence of a He signal in nickel spectra, suppression of peaks by the imaging gas, and the presence of adsorbed species such as CO^+ at low fields in the IAP signal from nickel and tungsten under UHV conditions.

These phenomena are interesting surface physics in themselves and will be discussed in the last chapter. Although many of these observations are original and have been or will be published, they are incidental to the major thrust of this chapter. With respect to obtaining depth profiles or understanding the effects of the field on the material properties of the sample, they are only experimental artifacts and will not be discussed in this chapter. It is important that an operator understand the basic physics of the instrument when using the FIM/IAP. For example if either an iron or nickel system is being investigated, the appearance of the CO^{+} peak ($m/n = 28$) could be confused with the Fe^{+2} peak of iron ($m/n = 28$) or the Ni^{+2} peak of nickel ($m/n = 29$).

Instrumentation

FIM/IAP

The instrumentation comprising the FIM/IAP at the University of Florida required a prolonged effort of this author and is a major result of the present study directed towards the understanding of the interactions of deuterium with defects in metals using the FIM/IAP. There are novel features in this instrument, many of which have already been described in the published literature. The instrument was designed specifically to overcome the special problems inherent to the presence of a hydrogen background. The combined FIM/IAP is a versatile, highly reliable instrument for metallurgical applications capable of H (or D) analysis and in this sense, unique. The operating characteristics are completely known and all of the instrumental parameters have been determined. Although the instrument was not designed for multiple users, (i.e. such as a commercial instrument would be), several scientists have learned to use it in a relatively short period of time. Some knowledge and experience in vacuum science is required.

Although the instrument was designed with a specific set of experiments in mind, it has been or is currently being used in a variety of studies. These include: the Fe-Mo-N system discussed in Chapter II [74], an underpotential deposition study of Cu on Pt [92,93], a study of sputter-deposited Nb on W*, and the present study. In addition, parts of the instrument can be used independently as a FIM/IAP, an ion gun, or as a computer system with a data acquisition capability. For example, H_2 and N_2 will be implanted into silicon and then analyzed by Rutherford Backscattering (RBS) and Electron Beam Induced Current (EBIC) (e.g. see Appendix B). The Tektronix 7912AD digitizer and 4052A computer were used at Shands Teaching Hospital at the University of Florida to capture the fast, focussed pressure burst in the Lithotripter (a non-surgical, non-invasive, kidney stone smasher) [94,95]. In this case the early FIM/IAP programs which stored waveforms on magnetic tape of the 4052A were used, essentially in an unmodified form. In addition to controlling the digitizer, the IAP programs which are written to control and display output data from the IAP can be modified to control other instruments over the GPIB or BCD/IO data busses. The FIM/IAP is much more than a "microscope" and the possibility of using it for interdisciplinary research has been proven. It will undoubtedly prove of further value.

---

*Moulton, W. G., Florida State University, private communication (1985).

FIM/TEM Specimen Holders

The two special FIM/TEM holders described in Chapter II are unique and are the first designed and constructed to answer specific questions raised about the field-effects in the samples used in this study. The "double-tilt" holder has not proven to be as useful as expected in helping to identify defects in implanted structures. It was thought that certain orientations and imaging conditions would be optimum, but at all orientations, the structure appeared mottled. Such contrast is difficult to interpret because of the severe overlap of multiple defect images. The best contrast was usually seen slightly off the Bragg condition for a "two-beam" case. Since the two single-axis rotation holders can easily achieve this type of image, they were used almost exclusively. However, the "double-tilt" holder should prove indispensible in identifying other types of defects in future work.

Methods/Techniques

Three major methods and/or techniques have been developed in this study which add to the capability for future research on ion implantation using the FIM/IAP. The first was the establishment of a procedure to determine depth profiles using the IAP without the presence of an imaging gas. This capability is often important because an imaging gas can alter raw data and resultant depth profiles. Several observations of the results of electric field interactions with the specimen are further complicated by the presence of an imaging gas. If such effects can be eliminated, so much the better. Integral with the methods developed is the need for TEM capabilities in conjunction with FIM/IAP techniques, especially for metallurgical applications. As a matter of course, we now routinely observe specimens by TEM for quality control. With the strict specimen selection criteria necessary for the depth profiling method (to obtain the geometric parameters) the TEM is absolutely essential.

The second method developed was the accomplishment of ion implantation of deuterium into FIM specimens in situ. The success of this procedure was directly related to properly designing the differential pumping system of the Colutron ion gun, beam line, and the FIM/IAP pumping system. These in turn controlled the partial pressure of deuterium in the FIM/IAP chamber which is absolutely critical to any meaningful studies of H or D in the specimen themselves. A discussion of the results of the control experiments on the introduction of deuterium into the FIM/IAP chamber will be presented in a later section of this chapter. Without this overall approach, the apparatus for introducing deuterium into the lattice, quenching the sample to cryogenic temperature to prevent diffusion of deuterium, and the cryogenic transfer of the specimen would be unwieldy and complicated. A comparison of the effect of ex situ and in situ implantation of nitrogen into specimens was made possible because of the apparatus designed for in situ deuterium implantation.

The third area of development comprised the data handling procedures for collecting, storing, and processing the tremendous amount of data collected in profile experiments. A typical experiment can take up to several thousand waveforms each requiring between 2.5 to 15 Mbytes of storage. Fortunately, the signal averaging processes built into the Tektronix 7912AD digitizer alleviates storage requirements since each desorbtion pulse does not require a separate waveform, but several are averaged together. However, it is important to be aware of the assumptions inherent with the use of averaging techniques, especially as they affect the detectability and analysis of single events such as field evaporation. If the number of traces of the digitizer is too high, the assumption that each pulse has, on the average, the same peak height is clearly not valid because of a sharp increase in signal when a major ring collapses. By trial and error, however, it could be shown that when the number of signal-averaged traces were small and the evaporation rate about one ring per five to eight waveforms, the averaging assumption was valid.

Convenient data handling procedures also include the storage and processing of a cumulative signal. Because a profile consists of so many waveforms, a small d.c. component in the waveform is also added in the accumulation process, as was shown in Chapter III. The validity of the technique for stripping this d.c. offset level for each experiment could be checked by direct observation of the spectra from which it is obtained. That is, each point on a profile could be cross-referenced to its corresponding spectrum.

Discussion Of Experimental Results

Control Experiments

This section will used to discuss those experiments related to the use of the FIM/IAP which affect the interpretation of data in a significant way. The experiments were reported in Chapter III in detail. Some of these results are as important as knowing the operating parameters of the IAP itself when spectra are collected. They must be taken into account when the instrument is set up for an experiment involving ion implantation, and/or extended depth profiling with or without the imaging gas.

Field effects

The experiments carried out with respect to field effects on the specimens are not decisive but were qualitatively helpful. Since the FIM/TEM "Field-Effect" holder did not have a cryogenic capability, certain points could not be deduced absolutely because:

1) the applied field was limited to 30% of the cryogenic field,
2) the specimens tend to field evaporate rapidly,
3) the flow stress for metals is lower at higher temperatures and defect mobilities vary even qualitatively with temperature.

Despite these problems, the field effect results gave qualitatively important results. If the applied field has an effect on defects structures even at lower fields, chances are it will be even worse under normal imaging conditions. The results from studies on He^+ implanted specimens are summarized below:

1) At room temperature, and at approximately 30% of the field value for evaporation at 65°K, the implanted defect microstructure is unaffected by field-induced stresses that can be detected to within the resolution limits of the TEM.
2) Quantitative image comparisons between specimens transferred between instruments could not be made because of the extreme sensitivity to slight differences in tilting conditions.
3) Qualitatively, there is no difference in defect density due to imaging or analyzing in the FIM/IAP that can be observed to

within the limits of obtaining the same tilt conditions in the TEM. This implies no alteration of the defect density or type during cycling between cryogenic and room temperatures.

4) Single dislocations are often unstable under imaging stresses and slip out of the specimen.

Ring counting experiments

The results of the ring counting experiments are an important means to cross check a depth scale for profiles obtained from the IAP when an imaging gas is absent. They verify the validity of the geometric model of the FIM specimens, (even though the latter must meet rather stringent selection criteria). In addition, these experiments show that the data presented as cumulative matrix signal versus ring number, or depth, have the geometric parameters sensitively presented within the curve. This can be understood by examining equation III-9. If l_0 is relatively large, the curvature is smaller and conversely, the parameter, α, does not affect the curvature as much as it determines the coefficient, K_α, of the cubic expression in h. The calculated curve can be fit to an experimentally determined curve to within 10%. The factors limiting the fit depend primarily on how well the parameters can be obtained from the TEM micrographs. It is important that the magnification be known as precisely as possible in the TEM. An important feature of this procedure is that the curves generated are independent of the evaporation rate and insensitive to the normal fluctuations in the data.

Automated data collection

The procedure from the ring counting studies proved to be invaluable for two reasons. First, the data could be taken in an automatic mode.

That is, the screen would not have to be watched constantly in order to note a ring collapse. Secondly, the complications due to the presence of an imaging gas can be overcome. This includes many of the field desorbtion problems associated with the imaging gas. The importance of these results for depth profiling are obvious. Typical ranges for deuterium for the energies used in this study can require for an experiment to run up to eight hours. Because of the background problem, the data must be taken continuously, i.e. pulsing must not be stopped because the deuterium in the background will field-adsorb. Such experiments require an operator's full attention.

Background gases

Adsorbed gases often appear in time-of-flight spectra at low field strengths. Their presence can be at best confusing and at worst lead to erroneous conclusions. Once their presence is understood, their effects can be easily factored out. Two examples of the influence of an imaging gas or the background gases are cited below. In IAP spectra taken under UHV conditions, there is a significant H_1^+ peak always present. This means that even though the neon imaging gas used is 99.999+% purity, a significant amount of hydrogen can still be introduced. Hydrogen is well known to reduce the evaporation field of many emitter materials. In light of this, the observation of the increased evaporation field for nickel when neon is present is a doubly anomalous phenomenon in that both hydrogen and the imaging gas should reduce the evaporation field separately.

The second example relates to the suppression by the imaging gas of a desorption peak at low field strengths. In an experiment on a 6 kV tip which showed the low-field desorption peaks of CO^+, another peak was seen between the voltages where the CO^+ disappeared (approximately 2 kV, d.c. + 2 kV, pulse) and where the nickel started to field evaporate (approximately 4.5 kV, d.c. + 2 kV, pulse). This peak had a mass-to-charge ratio between 14.5 and 16.0, but its exact mass was difficult to determine because there was no reference peak. (The CO^+ had vanished, and the Ni^{+2} signal had not yet appeared.) Neon was introduced into the chamber to be used as a known reference mass. The unknown peak was still visible at $1x10^{-8}$ Torr neon. When the neon pressure was raised such that its signal was seen in the IAP spectrum, the unknown peak disappeared. Apparently neon covered the surface and prevented the unknown surface specie from field desorbing. In the case of nitrogen-implanted tungsten, suppression of the desorbing bulk nitrogen by the imaging gas containing a significant neon partial pressure occurred. The condition was easily corrected by opening the valve to the exchange chamber and allowing the turbo-pump to decrease the neon pressure. When such difficulties arise, it is best simply to keep the offending gas out of the system. The calculation method for determining the depth scale is then the only method available.

Deuterium background

Because of the extremely high sensitivity to hydrogen, the IAP could become a valuable tool in studying hydrogen (deuterium)-metal systems. But as indicated above, deuterium presents a special background problem. The deuterium control experiments presented in Chapter III are thus important in establishing a methodology of extracting useful data from deuterium-metal systems.

Since the present FIM/IAP was especially designed to control the hydrogen background problem, and _in situ_ implantation of deuterium was a major research thrust, the effects of the deuterium background were of paramount importance. It was essential to keep the deuterium partial pressure low enough so that it did not interfere with the collection of data from implanted deuterium. This was a test of the system and it performed better than expected. With an ion source throughput of $1x10^{-4}$ Torr l/sec, the design requirements allowed a maximum pressure during implantation of $5x10^{-9}$ Torr. The total pressure in the chamber during implantation (the worst case), was less than $1x10^{-9}$ Torr.

Deuterium was implanted into the side of the FIM/IAP specimen holder under conditions simulating a typical implantation during the first time the chamber was exposed to deuterium. Subsequently, the spectra were observed in which the time interval between pulses was varied. This was a study of the field-enhanced adsorption of deuterium to the emitter at extremely low partial pressures. The time interval was varied between 0.5 sec and 200 sec. At intervals longer than 20 sec the spectra show D_1^+ peaks about half of the time. At intervals of 30 sec or longer, the D_1^+ signal was present greater than 90% of the time. When the FIM/IAP was brought up to atmosphere for repairs and subsequently pumped down, the D_1^+ peak was not seen in any subsequent spectra. It was expected that regurgitation of the deuterium from the ion and sublimation pumps would cause a deuterium background deuterium peak to worsen with time even if the chamber was backfilled to atmosphere. Fortunately, this is not the case. However, this should be monitored periodically. Apparently implanted deuterium can be differentiated from background deuterium without difficulty in the FIM/IAP of our laboratory.

Nitrogen Implantation In Nickel

Nickel specimens were severely damaged when nitrogen was implanted into them so that ring counting was not a feasible means for depth profiling and therefore, the calculation method for determining the depth had to be used. As it happens, nickel is particularly well suited for this method because tips made from its wire are oriented in a [111] direction, and the geometric model describes their shapes very well. This is contrasted with tungsten which has a [011] orientation and is flattened at the apex corresponding to the (011) pole.

There were several results which are important with respect to future applications of the FIM/IAP to studying ion implantation. First, the nickel specimens were not embrittled by the implantation of nitrogen as they were when deuterium was used. After implanting nitrogen, the nickel samples could still be field evaporated at relatively high rates without failure of the tips. This probably indicates that other ions may be implanted into nickel and successfully studied as well.

Although high field evaporation rates can be tolerated for nitrogen implanted into nickel, there seems to be a relationship between the field evaporation rate and the "bursts" which occur in the spectra unexpectedly during profiling. This relationship could not be quantified because the field evaporation rate varies greatly during an experiment. In fact, the definition of the field evaporation rate over many layers is itself slightly ambiguous. In one definition, the average number of pulses it takes to cause one monolayer of material to be removed is used. This value can be defined and held constant over many layers. However, over a large number of layers the radius of curvature of the tip increases and hence the number of atoms within the detector area increases. Thus the signals in the spectra also get very large. This is not desirable because it requires a change in the vertical amplifier gain in the middle of the experiment required the d.c. offset to be adjusted. This can cause problems when the data are analyzed and the d.c. level is stripped. the normally accepted method for expressing the evaporation rate is by the absolute number of ions per pulse. For nickel, this is reflected in the Ni^{+2} signal. However, this is difficult to maintain at a constant level because of the necessary and continual voltage increases required during an extended profile and the natural periodic increases in signal when a major pole collapses. Generally it can be said that at very mild evaporation rates the "bursts" were less likely to occur. At moderate to fast rates, there are at least a few which occurred.

The absence of a well defined implantation peak in the profiling studies of nitrogen in nickel was quite surprising. Implantation theory alone gave no obvious reason for this result. As was discussed in Chapter IV, the explanation is probably due to nitrogen acting in a fashion similar to sulfur. The difference between sulfur and nitrogen is that part of the nitrogen on the surface is detected while for sulfur it is not. In determining the activation energy for field desorbtion of species from an emitter at a given field strength, the most important parameter is the absorption energy (binding energy). The higher this energy, the more tightly it is bound to the surface. Sulfur is known to have a higher binding energy on nickel than does nitrogen. These results imply that stoichiometries reported from atom probe work involving nitrogen concentrations in a matrix could be in error. This error would tend to give measured nitrogen concentration less than the actual. It is not certain as yet whether a suitable correction could be made. There are two possible means for depth profiling implanted or diffused nitrogen with the methods developed in this study. One way would be to control the temperature of the sample in order to control the evaporation rate in another way (rather than with the voltage levels alone). Another possible alternative would be to use a pulsed laser atom probe (PLAP) instead of the IAP which uses only voltage pulses. The PLAP uses a laser to initiate the evaporation process (i.e. applying a thermal pulse to the tip). This technique also allows an investigation into the dependency of the desorbing species on the applied field because the laser power can be controlled to compensate for a change in the applied voltage.

The above explanation of the behavior of the nitrogen in nickel does not explain the observation of the falloff of the N^+ signal with depth. The possibility exists that this feature is associated with the defect depth distribution. Since implantation was seen to lower the evaporation field initially, there must be a change in the evaporation field as the sample is profiled through the damage region. From the theory of field evaporation, there must be an energy term which is increasing as the sample approaches the unimplanted region. This term must be the lattice binding energy which depends on the number of nearest neighbor atoms. The ion implantation would tend to reduce the number of nearest neighbors because of vacancies and vacancy clusters produced. In addition, the local asperities produced when a vacancy cluster is exposed to the surface would also tend to have higher fields associated with them and thus field evaporate more readily. Both of these conditions would lead to easier field evaporation of the specimen in the early stages of the profile. Unfortunately, these two reasons may explain the general shape of one curve at a given energy, but do not explain why two curves at different energies are similar.

There is another parameter that changes as a profile progresses, the pulse fraction. The pulse fraction is the ratio of the voltage pulse to the total field evaporation voltage (d.c. and pulse components). The experiments are performed with a constant pulse voltage and as the experiment continues, the pulse fraction decreases. Typically, the values start at about 37% and decrease to about 25%. Good atom probe practice requires that this level never falls below about 15% to avoid conditions in which some species may be d.c. field evaporated. It is uncertain at this time whether this parameter coupled with the above explanations can account for the similarity of the profile curves at different energies.

Future work is warranted in order to predict in which materials systems and under what conditions this anomalous behavior of nitrogen will occur.

Nitrogen Implantation In Tungsten

Microstructural damage of the nitrogen implanted tungsten emitters was sufficient to hinder FIM observations of ring collapse of the (011) planes. Qualitatively, the damage was similar to that observed for the He^+ implanted nickel samples. This similarity was probably not coincidental since the maximum energy transferred to a nickel atom by a helium ion is 24% of the primary energy, while for a nitrogen ion into tungsten the value is 27%. Since the rings could be discerned and the helium imaging gas did not affect the N^+ signal, depth profiling using the ring counting method was appropriate. Direct observation of the field evaporated structure during depth profiling made it possible to monitor the change in damage with depth. The operator could observe when the profile passed through the implanted volume and this observation corresponded well with the N^+ signal in the spectra. In addition, defect spirals could sometimes be seen in the image which lasted for several rings before disappearing. Such spirals can be attributed directly to dislocation loops caused by the implantation. The size of the loops can be estimated from the number of rings that collapse from the appearance to the disappearance of the spiral. The loop sizes found in this way corresponded to those seen separately in FIM micrographs from the (222) regions of implanted tips. These micrographs were not taken from specimens which were depth profiled because stopping to obtain an image interferes with the data collection process. The estimated sizes of the dislocation loops seen in the FIM by both methods were approximately 10-20 Å. This size agrees with the discussion presented in the section of Chapter I on the microstructure of implanted metals and explains why individual defects were not resolved by the TEM.

In contrast to the difficulties in obtaining profiles from nitrogen in nickel, nitrogen implanted into tungsten exhibited well defined implantation peaks. There are two possible explanations. First, the evaporation field for tungsten is much higher than for nickel (5.7 V/Å for tungsten, compared to 3.6 V/Å for nickel). Hence the implanted nitrogen is exposed to a higher field than in the nickel system. Secondly, the chemical nature of the nitrogen-tungsten system is different than the nitrogen-nickel system. The use of the PLAP might be able to determine which factor may be controlling. Support for the first explanation was obtained from the following (unintentional) experiment. During a period of time, the high voltage switch in the pulser deteriorated and only about 75% of the maximum voltage was attainable. The depth profiles of nitrogen obtained had no distinct implantation peak, and were similar in shape to the result from the nitrogen into nickel profiles. It is likely that the higher d.c. voltage required to compensate for the decreased pulse available caused some of the nitrogen to be field desorbed between pulses. When the switch was repaired, the nitrogen in tungsten profiles returned to normal.

An additional feature was observed in the nitrogen-tungsten profiles. A sub-surface peak extending from the surface to about 40 Å was present in most profiles. This peak should be differentiated from the true surface peak which is always seen before the first plane field evaporates, i.e. before any ring collapse. These subsurface peaks are not well understood at this time. For the highest energy used in this study (18 keV), this feature is not seen, but there is a smaller peak seen at approximately 49 Å. It is suggested that the sub-surface peak and the smaller peak in the 18 keV profile may be related to backscattered ions inside the material. These backscattered ions may come to rest in the more heavily damaged regions of the sample near the surface. Another possibility is that a surface barrier to the backscattered ions prevents them from escaping. Although the TRIMML code agrees with the experimental ranges for nitrogen implanted into tungsten quite well when the best fit choices for the screening length and Linhard-Scharff-Schiott constant are used, it does not predict either the sub-surface peak or the smaller peak in the high energy profile. Future work should include more implantations at higher energies to see if these hypotheses are consistent.

Applicability Of The TRIMML Code To Low Energy Ions

The fact that the TRIMML code does not predict the subsurface peaks described above is not surprising since it was developed primarily for high energy ions (>50 keV). The interactions at the very low energies (several eV) at the end of the ion's trajectory are probably more important for lower energies, but are not incorporated into the model. These interactions include trapping of the ions to defects, surface barriers for escape from the substrate, etc. In addition, there are few data that exist for ions at the high energies in materials other than silicon. As a consequence of this, there is no independent check of the parameters used in the model determined from low energy data. Therefore, comparisons made between experimental and calculated values as, was done in Table IV-1, should be viewed cautiously.

Reproducibility Of Profile Results

Curve shapes and total ions detected

The shapes of the profiles reproduce well for both nitrogen implanted into tungsten and nickel. Except for the one 18 keV N_2^+ implantation experiment of tungsten, all of the implantations at the energies used in this study were performed a minimum of twice. No irregularities were seen. It is appropriate at this point to comment on the varying levels of the cumulative N^+ signal in profiles of the same energy and fluence. Because the volume probed depends strongly on the geometric parameters of the emitter, one should not expect that the levels for two samples to be the same. But, because these parameters do not vary by much, the cumulative values should be on the same order and this is was is seen. Long slender (small α) specimens give lower values of the cumulative signal whereas wider angled specimens give higher values.

The exact concentration profile cannot be obtained at this time because the constant for the voltage per ion is not known. At the time of this writing, the time-gated mode of the IAP does not work well enough to obtain this value. It is found by ratioing the number of ions counted in a time-gated image to the signal in a spectrum collected under identical conditions. There is an alternative way of estimating this quantity. The number of nickel atoms within the volume probed can be calculated using the density. The constant for the voltage per ion, K_V is found by the cumulative nickel signal divided by the number of atoms in that volume. Using parameters from the data in Figure IV-5, given in Table V-1, and equation III-9, the volume probed is given as $\approx 8.3\text{x}10^{-18}$ cm^3. (This value is consistent with calculations from TEM micrographs.) This gives the total number of nickel atoms as $\approx 7.6\text{x}10^5$ and K_V as .07 mV/ion. The total number of N^+ ions detected in that experiment using this approach is $1.3\text{x}10^4$. From the observations of very low evaporation spectra, it can be said that these values are of the correct order.

Table V-1
Parameters For Figure IV-5
Used To Calculate K_V

Cumulative Ni^{+2} signal:	52.80 volts
Cumulative N^{+} signal:	.94 volts
depth probed:	406 Å = 4.06×10^{-6} cm
l_0:	3800 Å = 3.8×10^{-5} cm
α:	3.2°
density of nickel:	8.9 gm/cm^3
molecular weight of nickel:	58.7 gm/mole

Perhaps a better method of determining would be expressing it in an unconventional manner. Between ring collapses, the cumulative signal versus depth curves obtain an internal calibration mechanism. A cumulative matrix signal per monolayer can be found between ring collapses. (For averaging purposes, take it over several ring collapses.) In the same interval, the cumulative N^+ signal can be found. Taking the ratio of this to the cumulative matrix signal per monolayer would give a quantity which would be in equivalent monolayer units. This could then be transformed into concentration values.

Because of the uncertainty of K_V, it is inadvisable to put stock in any calculations of concentrations using it. For this reason, none of the profiles in this study have been calculated as concentration. The usefulness of doing the calculation of K_V is not that these profiles can be transformed into true concentration profiles, but that it gives a feel for the total number of atoms detected in an experiment.

Error analysis of geometric model

How well is the depth scale assigned to the profiles for the nitrogen in nickel experiments? There are several factors that go into answering this question. The first uncertainty lies with the digitizing of the TEM micrographs using the least squares routine. The following experiment was tried. Two thin straight lines on the digitizing plotter approximating a TEM micrograph were repeatedly digitized using the program, "TIPREDUCER." The resulting output parameters, α and l_0 vary by about 5%. When the calibration specimen for determining K_D was repeatedly digitized, it produces about a 10% envelope of curves at the higher depth ranges (approximately 1300 Å). At shallower depths, the curves have less differences. The largest depth for a nitrogen in nickel profile which used the calculation method was about 500 Å. Using the upper limit of 10%, it is safe to say that the depth attributed at each point along one of these profiles is within 10% of the true value.

Another factor which is important with respect to the reproducibility of these results is that the FIM specimens must meet stringent requirements to satisfy the geometric model. Specimens which do not pass these requirements are not used for the profiling experiments.

Deuterium Implantation In Nickel

The present work has demonstrated convincingly that the FIM/IAP can be used to study deuterium implanted into metal samples, if they have been implanted *in situ*. The deuterium background experiments showed conclusively that the D^+ signal detected in the IAP data during a profile experiment is coming from the bulk and not the background. However, it is important to emphasize that during a profiling experiment, pulsing should not be interrupted, i.e. by letting the emitter sit at its d.c.

potential, because then a significant D^+ background peak from adsorption will appear.

The fracture of the specimens during profiling is still puzzling and deserves further work. Essentially all of the specimens implanted with deuterium and subsequently depth profiled flashed during IAP profiling. The fracture mechanism is probably a complex function of the deuterium distribution, the defect structure, the energy of implantation, and the field-induced stresses (which are dependent on emitter geometry). Since the maximum energy transferred was very low, radiation damage per se was unlikely to be the major cause of fracture. In fact, since profiles of nitrogen-implanted nickel emitters were obtained without fractures, nickel was not embrittled by the damage caused by implantation alone. There is most likely an embrittling mechanism inherent to the hydrogen-nickel system. Furthermore, the fluences used in these studies were between 1×10^{16} and 5×10^{16} D^+/cm^2 and not considered high. A cumulative D^+ signal comparable to a cumulative Ni^{+2} signal of several monolayers was expected at the projected range. The implanted deuterium in nickel system acted as if the nickel was being embrittled by the deuterium. This was a surprising result since nickel is not known to be embrittled by hydrogen. Other observations during profiling studies also point to an unknown embrittling mechanism. In general, fracture occurred extremely fast and with no indications or warnings prior to the event during a run. The TEM micrographs of fractured specimens indicated that the failure sites were not anywhere close to the mean projected range of the implanted species (measured from the surface of the emitter), but rather much deeper. Routine observation of the specimens were performed beforehand and no defects were observed near the eventual fracture surfaces. Thus, they did not correspond to pre-existing defects, but were induced after implantation.

Results from one specimen which was implanted at two energies (D_2^+ at 3 and 5 keV) to the same fluence for each showed two deuterium releases during the profile. The second release corresponded to a flash in which the sample was fractured. It was originally thought that the two release stages could correspond to the depth of implantation for each energy. However, the calculated ranges were much shallower.

Carbon In Tungsten And Nickel

The inclusion of carbon in the implanted substrates is an important feature which must be accounted for since ion beams are used for modification of surface properties so frequently. When nickel or tungsten specimens were implanted *in situ*, no C^{+2} or C^+ peaks were ever detected, but when *ex situ* conditions were employed, the carbon peaks were always present. In all instances the ion beam used was carefully mass filtered to exclude extraneous ions. The carbon peaks were only present at shallow depths (≤ 30 Å), indicating that they were not implanted at the primary implantation energy, but were probably the result of knock-on events with the primary beam at the surface. There was also a difference seen in the distribution of the C^{+2} and C^+ peaks with depth. The C^+ peak was more prevalent near the surface (≤ 10 Å) and was usually not seen as deep as the C^{+2} peak. The source of the carbon in the *ex situ* samples was not due to exposure to atmosphere because nickel specimens which were implanted *in situ* had also been exposed to the atmosphere during transfer to the TEM and back to the FIM/IAP.

Although it has not been established in this study whether the absence of carbon for *in situ* implanted specimens was due to the cryogenic conditions or to the better vacuum, the results do indicate the importance of understanding the interactions of environmental parameters during ion implantation. Both of these environmental parameters would have the effect of lowering the presence of contamination of the sample during implantation. The primary source of the carbon is most likely in the form of CO, which is known to adsorb rapidly, however, no oxygen peak that could not be attributed to the slight oxidation of the emitter was ever seen at depths equivalent to those for carbon. Because of its importance in the formation of carbide phases which can modify surface properties, future studies should concentrate on the sources of this carbon and also determine under what conditions carbide phases can be induced to precipitate.

CHAPTER VI
CONCLUSIONS

The purpose of this study was to demonstrate that depth distributions of low energy ions implanted into metals could be obtained using the FIM/IAP. The modification of the near surface region by ion implantation has become increasingly commonplace. In particular nitrogen ions are often used to harden the surface of metals such as iron, nickel, titanium, etc. Yet the ability to measure the extent and nature of the implanted ions has not been adequate either spectroscopically or microstructurally. Field ion techniques are ideal for depth profiling because they offer the highest degree of depth resolution of any analytical instrument. However, there are questions of interpretation which arise from the use of FIM techniques. This study attempted to address them. In particular, there is the potential for alteration of the microstructure from stresses induced in emitters by the application of high electric fields. The TEM was used extensively to try to answer this point. The demonstration of the combined use of the TEM and the FIM/IAP in this study argues for the continued need to supplement and compare results from one instrumental technique with another.

The following sections will summarize the conclusions from each of the different areas in this study. In general, it can be said that the FIM/IAP can give the implanted depth of a particular species into a given metal substrate, but there are problems associated with its use which are unique to each specific system. The results of this study indicate paths for the ultimate solution to problems that may arise.

Depth Profiling Techniques

Two different methods were developed and successfully used in this study to obtain depth distributions of N_2^+ implanted into two metals, nickel and tungsten. One method, called the calculation method, was developed for metals which cannot be profiled with an imaging gas present. A second method, ring counting, was a modification of conventional FIM techniques that have been applied in atom probe work and when the image can be viewed. It too used the same data processing methods applied to calibration samples, with a few slight changes. The calculation method has a major advantage over ring counting in that data acquisition can be automated, if desired.

The calculation method was used for nickel because ion damage from implantation was sufficiently high such that the ring structure could not be discerned. Calibration samples showed that the model used for the geometry of the samples was appropriate. Two other points emerged from the calibration sample results. Firstly, they showed that natural fluctuations in the IAP signal are not reflected in the output of profiles. These fluctuations arise from raising the voltage during a profile, collapsing of major poles, and the decreasing field evaporation rate at constant voltage associated with the increasing radius of curvature. Secondly, they showed that extended depth profiles can be obtained without the imaging gas being present. Typically, depths of 1500 Å were relatively easy to achieve. It was also shown that TEM micrographs taken before and after depth profiling could be used to obtain the total distance probed and thus serve as a check on the calculated depth scale.

The ring counting method worked fine for N_2^+ implanted tungsten. It has several advantages to its use. The operator could observe the degree of damage in the FIM image as the experiment progressed and could essentially tell when the implanted region had been removed. These visual observations correlated well with the spectra obtained. In addition, specific defects could be seen while the experiment is in progress. Spirals indicating the presence of dislocation loops were seen on the major pole used for ring counting. These spirals were visible only for a limited number of rings and thereby the size of the loops could be obtained. In general, ring counting method is the preferred means of depth profiling if it can be used.

To a large extent, the success of both profiling techniques was due to the development and implementation of computer programs for collecting and handling the data. These programs were written so that information could be exchanged between them easily, i.e. they had the same data file formats. In addition, the large amount of storage afforded by the Tektronix 4909 file manager made some aspects of the study much easier, e.g. the ability to cross reference features on the profiles with the actual spectra. This ability sets this instrument apart from other atom probe instruments.

Field-Induced Stresses

The two TEM holders were developed for this study specifically to investigate the effects of the field-induced stress on the implanted defect structure. The "Double-tilt" holder was designed in order to be able to identify defects using precise diffraction and diffraction contrast imaging. However, this holder had limited use for the present study because the size of the defects caused by implantation was on too fine a scale and also because of the large amount of overlapping of defects in the samples. It should have many other uses in future work, e.g. phase identification, defect analysis, etc. The best imaging conditions for implanted tips were found to be slightly off the Bragg "two"-beam condition. The "Field-effect" holder was developed to see directly the effects of applying a field to an emitter. Although there is a difference between the conditions of a specimen in this holder (at room temperature) and those found in the FIM, it provides the best current answer to questions about the effects of applied fields on the implanted structure. The major results of the TEM work were as follows:

1) At room temperature, and at approximately 30% of the field for evaporation at 65°K, the implanted defect microstructure was unaffected by field-induced stresses within the resolution limits of the TEM.
2) Quantitative image comparisons between specimens transferred between instruments cannot be made because of the extreme image sensitivity to slight differences in tilting conditions.
3) Qualitatively, there was no difference in defect density due to imaging or analyzing in the FIM/IAP, within the limits of obtaining the same tilt conditions in the TEM.

Nitrogen Implantation

Nitrogen In Nickel

The results from the work on implantation of N_2^+ in nickel indicate that the nitrogen is behaving in a fashion similar to sulfur on nickel [85]. The nitrogen "bursts" seen in profiles and spectra, and the experiment in which the refrigerator shut down leads to the conclusion that the nitrogen atoms cling to the surface and resist desorption even though the nickel matrix field evaporates. However, the presence of some nitrogen in the spectra indicates that it is not as tightly bound as sulfur. There is a strong temperature dependence in the way nitrogen desorbs from the nickel surface. It is anticipated that a temperature controlled sample holder should be able to show that the nitrogen implanted into nickel can be profiled with the methods developed in this study.

The present results suggest serious difficulties with results of conventional atom probe experiments involving analyses of phases containing nitrogen. Since the IAP obtains a complete spectrum for each evaporation pulse, it contains details which conventional atom probe spectra miss. For example, the conventional atom probe is unable to detect the "bursts" which were seen in the IAP spectra and profiles. Therefore, in an atom probe study, the nitrogen composition could be reported as substantially less than the true composition and its depth distribution substantially spread.

Nitrogen In Tungsten

The results of N_2^+ implanted tungsten showed that the IAP can indeed profile a system which is well behaved. The experimentally determined ranges agree nicely with the TRIMML results when the proper constants are found. However, the peaks at shallower depths are not understood. They may be associated with backscattering of the ions inside the metal, but this explanation is uncertain. It is possible that, because of the of the great depth sensitivity of the FIM/IAP, these peaks have not been seen before.

In Situ Implantation Results

Two distinct conclusions can be made from the use of *in situ* ion implantation in this study. The first is that it is possible to use *in situ* implantation for studying deuterium. This study has shown that proper design of the differential pumping of the ion gun coupled to the FIM/IAP chamber keeps the deuterium background pressure sufficiently low. This means that, with the proper precautions, implanted deuterium can be distinguished from background deuterium despite the adsorption of hydrogen (deuterium) onto the emitter which occurs simultaneously in the FIM. The second result is that carbon is seen in the spectra of specimens implanted *ex situ*, but not those implanted *in situ*. Since most experimental and commercial implantations are performed under conditions similar to those designated *ex situ* in this study, they may also have unintentionally implanted carbon (by knock-on events). These observations should open up an area of investigation in the FIM/IAP that includes microscopic and analytical studies of carbide phases which precipitate as a result of the beam carburization.

Deuterium Embrittlement Of Nickel

Since the TEM results indicated that no pre-existing defects were contained in the specimens used in this study and from the separate observation that nitrogen-implanted nickel tips could be successfully profiled, the results in this study indicated strongly that nickel is embrittled by deuterium. Although, it is known that the fracture is intragranular, it is very difficult to apply any of the embrittlement mechanisms discussed in Chapter I to this problem. Since embrittlement occurred in nearly all the samples profiled, it is clear that the mechanism must involve the interaction of the defects caused by implantation and the deuterium. It must also account for the fracture occurring further down the shank of the specimen where both the defect and implanted deuterium densities are very low and close to the surface. It is difficult to speculate on a mechanism that incorporates these features.

FIM/IAP Observations

A number of observations were made during the course of this study which affect the proper operation of the FIM/IAP and the interpretation of data, but do not bear on the implantation results directly. These are summarized below:

1) Neon suppresses the N^+ signal in tungsten. It also suppresses an adsorbed species (m/n = 14.5-16) which is difficult to identify.
2) A CO^+ peak is present at low fields for all specimens. The magnitude of this peak is dependent on the interval between

pulses and the field strength. A maximum in the CO^+ signal is seen as the field is increased, but decreases to zero well below the fields required for field evaporation of the substrate.

3) The evaporation field for several metals (nickel, iron, and tungsten) are lowered by ion implantation.
4) The evaporation field for nickel is raised when neon is used as the imaging gas. This is the only metal for which this behavior has been observed.
5) Implanted helium cannot be detected in a system in which the evaporation field for the metal is less than the ionization field for helium.

CHAPTER VII
SUGGESTED FUTURE WORK

Many of the ideas for future work presented in this chapter are derived from the observations made in the control experiments performed in Chapter III and from an extension of the experiments in Chapter IV. Several of the experiments suggested parallel the ion beam work of Myers et al. [96-101]. Still others are tied to near-future modifications of the Colutron ion gun and FIM/IAP. This chapter will outline some experiments which are be possible but not yet feasible and some that are capable of being performed with the present instrument.

Nitrogen In Nickel

The question of why the nitrogen behaves as it does in nickel during depth profiling deserves further attention. The present results suggest that there is a critical temperature dependence on the way nitrogen desorbs from nickel. Two experimental approaches are suggested. The first would use the new temperature controlled FIM specimen stage to investigate this dependency. A series of depth profiles should be taken at temperatures above that used for this study (65°K). An early experiment should recreate the accidental one in which the refrigerator shut down in order to see the relation of the spectra corresponding to the release of nitrogen and the high evaporation rate with temperature. The second approach should use a pulsed laser atom probe to desorb the nitrogen. By varying the laser power relative to the applied field to, information on the field dependence of the desorbing nitrogen could be obtained. The base temperature of the tip can also be controlled. The primary goal of both approaches is to carefully control the field evaporation rate by a means other than with the voltage.

Similar studies should be undertaken for nitrogen as well for other interstitial-type elements in other metals. These others would include carbon. oxygen, phosphorus, and sulfur. Interstial are extremely important in BCC metals and can affect phase stability decisively even when present at very low levels. Such a series of studies would be of far reaching importance and are well suited to the FIM/IAP, especially when used in conjunction with TEM.

Nitrogen In Tungsten

The tungsten work on nitrogen in tungsten should be continued at higher implantation energies to see if the peaks at shallow depths persist or if there is a single implantation peak. The question arises, "Are the shallow peaks (and surface peaks) only present for low energy implantation energies or is the FIM/IAP so sensitive that these peaks have only been observed by other means?" By extending the range of ion energies, the constants used for the TRIMML program may be more accurately determined for this system. The tungsten system also acts as a gauge to measure the performance of other systems.

Carbon In Metals

Because many of the commercial alloys being modified by ion implantation contain strong carbide formers, the incidental inclusion of carbon in implanted substrates is an important feature which must be better understood. The present study has shown that cryogenic temperatures and good vacuum conditions can eliminate the presence of carbon in the target material. Other studies indicate that the carbide phases will not occur when elevated temperatures are used. Thus, a battery of *in situ* implantations in which the sample temperature is controlled in order to determine which of the above parameters are the most important is suggested. It should be pointed out that the presence of the carbon is not necessarily bad since carbide phases can be beneficial.

A more precise set of experiments should be undertaken to investigate the reasons for the change in the distribution of the C^{+2} and C^{+} peaks with depth. It is probably related to the distribution of carbon atoms in the near-surface region. The FIM/IAP is aptly suited for this type of study.

Deuterium In Metals

Deuterium Implanted Nickel Emitter Failure

The phenomena of the embrittling of the nickel emitters with deuterium implantation should be investigated further. The first set of experiments should determine whether hydrogen implantation produces the same results. If so, then hydrogen should be used for the embrittlement studies instead of deuterium in order to minimize the deuterium background build-up. These studies should include experiments to determine the fluence, energy, and implantation temperature dependencies.

The results of such work will have implications on deuterium implantation studies of other metals and/or alloy systems using the FIM/IAP.

Fracture of the specimens may be detectable without collecting the enormous amount of data normally required in an IAP depth profiling experiment. This could be done by setting the experiment to not store all the waveforms. The digitizer would be set up with the vertical amplifier at a lower than normal gain and although the Ni^{+2} signals would be quite small, the large, off-scale peaks associated with specimen fracture would be seen. The resulting spectra should be examined to look for the large release of the implanted species.

Of course, the interaction of hydrogen with metals is an important problem area in materials science. The present work has demonstrated the feasibility of using the FIM/IAP to studying in situ deuterium implanted specimens. This effort should be extended to other metal substrates until one is found in which embrittlement is not a problem. Tungsten is the most likely candidate. The earlier work of Kellogg and Panitz [45] and Panitz [47] indicated that very low energy (< 300 eV), high fluence studies are possible. Preliminary results in the present studies using 5 keV D_2^+ ion energies and very low fluences indicate that depth profiling of tungsten without failure of the emitters is possible.

The suggested areas of investigation in the following section depend on whether a suitable metal system can be found in which the specimens are not embrittled by the implanted deuterium.

Deuterium Redistribution

Cryogenic/room temperature experiments

With the ability to determine the depth distribution of deuterium implanted into metals and trapped to defects, the study of the redistribution of deuterium between trap types is possible. Simple experiments of implanting specimens with deuterium and letting them warm to room temperature are possible with the present FIM/IAP specimen stage. In nickel, warming a D^+-only implanted tip should result in the release of the deuterium from the sample [98]. If He^+ ions are implanted into the nickel prior to D^+ ion implantation, the release of the deuterium from the weaker trap types caused by D^+ ion implantation to the stronger He bubble traps will occur below room temperature [99]. The release stage from these types of traps is well above room temperature. If the He is implanted at different energies in various specimens and subsequently implanted with deuterium and raised to room temperature, the deuterium depth profiles of these specimens should reflect the energy dependence of the implanted He. With the use of the new temperature controlled FIM/IAP specimen stage (see Appendix A), the release temperature stage should be able to be found by depth profiling several specimens, each at different temperatures.

It was originally thought that the deuterium trapped to the helium bubbles, might be correlated with the helium signal in the IAP spectra and thus find the ratio of D atoms to He atoms. However as was discussed in Chapter III, the He signal cannot be detected with nickel. However, this possibility should be checked with one of the refractory metals (such as W, Mo, or Pt). In these metals, the evaporation field is higher than the ionization field for He.

Temperature-controlled experiments

The use of the new specimen stage will present other experimental opportunities. As the temperature is raised, depending on the number and strength of higher energy traps, the deuterium will be released from the bulk metal at certain temperatures. The D^+ peak should be able to be monitored with desorption pulsing as it comes to the surface. Field desorbtion refers to the desorbtion of less tightly bound surface species as compared to the matrix, i.e., field evaporation does not occur. This procedure will not be straightforward because field evaporation is a thermal process. This means that a reliable method must be found to lower the d.c. voltage as the temperature is increased. This can be accomplished in two ways, both would require computer control. The first involves a calibration sample of known radius in which the evaporation voltage as a function of temperature is found. This method probably will not be the best since the field on an emitter as a function of voltage is slightly dependent on specimen geometry, i.e., shank half-angle. It is also complicated by the lowering of the evaporation field by ion implantation discussed in Chapter III. The second method employs analyzing each spectrum for the matrix signal and lowering the voltage until the signal is not present. This method has its disadvantages in that the feedback loop is rather slow. Perhaps a combination of the two methods would prove best.

These temperature ramping experiments will have another complication due to the field dependence of the H_2^+/H^+ ratio. This ratio would need to be determined as a function of temperature for a given metal. This may not be a serious problem, because the deuterium would appear as D_1^+ in the IAP spectra and also as $(HD)^+$, and D_2^+. Another problem which should be addressed is to determine the temperature at which the metal used has an evaporation field which becomes less than the ionization field for hydrogen. Again, this situation could require the use of a refractory metal if higher temperatures are desired. These are quite simple control experiments in general terms, but will require a bit of expertise at running the FIM/IAP. Fortunately, the interface programs for the control of the Scientific Instruments model 5500 temperature controller have been written (see Appendix D). Only minor modifications to the program "IAPRING.HV" would be required for these experiments.

Field-Induced Stresses

Field-induced stresses have been a persistent question with FIM techniques. Although the use of the FIM/TEM "Field-Effect" holder did not fully answer all the questions with respect to the effects on the implanted defect structure, it did shed considerable light on the subject. This holder has not yet been fully utilized. It is a means of applying a stress state in the TEM which can be completely determined by finite element analysis [102]. The stress state of the specimen is similar to that ahead of crack tip in a brittle material.

If a cryogenic "Field-Effect" holder can be constructed, with the capability of applying up to 7 kV to the specimen _in situ_ TEM, all of the questions pertaining to field effects can be answered. However, the design of this holder will be complex because of the somewhat conflicting requirements of stability, high voltage, cryogenic design, and physical dimensions.

When used in conjunction with the FIM/IAP, the "Double-Tilt" holder and the "Field-Effect" holder are an especially powerful combination. Defects such as grain boundaries or dislocations, or second phases such as precipitates can be completely analyzed with the use of the "Double-Tilt" holder and the effects of the applied field-induced stress determined with the "Field-Effect" holder. In addition, low energy ion implantation of interstitial elements with an appropriate heat treatment, can provide atmospheres around dislocations or segregation to boundaries. The effects the atmospheres have on the defect with respect to the field-induced stresses can be observed.

Implantation Depths

Data on implantation depths for various ions into elements other than silicon simply does not exist for relatively low energies (<50 keV). This data now can be generated. The Colutron ion gun is capable of using many types of charges, both gaseous and solid. Many different metal systems have been investigated with FIM techniques. The possibility exists for producing a much needed data base for a multitude of systems involving low energy ion implantation. The addition of the side-implantation port on the ion beam line (discussed below) could also be most helpful in this respect.

Orthogonal Axis Implantation

Perhaps some of the most exciting potential applications of the present FIM/IAP and Colutron ion gun combination will occur when the beam line of the ion gun is modified to accept FIM specimens such that they may be implanted perpendicular to the emitters' axes. The Colutron ion gun is capable of using solid charges. Thus, the relatively new field of ion implantation metallurgy can be extensively studied on these samples. The microstructures of the implanted specimens can be observed with both FIM and TEM, without any further specimen preparation. With proper heat treatments, precipitation processes with both metastable phases and equilibrium phases have been seen to occur with ion metallurgy [103-105]. In addition, since the implantation is done from the side of the specimen, an interface is created between the implanted and unimplanted regions of the specimen. This interface can be observed by FIM as was seen by Loberg and Nordén who implanted 20 keV Ar^+ into tungsten and could see the damaged and undamaged regions in the image [106]. These authors also correlated the FIM image with TEM images to obtain the depth range of the Ar^+ ions. Clearly from the standpoint of ion metallurgy these studies will be quite exciting because the resulting implantation microstructures can be observed in cross section in both the FIM and TEM and also be readily studied with the analytical methods available (i.e., IAP and atom probe - FIM, Energy Dispersive X-ray analysis (EDX), Electron Energy Loss Spectroscopy (EELS), and convergent beam diffraction - TEM).

With respect to the deuterium work, implantation from the side is a method for obtaining trap types such as solute and interstitial atoms, precipitates, and interfaces which would be impossible to find in normally prepared FIM specimens because of the small volume studied. These specimens, implanted from the side, heat treated or processed in some manner, could be transferred to the FIM/IAP and implanted from the front with deuterium. The trapping of deuterium should be able to be observed in the IAP time-gated mode of operation to directly see the trapping of the deuterium to these trap sites. In addition, the time-gated mode offers an advantage from the FIM mode, the specimen need not be held at cryogenic temperatures to form the image, since the image is formed by the field evaporated ions themselves. The possibility of room temperature evaporation may alleviate some of the problems discussed above.

Implantation Lowering Of Evaporation Field

For future work with ion implanted specimens using the FIM/IAP, or a conventional atom probe, the dependence on the mass, and energy of implanted species should be found in order to account for it during operating the IAP. Preliminary observations in nickel have shown a decrease in evaporation field for He^+, D_1^+, D_2^+, and N_2^+. There also appears to be a mass dependence, but little dependence on energy (in the 5 to 10 keV range). These are only qualitative observations which indicate a tendency; there are only a small base of data supporting these statements. There are also questions of what the ion fluence and temperature during implantation will have on the evaporation field. These dependencies, if they are there, should be able to be found in a straightforward set of experiments using the FIM/IAP and Colutron ion gun combination.

APPENDIX A
IMPROVED FIM SPECIMEN HOLDER WITH TEMPERATURE CONTROL

Geometrically, there is little difference between the new holder and the old one. There are several cryogenic improvements which have been incorporated along with the addition of the thermocouple and heater. The concentric outer copper cylinder, boron nitride insulator, and inner copper rod all are tapered to the same angle and fit together tightly. This improves the heat transfer from the inner rod to the outer cylinder. The outer cylinder is made from one piece of copper and does not have the stainless steel front end that the old holder has. The mechanical support rods coming down from the manipulator are made from thin-walled stainless steel tubing which is a poor thermal conductor. The original holder has solid stainless steel rods which have both a better thermal path and a larger thermal mass. The sample holder also has a radiation shield attached to the first stage of the Air Products Displex refrigerator. These changes should bring the ultimate temperature considerably below the 65°K temperature of the old holder.

The attachment of the braid to the outer cylinder's collar differs also. The original braid was silver-soldered to the button and the cylinder collar. The new braid has been TIG-welded to the button and to a plate which is clamped to the collar. A special technique was used to TIG-weld the copper and to keep it from oxidizing. An incubator was modified to accept the TIG electrode and to have Argon or Helium flow through it. The braid was clamped by two pieces of copper to both hold the end to be welded and act as a heat sink. The inert gas was left flowing until the piece cooled. The mating surfaces were then polished to a flat surface. Gold leaf, .002 in. thick, is used as a gasket to improve the heat transfer. This braid design has the added benefit that in the future a new holder design can also use it.

The heater is a length of nichrome wire having a resistance of approximately 12 ohms. Four alumina tubes are bound to the outer cylinder with stainless steel bands. The nichrome wire was first wound in a spiral and then pulled through the tubes. Alumina fish-spine beads are used for insulating the bare wire. The heater and thermocouple wires are thermally sunk to the end cryogenic button. A specially designed lavite block is used to make a nichrome to copper wire contact and make chromel/chromel and gold/gold contacts. These connections are made before the button is bolted to the second stage of the refrigerator. The wires are led from the electrical feed through to the radiation shield and then to the button.

Figure A-1 shows three different views of the specimen holder, with the braid attached, and stainless steel mechanical support.

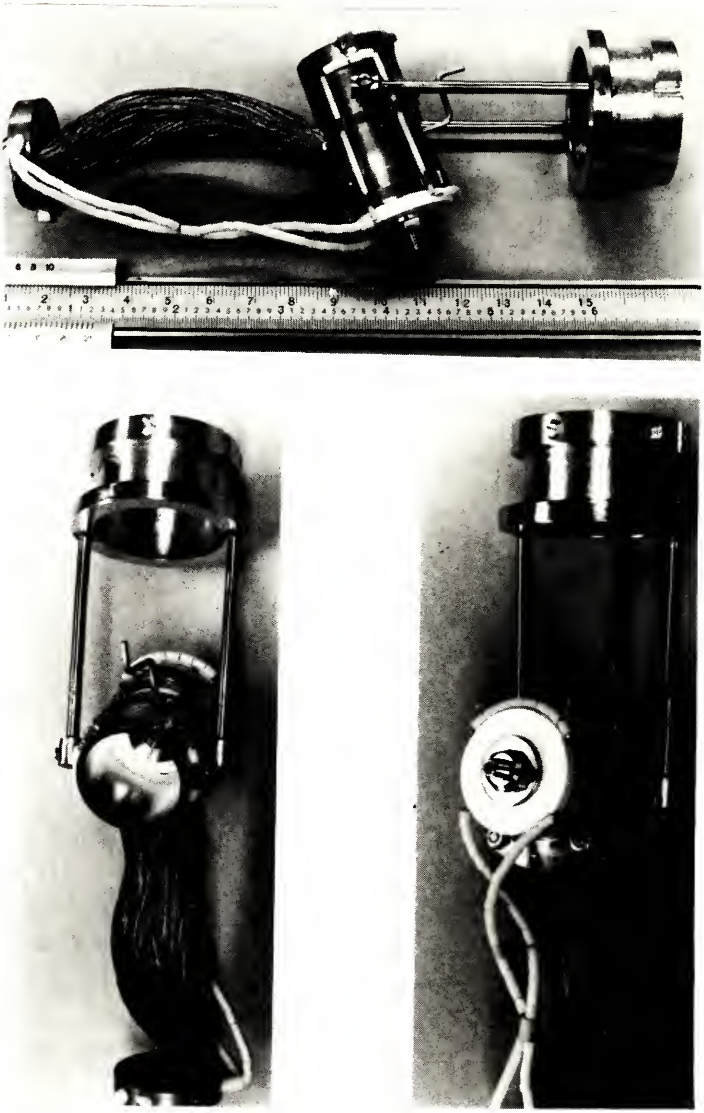

Figure A-1 Three different views of the new temperature controlled FIM/IAP specimen holder.

APPENDIX B
ALIGNMENT OF THE COLUTRON ION GUN

When the Colutron ion gun was coupled to the FIM/IAP, a problem arose which is common when an ion gun is attached to a pre-existing system: the ion beam could not be aligned by line-of-sight methods such as using a phosphor screen because of the lack of a viewing port. The ion beam current striking the sample holder is monitored by removing the high voltage lead and replacing it with a Keithley 610B electrometer. However, monitoring the ion current also cannot be used to center the beam because the size of the sample holder is much larger than the 2 mm beam spot size. In addition, the centering of the ion beam is extremely critical because the field emitter positioned in the exact center of the specimen holder and has only a .010" diameter cross section. Therefore, an alternative method was required for alignment.

Anhydrous tungsten trioxide is known to turn from yellow to blue when protons are injected into it under electrochemical conditions. Specimen stools with Scotch double-stick tape were pressed into a container containing WO_3 powder and excess powder tapped off. These prepared stools were then placed in the FIM/IAP and exposed to a H_2^+ beam under conditions similar to normal FIM specimens. A dark, bluish spot is visible on the stool when it is removed from the FIM/IAP. The Huntington manipulator is adjusted for the next stool accordingly with respect to the relative spot position. In addition, the size of the spot gives the approximate beam spot size. Figure B-1 shows a sequence of ten

H_2^+-irradiated WO_3 samples in the alignment of the sample holder with the beam.

There were some anticipated problems with the use of the Scotch tape, but they proved to be minor. The vacuum conditions were not noticeably affected either with or without the ion beam on. If the stools were used at room temperature there were no charging effects, but at cryogenic temperatures, initially the current would jump and then settle down to a constant value. Whether beam heating, thinning of the tape, improved conductivity due to the hydrogen injection, or a combination of these is occurring is not known, but charging does not present a serious problem at cryogenic temperatures.

The WO_3 method provides a visual means of finding the beam location and the approximate beam size. After the ion beam was aligned, a silicon sample with a TEM copper grid covering it was implanted. This sample was then imaged in a scanning electron microscope (SEM) using the SEI (Secondary Electron Image) signal. Figure B-2 shows the SEM micrograph of this sample. The exact beam size and shape is obtained from this micrograph. EBIC (Electron Beam Induced Current) images show the contrast better, but the SEI image is suitable.

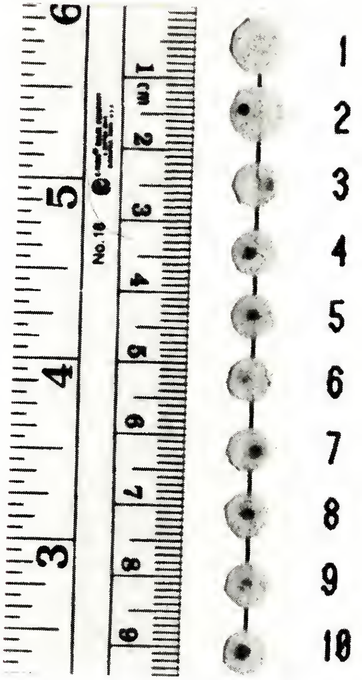

Figure B-1 Ten WO_3 samples exposed to 8 keV H_2^+ ions. Between each sample, the manipulator settings of the FIM/IAP were changed in an attempt to find the correct ones for alignment. In trial number 1, the beam had just hit the edge of the target. In trial 2, the exposure was not long enough to produce the very heavy spots seen in the subsequent trials (in the later runs, the time of exposure was increased), and so was highlighted with a black pen in order to be photographed. Between trials 1 and 8, the manipulator settings were changed. Between trials 8 and 10 the same settings were used and are those used for implanting FIM specimens. The manipulator settings were reset back to their normal positions each time the samples were exchanged with the exchange mechanism of the FIM/IAP. The spots indicate the approximate size and shape of the ion beam.

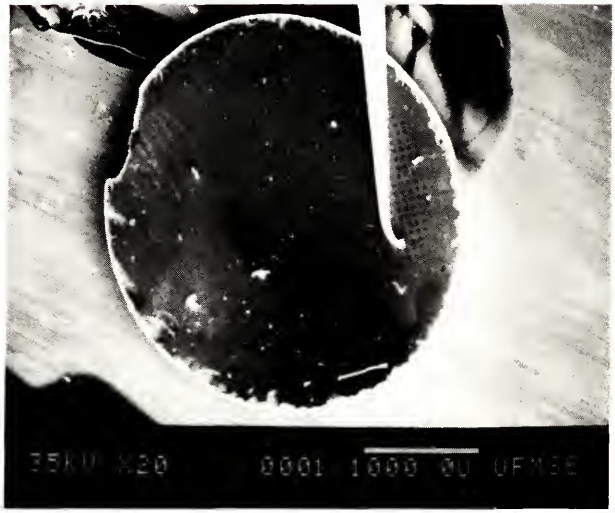

Figure B-2 Scanning Electron Microscope image of an 8 keV H_2^+ ion implanted 3 mm silicon disk. The cross-hatched area is the result of placing a TEM grid over half of the sample. The image is not seen to be circular because it was recorded while tilted in the microscope and without the tilt correction on. This example shows that the beam size can be found quite easily.

APPENDIX C
MEASURED TIME DELAYS

Table C-1 lists the delays and their values, all determined with the 7912AD. In some cases the delays are intentional in order to compensate for other delays. For example the delay of the desorption pulse line was introduced by having a 52.3 meter cable to balance the delay of the Krytron switch circuitry of the channel plate pulser. All the delays are measured by splitting an input pulse into the device or cable for which the delay is to be measured and one channel of the digitizer. The delay is then measured between the displayed trigger pulse and output signal of the device which is fed into the other channel. One exception to this procedure was the measurement of the time difference between the vertical amplifier and the "Z"-intensification displayed on the digitizer. In this case an input pulse was split into two equal length cables; one going to the one channel of the digitizer and one into the "Z"-intensification input. The digitizer was triggered by the vertical amplifier and the pulse displayed in a normal trace. Because of the delay between the vertical amplifier and "Z"-in, the intensified portion of the trace was displaced by the time difference. The position of the displayed pulse was constant between waveforms and was noted. The main intensity of the digitizer was turned down until only the intensified portion was being displayed. When this was digitized, the 7912AD fills in those points not detected with an interpolated straight line. There is a small amplitude, jagged curve occurring in the portion of the trace where it was intensified. The start of this is noted. The time delay is the difference between the two values found. The measured value was 39 nsec. This also yields the width of the pulse which is set at 50 nsec.

Table C-1
FIM/IAP Delay Times

TOF Mode Delay	Figure II-6 label	Delay (nsec)	Cable length (m)
Cable, Tee pickoff to Ch1	A	13.1	2.62
Cable, CEMA output to Ch2	B	13.1	2.62

Time-Gated Mode Delay	Figure II-8 label	Delay (nsec)	Cable length (m)
Cable, desorption pick-off to delay generator	B	6	2.77
Cable, CT-3 to Des. pickoff	internal to Des. pulser	6	2.77
Delay generator (0 settting)	C	47	N/A
Cable, Delay gen. to gate pulse trigger	D	6	2.77
Krytron Switch	E (internal to gate pulser)	185	N/A
Cable, Delay gen. to Digitizer trigger	J	6	2.77
Cable, Gate pulse line	F	7.5	1.5
Cable, CT-3 to Gate pickoff	internal to gate pulser	6	2.77
Cable, Desorption pulse line	G	267*	53.2
Vertical amplifier (Z intense."Z"-in)	H (internal to digitizer)	39	N/A
Cable, Gate pickoff to "Z"-in	I	53.6*	10.7

* indicates an intentional delay used for compensating other delays.

APPENDIX D
FIM/IAP TEK BASIC PROGRAMS

The Tektronix 4052A uses an extended form of the BASIC programming language. In this section a brief description of the programs which have been developed for the FIM/IAP will be given. Each program listing will be given starting on the following page.

IAPRING.HV

This program is the main data collection program. User-defined keys can collect, create data files, recall and store waveforms from/to memory, control the Bertan 205A-30R power supply, display the spectrum, calculate mass-to-charge ratios,and turn on the voltage ramp feature. The control section from statement number 60000 will continuously loop, collecting spectra. Voltage control can be done manually or with the voltage ramp feature. When data are being collected in this manner, a previous spectrum is stored on the file manager during the same time as the digitizer is collecting the next one. There is very little delay between spectra in this way. The number of waveforms in each data file is limited to 500; new files are created automatically having the same generic file name. The control section of the program is run by entering the command, "Run 60000."

```
1 INIT
2 ON SRQ THEN 21000  !                    IAPRING.HV
3 GO TO 100
4 GO TO 1000
8 GO TO 2000
12 GO TO 3000
16 GO TO 4000
20 GO TO 5000
24 GO TO 6000
28 GO TO 7000
32 GO TO 8000
36 GO TO 9000
40 GO TO 10600
44 GO TO 10000
48 GO TO 12000
52 GO TO 13000
56 GO TO 14000
60 GO TO 15000
64 GO TO 16000
68 GO TO 17000
72 GO TO 18000
76 GO TO 19000
80 GO TO 20000
90 REM 7912AD/4050-Series [IAPDATA] IAPRING.HV"
92 REM
93 REM
94 REM Version WALCK 04/01/85
99 REM
100 REM
105 Skipper=2
110 G$="G"
120 DIM D$(1000)
130 CALL "STATUS","UNIT:ALL",D$
140 PRINT "L",D$
150 DIM D$(200)
160   !CALL "WAIT",5
170   !CALL "IDENTIFY","uni:0  [iapdata]"
172 CALL "DIRECT",D$
174 B$=SEG(D$,6,12)
176 B$=B$&" "&SEG(D$,119,17)
178 PRINT "K",B$,"J"
180 CALL "OPEN","INDEXFILENAME LFN:2"
190 DIM B$(400)
200 INPUT #2,65000:S$
210 Indexfile$=S$
220 CLOSE 2
230 B$=S$&" is the current indexed file being used for data storage_"
240 B$=B$&"Do you still want this file to be used? (y/n) "
250 GOSUB 11900
260 IF X=0 THEN   !     Will go to 10000 and either create a new file or
270    GOSUB 10000  !   use an old one.
280 END IF
```

```
282 Temelktr=0
284 Filenum=0
290 GOSUB 11000
300 SET KEY
310 GO TO 300
900   !
910   !
920   !
930   !
940   !
1000 REM                                                  ACQUIRE WAVEFORM
1020 SET NOKEY
1030 N$=" "
1035 Fileid$=""
1040 L=0
1050 Title$=""
1060   !PRINT "L ","ACQUIRE CURRENT WAVEFORM"
1070 CLOSE
1080 GOSUB 23000
1100 VIEWPORT 14,110,10,90
1110   !PRINT "L ","  WAVEFORM FROM CURRENT SETUP"
1120   !GOSUB 24000
1130 IF Recclamp<=0 THEN
1140    GOSUB 28000
1150 END IF
1155 GOSUB 32000
1160 RETURN
1900   !
1910   !
1920   !
1930   !
1940   !
2000   !INCREASE VOLTAGE
2020 SET NOKEY
2030 Meters$="12345678"
2040 CALL "IOBCD",Meters$,I1,I2
2050 Met1$=SEG(Meters$,1,4)
2060 V=VAL(Met1$)*0.01
2070 Vnew=V+Vinc
2080 Vprog=Vnew*1.06-0.012
2090 Vprog=INT(Vprog*1000)/1000
2110 PRINT @4:"P";Vprog;"KG"
2115 CALL "wait",0.75
2120 RETURN
3000   !RESET
3020 SET NOKEY
3030 PRINT @4:"R"
3040 CALL "BSETUP","IIII",0,High
3050 RETURN
4000   !INCREASE VOLTAGE
4006 Meters$="12345678"
4010 SET NOKEY
```

```
4020 CALL "IOBCD",Meters$,I1,I2
4030 Met1$=SEG(Meters$,1,4)
4040 V=VAL(Met1$)*0.01
4050 Vnew=V+0.1
4060 Vprog=Vnew*1.06-0.012
4070 Vprog=INT(Vprog*1000)/1000
4080 PRINT @4:"P";Vprog;"KG"
4085 CALL "wait",0.75
4090 RETURN
5000 REM                                Acquire from INDEXFILE$ file ON 4909
5020 SET NOKEY
5030 Title$=""
5040 PRINT "L ","HHHHHJust a minute, please, I'm finding the last rec";
5050 PRINT "ord number."
5060 GOSUB 26000
5080 IF X=0 THEN 5460
5102 Filenum=X
5120 CALL "RLOCATE","4 INDEX:";Filenum
5130 IF TYP(4)=4 THEN 5180
5140 PRINT "JINVALID FILE --- PLEASE SELECT ANOTHER"
5160 GO TO 5460
5180 IF A1<=0 THEN 5300
5300 DELETE A
5320 READ #4:N$,A1,A2,A3,X,X,H$,V$
5340 DIM A(A1)
5360 READ #4:A,X,Y,Y,Vdc,Vp,Ddatetime$,Specid$,Ktr,Numavgf
5370 CLOSE 4
5380 IF X=1 THEN 5420
5400 PRINT "JWARNING --- NON-UNIFORM SAMPLNG RATE IGNORED";G$;
5420 VIEWPORT 14,110,10,90
5430 PAGE
5440 GOSUB 24000
5460 CLOSE 4
5465   !GOSUB 32000
5480 RETURN
5900   !
5910   !
5920   !
5930   !
5940   !
6000   !SHUTDOWN
6020 SET NOKEY
6030 PRINT @4:"S"
6040 RETURN
7000   !DECREASE VOLTAGE
7020 SET NOKEY
7030 Meters$="12345678"
7040 CALL "IOBCD",Meters$,I1,I2
7050 Met1$=SEG(Meters$,1,4)
7060 V=VAL(Met1$)*0.01
7070 Vnew=V-Vinc
7080 Vprog=Vnew*1.059-0.012
```

```
7090 Vprog=INT(Vprog*1000)/1000 MAX 0
7100 PRINT @4:"P";Vprog;"KG"
7105 CALL "wait",0.75
7110 RETURN
8000 SET NOKEY   !              REGRAPH WFM ON SCREEN
8005 PAGE
8007 VIEWPORT 14,110,10,90
8008 Lun=32
8010 GOSUB 24000
8020 SET KEY
8030 RETURN
8900   !
8910   !
8920   !
8930   !
8940   !
9000   !INCREASE VOLTAGE
9006 Meters$="12345678"
9010 SET NOKEY
9020 CALL "IOBCD",Meters$,I1,I2
9030 Met1$=SEG(Meters$,1,4)
9040 V=VAL(Met1$)*0.01
9050 Vnew=V-0.1
9060 Vprog=Vnew*1.06-0.012
9070 Vprog=INT(Vprog*1000)/1000 MAX 0
9080 PRINT @4:"P";Vprog;"KG"
9085 CALL "wait",0.75
9090 RETURN
10000 REM              CREATE AN INDEXED FILE, & PUT IT IN INDEXFILENAME
10005 Idum=0
10010 CALL "open","indexfilename lfn:2"
10020 PRINT "LINDEX","HHHHHHHHFILENAME"
10025 Indexlast=0
10030 CALL "RPOSITION",2,L$
10035 L$=REP("",1,20)
10040 Indexktr=VAL(L$)
10050 INPUT #2,Indexktr:S$
10060 PRINT Indexktr,"HHHHHHHH";S$
10070 IF Indexktr=>65000 THEN 10150
10080 CALL "RLOCATE",2,"NEXT"
10090 Indexlast=Indexktr
10100 GO TO 10030
10150 REM S$ IS CURRENT INDEXFILE$ BEING USED (INDEX:65000)
10160 REM & SHOULD BE DUPLICATED IN LIST ONCE.
10170 REM INDEXLAST IS LAST INDEX USED PRIOR TO 65000
10180 B$="HAVE ANY OF THESE BEEN DELETED? (Y/N) "
10190 GOSUB 11900
10200 IF X=0 THEN 10290
10210 PRINT "HOW MANY? ";
10220 INPUT Bb
10230 DIM B(Bb)
10240 PRINT "ENTER INDEX NUMBERS. ";
```

```
10250 INPUT B
10260 FOR I=1 TO Bb
10270    CALL "DRECORD","LFN:2 INDEX:";B(I)
10280 NEXT I
10282 GOSUB 27000
10284 IF Idum>0 THEN 10005
10290 B$="Are any of these (WITH INDEX < 65000) the desired file? (Y/N)"
10300 GOSUB 11900
10310 IF X=1 THEN
10320    PRINT "Enter the indexed number of file you want to use. ";
10330    INPUT Indexktr
10340    INPUT #2,Indexktr:S$
10350    PRINT #2,65000:S$  !puts the old file to be used in record#
         65000
10360    Indexfile$=S$
10370 ELSE
10380    REM NEW INDEXED FILE TO BE CREATED
10390    PRINT "What is the name of new indexed file you wish to use
         for "
10400    PRINT "data storage? ";
10410    INPUT Indexfile$
10415    Indexfile$=Indexfile$&".fl"
10420    Indexktr=Indexlast+1
10430    PRINT #2,65000:Indexfile$
10440    PRINT #2,Indexktr:Indexfile$
10500    CALL "CREATE","B","N",Indexfile$
10510    CALL "OPEN",Indexfile$,"LFN:3"
10520    WRITE #3,65000:0  !   INDEX #65000 IS WHERE LAST FILENUM IS PUT
10525    WRITE #3,65001:500  !REC LIMIT=500
10530    CLOSE 3
10540    PRINT "INDEXED FILE, ";Indexfile$;" CREATED AND 0 PUT IN INDEX"
10550    PRINT " 65000 FOR LAST FILE USED."
10560    PRINT Indexfile$;" WAS ALSO PUT IN FILE 'INDEXFILENAME'."
10565    CALL "WAIT",1
10570 END IF
10580 CLOSE 2
10590 RETURN
10600 REM
10610 REM              ADD ANOTHER FLITETIME TO LIST & INDICATE WHERE
10620 CALL "OPEN","FLYTIMES LFN:6"
10630 IF Ktrtof=0 THEN 10670
10640 FOR I=1 TO Ktrtof
10650    INPUT #6:Flytime,Flitemkr
10660 NEXT I
10670 Flytime=(Arraycursor-It0)*A3
10680 Flitemkr=Arraycursor
10690 PRINT #6:Flytime,Flitemkr
10700 CLOSE 6
10710 Ktrtof=Ktrtof+1
10720 PRINT "G"
10730 MOVE Arraycursor-It0+1,A(Arraycursor)
10740 FOR I=1 TO 10
```

```
10750    RDRAW 0,0
10760 NEXT I
10770 MOVE Flitemkr-It0+1,0
10780 DASH 85
10790 RDRAW 0,-A2
10800 DASH 0
10810 HOME
10820 DELETE Masses,Premasses
10830 DIM Masses(Ktrtof),Premasses(Ktrtof)
10840 Masses=0
10850 Premasses=0
10860 RETURN
10900   !
10910   !
10920   !
10930   !
10940   !
11000 OFF SRQ   !                                                Initialize
11002 ON SRQ THEN 21200
11010 SET NOKEY
11020 DIM A$(100),L$(300),Q(20),B$(144),Fileid$(400)
11030 PRINT "L ","4050-SERIES/7912AD IAPSCALED"
11040 PRINT "  ","Copyright (c) 1980 Tektronix, Inc."
11050 PRINT "  ","       All rights reserved."
11060 REM SET ENVIRONMENT
11065 P2=2000
11070 DATA 4,1,4,1,1,1,3,1,4,1,1,1,4,1,3,1,1,1
11090 Meters$="ITISOFFF"
11100 DIM High(6),Start(6),Sstop(6)
11110 READ High,Start,Sstop
11120 CALL "BSETUP","IIII",0,High  !SETS ROM OUTPUT PINS 39&27 HIGH(+5V)
11130 Title$=""
11132 Rampind=-1
11134 Rampint=0.05
11136 Recclamp=500
11140 G$="G"
11145 Q1=1
11150 Q2=1
11155 Vinc=0.02
11160 Gnd=0
11170 CALL "RATE",9600,0,2  !SET BAUD RATE AND PARAMS. FOR PAPER TIGER
11175 CALL "CMFLAG",0  !NO INTERFACE BUFFER OVERFLOW FLAGGING,
11176   !                WILL NOT ALLOW FULL PROGRAM TO BE LISTED!
11177 REM******* FOR EPSON PRINTER, PUT PRI@37,26:1 HERE.
11178 REM       (ADDS CR+LF) REMEMBER TO PUT PRI@37,26:0 AT END!
11190 Nrpt=512
11200 Arraycursor=256
11201 It0=1
11202 Lefty=1
11204 Righty=1
11206 Ktrtof=0
11210 Q4=0
```

```
11212 B$="JJENTER NUMBER OF WFM'S TO BE AVGED(1<=2^N>=64)."
11214 PRINT B$
11216 INPUT Numavg
11220 Numavgf=Numavg
11225 PRINT "GGGGG"
11230 PRINT "GG","WARNING: DESORB PULSE MUST BE MORE THAN 2 DIV HIGH!__"
11240 Q7=1
11242 Tfilenum=0
11245 Fileid$=""
11255 File4909ind=-1
11260 Spectraktr=0
11265 Ktr=0
11270 Q8=1
11272 B$="JJIs printer available for tape directory (y/n)?"
11274 GOSUB 11900
11276 Q9=X
11277 IF Q9=0 THEN
11278    CALL "CMFLAG",0  !NO PRINTER AVAILABLE
11279 END IF
11380 DATA 0,0,0,0,1,0,"S","V",0,0  !!             INITIALIZE WAVEFORMS
11390 READ A1,A2,A3,A4,A5,B1,H$,V$,Vdc,Vp
11400 GOSUB 40000  !                          CHECK DATE & SPECIMEN ID
11410 Ind=1
11470 REM INITIALIZE ZERO REFS, ETC
11490 Q3=1
11500 REM SET NO-LOOP MODE
11510 Q0=0
11520 REM DEFINE CYCLE
11530 Q=-1
11550 U=1  ! DEFINES 7912AD ADDRESS TO BE 1
11560 U=INT(U)
11570 IF U<1 OR U>30 THEN 11540
11580 PRINT @U,0:"ID?"
11590 INPUT @U,0:A$
11600 IF POS(A$,"7912AD",1)<>0 THEN 11625
11610 PRINT "JIMPROPER RESPONCE FROM ADDRESS ";U;",0 --- ";A$
11620 STOP
11625 ON SRQ THEN 21200
11630 GOSUB 32000
11640 RETURN
11900 REM                                              Query user routine
11910 X=0
11920 PRINT B$;G$
11930 INPUT A$
11940 A$=SEG(A$,1,1)
11950 IF A$="N" THEN 11980
11960 IF A$<>"Y" THEN 11920
11970 X=1
11980 RETURN
11990   !
11991   !
11992   !
```

```
11993   !
11994   !
12000 REM *********************CURSOR MOVE LEFT ************************
12005 SET NOKEY
12010 Arraycursor=Arraycursor-1
12020 IF Arraycursor<=It0 THEN
12030    Arraycursor=512
12040    GO TO 12070
12050 END IF
12060 MOVE Arraycursor-It0,A(Arraycursor)
12070 RDRAW 0,0
12090 RETURN
12910   !
12920   !
12930   !
12940   !
13000 REM *********************CURSOR MOVE RIGHT ********************
13005 SET NOKEY
13010 Arraycursor=Arraycursor+1
13020 IF Arraycursor=>Nrpt THEN
13030    Arraycursor=It0  !
13040    GO TO 13070
13050 END IF
13060 MOVE Arraycursor-It0+1,A(Arraycursor)
13070 RDRAW 0,0
13090 RETURN
13900   !
13910   !
13920   !
13930   !
13940   !
14000   !SET VOLTAGE TO ZERO
14020 SET NOKEY
14030 PRINT @4:"P";0;"KG"
14040 RETURN
15000 REM                                  Save current waveform on file
15010 SET NOKEY
15020 PRINT "L ","SAVE WAVEFORM ON FILE"
15030 GOSUB 29000
15040 N$=Specid$&" "&"#"
15050 N$=N$&Spectraktr$&"     "&Ddatetime$
15060 CALL "OPEN",Indexfile$,"LFN:4"
15070 READ #4,65000:Filektr
15090 B$=STR(Filektr+1)
15100 B$="This WFM will be sTored in record#"&B$
15110 B$=B$&". _Is this ok? (y/n) "
15120 GOSUB 11900
15130 IF X=0 THEN 15160
15133 Filenum=Filektr+1
15140 WRITE #4,Filenum:N$,A1,A2,A3,0,1,H$,V$,A,1,0,A3,Vdc,Vp,Ddatetime$
15150 WRITE #4:Specid$,Spectraktr,Numavgf
15155 WRITE #4,65000:Filenum
```

```
15160 CLOSE 4
15161 Recclamp=Recclamp-1
15162 IF Recclamp<=0 THEN
15163    GOSUB 28000
15164 END IF
15165 GOSUB 8000
15170 GOSUB 32000
15180 RETURN
15900   !
15910   !
15920   !
15930   !
15940   !
16000 REM            TURN AUTO-STORE MODE ON/OFF (4909) NEXT IAPDATAXXXX
16010 SET NOKEY
16020 PAGE
16030 PRINT "JJJJJJJJ"
16040 Rampind=-Rampind
16050 IF Rampind=1 THEN
16060    PRINT "Voltage ramp is now on. Every ";Rampint*100;
16065    PRINT " minutes, voltage will"
16067    PRINT "be raised by vinc(";Vinc;") kv."
16070    PRINT "To turn off, press key 16 again."
16080 ELSE
16090    PRINT "Voltage ramp is now off. To turn back on"
16100    PRINT "again, press key 16 again."
16120 END IF
16130 RETURN
16900   !
16910   !
16920   !
16930   !
16940   !
17000   !incrase voltage increment by 10%
17010 SET NOKEY
17020 Vinc=INT(Vinc*1.1*1000)/1000
17025 PRINT "LJVINC= ";Vinc
17030 RETURN
18000 REM       USE CURSOR POSITION TO FIND DC OFFSET IN DIVISION UNITS
18010 PRINT "LJJJJJJJJJJJUSE CURSOR TO FIND DC OFFSET."
18020 PRINT "JWHEN SET, PRESS GND KEY (KEY 18)"
18025 CALL "WAIT",3
18030 Gnd=A(Arraycursor)/A2+Gnd
18035 PAGE
18036 A=A-A(Arraycursor)
18040 GOSUB 24000
18045 PRINT "JJJJJJJJJJJJJJJJJJJOFFSET=_";Gnd
18050 RETURN
18900   !
18910   !
18920   !
18930   !
```

```
18940  !
19000 REM CALCULATE M/N¯S AND MARK TIMES
19005 SET NOKEY
19006 Alpha=0.2  !MAY CHANGE THIS VALUE IF YOU LIKE
19010 IF Ktrtof=0 THEN 19440
19020 DIM Flytym(Ktrtof),Tmarker(Ktrtof),Massescalc(Ktrtof)
19030 CALL "OPEN","FLYTIMES LFN:6 TACCESS:READ "
19040 PRINT "L";Specid$
19050 PRINT "FILE: ";Indexfile$;"   INDEX:";Filenum;"   KTR#";Ktr," ";
19055 PRINT " ","H";Ddatetime$
19060 PRINT @40:"JJJJJJJ";Ddatetime$,Specid$,"FILE NO.";Filenum
19070 PRINT @40:"#";Ktr
19080 PRINT "JNUMBER","TOF(USEC)","PREVIOUS MASS","CURSOR INDEX"
19090 PRINT @40:"JNUMBER","TOF(USEC)","PREVIOUS MASS","CURSOR INDEX"
19100 FOR I=1 TO Ktrtof
19110    INPUT #6:Flytym(I),Tmarker(I)
19120    PRINT USING 19150:I,Flytym(I)/1.0E-6,Premasses(I),Tmarker(I)
19130    PRINT @40: USING 19150:I,Flytym(I)/1.0E-6,Premasses(I),
         Tmarker(I)
19140 NEXT I
19150 IMAGE 3T,2D,20T,2D.3D,40T,3D.2D,60T,3D
19160 CLOSE 6
19170 PRINT "JWHICH IS THE STANDARD?  ENTER ITS NUMBER. ";
19180 INPUT I
19190 PRINT "JWHAT IS ITS MASS TO CHARGE RATIO? ";
19200 INPUT Mton
19202 Massescalc=0
19204 Factor=0.193*(Vdc+Alpha*Vp)/0.15¯2/1.0E-12
19210 Flytym=Flytym¯2
19220 Masses=Flytym
19222 Massescalc=Flytym
19224 Massescalc=Massescalc*Factor
19230 Masses=Masses/Flytym(I)
19240 Masses=Masses*Mton
19250 Flytym=SQR(Flytym)
19260 Premasses=Masses
19270 Massind=1
19280 PRINT @40:"JJ"
19282 PRINT "JJ"
19290 PRINT @40:"THE FOLLOWING ARE THE MASSES CALCULATED BY RATIO BASED"
19292 PRINT "THE FOLLOWING ARE THE MASSES CALCULATED BY RATIO BASED"
19300 PRINT @40:"UPON MASS ";Mton;" AT TIME ";Flytym(I)/1.0E-6;" USEC ";
19302 PRINT "UPON MASS ";Mton;" AT TIME ";Flytym(I)/1.0E-6;" USEC ";
19305 PRINT @40:"AND TOF EQUATION "
19306 PRINT @40:"USING ALPHA= ";Alpha;" :J"
19307 PRINT "AND TOF EQUATION "
19308 PRINT "ALPHA= ";Alpha;" :J"
19310 PRINT "NUMBER","TIME(USEC)","RATIO M/N","CALC M/N"
19320 PRINT @40:"NUMBER","TIME(USEC)","RATIO M/N","CALC M/N"
19330 FOR I=1 TO Ktrtof
19340    PRINT USING 19360:I,Flytym(I)/1.0E-6,Masses(I),Massescalc(I)
19350    PRINT @40: USING 19360:I,Flytym(I)/1.0E-6,Masses(I),
          Massescalc(I)
19360     IMAGE2X,2D,15X,2D.3D,12X,3D.2D,11X,3D.2D
19370 NEXT I
19375 PRINT @40:"L"
19380 CALL "WAIT",6
19390 PAGE
19410 GOSUB 50000
19420    !GOSUB 19520
19430    !GOSUB 19610
19438 SET KEY
19440 RETURN
19450 PAGE
19460 PRINT "JJJJJYOU MUST MARK THE FLIGHT TIMES WITH KEY10 FIRST,
      SILLY."
19470 PRINT "GGGGGGGGGGGGGGG"
19480 CALL "WAIT",3
19490 PAGE
19500 GOSUB 24000
19510 RETURN
19520 REM MARK TIMES WITH DASHED LINES ON GRAPH
19530 DASH 85
19540 FOR I=1 TO Ktrtof
19550    MOVE @Lun:Tmarker(I)-It0+1,0
19560    RDRAW @Lun:0,-A2
19570 NEXT I
19580 DASH 0
19590 HOME
19600 RETURN
19610 REM WRITE THE MASSES ON RIGHT SIDE OF GRAPH
19620 HOME @Lun:
19630 PRINT @Lun:"JJJ"
19640 IF Lun=3 THEN 19670
19650 PRINT @Lun: USING "64"" "",""M/N""":
19660 GO TO 19690
19670 MOVE @Lun:533.5,W2-1.0E-3
19680 PRINT @Lun:"M/NHHHHHJ";
19690 FOR I=1 TO Ktrtof
19700    IF Lun=3 THEN 19730
19710    PRINT @Lun: USING "62"" "",3D.2D":Masses(I)
19720    GO TO 19740
19730    PRINT @Lun: USING "3D.2D,""HHHHHHJ"",S":Masses(I)
19740 NEXT I
19750 HOME
19760 RETURN
19770   !
19780   !
19790   !
19800   !
19810   !
20000 REM        RESET (TOFFILE) & SET KTRTOF TO 0
20005 DELETE Masses,Premasses
20010 Ktrtof=0
```

```
20020 CALL "open","flytimes lfn:6"
20025 Massind=0
20030 CLOSE 6
20035 PRINT "G"
20036 Arraycursor=It0
20040 RETURN
20900   !
20910   !
20920   !
20930   !
20940   !
21000 REM                                                 Temp serial poll
21040 X=1
21060 X=INT(X)
21080 IF X<1 OR X>30 THEN 21020
21100 POLL P1,P2;X,0
21120 POLL P1,P2;X,1
21140 POLL P1,P2;X,2
21150 POLL P1,P2;2;3;4
21160 RETURN
21200 REM                                                 Real serial poll
21220 POLL P1,P2;U,0;2;3;4
21225 REM  7912AD OPC SRQ HANDLER
21230 IF P2=82 OR P2=66 OR P2=2 OR P2=64 AND P1=1 THEN 21252
21240 PRINT "SRQ FROM ";P1;",","STATUS = ";P2
21250 GO TO 21260
21252 GOSUB 56000
21260 RETURN
22000 REM                                FILEID$ CONCANTENATION ROUTINE
22001 REM                        RETURNS S$ AND IAP$ IN FORM: IAPDATAxxxx
22010 Iap$="IAPDATA"
22020 Sp$="0000"
22030 S$=STR(Filenum)
22040 S$=REP("",1,1)
22050 S$=Sp$&S$
22060 X=LEN(S$)
22070 Y=X-4
22080 S$=REP("",1,Y)
22090 S$=Iap$&S$
22100 Iap$=S$
22110 RETURN
23000 REM                                           Acquire waveform into A
23001 Filenum=0
23002 Numavg$=STR(Numavg)
23004 Digsa$="DIG SA,"&Numavg$
23010 IF A1<=0 THEN 23080
23070 REM FIRST GET VERTICAL SCALE
23080 PRINT @U,0:"VS2?"
23090 INPUT @U,0:V1,V1
23095 Vs2=V1
23100 REM SET UP CONSTANTS
23105 A2=ABS(V1)
```

```
23110 C1=ABS(V1)*256*8/1024
23120 C2=C1/256
23130 PRINT @U,0:"GRI?"  !NEEDED,BUT WHY?
23140 INPUT @U,0:B$  !NEEDED,BUT WHY?
23150 PRINT @U,0:"GRI 0"
23180 P2=1000
23190 PRINT @1,0:"OPC ON"
23195 PRINT @U,0:Digsa$
23200   !CALL "WAIT",1
23201 GOSUB 55000
23202 GO TO Skipper OF 23203,23204
23203 GOSUB 58000
23204 IF P2=82 OR P2=66 OR P2=2 OR P2=64 THEN 23210
23205 PRINT USING 60110:Temelktr,Filenum,Ktr,Ktr*Numavg
23206 GO TO 23204
23210 PRINT @U,0:B$;"OPC OFF;DEF ON;READ SA;"
23215 Skipper=1
23220 WBYTE @64+U,96:
23230 RBYTE X,X,Y
23240 A1=(X*256+Y-1)/2
23250 DELETE A
23260 DIM A(A1)
23270 GO TO Q1+1 OF 23380,23280
23280 REM FAST READ
23300 DELETE V1,V2
23310 DIM V1(A1,2),V2(2,1)
23320 V2(1,1)=C1
23330 V2(2,1)=C2
23340 RBYTE V1
23350 A=V1 MPY V2
23360 DELETE V1,V2
23440 RBYTE X,Y
23450 REM NOW READ HORIZONTAL SCALE
23460 PRINT @U,0:"HS2?"
23470 INPUT @U,0:A3,A3
23480 A3=A3/51.2
23500 A=A/2^(LGT(Numavg)/LGT(2)-1)
23510 A=A-Gnd*A2
23520 H$="S"
23530 V$="V"
23560 IF Ind=-1 THEN 23640
23570 CALL "OPEN","DATE LFN:1"
23580 INPUT #1:Specid$,Spectraktr
23590 Spectraktr=Spectraktr+1
23600 CALL "RLOCATE","1 POSITION:0"
23610 INPUT #1:Specid$
23620 PRINT #1:Spectraktr
23625 Ktr=Spectraktr
23630 CALL "TIME",Ddatetime$
23650 PRINT #1:Ddatetime$
23660 GOSUB 57000
23665 Numavgf=Numavg
```

```
23670 CLOSE 1
23680 REM IF AUTO-STORE MODE ON, GET STORE IN NEXT IAPDATAXXXX FILE
23690 IF File4909ind=1 THEN
23700    GOSUB 58000
23710 END IF
23800 RETURN
24000 REM                                   Graph waveform A at screen
24020 Lun=32
24030 VIEWPORT 14,110,10,90
24050 GOSUB 50000
24960 HOME
24970 PRINT "_____"
24990 RETURN
25000 REM GRAPH AT PLOTTER
25010 VIEWPORT 14,130,10,90
25020 Lun=3
25030 GOSUB 50000
25040 RETURN
26000 REM               Do tape directory from INDEXED file, INDEXFILE$
26005 P=POS(Indexfile$,".F",1)
26010 Bb$=SEG(Indexfile$,1,P-1)
26015 CALL "OPEN",Bb$;".F*","LFN:4"
26017 READ #4,65000:Filektr
26018 READ #4,65001:Reclimit
26020 GOSUB 26800
26040 B$="JDo you want a file directory (Y/N) ?"
26045 GOSUB 11900
26050 IF X=0 THEN 26255
26055 PRINT "JGInput beginning file number for directory 1-";Filektr;"."
26060 INPUT Beginfilenum
26065 PRINT "JGInput ending file number for directory."
26070 INPUT Lastfilenum
26075 Lastfilenum=Lastfilenum MIN Filektr
26080 PAGE
26085 PRINT "J ","4 9 0 9   F I L E SJJ"
26090 PRINT "File Number","Contents","    Date     Time"
26095 GO TO Q9+1 OF 26115,26100
26100 CALL "TIME",Ddatetime$
26105 PRINT @40:"J","4 9 0 9  F I L E S            ";Ddatetime$;"JJ"
26110 PRINT @40:"File Number","Contents"
26115 READ #4,65000:Clamp
26120 I=Beginfilenum-1
26125 I=I+1
26129   !
26130 IF I>Clamp THEN
26135    CALL "OPEN","LFN:4 NEXT"
26140    READ #4,65000:Clamp
26145 END IF
26150 Filenum=I
26155 CALL "RLOCATE","4 INDEX:";I
26160 GO TO TYP(4)+1 OF 26165,26165,26180,26180,26195
26165 PRINT I,"<Empty>"
```

```
26170 GO TO Q9+1 OF 26175,26210
26175 GO TO 26235
26180 PRINT I,"<Unknown>"
26185 GO TO Q9+1 OF 26190,26220
26190 GO TO 26235
26195 READ #4:A$
26200 PRINT I,A$
26205 GO TO Q9+1 OF 26235,26230
26210 PRINT @40:I,"<Empty>"
26215 GO TO 26235
26220 PRINT @40:I,"<Unknown>"
26225 GO TO 26235
26230 PRINT @40:I,A$
26235 IF I<Lastfilenum THEN 26125
26236   !
26240 GO TO Q9+1 OF 26250,26245
26245 PRINT @40:"L"
26250 REM
26255 Last=Filektr
26260 PRINT "JEnter number of desired file (0 if none/1--";Last;"):";G$;
26265 INPUT X
26270 X=INT(X)
26275 IF X=0 THEN 26300
26280 IF X<1 OR X>Filektr THEN 26255
26285 CLOSE 4
26290 S=INT((X-1)/Reclimit)+1  !S=INT(X/500)+1
26295 CALL "OPEN",Bb$;".F";S,"LFN:4"
26300 RETURN
26800 CALL "ONERR",26900
26810 Skip=1
26820 CALL "OPEN","LFN:4 NEXT"
26830 READ #4,65000:Filektr
26840 GO TO Skip OF 26820,26850
26850 CLOSE 4
26860 CALL "OPEN",Bb$;".F* LFN:4"
26865 CALL "OFFERR"
26870 RETURN
26900 Skip=2  !REC DOES NOT EXIST, PREVIOUS FILKTR WAS LAST
26910 RETURN
27000 REM       REPACK THE FILE 'INDEXFILENAME' INDICES
27010 J=1
27020 CLOSE 2
27030 CALL "OPEN","INDEXFILENAME LFN:2"
27040 CALL "RPOSITION",2,L$
27050 L$=REP("",1,20)
27060 Idum=VAL(L$)
27070 IF Idum=>65000 THEN 27140
27080 INPUT #2,Idum:B$
27090 CALL "DRECORD","LFN:2 INDEX:";Idum
27100 PRINT #2,J:B$
27110 J=J+1
27120 CALL "RLOCATE",2,"NEXT"
```

```
27130 GO TO 27040
27140 CLOSE 2
27150 RETURN
28000 REM                                ROUTINE TO LIMIT NUMBER OF RECORDS
28010 CLOSE 3
28020 P=POS(Indexfile$,".f",1)
28030 B$=SEG(Indexfile$,P+2,10)
28035 L$=SEG(Indexfile$,1,P+1)
28040 Recgroupktr=VAL(B$)+1
28050 Recgroup$=STR(Recgroupktr)
28060 Recgroup$=REP("",1,1)
28070 Indexfile$=L$&Recgroup$
28080 CALL "CREATE","B","N",Indexfile$
28090 CALL "OPEN",Indexfile$,"LFN:3"
28100 WRITE #3,65000:Filektr+1
28101 WRITE #3,65001:500  !REC LIMIT=500
28110 CALL "OPEN","INDEXFILENAME LFN:2"
28120 REM PUT INFO IN FILE, 'INDEXFILENAME'
28130 Indexlast=0
28140 CALL "RPOSITION",2,L$
28150 L$=REP("",1,20)
28160 Indexktr=VAL(L$)
28170 IF Indexktr=>65000 THEN 28300
28180 CALL "RLOCATE",2,"NEXT"
28190 Indexlast=Indexktr
28200 GO TO 28140
28300 PRINT #2,Indexlast+1:Indexfile$
28310 PRINT #2,65000:Indexfile$
28320 CLOSE 2
28330 Recclamp=500
28335 CLOSE 3
28340 RETURN
29000 REM                                          Check for waveform present
29020 X=1
29040 IF A1>0 THEN 29120
29060 PRINT "JSorry --- No waveform acquired.  Press key 1,2,3,4 or 5";
29080 PRINT "¯first.";G$
29100 X=0
29120 RETURN
30000 REM                     Check for waveform, power of two, and <=1024
30020 X=0
30040 IF A1>0 THEN 30100
30060 PRINT "JSorry --- No waveform acquired.  Press key 1,2,3,4 or 5";
30080 GO TO 30240
30100 IF A1=2¯INT(LOG(A1)/LOG(2)) THEN 30160
30120 PRINT "JSorry --- Waveform size must be a power of two.";G$
30140 GO TO 30240
30160 IF A1<=1024 THEN 30220
30180 PRINT "JSorry --- Waveform size must be <= 1024";G$
30200 GO TO 30240
30220 X=1
30240 RETURN
```

```
32000 REM                                                    Do "NEXT KEY" jazz
32020 SET KEY
32760 HOME
32780 RETURN
39000 REM                                                       Images and data
39020 IMAGE 36T,10A,3E,3A
39040 IMAGE 3T,4A," level:",3D.2D,A
39060 IMAGE 10T,12A,6E,"S"
39080 IMAGE  4D.D
40000 CALL "OPEN","DATE LFN:1"
40006 Spectraktr$=""
40010 Specid$=""
40015 ON EOF (1) THEN 47000
40020 INPUT #1:Specid$,Spectraktr
40030 CALL "time",Ddatetime$
40040 B$="The current date/time on file manager is_"&Ddatetime$
40060 B$=B$&"."  !                                 __Is this correct (y/n)
40070 PRINT "J",B$,"J"
40080   !GOSUB 11900
40100   !IF X=1 THEN 41000
40120   !GOSUB 45000  !CHANGE DATE
41000 IMAGE
41002 Ttime$=SEG(Ddatetime$,11,5)
41004 Sttime$="*5"&Ttime$
41006 PRINT @2:Sttime$
41010 B$="The current specimen ID# is "&Specid$
41020 B$=B$&". Is this correct (Y/N)?"
41030 GOSUB 11900
41040 IF X=1 THEN 41060
41050 GOSUB 46000
41060 B$="The current spectra counter is "&STR(Spectraktr)
41070 B$=B$&". Is this correct (Y/N)?"
41080 GOSUB 11900
41090 IF X=1 THEN 41120
41100 PRINT "INPUT CORRECT SPECTRA COUNT FOR SAMPLE ID# ";Specid$
41110 INPUT Spectraktr
41120 CALL "RLOCATE","1 POSITION:0"
41150 PRINT #1:Specid$
41160 PRINT #1:Spectraktr
41170 PRINT #1:Ddatetime$
42000 CLOSE 1
42010 RETURN
45000 PRINT "INPUT DATE AND TIME, PLEASE G, USING:DD-MON-YY HH:MM"
45004 PRINT "________ _____HHHHHHHHHHHHHHH";
45020 INPUT Ddatetime$
45080 CALL "SETTIM",Ddatetime$
45090 RETURN
46000 PRINT "INPUT SPECIMEN ID, PLEASE G";  !       CHANGE SPECIMEN ID
46010 INPUT Specid$
46050 RETURN
47000 GOSUB 45000  !!                                      EOF ROUTINE
47005 PRINT "GGGGGGGGGGGGGGGGGGGGGGGGGGGGGGGGGGGGG"
```

```
47010 RETURN
50000 REM
50020 REM                                   Graph waveform A at LUN (32 or 3)
50040 CALL "MAX",A,V,Lines
50060 Lines=INT(V/A2)+1
50080 IF Lines<=2 THEN
50100    Lines=Lines+1
50120 END IF
50140 REM FINALLY, COMPUTE TOP OF GRAPH
50160 W1=-A2
50180 W2=Lines*A2
50200 WINDOW 1,A1,W1,W2
50220 AXIS @Lun:A1/40,A2/5,1,-A2
50240 FOR I=1 TO 10
50260    AXIS @Lun:0,0,I*51.2,A2*(I-1)
50280 NEXT I
50300 REM SET W3 AS VERTICAL LABLE SCALING
50305 Title$=SEG(Title$,1,50)
50308 HOME @Lun:
50309 PRINT @Lun,17:2,3.9
50310 PRINT @Lun:"  ","HHHHH";Title$
50311 PRINT @Lun,7:
50320 A$=" "
50340 A$=A$&V$
50360 MOVE @Lun:1,W2
50380 P=INT(LGT(A2))
50400 PRINT @Lun:"HHHHHHHK";"1.0E";P;A$;
50410 PRINT @Lun,17:2,3.9
50420 PRINT @Lun:" ",Specid$;" #";Ktr;" ";Ktr*Numavg;"    ";Ddatetime$
50450 PRINT @Lun,7:
50460 REM PRINT VERTICAL LABLES
50480 FOR I=0 TO Lines+1
50500    MOVE @Lun:1,(W2-W1)/(Lines+1)*I+W1
50520    PRINT @Lun: USING """HHHHH"",4D.":(W1+I*A2)/10¯P
50540 NEXT I
50560 REM SET W3 TO HORIZONTAL LABLE SCALING
50580 W3=INT(LGT(A3*A1))
50600 A$=""
50620 IF W3=0 THEN 50680
50640 A$=STR(10¯W3)
50660 A$=A$&" "
50680 A$=A$&H$
50700 MOVE @Lun:200,W1
50720 PRINT @Lun:"JJ";A$;"ec "
50730 PRINT @Lun,17:2,3.9
50740 PRINT @Lun:"    KVDC=";Vdc;"   KVP=";Vp;"   ";Numavgf;" Pulses";
50746 PRINT @Lun:"    ";"FILE: ";Indexfile$;"  REC# ";Filenum;"¯"
50750 PRINT @Lun,7:
50760 REM PRINT HORIZONTAL LABLES
50780 FOR I=0 TO 10 STEP Q3
50800    MOVE @Lun:I*(A1-1)/10+1,W1
50820    PRINT @Lun: USING """HHJ"",2D.D,S":I*(A1-1)/10*A3/10¯W3
```

```
50840 NEXT I
50860 CALL "CROSS",A,1.5*A2,It0
50880 It0=It0-2
50900 IF It0-INT(It0)<0.5 THEN
50920    It0=INT(It0)
50940    GO TO 51000
50960 END IF
50980 It0=INT(It0)+1
51000 IF It0<=0 THEN
51020    It0=1
51040 END IF
51060 DIM Xx(512)
51070 Xx=1
51080 CALL "INT",Xx,Xx
51090 Xx=Xx+1
51100 Xx=Xx-It0
51105 MOVE @Lun:Xx(It0),A(It0)
51110 DRAW @Lun:Xx,A
51140 HOME
51160 IF Ktrtof=0 THEN 51290
51162 PRINT @Lun,17:2,3.9
51180 GOSUB 19520
51190 GOSUB 19610
51192 PRINT @Lun,7:
51290 PRINT "G¯    "
51295 Lun=32
51300 RETURN
55000 REM              PULSE STARTER ROUTINE, PIN39
55010 CALL "BSETUP","IIII",0,Start
55020 CALL "WAIT",0.1
55030 CALL "BSETUP","IIII",0,High
55035 PRINT "G"
55040 RETURN
55555 REM
56000 REM              PULSE STOPPER ROUTINE, PIN27
56010 CALL "BSETUP","IIII",0,Sstop
56020   !CALL "WAIT",0.2
56030   !CALL "BSETUP","IIII",0,High
56035 PRINT "G"
56040 RETURN
56555 REM
57000 REM                       VOLTAGES I/O ROUTINE FROM METERS
57010 CALL "IOBCD",Meters$,I1,I2
57020 Met1$=SEG(Meters$,1,4)
57030 Met2$=SEG(Meters$,5,4)
57040 Vdc=VAL(Met1$)*0.01
57050 Vp=VAL(Met2$)*0.01
57060 RETURN
58000 REM             GET LAST FILEKTR FROM RECORD 65000 IN INDEXFILE$ AND
58010 REM             STORE WFM IN NEXT ONE
58020 CALL "OPEN",Indexfile$,"LFN:3"
58030 READ #3,65000:Filektr
```

```
58040 Filenum=Filektr+1
58050 REM                                                 STORE DATA
58060 Spectraktr$=STR(Spectraktr)
58100 N$=Specid$&" #"&Spectraktr$
58110 N$=N$&"    "&Ddatetime$
58120 WRITE #3,Filenum:N$,A1,A2,A3,0,1,H$,V$,A,1,0,A3,Vdc,Vp,Ddatetime$
58130 WRITE #3:Specid$,Spectraktr,Numavgf
58140 WRITE #3,65000:Filenum  !         KEEPS TRACK OF LAST RECORD USED
58145 Recclamp=Recclamp-1
58150 CLOSE 3
58160 RETURN
60000 REM
60010 REM
60020 REM
60030 Temelktr=1
60035 Iiiktr=1
60040 GOSUB 1000
60045 IF Rampind=1 THEN
60050    INPUT @2:Tt,Tt
60060    IF Tt>Rampint THEN
60070       GOSUB 2000
60080       PRINT @2:"*50000"
60090    END IF
60095 END IF
60100 PRINT USING 60110:Temelktr,Filenum,Ktr,Ktr*Numavg
60110 IMAGE "_",3(4d,4X),7D
60120 Temelktr=Temelktr+1
60130 IF Iiiktr=10 THEN
60140    PAGE
60150    CALL "disp",A
60160    Iiiktr=Iiiktr+1
60170    GO TO 60035
60180 END IF
60190 Iiiktr=Iiiktr+1
60200 GO TO 60040
60300 FOR Ijk=Kji TO 4000
60310    X=Ijk
60320    CALL "open",Indexfile$,"lfn:4"
60330    GOSUB 5080
60340 NEXT Ijk
```

IAP2TAPE

This program is very similar to "IAPRING.HV" except it does not collect data or control the Bertan 205A-30R high voltage power supply. This program has routines which are suited for displaying and manipulating the data previously taken with "IAPRING.HV" program. It contains routines for sequentially viewing selected files. In addition, files can be stored and retrieved from magnetic tape. This feature allows the deletion of the files containing spectra to allow for additional experiments to be performed and also stored on the 4909 file manager. Outputting the waveforms on the Tektronix 4662 Interactive Plotter is most easily done with this program. Most of the User-defined keys employed in "IAPRING.HV" are used to find information from the recorded waveforms on the screen. These keys include lighting the location of the cursor, finding the time difference between two marked positions, calculating the mass-to-charge ratios by the ration method and direct time-of-flight calculations independently from each other.

```
1 INIT
2 ON SRQ THEN 21000  !                 IAP2TAPE
3 GO TO 100
4 GO TO 1000
8 GO TO 2000
12 GO TO 3000
16 GO TO 4000
20 GO TO 5000
24 GO TO 6000
32 GO TO 8000
40 GO TO 10600
44 GO TO 10000
```

```
48 GO TO 12000
52 GO TO 13000
56 GO TO 14000
60 GO TO 15000
64 GO TO 16000
68 GO TO 25000
72 GO TO 18000
76 GO TO 19000
80 GO TO 20000
90 REM 7912AD/4050-Series [IAPDATA] IAP2TAPE
94 REM Version WALCK 04/01/85
99
100 REM
105 Skipper=2
110 G$="G"
120 DIM D$(1000)
130 CALL "STATUS","UNIT:ALL",D$
140 PRINT "L",D$
150 DIM D$(200)
160   !CALL "WAIT",5
170 CALL "IDENTIFY","uni:0  [iapdata]"
172 CALL "DIRECT",D$
174 B$=SEG(D$,6,12)
176 B$=B$&" "&SEG(D$,119,17)
178 PRINT "K",B$,"J"
180 CALL "OPEN","INDEXFILENAME LFN:2"
190 DIM B$(400)
200 INPUT #2,65000:S$
210 Indexfile$=S$
220 CLOSE 2
230 B$=S$&" is the current indexed file being used for data storage_"
240 B$=B$&"Do you still want this file to be used? (y/n) "
250 GOSUB 11900
260 IF X=0 THEN   !     Will go to 10000 and either create a new file or
270    GOSUB 10000  !   use an old one.
280 END IF
282 Temelktr=0
284 Filenum=0
290 GOSUB 11000
300 SET KEY
310 GO TO 300
900   !
910   !920   !
930   !
940   !
1000 REM                                              AUTO FILE RETREIVAL
1010 PRINT "L INPUT FIRST FILE TO OUTPUT TO SCREEN. ";
1020 INPUT Iii
1030 PRINT " INPUT THE LAST. ";
1040 INPUT Kji
1050 FOR Ijk=Iii TO Kji
1060    X=Ijk
```

```
1070    CALL "open",Indexfile$,"lfn:4"
1072    READ #4,65001:Reclimit
1074    GOSUB 26285
1080    GOSUB 5080
1085      !GOSUB 16000
1090 NEXT Ijk
1100 RETURN
2000 REM CHANGE FILE BY -1
2010 CALL "OPEN","INDEXFILENAME LFN:2"
2020 Indexktr=Indexktr-1
2030 INPUT #2,Indexktr:S$
2040 PRINT #2,65000:S$
2050 Indexfile$=S$
2060 PRINT "LNEW FILE: ";Indexfile$
2070 CLOSE 2
2080 RETURN
3000 REM CHANGE FILE BY +1
3010 CALL "OPEN","INDEXFILENAME LFN:2"
3020 Indexktr=Indexktr+1
3030 INPUT #2,Indexktr:S$
3040 PRINT #2,65000:S$
3050 Indexfile$=S$
3060 PRINT "LNEW FILE: ";Indexfile$
3070 CLOSE 2
3080 RETURN
4000 REM          Get NEXT Wfm
4005 SET NOKEY
4010 X=Filenum+1
4015 CLOSE 4
4020 CALL "open",Indexfile$,"lfn:4"
4030 GOSUB 5102
4035 SET KEY
4040 RETURN
5000 REM                            Acquire from INDEXFILE$ file ON 4909
5020 SET NOKEY
5030 Title$=""
5040 PRINT "L ","HHHHHJust a minute, please, I'm finding the last rec";
5050 PRINT "ord number."
5060 GOSUB 26000
5080 IF X=0 THEN 5460
5102 Filenum=X
5120 CALL "RLOCATE","4 INDEX:";Filenum
5130 IF TYP(4)=4 THEN 5180
5140 PRINT "JINVALID FILE --- PLEASE SELECT ANOTHER"
5160 GO TO 54605180 IF A1<=0 THEN 5300
5300 DELETE A
5320 READ #4:N$,A1,A2,A3,X,X,H$,V$
5340 DIM A(A1)
5360 READ #4:A,X,Y,Y,Vdc,Vp,Ddatetime$,Specid$,Ktr,Numavgf
5370 CLOSE 4
5380 IF X=1 THEN 5420
5400 PRINT "JWARNING --- NON-UNIFORM SAMPLNG RATE IGNORED";G$;
```

```
5420 VIEWPORT 14,110,10,90
5430 PAGE
5440 GOSUB 24000
5460 CLOSE 4
5465   !GOSUB 32000
5480 RETURN
5900   !
5910   !
5920   !
5930   !
5940   !
6000 REM                                           Acquire from file
6010 ON EOF (0) THEN 6270
6020 SET NOKEY
6030 Title$=""
6040 PRINT "L ","READ WAVEFORM FROM MAGNETIC TAPE FILE"
6050 GOSUB 6340
6060 IF X=0 THEN 5460
6070 FIND X
6080 Tfilenum=X
6090 IF TYP(0)=4 THEN 6120
6100 PRINT "JINVALID FILE --- PLEASE SELECT ANOTHER"
6110 GO TO 5460
6120 IF A1<=0 THEN 6180
6130 DELETE B
6140 B1=A1
6150 B3=A3
6160 DIM B(B1)
6170 B=A
6180 DELETE A
6190 READ @33:N$,A1,A2,A3,X,X,H$,V$
6200 DIM A(A1)
6210 READ @33:A,X,Y,Y,Vdc,Vp,Ddatetime$,Specid$,Ktr,Numavgf
6215 READ @33:Recnum
6216 Filenum=Recnum
6220 IF X=1 THEN 6240
6230 PRINT "JWARNING --- NON-UNIFORM SAMPLNG RATE IGNORED";G$;
6240 VIEWPORT 14,110,10,90
6250 PAGE
6260 RETURN
6270 Ttim=0
6280 RETURN
6290   !
6300   !
6310   !
6320   !
6330   !6340 REM                        Do tape directory from files 3-50
6350 B$="JDo you want a tape directory (Y/N) ?"
6360 GOSUB 11900
6370 IF X=0 THEN 6690
6380 PRINT "JGInput beginning file number for directory(1-53)."
6390 INPUT Beginfilenum
```

```
6400 PRINT "JGInput ending file number for directory(2-54)."
6410 INPUT Lastfilenum
6420 PAGE
6430 PRINT "J ","T A P E   F I L E SJJ"
6440 PRINT "File Number","Contents","Date       Time"
6450 GO TO Q9+1 OF 6480,6460
6460 PRINT @40:"J","T A P E  F I L E S                    ";Dedate$;"JJ"
6470 PRINT @40:"File Number","Contents"
6480 FOR I=Beginfilenum TO Lastfilenum
6490    FIND I
6500    GO TO TYP(0)+1 OF 6510,6510,6540,6540,6570
6510    PRINT I,"<Empty>"
6520    GO TO Q9+1 OF 6530,6600
6530    GO TO 6650
6540    PRINT I,"<Unknown>"
6550    GO TO Q9+1 OF 6560,6620
6560    GO TO 6650
6570    READ @33:A$
6580    PRINT I,A$
6590    GO TO Q9+1 OF 6650,6640
6600    PRINT @40:I,"<Empty>"
6610    GO TO 6650
6620    PRINT @40:I,"<Unknown>"
6630    GO TO 6650
6640    PRINT @40:I,A$
6650 NEXT I
6660 GO TO Q9+1 OF 6680,6670
6670 PRINT @40:"L"
6680 REM
6690 PRINT "JEnter number of desired file (0 if none/1--54):";G$;
6700 INPUT X
6710 X=INT(X)
6720 IF X=0 THEN 6740
6730 IF X<1 OR X>54 THEN 6690
6740 RETURN
6750 REM                                       Check for waveform present
6760 X=1
6770 IF A1>0 THEN 6810
6780 PRINT "JSorry --- No waveform acquired.  Press key 1,2,3,4 or 5";
6790 PRINT " first.";G$
6800 X=0
6810 RETURN
6820 REM                     Check for waveform, power of two, and <=1024
6830 X=0
6840 IF A1>0 THEN 6870
6850 PRINT "JSorry --- No waveform acquired.  Press key 1,2,3,4 or 5";
6860 GO TO 6940
6870 IF A1=2^INT(LOG(A1)/LOG(2)) THEN 6900
6880 PRINT "JSorry --- Waveform size must be a power of two.";G$
6890 GO TO 6940
6900 IF A1<=1024 THEN 6930
6910 PRINT "JSorry --- Waveform size must be <= 1024";G$
```

```
6920 GO TO 6940
6930 X=1
6940 RETURN
8000 SET NOKEY   !              REGRAPH WFM ON SCREEN
8005 PAGE
8007 VIEWPORT 14,110,10,90
8008 Lun=32
8010 GOSUB 24000
8020 SET KEY
8030 RETURN
8900   !
8910   !
8920   !
8930   !
8940   !
10000 REM              CREATE AN INDEXED FILE, & PUT IT IN INDEXFILENAME
10005 Idum=0
10010 CALL "open","indexfilename lfn:2"
10020 PRINT "LINDEX","HHHHHHHHFILENAME"
10025 Indexlast=0
10030 CALL "RPOSITION",2,L$
10035 L$=REP("",1,20)
10040 Indexktr=VAL(L$)
10050 INPUT #2,Indexktr:S$
10060 PRINT Indexktr,"HHHHHHHH";S$
10070 IF Indexktr=>65000 THEN 10150
10080 CALL "RLOCATE",2,"NEXT"
10090 Indexlast=Indexktr
10100 GO TO 10030
10150 REM S$ IS CURRENT INDEXFILE$ BEING USED (INDEX:65000)
10160 REM & SHOULD BE DUPLICATED IN LIST ONCE.
10170 REM INDEXLAST IS LAST INDEX USED PRIOR TO 65000
10180 B$="HAVE ANY OF THESE BEEN DELETED? (Y/N) "
10190 GOSUB 11900
10200 IF X=0 THEN 10290
10210 PRINT "HOW MANY? ";
10220 INPUT Bb
10230 DIM B(Bb)
10240 PRINT "ENTER INDEX NUMBERS. ";
10250 INPUT B
10260 FOR I=1 TO Bb
10270    CALL "DRECORD","LFN:2 INDEX:";B(I)
10280 NEXT I
10282 GOSUB 27000
10284 IF Idum>0 THEN 10005
10290 B$="Are any of these (WITH INDEX < 65000) the desired file? (Y/N)"
10300 GOSUB 11900
10310 IF X=1 THEN
10320    PRINT "Enter the indexed number of file you want to use. ";
10330    INPUT Indexktr
10340    INPUT #2,Indexktr:S$
10350    PRINT #2,65000:S$  !puts the old file to be used in record#
```

```
         65000
10360    Indexfile$=S$
10370 ELSE
10380    REM NEW INDEXED FILE TO BE CREATED
10390    PRINT "What is the name of new indexed file you wish to use
         for "
10400    PRINT "data storage? ";
10410    INPUT Indexfile$
10415    Indexfile$=Indexfile$&".f1"
10420    Indexktr=Indexlast+1
10430    PRINT #2,65000:Indexfile$
10440    PRINT #2,Indexktr:Indexfile$
10500    CALL "CREATE","B","N",Indexfile$
10510    CALL "OPEN",Indexfile$,"LFN:3"
10520    WRITE #3,65000:0  !   INDEX #65000 IS WHERE LAST FILENUM IS PUT
10525    WRITE #3,65001:500  !REC LIMIT=500
10530    CLOSE 3
10540    PRINT "INDEXED FILE, ";Indexfile$;" CREATED AND 0 PUT IN INDEX"
10550    PRINT "65000 FOR LAST FILE USED."
10560    PRINT Indexfile$;" WAS ALSO PUT IN FILE 'INDEXFILENAME'."
10565    CALL "WAIT",1
10570 END IF
10580 CLOSE 2
10590 RETURN
10600 REM
10610 REM               ADD ANOTHER FLITETIME TO LIST & INDICATE WHERE
10620 CALL "OPEN","FLYTIMES LFN:6"
10630 IF Ktrtof=0 THEN 10670
10640 FOR I=1 TO Ktrtof
10650    INPUT #6:Flytime,Flitemkr
10660 NEXT I
10670 Flytime=(Arraycursor-It0)*A3
10680 Flitemkr=Arraycursor
10690 PRINT #6:Flytime,Flitemkr
10700 CLOSE 6
10710 Ktrtof=Ktrtof+1
10720 PRINT "G"
10730 MOVE Arraycursor-It0+1,A(Arraycursor)
10740 FOR I=1 TO 10
10750    RDRAW 0,0
10760 NEXT I
10770 MOVE Flitemkr-It0+1,0
10780 DASH 85
10790 RDRAW 0,-A2
10800 DASH 0
10810 HOME
10820 DELETE Masses,Premasses
10830 DIM Masses(Ktrtof),Premasses(Ktrtof)
10840 Masses=0
10850 Premasses=0
10860 RETURN
10900   !
```

```
10910   !
10920   !
10930   !
10940   !
11000 OFF SRQ   !                                               Initialize
11002 ON SRQ THEN 21200
11010 SET NOKEY
11020 DIM A$(100),L$(300),Q(20),B$(144),Fileid$(400)
11030 PRINT "L ","4050-SERIES/7912AD IAPSCALED"
11040 PRINT "¯ ","Copyright (c) 1980 Tektronix, Inc."
11050 PRINT "  ","       All rights reserved."
11060 REM SET ENVIRONMENT
11065 P2=2000
11070 DATA 4,1,4,1,1,1,3,1,4,1,1,1,4,1,3,1,1,1
11090 Meters$="ITISOFFF"
11100 DIM High(6),Start(6),Sstop(6)
11110 READ High,Start,Sstop
11120 CALL "BSETUP","IIII",0,High  !SETS ROM OUTPUT PINS 39&27 HIGH(+5V)
11130 Title$=""
11132 Rampind=-1
11134 Rampint=0.05
11136 Recclamp=500
11140 G$="G"
11145 Q1=1
11150 Q2=1
11155 Vinc=0.02
11160 Gnd=0
11170 CALL "RATE",9600,0,2  !SET BAUD RATE AND PARAMS. FOR PAPER TIGER
11175 CALL "CMFLAG",0  !NO INTERFACE BUFFER OVERFLOW FLAGGING,
11176   !                 WILL NOT ALLOW FULL PROGRAM TO BE LISTED!
11177 REM******* FOR EPSON PRINTER, PUT PRI@37,26:1 HERE.
11178 REM       (ADDS CR+LF) REMEMBER TO PUT PRI@37,26:0 AT END!
11190 Nrpt=512
11200 Arraycursor=1
11201 It0=1
11202 Lefty=1
11204 Righty=1
11206 Ktrtof=0
11210 Q4=0
11212 B$="JJENTER NUMBER OF WFM'S TO BE AVGED(1<=2¯N>=64)."
11214   !PRINT B$
11216 Numavg=1  !        INPUT NumaG
11220 Numavgf=Numavg
11225 PRINT "GGGGG"
11230 PRINT "GG","WARNING: DESORB PULSE MUST BE MORE THAN 2 DIV HIGH!__"
11240 Q7=1
11242 Tfilenum=0
11245 Fileid$=""
11255 File4909ind=-1
11260 Spectraktr=0
11265 Ktr=0
11270 Q8=1
```

```
11272   !B$="JJIs printer available for tape directory (y/n)?"
11274   !GOSUB 11900
11276 Q9=0  !Q9=X
11277 IF Q9=0 THEN 11278    CALL "CMFLAG",0  !NO PRINTER AVAILABLE
11279 END IF
11380 DATA 0,0,0,0,1,0,"S","V",0,0  !!            INITIALIZE WAVEFORMS
11390 READ A1,A2,A3,A4,A5,B1,H$,V$,Vdc,Vp
11400 GOSUB 40000  !                         CHECK DATE & SPECIMEN ID
11410 Ind=1
11470 REM INITIALIZE ZERO REFS, ETC
11490 Q3=1
11500 REM SET NO-LOOP MODE
11510 Q0=0
11520 REM DEFINE CYCLE
11530 Q=-1
11550 U=1  ! DEFINES 7912AD ADDRESS TO BE 1
11560 U=INT(U)
11570 IF U<1 OR U>30 THEN 11540
11580   !PRINT @U,0:"ID?"
11590   !INPUT @U,0:A$
11600 IF POS(A$,"7912AD",1)<>0 THEN 11625
11610   !PRINT "JIMPROPER RESPONCE FROM ADDRESS ";U;",0 --- ";A$
11620   !STOP
11625 ON SRQ THEN 21200
11630 GOSUB 32000
11640 RETURN
11900 REM                                           Query user routine
11910 X=0
11920 PRINT B$;G$
11930 INPUT A$
11940 A$=SEG(A$,1,1)
11950 IF A$="N" THEN 11980
11960 IF A$<>"Y" THEN 11920
11970 X=1
11980 RETURN
11990   !
11991   !
11992   !
11993   !
11994   !
12000 REM ********************CURSOR MOVE LEFT ***********************
12005 SET NOKEY
12010 Arraycursor=Arraycursor-1
12020 IF Arraycursor<=It0 THEN
12030    Arraycursor=512  !It0
12040    GO TO 12060
12050 END IF
12060 MOVE Arraycursor-It0,A(Arraycursor)
12070 RDRAW 0,0
12090 RETURN
12910   !
12920   !
```

```
12930   !
12940   !
13000 REM ********************CURSOR MOVE RIGHT ********************
13005 SET NOKEY
13010 Arraycursor=Arraycursor+1
13020 IF Arraycursor=>Nrpt THEN 13030    Arraycursor=It0  !Nrpt
13040    GO TO 13060
13050 END IF
13060 MOVE Arraycursor-It0+1,A(Arraycursor)
13070 RDRAW 0,0
13090 RETURN
13900   !
13910   !
13920   !
13930   !
13940   !
14000 REM          Get NEXT Wfm
14010 SET NOKEY
14020 X=Filenum-1
14030 CLOSE 4
14040 CALL "open",Indexfile$,"lfn:4"
14050 GOSUB 5102
14060 SET KEY
14070 RETURN
15000 REM                                 Save current waveform on file
15010 SET NOKEY
15020 PRINT "L ","SAVE WAVEFORM ON FILE"
15030 GOSUB 29000
15040 N$=Specid$&" "&"#"
15050 N$=N$&Spectraktr$&"     "&Ddatetime$
15060 CALL "OPEN",Indexfile$,"LFN:4"
15070 READ #4,65000:Filektr
15090 B$=STR(Filektr+1)
15100 B$="This WFM will be sTored in record#"&B$
15110 B$=B$&". _Is this ok? (y/n) "
15120 GOSUB 11900
15130 IF X=0 THEN 15160
15133 Filenum=Filektr+1
15140 WRITE #4,Filenum:N$,A1,A2,A3,0,1,H$,V$,A,1,0,A3,Vdc,Vp,Ddatetime$
15150 WRITE #4:Specid$,Spectraktr,Numavgf
15155 WRITE #4,65000:Filenum
15160 CLOSE 4
15161 Recclamp=Recclamp-1
15162 IF Recclamp<=0 THEN
15163    GOSUB 28000
15164 END IF
15165 GOSUB 8000
15170 GOSUB 32000
15180 RETURN
15900   !
15910   !
15920   !
```

```
15930   !
15940   !
16000 REM                                  Save current waveform on file
16005 Recnum=Filenum
16010 SET NOKEY
16020 PRINT "L ","SAVE WAVEFORM ON MAGNETIC TAPE FILE"
16022 PRINT "JJJJ  ",Specid$;" #";Ktr,"     ";Ddatetime$,"J"
16024 PRINT "     KVDC=";Vdc;"   KVP=";Vp;"   ";Numavgf;" Pulses";16026
PRINT "    ";"FILE: ";Indexfile$;"  REC# ";Filenum
16028 PRINT
16030 GOSUB 29000
16040 IF X=0 THEN 16150
16070 GOSUB 6340
16080 IF X=0 THEN 16150
16090 Tfilenum=X
16100 KILL X
16110 FIND X
16120 WRITE @33:N$,A1,A2,A3,0,1,H$,V$,A,1,0,A3,Vdc,Vp,Ddatetime$,Specid$
16130 WRITE @33:Ktr,Numavgf,Recnum
16140 CLOSE
16150   !
16160 RETURN
16170   !
16180   !
16190   !
16200   !
16210   !
18000 REM       USE CURSOR POSITION TO FIND DC OFFSET IN DIVISION UNITS
18010 PRINT "LJJJJJJJJJJJUSE CURSORTO FIND DC OFFSET."
18020 PRINT "JWHEN SET, PRESS GND KEY (KEY 18)"
18025 CALL "WAIT",3
18030 Gnd=A(Arraycursor)/A2+Gnd
18035 PAGE
18036 A=A-A(Arraycursor)
18040 GOSUB 24000
18045 PRINT"JJJJJJJJJJJJJJJJJə _JOFFSET=_";Gnd
18050 RETURN
18900   !
18910   !
18920   !
18930   !
18940   !
19000 REM CALCULATE M/N`S AND MARK TIMES
19005 SET NOKEY
19006 Alpha=0.2  !MAY CHANGE THIS VALUE IF YOU LIKE
19010 IF Ktrtof=0 THEN 19440
19020 DIM Flytym(Ktrtof),Tmarker(Ktrtof),Massescalc(Ktrtof)
19030 CALL "OPEN","FLYTIMES LFN:6 TACCESS:READ "
19040 PRINT "L";Specid$
19050 PRINT "FILE: ";Indexfile$;"   INDEX:";Filenum;"   KTR#";Ktr," ";
19055 PRINT " ","H";Ddatetime$
19060 PRINT @40:"JJJJJJJ";Ddatetime$,Specid$,"FILE NO.";Filenum
```

```
19070 PRINT @40:"#";Ktr
19080 PRINT "JNUMBER","TOF(USEC)","PREVIOUS MASS","CURSOR INDEX"
19090 PRINT @40:"JNUMBER","TOF(USEC)","PREVIOUS MASS","CURSOR INDEX"
19100 FOR I=1 TO Ktrtof
19110    INPUT #6:Flytym(I),Tmarker(I)
19120    PRINT USING 19150:I,Flytym(I)/1.0E-6,Premasses(I),Tmarker(I)
19130    PRINT @40: USING 19150:I,Flytym(I)/1.0E-6,Premasses(I),
         Tmarker(I)
19140 NEXT I
19150 IMAGE 3T,2D,20T,2D.3D,40T,3D.2D,60T,3D
19160 CLOSE 619170 PRINT "JWHICH IS THE STANDARD?  ENTER ITS NUMBER.";
19180 INPUT I
19190 PRINT "JWHAT IS ITS MASS TO CHARGE RATIO? ";
19200 INPUT Mton
19202 Massescalc=0
19204 Factor=0.193*(Vdc+Alpha*Vp)/0.15^2/1.0E-12
19210 Flytym=Flytym^2
19220 Masses=Flytym
19222 Massescalc=Flytym
19224 Massescalc=Massescalc*Factor
19230 Masses=Masses/Flytym(I)
19240 Masses=Masses*Mton
19250 Flytym=SQR(Flytym)
19260 Premasses=Masses
19270 Massind=1
19280 PRINT @40:"JJ"
19282 PRINT ""
19290 PRINT @40:"THE FOLLOWING ARE THE MASSES CALCULATED BY RATIO BASED"
19292 PRINT "THE FOLLOWING ARE THE MASSES CALCULATED BY RATIO BASED"
19300 PRINT @40:"UPON MASS ";Mton;" AT TIME ";Flytym(I)/1.0E-6;" USEC ";
19302 PRINT "UPON MASS ";Mton;" AT TIME ";Flytym(I)/1.0E-6;" USEC ";
19305 PRINT @40:"AND TOF EQUATION "
19306 PRINT @40:"USING ALPHA= ";Alpha;" :J"
19307 PRINT "AND TOF EQUATION "
19308 PRINT "ALPHA= ";Alpha;" :J"
19310 PRINT "NUMBER","TIME(USEC)","RATIO M/N","CALC M/N"
19320 PRINT @40:"NUMBER","TIME(USEC)","RATIO M/N","CALC M/N"
19330 FOR I=1 TO Ktrtof
19340    PRINT USING 19360:I,Flytym(I)/1.0E-6,Masses(I),Massescalc(I)
19350    PRINT @40: USING 19360:I,Flytym(I)/1.0E-6,Masses(I),
         Massescalc(I)
19360    IMAGE2X,2D,15X,2D.3D,12X,3D.2D,11X,3D.2D
19370 NEXT I
19375 PRINT @40:"L"
19380 CALL "WAIT",6
19390 PAGE
19410 GOSUB 50000
19420   !GOSUB 19520
19430   !GOSUB 19610
19438 SET KEY
19440 RETURN
19450 PAGE
```

```
19460 PRINT "JJJJJYOU MUST MARK THE FLIGHT TIMES WITH
KEY10 FIRST, SILLY      ."
19470 PRINT "GGGGGGGGGGGGGGGG"
19480 CALL "WAIT",3
19490 PAGE
19500 GOSUB 24000
19510 RETURN
19520 REM MARK TIMES WITH DASHED LINES ON GRAPH
19530 DASH 85
19540 FOR I=1 TO Ktrtof
19550    MOVE @Lun:Tmarker(I)-It0+1,0
19560    RDRAW @Lun:0,-A2
19570 NEXT I19580 DASH 0
19590 HOME
19600 RETURN
19610 REM WRITE THE MASSES ON RIGHT SIDE OF GRAPH
19620 HOME @Lun:
19630 PRINT @Lun:"JJJ"
19640 IF Lun=3 THEN 19670
19650 PRINT @Lun: USING "64"" "",""M/N""":
19660 GO TO 19690
19670 MOVE @Lun:533.5,W2-1.0E-3
19680 PRINT @Lun:"M/NHHHHHJ";
19690 FOR I=1 TO Ktrtof
19700    IF Lun=3 THEN 19730
19710    PRINT @Lun: USING "62"" "",3D.2D":Masses(I)
19720    GO TO 19740
19730    PRINT @Lun: USING "3D.2D,""HHHHHHJ"",S":Masses(I)
19740 NEXT I
19750 HOME
19760 RETURN
19770   !
19780   !
19790   !
19800   !
19810   !
20000 REM         RESET (TOFFILE) & SET KTRTOF TO 0
20005 DELETE Masses,Premasses
20010 Ktrtof=0
20020 CALL "open","flytimes lfn:6"
20025 Massind=0
20030 CLOSE 6
20035 PRINT "G"
20036 Arraycursor=It0
20040 RETURN
20900   !
20910   !
20920   !
20930   !
20940   !
21000 REM                                               Temp serial poll
21040 X=1
```

```
21060 X=INT(X)
21080 IF X<1 OR X>30 THEN 21020
21100 POLL P1,P2;X,0
21120 POLL P1,P2;X,1
21140 POLL P1,P2;X,2
21150 POLL P1,P2;2;3;4
21160 RETURN
21200 REM                                                     Real serial poll
21220 POLL P1,P2;U,0;2;3;4
21225 REM  7912AD OPC SRQ HANDLER
21230 IF P2=82 OR P2=66 OR P2=2 OR P2=64 AND P1=1 THEN 21252
21240 PRINT "SRQ FROM ";P1;",","STATUS = ";P2
21250 GO TO 21260
21252 GOSUB 56000
21260 RETURN
22000 REM                                      FILEID$ CONCANTENATION ROUTINE
22001 REM                          RETURNS S$ AND IAP$ IN FORM: IAPDATAxxxx
22010 Iap$="IAPDATA"
22020 Sp$="0000"
22030 S$=STR(Filenum)
22040 S$=REP("",1,1)
22050 S$=Sp$&S$
22060 X=LEN(S$)
22070 Y=X-4
22080 S$=REP("",1,Y)
22090 S$=Iap$&S$
22100 Iap$=S$
22110 RETURN
23000 REM                                                 Acquire waveform into A
23001 Filenum=0
23002 Numavg$=STR(Numavg)
23004 Digsa$="DIG SA,"&Numavg$
23010 IF A1<=0 THEN 23080
23070 REM FIRST GET VERTICAL SCALE
23080 PRINT @U,0:"VS2?"
23090 INPUT @U,0:V1,V1
23095 Vs2=V1
23100 REM SET UP CONSTANTS
23105 A2=ABS(V1)
23110 C1=ABS(V1)*256*8/1024
23120 C2=C1/256
23130 PRINT @U,0:"GRI?"  !NEEDED,BUT WHY?
23140 INPUT @U,0:B$  !NEEDED,BUT WHY?
23150 PRINT @U,0:"GRI 0"
23180 P2=1000
23190 PRINT @1,0:"OPC ON"
23195 PRINT @U,0:Digsa$
23200   !CALL "WAIT",1
23201 GOSUB 55000
23202 GO TO Skipper OF 23203,23204
23203 GOSUB 58000
23204 IF P2=82 OR P2=66 OR P2=2 OR P2=64 THEN 23210
```

```
23205 PRINT USING 60110:Temelktr,Filenum,Ktr,Ktr*Numavg
23206 GO TO 23204
23210 PRINT @U,0:B$;"OPC OFF;DEF ON;READ SA;"
23215 Skipper=1
23220 WBYTE @64+U,96:
23230 RBYTE X,X,Y
23240 A1=(X*256+Y-1)/2
23250 DELETE A
23260 DIM A(A1)
23270 GO TO Q1+1 OF 23380,23280
23280 REM FAST READ
23300 DELETE V1,V2
23310 DIM V1(A1,2),V2(2,1)
23320 V2(1,1)=C1
23330 V2(2,1)=C2
23340 RBYTE V1
23350 A=V1 MPY V2
23360 DELETE V1,V223440 RBYTE X,Y
23450 REM NOW READ HORIZONTAL SCALE
23460 PRINT @U,0:"HS2?"
23470 INPUT @U,0:A3,A3
23480 A3=A3/51.2
23500 A=A/2^(LGT(Numavg)/LGT(2)-1)
23510 A=A-Gnd*A2
23520 H$="S"
23530 V$="V"
23560 IF Ind=-1 THEN 23640
23570 CALL "OPEN","DATE LFN:1"
23580 INPUT #1:Specid$,Spectraktr
23590 Spectraktr=Spectraktr+1
23600 CALL "RLOCATE","1 POSITION:0"
23610 INPUT #1:Specid$
23620 PRINT #1:Spectraktr
23625 Ktr=Spectraktr
23630 CALL "TIME",Ddatetime$
23650 PRINT #1:Ddatetime$
23660 GOSUB 57000
23665 Numavgf=Numavg
23670 CLOSE 1
23680 REM IF AUTO-STORE MODE ON, GET STORE IN NEXT IAPDATAXXXX FILE
23690 IF File4909ind=1 THEN
23700    GOSUB 58000
23710 END IF
23800 RETURN
24000 REM                                       Graph waveform A at screen
24020 Lun=32
24030 VIEWPORT 14,110,10,90
24050 GOSUB 50000
24960 HOME
24970 PRINT "_____"
24990 RETURN
25000 REM GRAPH AT PLOTTER
```

```
25010 VIEWPORT 14,130,12,90  !???
25020 Lun=3
25030 GOSUB 50000
25040 RETURN
26000 REM                  Do tape directory from INDEXED file, INDEXFILE$
26005 P=POS(Indexfile$,".F",1)
26010 Bb$=SEG(Indexfile$,1,P-1)
26015 CALL "OPEN",Bb$;".F*","LFN:4"
26017 READ #4,65000:Filektr
26018 READ #4,65001:Reclimit
26020 GOSUB 26800
26040 B$="JDo you want a file directory (Y/N) ?"
26045 GOSUB 11900
26050 IF X=0 THEN 26255
26055 PRINT "JGInput beginning file number for directory 1-";Filektr;"."
26060 INPUT Beginfilenum
26065 PRINT "JGInput ending file number for directory."
26070 INPUT Lastfilenum
26075 Lastfilenum=Lastfilenum MIN Filektr
26080 PAGE 26085 PRINT "J ","4 9 0 9   F I L E SJJ"
26090 PRINT "File Number","Contents","     Date      Time"
26095 GO TO Q9+1 OF 26115,26100
26100 CALL "TIME",Ddatetime$
26105 PRINT @40:"J","4 9 0 9  F I L E S             ";Ddatetime$;"JJ"
26110 PRINT @40:"File Number","Contents"
26115 READ #4,65000:Clamp
26120 I=Beginfilenum-1
26125 I=I+1
26129   !
26130 IF I>Clamp THEN
26135    CALL "OPEN","LFN:4 NEXT"
26140    READ #4,65000:Clamp
26145 END IF
26150 Filenum=I
26155 CALL "RLOCATE","4 INDEX:";I
26160 GO TO TYP(4)+1 OF 26165,26165,26180,26180,26195
26165 PRINT I,"<Empty>"
26170 GO TO Q9+1 OF 26175,26210
26175 GO TO 26235
26180 PRINT I,"<Unknown>"
26185 GO TO Q9+1 OF 26190,26220
26190 GO TO 26235
26195 READ #4:A$
26200 PRINT I,A$
26205 GO TO Q9+1 OF 26235,26230
26210 PRINT @40:I,"<Empty>"
26215 GO TO 26235
26220 PRINT @40:I,"<Unknown>"
26225 GO TO 26235
26230 PRINT @40:I,A$
26235 IF I<Lastfilenum THEN 26125
26236   !
```

```
26240 GO TO Q9+1 OF 26250,26245
26245 PRINT @40:"L"
26250 REM
26255 Last=Filektr
26260 PRINT "JEnter number of desired file (0 if none/1--";Last;"):";G$;
26265 INPUT X
26270 X=INT(X)
26275 IF X=0 THEN 26300
26280 IF X<1 OR X>Filektr THEN 26255
26285 CLOSE 4
26290 S=INT((X-1)/Reclimit)+1  !S=INT(X/500)+1
26295 CALL "OPEN",Bb$;".F";S,"LFN:4"
26300 RETURN
26800 CALL "ONERR",26900
26810 Skip=1
26820 CALL "OPEN","LFN:4 NEXT"
26830 READ #4,65000:Filektr
26840 GO TO Skip OF 26820,26850
26850 CLOSE 4
26860 CALL "OPEN",Bb$;".F* LFN:4"
26865 CALL "OFFERR"
26870 RETURN 26900 Skip=2  !REC DOES NOT EXIST, PREVIOUS FILKTR WAS LAST
26910 RETURN
27000 REM       REPACK THE FILE 'INDEXFILENAME' INDICES
27010 J=1
27020 CLOSE 2
27030 CALL "OPEN","INDEXFILENAME LFN:2"
27040 CALL "RPOSITION",2,L$
27050 L$=REP("",1,20)
27060 Idum=VAL(L$)
27070 IF Idum=>65000 THEN 27140
27080 INPUT #2,Idum:B$
27090 CALL "DRECORD","LFN:2 INDEX:";Idum
27100 PRINT #2,J:B$
27110 J=J+1
27120 CALL "RLOCATE",2,"NEXT"
27130 GO TO 27040
27140 CLOSE 2
27150 RETURN
28000 REM                              ROUTINE TO LIMIT NUMBER OF RECORDS
28010 CLOSE 3
28020 P=POS(Indexfile$,".f",1)
28030 B$=SEG(Indexfile$,P+2,10)
28035 L$=SEG(Indexfile$,1,P+1)
28040 Recgroupktr=VAL(B$)+1
28050 Recgroup$=STR(Recgroupktr)
28060 Recgroup$=REP("",1,1)
28070 Indexfile$=L$&Recgroup$
28080 CALL "CREATE","B","N",Indexfile$
28090 CALL "OPEN",Indexfile$,"LFN:3"
28100 WRITE #3,65000:Filektr+1
28101 WRITE #3,65001:500  !RECLIMIT=500
```

```
28110 CALL "OPEN","INDEXFILENAME LFN:2"
28120 REM PUT INFO IN FILE, 'INDEXFILENAME'
28130 Indexlast=0
28140 CALL "RPOSITION",2,L$
28150 L$=REP("",1,20)
28160 Indexktr=VAL(L$)
28170 IF Indexktr=>65000 THEN 28300
28180 CALL "RLOCATE",2,"NEXT"
28190 Indexlast=Indexktr
28200 GO TO 28140
28300 PRINT #2,Indexlast+1:Indexfile$
28310 PRINT #2,65000:Indexfile$
28320 CLOSE 2
28330 Recclamp=500
28340 RETURN
29000 REM                                   Check for waveform present
29020 X=1
29040 IF A1>0 THEN 29120
29060 PRINT "JSorry --- No waveform acquired.  Press key 1,2,3,4 or 5";
29080 PRINT " first.";G$
29100 X=0
29120 RETURN
30000 REM                    Check for waveform, power of two, and <=1024
30020 X=030040 IF A1>0 THEN 30100
30060 PRINT "JSorry --- No waveform acquired.  Press key 1,2,3,4 or 5";
30080 GO TO 30240
30100 IF A1=2^INT(LOG(A1)/LOG(2)) THEN 30160
30120 PRINT "JSorry --- Waveform size must be a power of two.";G$
30140 GO TO 30240
30160 IF A1<=1024 THEN 30220
30180 PRINT "JSorry --- Waveform size must be <= 1024";G$
30200 GO TO 30240
30220 X=1
30240 RETURN
32000 REM                                               Do "NEXT KEY" jazz
32020 SET KEY
32760 HOME
32780 RETURN
39000 REM                                                  Images and data
39020 IMAGE 36T,10A,3E,3A
39040 IMAGE 3T,4A," level:",3D.2D,A
39060 IMAGE 10T,12A,6E,"S"
39080 IMAGE  4D.D
40000 CALL "OPEN","DATE LFN:1"
40006 Spectraktr$=""
40010 Specid$=""
40015 ON EOF (1) THEN 47000
40020 INPUT #1:Specid$,Spectraktr
40030 CALL "time",Ddatetime$
40040 B$="The current date/time on file manager is_"&Ddatetime$
40060 B$=B$&"."  !                      __Is this correct (y/n)
40070 PRINT "J",B$,"J"
```

```
40080   !GOSUB 11900
40100   !IF X=1 THEN 41000
40120   !GOSUB 45000  !CHANGE DATE
41000 IMAGE
41002 Ttime$=SEG(Ddatetime$,11,5)
41004 Sttime$="*5"&Ttime$
41006   !PRINT @2:Sttime$
41010 B$="The current specimen ID# is "&Specid$
41020 B$=B$&". Is this correct (Y/N)?"
41030   !GOSUB 11900
41035 X=1
41040 IF X=1 THEN 41060
41050 GOSUB 46000
41060 B$="The current spectra counter is "&STR(Spectraktr)
41070 B$=B$&". Is this correct (Y/N)?"
41080   !GOSUB 11900
41085 X=1
41090 IF X=1 THEN 41120
41100 PRINT "INPUT CORRECT SPECTRA COUNT FOR SAMPLE ID# ";Specid$
41110 INPUT Spectraktr
41120 CALL "RLOCATE","1 POSITION:0"
41150 PRINT #1:Specid$
41160 PRINT #1:Spectraktr
41170 PRINT #1:Ddatetime$
42000 CLOSE 1
42010 RETURN 45000 PRINT "INPUT DATE AND TIME, PLEASE G, USING:DD-MON-YY
    HH:MM"
45004 PRINT "______________HHHHHHHHHHHHHHH";
45020 INPUT Ddatetime$
45080 CALL "SETTIM",Ddatetime$
45090 RETURN
46000 PRINT "INPUT SPECIMEN ID, PLEASE G";  !       CHANGE SPECIMEN ID
46010 INPUT Specid$
46050 RETURN
47000 GOSUB 45000  !!                                  EOF ROUTINE
47005 PRINT "GGGGGGGGGGGGGGGGGGGGGGGGGGGGGGGGGGGGGG"
47010 RETURN
50000 REM
50020 REM                          Graph waveform A at LUN (32 or 3)
50040 CALL "MAX",A,V,Lines
50060 Lines=INT(V/A2)+1
50080 IF Lines<=2 THEN
50100    Lines=Lines+1
50120 END IF
50140 REM FINALLY, COMPUTE TOP OF GRAPH
50160 W1=-A2
50180 W2=Lines*A2
50200 WINDOW 1,A1,W1,W2
50220 AXIS @Lun:A1/40,A2/5,1,-A2
50240 FOR I=1 TO 10
50260    AXIS @Lun:0,0,I*51.2,A2*(I-1)
50280 NEXT I
```

```
50300 REM SET W3 AS VERTICAL LABLE SCALING
50305 Title$=SEG(Title$,1,50)
50308 HOME @Lun:
50309 PRINT @Lun,17:2,3.9
50310 PRINT @Lun:"  ","HHHHH";Title$
50311   !PRINT @Lun,7:
50320 A$=" "
50340 A$=A$&V$
50360 MOVE @Lun:1,W2
50380 P=INT(LGT(A2))
50400 PRINT @Lun:"HHHHHHHK";"1.0E";P;A$;
50410 PRINT @Lun,17:2,3.9
50420 PRINT @Lun:" ",Specid$;" #";Ktr,"      ";Ddatetime$
50450   !PRINT @Lun,7:
50460 REM PRINT VERTICAL LABLES
50480 FOR I=0 TO Lines+1
50500    MOVE @Lun:1,(W2-W1)/(Lines+1)*I+W1
50520    PRINT @Lun: USING """HHHHH"",4D.":(W1+I*A2)/10^P
50540 NEXT I
50560 REM SET W3 TO HORIZONTAL LABLE SCALING
50580 W3=INT(LGT(A3*A1))
50600 A$=""
50620 IF W3=0 THEN 50680
50640 A$=STR(10^W3)
50660 A$=A$&" "
50680 A$=A$&H$
50700 MOVE @Lun:200,W1
50720 PRINT @Lun:"JJ";A$;"ec "
50730 PRINT @Lun,17:2,3.950740 PRINT @Lun:"    KVDC=";Vdc;"   KVP=";Vp;"
       ";Numavgf;" Pulses";
50746 PRINT @Lun:"    ";"FILE: ";Indexfile$;"  REC# ";Filenum;"^"
50750   !PRINT @Lun,7:
50760 REM PRINT HORIZONTAL LABLES
50780 FOR I=0 TO 10 STEP Q3
50800    MOVE @Lun:I*(A1-1)/10+1,W1
50820    PRINT @Lun: USING """HHJ"",2D.D,S":I*(A1-1)/10*A3/10^W3
50840 NEXT I
50860 CALL "CROSS",A,1.5*A2,It0
50880 It0=It0-2
50900 IF It0-INT(It0)<0.5 THEN
50920    It0=INT(It0)
50940    GO TO 51000
50960 END IF
50980 It0=INT(It0)+1
51000 IF It0<=0 THEN
51020    It0=1
51040 END IF
51060 DIM Xx(512)
51070 Xx=1
51080 CALL "INT",Xx,Xx
51090 Xx=Xx+1
51100 Xx=Xx-It0
```

```
51105 MOVE @Lun:Xx(It0),A(It0)
51110 DRAW @Lun:Xx,A
51140 HOME
51160 IF Ktrtof=0 THEN 51290
51162 PRINT @Lun,17:2,3.9
51180 GOSUB 19520
51190 GOSUB 19610
51192 PRINT @Lun,7:
51290 PRINT "G     "
51295 Lun=32
51300 RETURN
55000 REM            PULSE STARTER ROUTINE, PIN39
55010 CALL "BSETUP","IIII",0,Start
55020 CALL "WAIT",0.1
55030 CALL "BSETUP","IIII",0,High
55035 PRINT "G"
55040 RETURN
55555 REM
56000 REM            PULSE STOPPER ROUTINE, PIN27
56010 CALL "BSETUP","IIII",0,Sstop
56020   !CALL "WAIT",0.2
56030   !CALL "BSETUP","IIII",0,High
56035 PRINT "G"
56040 RETURN
56555 REM
57000 REM                   VOLTAGES I/O ROUTINE FROM METERS
57010 CALL "IOBCD",Meters$,I1,I2
57020 Met1$=SEG(Meters$,1,4)
57030 Met2$=SEG(Meters$,5,4)
57040 Vdc=VAL(Met1$)*0.01
57050 Vp=VAL(Met2$)*0.01
57060 RETURN
58000 REM           GET LAST FILEKTR FROM RECORD 65000 IN INDEXFILE$ AND
58010 REM           STORE WFM IN NEXT ONE
58020 CALL "OPEN",Indexfile$,"LFN:3"
58030 READ #3,65000:Filektr
58040 Filenum=Filektr+1
58050 REM                                                           STORE DATA
58060 Spectraktr$=STR(Spectraktr)
58100 N$=Specid$&" #"&Spectraktr$
58110 N$=N$&"     "&Ddatetime$
58120 WRITE #3,Filenum:N$,A1,A2,A3,0,1,H$,V$,A,1,0,A3,Vdc,Vp,Ddatetime$
58130 WRITE #3:Specid$,Spectraktr,Numavgf
58140 WRITE #3,65000:Filenum  !         KEEPS TRACK OF LAST RECORD USED
58145 Recclamp=Recclamp-1
58146 IF Recclamp<=0 THEN
58147    GOSUB 28000
58148 END IF
58150 CLOSE 3
58160 RETURN
60000 REM
60010 REM
```

```
60020 REM
60030 Temelktr=1
60035 Iiiktr=1
60040 GOSUB 1000
60045 IF Rampind=1 THEN
60050    INPUT @2:Tt,Tt
60060    IF Tt>Rampint THEN
60070       GOSUB 2000
60080       PRINT @2:"*50000"
60090    END IF
60095 END IF
60100 PRINT USING 60110:Temelktr,Filenum,Ktr,Ktr*Numavg
60110 IMAGE "_",3(4d,4X),7D
60120 Temelktr=Temelktr+1
60130 IF Iiiktr=10 THEN
60140    PAGE
60150    CALL "disp",A
60160    Iiiktr=Iiiktr+1
60170    GO TO 60035
60180 END IF
60190 Iiiktr=Iiiktr+1
60200 GO TO 60040
60300 FOR Ijk=Kji TO 4000
60310    X=Ijk
60320    CALL "open",Indexfile$,"lfn:4"
60330    GOSUB 5080
60340 NEXT Ijk
```

PEAKPICKOFF.FAST

This program is identical with IAPRING.HV except the control program section from statement 60000. Only this portion of the program will be listed. This program will automatically find the peak heights of up to eight mass peaks and store this value in a new data file. One file is created to record the information on number of peaks, masses, and number of spectra collected. For n peaks, n files will be created and opened with the respective peak heights stored in the appropriate file. These files have a generic name with a number appended to them. For example if the generic file name is "PEAK" and only one mass peak is to be found, the files, "PEAK.PF0 and "PEAK.PF1" would be created. The spectra and the pickoff process can be viewed during execution of this program. Pressing user-defined key #1 toggles this feature on and off. Considerable time can be saved by executing this program without displaying the spectra. It is suggested that the operator views only the first ten to twenty spectra to insure that the program is operating properly. Periodic spot checks can be made by pressing key #1 again.

```
1   !                                          PEAKPICKOFF.FAST PROGRAM
90 REM 7912AD/4050-Series [IAPDATA] PEAKPICKOFF.FAST
94 REM Version WALCK 04/01/85

     300 SET KEY  !             SECTION PERTAINING TO GRAPHING ROUTINE
310 PRINT "JJKEY#1 TOGGLES GRAPHING ROUTINE ON/OFF."
320 RETURN
900   !
910   !
920   !
930   !
940   !
1000 Iwantgraph=-Iwantgraph
```

```
1005 RETURN
1900   !
1910   !
1920   !
1930   !
1940   !

60000 REM                        peak pickoff routine
60001 CLOSE
60002 SET KEY
60005 PRINT "LJJHave you marked the time windows with the ref. peak ";
60008 PRINT "first, then the restin the desired order?  (There must be";
60009 PRINT " a min & max for each peak.)"
60010 INPUT Q$
60012 IF Q$<>"y" THEN
60015    PRINT "JThen mark them now using keys 20,2,3,&10. Then start
         again."
60018    STOP
60022 END IF
60024 P=POS(Indexfile$,".",1)
60026 Peaksfile$=SEG(Indexfile$,1,P-1)
60028 PRINT "JWhat is the reference file number with marked peaks? ";
60029 INPUT Reffile
60032 Peaks=Ktrtof/2
60040 PRINT "JJThere will be ";Peaks+1;" files created. ";Peaksfile$;
60050 PRINT ".PFO _will have # of peaks, masses, & number of waveforms."
60060 PRINT "JEnter the mass to charge ratios, ref. peak first, ";
60065 PRINT "followed by the rest  in the order that they were marked."
60070 DIM Mass(Peaks)
60080 INPUT Mass
60160 IF Ktrtof<>Peaks*2 THEN
60170    PRINT "Something is wrong weeth markers.J_FEEX IT, PEDRO!"
60180    STOP
60190 END IF
60200 PRINT "LWhat is the first file of ";Indexfile$;" to be used? ";
60210 INPUT Filestart
60220 PRINT "What is the last? ";
60230 INPUT Filestop
60234 CALL "ONERR",85
60240 FOR I=0 TO Peaks  !create peaks+1
60250    CALL "create","A","D",Peaksfile$;".PF";I
60254    CALL "OFFERR"
60260 NEXT I
60270 CALL "open",Peaksfile$;".PFO","lfn:9"
60280 PRINT #9:Peaks,Mass,Filestop-Filestart+1
60285 PRINT #9:Filestart,Filestop,"#PEAKS,MASSES,RECS,FILESTART,FILESTOP"
60290 CLOSE 9
60300 I=Peaks
60310 DIM Tpkmin(I),Tpkmax(I),Twidth(I),Lead(I)
60320 CALL "open","flytimes lfn:6"
60330 FOR I=1 TO Peaks
60340    INPUT #6:Tpkmin(I),Dum
```

```
60350    INPUT #6:Tpkmax(I),Dum
60360    Twidth(I)=Tpkmax(I)-Tpkmin(I)
60370 NEXT I
60380 CLOSE 6
60390 P=POS(Indexfile$,".",1)
60400 Fgrp$=Indexfile$
60410 Fgrp$=REP("",P,10)
60420 CALL "open",Fgrp$;".F*","lfn:8"
60430 READ #8,65000:Lastrec
60435 GOSUB 64270  !set discriminator level
60438 GOSUB 64700  !     CALCULATE MARKED TIMES FOR FIRST FILE
60440 REM                                      Open all peaksfile$
60450 FOR I=1 TO Peaks
60460    CALL "open",Peaksfile$;".PF";I,"lfn:";I
60470 NEXT I
60480 REM MAY HAVE TO CHANGE ALL CLOSE TO CLOSE N
60490 Skipclos$="skip"
60500 FOR Iiii=Filestart TO Filestop  ! looping with rec #
60510    IF Iiii=Lastrec+1 THEN
60520       GOSUB 63000  !open next indexfile$
60530    END IF
60540    X=Iiii
60550    GOSUB 5102
60600    REM                   DEAL WITH PEAKS
60610    Isub=1  !FOR REF PEAK
60620    GOSUB 64000
60630    REM FIND LEADING EDGE OF REF. PEAK
60650    Leadtest=1
60660    CALL "cross",B,Vbmax*0.3,Ibleadt,Leadtest
60670    IF Ibleadt<Ibmax THEN
60675       IF Ibleadt=-1 THEN 60712
60680       Iblead=INT(Ibleadt-1)
60690       Leadtest=Leadtest+1
60700       GO TO 60660
60710    END IF
60712    IF Iblead<0 THEN
60714       Iblead=Ibmax-INT(Twidth(1)/A3*0.25)
60716    END IF
60720    Ialead=Iblead+Ipkmin-1
60730    Pkflytime1=(Ialead-It0)*A3  !tof of ref peak
60732    Tflytime1=SQR(Mass(1)/0.193/(Vdc+Alpha*Vp))*0.15*1.0E-6
60734    IF Pkflytime1>1.05*Tflytime1 OR Pkflytime1<0.95*Tflytime1 THEN
60736       Pkflytime1=Tflytime1
60738    END IF
60740    Tpkmin(1)=Pkflytime1-0.25*Twidth(1)
60750    Tpkmax(1)=Tpkmin(1)+Twidth(1)
60752    IF Vbmax<=Vdiscrim(1) THEN
60754       Vbmax=0
60756    END IF
60760    PRINT #1:Vbmax  !put in peaksfile$.pf1
60770    REM    now, for the other peaks found by ratioing with ref peak
60775    IF Peaks=1 THEN 60840
```

```
60780    FOR Jj=2 TO Peaks
60790       Pkflytime_calc=SQR(Mass(Jj)/Mass(1))*Pkflytime1
60800       Tpkmin(Jj)=Pkflytime_calc-0.25*Twidth(Jj)
60810       Tpkmax(Jj)=Tpkmin(Jj)+Twidth(Jj)
60815       Isub=Jj
60820       GOSUB 64000  ! find max of peak
60822       IF Vbmax<=Vdiscrim(Jj) THEN
60824          Vbmax=0
60826       END IF
60830       PRINT #Jj:Vbmax
60835    NEXT Jj
60840 NEXT Iiii
60850 CLOSE
60900 PAGE
60920 DIM B$(1000)
60930 CALL "directory",Peaksfile$;".f*",B$
60940 PRINT B$
60950 END
60960   !
60970   !
60980   !
60990   !
61000 REM                                  DUPLICATE FILENAME HANDLER
61010 CALL "DSKERR",B$
61020 PRINT "J",B$
61030 B$="DO YOU WISH TO ALTER "&Peaksfile$&"? Y/N "
61040 GOSUB 11900
61050 IF X=1 THEN
61060    PRINT "Change peaksfile$ with edit keys."
61070    ALTER Peaksfile$,Peaksfile$
61080    CALL "CREATE","A","D",Peaksfile$;".PF";I
61090    RETURN
61100 END IF
61110 B$="Do you want to delete them? y/n "
61120 GOSUB 11900
61130 IF X=1 THEN
61140    B$="Are you sure? "
61150    GOSUB 11900
61160    IF X=1 THEN
61170       CALL "delete",Peaksfile$;".pf*","nin"
61180       CALL "create","A","D",Peaksfile$;".pf";I
61190    END IF
61210    RETURN
61220 ELSE
61300    PRINT "FEEX IT YOURSELF, PEDRO"
61310    STOP
61320 END IF
63000 REM       open next indexfile$ & read last rec#
63010 P=POS(Indexfile$,".",1)
63020 Fgrp$=Indexfile$
63030 Fgrp$=REP("",P,10)
63040 CALL "open","lfn:8 next"
```

```
63050 READ #8,65000:Lastrec  ! last rec in this file
63060 RETURN
64000 REM                         peak pickoff routine
64010 Iwidth=INT(Twidth(Isub)/A3+1)
64020 DIM B(Iwidth),Bx(Iwidth)
64030 Ipkmin=INT(Tpkmin(Isub)/A3+It0)
64032 IF Ipkmin+Iwidth-1>512 THEN
64034    Ipkmin=513-Iwidth
64036 END IF
64040 FOR I=1 TO Iwidth
64050    B(I)=A(Ipkmin+I-1)
64060 NEXT I
64070 Bx=1
64080 CALL "int",Bx,Bx
64090 Bx=Bx+Ipkmin
64100 Bx=Bx-It0
64110 Bx=Bx-1
64115 CALL "max",B,Vbmax,Ibmax
64120 GO TO Iwantgraph+2 OF 64260,64260,64130
64130 MOVE Bx(1),-A2
64140 DASH 85
64150 DRAW Bx(1),B(1)
64160 DASH 0
64170 DRAW Bx,B
64180 DASH 85
64190 DRAW Bx(Iwidth),-A2
64200 DASH 0
64220 MOVE Ibmax+Ipkmin-It0-1,B(Ibmax)
64230 FOR I=1 TO 50
64240    RDRAW 0,0
64250 NEXT I
64260 RETURN
64270 REM                               set discriminator level
64505 DIM Vdiscrim(Peaks)
64507 Vdiscrim=0
64510 PRINT "Do you want to set a discriminator level for any of the ";
64520 PRINT "peaks? y/n ";
64530 INPUT Q$
64540 IF Q$="y" THEN
64550    FOR I=1 TO Peaks
64560       PRINT I,Mass(I)
64570    NEXT I
64580    PRINT "How many masses are there that need discrim. levels set?
        ";
64590    INPUT Levnum
64600    FOR I=1 TO Levnum
64610       PRINT "Enter index for mass. ";
64620       INPUT Jkl
64630       PRINT "Enter discriminator level in volts. ";
64640       INPUT Vdiscrim(Jkl)
64650    NEXT I
64660 END IF
```

```
64670 RETURN
64700 REM              FIND MARKED TIMES FOR FIRST FILE USED
64710 X=Reffile
64730 GOSUB 5080
64740 Vref=Vdc+0.2*Vp
64750 X=Filestart
64760 GOSUB 5080
64770 Vstart=Vdc+0.2*Vp
64790 Tpkmin=SQR(Vref/Vstart)*Tpkmin
64800 Tpkmax=Tpkmin+Twidth
64810 RETURN
```

PEAKCUMULATOR

This program will find the cumulative values of the values found with the "PEAKPICKOFF.RATIO" program. The same number of new files will be created as was created previously. The new files will have the same generic name, but with ".CUM1" substituted for ".PF1." The only information required for this program is the generic name of the files.

```
100 REM                                             PEAKCUMULATOR PROGRAM
110 PRINT "L What is the generic name for files with peak values? ";
120 INPUT Peaksfile$
130 CALL "open",Peaksfile$;".pf* lfn:1"
140 INPUT #1:Adim
150 DIM A(Adim)
160 INPUT #1:A
170 INPUT #1:Recs
180 FOR I=1 TO Adim  !# of peaks & files to be created for cum
190    CALL "create","A","D",Peaksfile$;".cum";I
200    CALL "open","lfn:1 next"
210    CALL "open",Peaksfile$;".cum";I,"lfn:2"
220    Cum=0
230    FOR J=1 TO Recs
240       INPUT #1:Peakvalue
250       Cum=Cum+Peakvalue
260       PRINT #2:Cum
270    NEXT J
280    CLOSE 2
290 NEXT I
300 CLOSE
310 PAGE
320 DIM B$(1000)
330 CALL "directory",Peaksfile$;".cum*",B$
340 PRINT "L",B$
350 END
```

DATAREDUCER

This program is used for several reasons. It produces the files generic.CUMn, generic.CUMDISCn, and generic.DEPTH. The first two are used to find the d.c. offset and discriminator level. If the ring counting method has been used, the program execution is halted after these files are produced. If the calculation method is used, the program prompts for the α and l_0 values and then claculates an array for the depth from the reference peak. The cumulative signal of interest versus the depth is then graphed by plotting the array in one of the generic.CUMDISCn files against the array in generic.DEPTH.

```
1 INIT  !                                              DATAREDUCER PROGRAM
2 CALL "onerr",40000
3 GO TO 100
4 GO TO 21000
24 GO TO 6000
28 GO TO 7000
64 GO TO 16000
68 GO TO 17000
100 Beta=20
110 Kd=5.1597E-5
115 SET DEGREES
120 Cb=COS(Beta)
130 Sb=SIN(Beta)
140 Ccurs=1
150 Skippy=3
160 Dcoffset=0
170 Vdiscr=0
180 PRINT "LCAUTION, You will have problems if there are more than
    about "
190 PRINT "2700 data points.JJJ"
200 PRINT "The *.pf* should have been copied to the [peakfiles]
directory."
210 PRINT "JJ"
300 REM                                              PEAKCUMULATOR PROGRAM
310 PRINT "    What is the generic name for files with peak values? JJ"
320 INPUT Peaksfile$
```

```
330 CALL "open",Peaksfile$;".pf* lfn:1"
340 INPUT #1:Adim
350 DIM A(Adim)
360 INPUT #1:A
370 INPUT #1:Recs
375   !Recs=2384  !temp*****************************************
380 FOR I=1 TO Adim  !# of peaks & files to be created for cum
382    F$=STR(I)
384    E$=".cum"&F$
390    CALL "create","A","D","[peakfiles]",Peaksfile$;".cum";I
395    GO TO Skippy OF 500,400,400
400    CALL "open","lfn:1 next"
410    CALL "open","[peakfiles]",Peaksfile$;".cum";I,"lfn:2"
420    Cum=0
430    FOR J=1 TO Recs
440       INPUT #1:Peakvalue
450       Cum=Cum+Peakvalue
460       PRINT #2:Cum
470    NEXT J
480    CLOSE 2
490 NEXT I
500 CLOSE
505 Skippy=3
510 PAGE
515 CALL "COPY",Peaksfile$;".PF*","TO [PEAKFILES]",Peaksfile$;".PF*"
520 DIM B$(1000)
530 CALL "directory","[peakfiles]",Peaksfile$;".cum*",B$
540 PRINT "L",B$
560 PRINT "The ref. file will be the x-axis of the cum-cum graph. What"
570 PRINT "is the peak's name? ";
580 INPUT Xpeakname$
590 PRINT "Of the ";Adim;" peaks above, which one is of interest for the
    "
600 PRINT "y-axis? ";
610 INPUT Pnum
620 PRINT "What is this peak's name? ";
630 INPUT Ypeakname$
640 DIM X(Recs),Y(Recs)
650 CALL "open","[peakfiles]",Peaksfile$;".cum1 lfn:1"
660 INPUT #1:X
670 CALL "open","[peakfiles]",Peaksfile$;".cum";Pnum,"lfn:2"
680 INPUT #2:Y
690 CLOSE
700 Title$="cumulative "&Ypeakname$&" vs "&" cumulative "&Xpeakname$
710 PAGE
720 CALL "max",X,Xmax,I
730 CALL "max",Y,Ymax,I
740 GOSUB 50000
750 HOME
760 PRINT "JJJJ"
770 PRINT "Use keys 6, 7, & 16 to find and set left marker."
780 PRINT "Use keys 6, 7, & 17 to find and set right marker."
```

```
790 PRINT "Markers should denote linear portion of the graph."
800 PRINT "After doing this, restart program with key#1."
810 END
6000 REM cursor left
6010 Ccurs=Ccurs-1
6020 IF Ccurs<1 THEN
6030    Ccurs=Recs
6040 END IF
6050 MOVE X(Ccurs),Y(Ccurs)
6060 RDRAW 0,0
6070 RETURN
7000 REM cursor right
7010 Ccurs=Ccurs+1
7020 IF Ccurs>Recs THEN
7030    Ccurs=1
7040 END IF
7050 MOVE X(Ccurs),Y(Ccurs)
7060 RDRAW 0,0
7070 RETURN
16000 REM left marker set
16010 Lcursor=Ccurs
16015 PRINT "G"
16016 RDRAW 0,0
16020 RETURN
17000 REM right marker set
17010 Rcursor=Ccurs
17015 PRINT "G"
17016 RDRAW 0,0
17020 RETURN
18015 PRINT "G"
18016 RDRAW 0,0
21000 REM restarting place after linear part is marked
21010 CLOSE
21013 F$=STR(Pnum)
21015 E$=".cumdisc"&F$
21020 CALL "open",Peaksfile$;".pf";Pnum,"lfn:1"
21022 CALL "create","A","D","[peakfiles]",Peaksfile$;".cumdisc";Pnum
21024 CALL "open","[peakfiles]",Peaksfile$;".cumdisc";Pnum,"lfn:2"
21028 GO TO Skippy OF 21288,21030,21030
21030 INPUT #1:Y
21040 CLOSE 1
21050 Dcoffset=0
21060 FOR I=Lcursor TO Rcursor
21070    Dcoffset=Dcoffset+Y(I)
21080 NEXT I
21090 Dcoffset=Dcoffset/(Rcursor-Lcursor+1)
21100 Y=Y-Dcoffset
21110   !PRINT "LInput discriminator level. ";
21115 Vdiscr=5.0E-4  !YOU MAY CHANGE THIS VALUE
21120   !INPUT Vdiscr
21130 FOR I=1 TO Recs
21140    IF Y(I)<Vdiscr THEN
```

```
21150       Y(I)=0
21160    END IF
21170 NEXT I
21180 Ssum=0
21190 FOR I=1 TO Recs
21200    Ssum=Ssum+Y(I)
21210    Y(I)=Ssum
21220 NEXT I
21230 Title$="Cumulative "&Ypeakname$&" vs Cumulative "&Xpeakname$
21240 PAGE
21280 PRINT #2:Y
21285 GO TO 21290
21288 INPUT #2:Y
21289 Skippy=3
21290 CLOSE
21291 PRINT USING 21296:Dcoffset,Vdiscr
21292 GOSUB 50000
21296 IMAGE"L^JDC OFFSET= "2E "     DISCRIMINATOR= "1E
21300 PRINT "^JJJJJInput alpha & LO in (hkl) units."
21302 PRINT "alpha? ";
21304 INPUT Alpha
21306 PRINT "LO? ";
21308 INPUT LO
21310 Sa=SIN(Alpha)
21320 Ka=Sa/(1-Sa)
21330 K=Kd*PI*(Ka^2*Sb^2-Ka^3*(1-Cb)^2)/3
21500 PRINT "Input estimated number of layers.";
21510 INPUT Layers
21520 REM calculate cum ni from est & check that > x(recs),(xmax)
21530 Cumnicalc=K*(Layers^3+3*LO*Layers^2+3*LO^2*Layers)
21540 IF Cumnicalc<X(Recs) THEN
21550    Layers=Layers+10
21560    GO TO 21530
21570 END IF
21582 CALL "create","A","D","[peakfiles]",Peaksfile$;".depth"
21584 CALL "open","[peakfiles]",Peaksfile$;".depth lfn:1"
21588 GO TO Skippy OF 30000,21590,21590
21590 DELETE Y
21591 DIM Testcum(INT(Layers+1))
21595 FOR I=1 TO INT(Layers)+1
21600    Testcum(I)=K*(I^3+3*LO*I^2+3*LO^2*I)
21625 NEXT I
21630 FOR I=1 TO Recs
21635    Temp=X(I)
21640    CALL "cross",Testcum,Temp,Depth
21642    IF Depth=-1 THEN
21644       Depth=X(I)/Testcum(1)
21646    END IF
21650    PRINT #1:Depth
21660 NEXT I
21670 DELETE Testcum
21680 DIM Y(Recs)
```

```
21690 CALL "open","[peakfiles]",Peaksfile$;".cumdisc";Pnum,"lfn:3"
21700 INPUT #3:Y
21710 CLOSE 3
30000 CALL "rlocate","1 position:0"
30010 INPUT #1:X
30020 CLOSE 1
30030 Skippy=3
30040 Title$="Cumulative "&Ypeakname$&" vs Depth (hkl) Layers"
30050 Xmax=Layers
30060 PAGE
30070 PRINT "JALPHA= ";Alpha,"LO= ";LO
30080 GOSUB 50000
30090 END
40000 REM duplicate file handling routine
40010 DIM B$(500)
40020 CALL "DSKERR",B$
40030 PRINT "L",B$
40034 PRINT "JJThe file name is: ";Peaksfile$;E$,"JJJ"
40040 PRINT "If error is duplicate file, you have a choice.  You may "
40050 PRINT "restore the new data on the old file, or use the old data.J
      "
40060 PRINT "Do you want to use the old data? (Y/N) ";
40070 INPUT Q$
40080 IF Q$="n" THEN
40090    Skippy=2
40100 ELSE
40110    Skippy=1
40120 END IF
40125 PAGE
40130 RETURN
50000 REM graph routine y vs x
50010 WINDOW 0,Xmax,0,Ymax
50020 VIEWPORT 10,120,10,90
50030 AXIS Xmax,Ymax
50040 MOVE Xmax,0
50050 PRINT USING 50060:Xmax
50060 IMAGE"JHH",3d.2d
50070 MOVE 0,Ymax
50080 PRINT USING 50090:Ymax
50090 IMAGE"HHHHH", 2d.2d
50100 MOVE 0,0
50110 DRAW X,Y
50115 PRINT "_",Title$;"   ";"[peakfiles] ";Peaksfile$
50117 COPY
50120 RETURN
```

CUMVSRING

This program is used for producing the cumulative IAP signal versus ring count data as described in Chapter III. Peak values are accumulated to the pulse number which corresponds to a ring collapse. The cumulated values are stored in a new file on the file manager. The index number of the cumulated datum point corresponds to the ring collapse number which is associated with that value. If a ring collapse occurred in the middle of the a spectrum, e.g. on the fourth pulse out of eight, a fractional part of the peak height is added to the cumulated value, in this example one-half would be added. The resultant information is graphed. Because of the manner in which the control "Cum Ni vs Ring Count" curve is generated, no manipulation of data acquired during regular profiling experiments will need to be performed in order to compare that data to the curve generated to provide the depth scale for that particular specimen. This program will also generate a theoretical curve based on the geometric emitter parameters, α, the shank half-angle, and l_0, the cone apex to initial surface distance. A linearly-weighted-average, proportionality constant, K_D, can also found with this program.

```
1   !
2 Lun=32  !                                    CUMVSRING.PROG
3 GO TO 100
12 GO TO 3000  !   KEY:3  >>>> GRAPH THEORETICAL CURVE
20 GO TO 20000  !  KEY:5  >>>> GRAPH CUM SIGNAL STORED ON FILE
40 GO TO 2300  !   KEY:10 >>>> REGRAPH, SAME PARAMETERS
44 GO TO 560  !    KEY:11 >>>> RUN AGAIN,BUT CUMVSRING$ FILE GIVES ERROR
52 GO TO 13000  !  KEY:13 >>>> ENTER ALPHA AND LO
64 GO TO 16000  !  KEY:16 >>>> GRAPH DIF3(Y)/DIF3(X) VS X
72 GO TO 18000  !  KEY:18 >>>> FIND KD FROM RINGCOUNT EXPERIMENT
80 GO TO 2000  !   KEY:20 >>>> REGRAPH, CHANGE GRAPH PARAMETERS
90 GO TO 21000
100 REM                                   CUMVSRING.PROG
101 SET DEGREES
105 A$=""
106 B$=""
110 Title$=""
120 PAGE
140 PRINT "JWhat is generic name for files being reduced? ";
150 INPUT Peaksfile$
160 CALL "open",Peaksfile$;".pf0 lfn:1"
170 INPUT #1:Adim
180 DIM Massnums(Adim)
190 INPUT #1:Massnums
200 INPUT #1:Recs
210 INPUT #1:Filestart,Filestop
230 CLOSE
240 PRINT "JThe pulsenum file should have the extension, '.cnt'."
250 Pulsenum$=Peaksfile$&".cnt"
260 PRINT "JWhat is number of rings collapsed? ";
270 INPUT Nrings
280 PRINT "JInput the dcoffset and discriminator levels? (x,y) ";
290 INPUT Dcoffset,Vdiscr
300 PRINT "JWhat is .pf(n) extension number for the mass of interest? ";
310 INPUT Pnum$
320 Pnum=VAL(Pnum$)
340 Vsignal$=Peaksfile$&".pf"&Pnum$
350 Cumvsring$=Peaksfile$&".cumvsring"&Pnum$
355 Title$=Cumvsring$
560 CALL "OPEN",Vsignal$,"LFN:1"
570 CALL "OPEN",Pulsenum$,"LFN:2"
580 CALL "ONERR",90
590 CALL "CREATE","A","D",Cumvsring$
600 CALL "OPEN",Cumvsring$,"LFN:9"
610 DIM Cum(Nrings),Pulsenum(Nrings),Y(Nrings)
620 RESTORE
630 DATA 0,0,8
640 READ Dumcum,Ktr2,Numavg
650 Cum=0
660 CALL "TIME",B$
670 A$="JJSTART TIME WAS "&B$
680 INPUT #2:Pulsenum
```

```
682 PRINT "LRing#","Spectra#","PULSE","PARTITION"
684 I=1  !I is ring #
690 Ktr=Filestart-1
700 Ktr=Ktr+1  !ktr is  for spectra#
710 INPUT #1:V
712 V=V-Dcoffset
714 IF V<Vdiscr THEN
716    V=0
718 END IF
720 IF Ktr*Numavg=>Pulsenum(I) THEN   ! ring collapsed occurred
730    S=Pulsenum(I)-(Ktr-1)*Numavg  !s is fractional partition
740    Cum(I)=Dumcum+V*S/Numavg
750    I=I+1
760    REM  Check to see if multiple collapses within one spectrum
765    IF I=Nrings+1 THEN 950  !ESCAPE, DONE!
770    S=Pulsenum(I)-(Ktr-1)*Numavg
780    IF S<=Numavg THEN
790       PRINT I,Ktr,Pulsenum(I),S
800    END IF
810    GO TO 720
820 END IF
830 Dumcum=Dumcum+V
840 GO TO 700
950 PRINT #9:Cum
960 CLOSE
970 PRINT "JFile being used is: ";Vsignal$;". Mass is ";Massnums(Pnum)
980 PRINT "JEnter the orientation (hkl) and tip material as it will ";
990 PRINT "be printed. ";
1000 INPUT Xlbl$
1010 PRINT "JEnter the name of the peak used for y-axis. ";
1020 INPUT Ylbl$
2000   !GRAPH
2100 PAGE
2102 PRINT A$
2104 PRINT "JFINISH TIME WAS ";B$
2106 Y=Cum
2110 CALL "MAX",Y,Vmax,Iimax
2120 PRINT "JJJTHE MAX CUM VALUE IS ";Vmax;".  ENTER MAX FOR GRAPH."
2130 INPUT Vmax
2140 PRINT "JTHE NUMBER OF RINGS IS ";Nrings;". ENTER XMAX FOR GRAPH."
2150 INPUT Xmax
2160 PRINT "ENTER DESIRED X-TIC INTERVAL. ";
2170 INPUT Xtic
2180 PRINT "JENTER Y-TIC INTERVAL. ";
2190 INPUT Ytic
2200 WINDOW 0,Xmax,0,Vmax
2210 PRINT "JENTER LABEL INTERVALS,X THEN Y. ";
2220 INPUT Xlbl,Ylbl
2300 PAGE
2310 VIEWPORT 15,110,10,90
2320 AXIS @Lun:Xtic,Ytic
2325 AXIS @Lun:Xtic,Ytic,Xmax,Vmax
```

```
2330 FOR I=Xlbl TO Xmax STEP Xlbl
2340    MOVE @Lun:I,0
2350    PRINT @Lun:"J";I/100
2360 NEXT I
2370 FOR I=Ylbl TO Vmax STEP Ylbl
2380    MOVE @Lun:0,I
2390    PRINT @Lun:"HHH";I
2400 NEXT I
2402 MOVE @Lun:0,0
2404 PRINT @Lun:"HJ0"
2410 DIM X(Nrings)
2420 X=1
2430 CALL "INT",X,X
2440 X=X+1
2450 MOVE @Lun:0,0
2460   !DRAW @Lun:X,CUM !IF ERROR HERE, ASSIGN Y=CUM IN CALLING PROGRAM
2465 DRAW @Lun:X,Y
2470 MOVE @Lun:Xmax/2,0
2480 PRINT @Lun:"JJJHHHHHHH";Xlbl$;" RING COUNT (x100)^"
2490 MOVE @Lun:0,0.67*Vmax
2491 PRINT @Lun,25:90
2492 PRINT @Lun:"JHHHHHHKKKCUM ";Ylbl$;"^"
2495 PRINT @Lun,7:
2500 PRINT @Lun,17:1.792*1.3,2.816*1.3
2510 HOME @Lun:
2520 PRINT @Lun:" "," ","HHHHHHHHHHHJ";Title$
2530 PRINT @Lun,7:
2535 Lun=32
2537 DASH 0
2540 END
3000 REM                                                    THEORETICAL CURVE
3010   !FOR Kd=1.8E-7 TO 1.9E-7 STEP 1.0E-8
3020   !FOR L0=1000 TO 2600 STEP 200
3030 DASH 51
3060 RESTORE 3070
3070 DATA 2.03,20,1.4393E-4
3080 READ D111,Beta,Kd
3090 Sa=SIN(Alpha)
3100 Sb=SIN(Beta)
3110 Cb=COS(Beta)
3120 B=3*L0
3130 C=3*L0^2
3135 Ka000=Sa/(1-Sa)
3140 Kalpha=PI*(Ka000^2*Sb^2-Ka000^3*(1-Cb)^2)/3
3150 DIM Cumtheo(Xmax),X(Xmax),Dummy(Xmax)
3160 X=1
3170 CALL "int",X,X
3180 X=X+1
3190 Cumtheo=X^3
3200 Dummy=X^2
3210 Dummy=Dummy*B
3220 Cumtheo=Cumtheo+Dummy
```

```
3230 Dummy=C*X
3240 Cumtheo=Cumtheo+Dummy
3250 Cumtheo=Cumtheo*Kalpha
3260 Cumtheo=Cumtheo*Kd
3270 MOVE @Lun:0,0
3280 DRAW @Lun:X,Cumtheo
3281   !PRINT Kd
3282   !PRINT LO
3285   !NEXT Kd
3286   !NEXT LO
3287 DASH 0
3289 Lun=32
3290 END
13000 REM                              ENTER ALPHA AND LO
13010 PAGE
13020 PRINT "JEnter LO in n(111) units. G";
13030 INPUT LO
13040 PRINT "JEnter emitter half-angle, Alpha, in degrees. G";
13050 INPUT Alpha
13060 RETURN
16000 REM                        FIND DIF3(Y)/DIF3(X) VS X
16010 DIM Xx(Nrings),Yy(Nrings)
16020 CALL "DIF3",X,Xx
16030 CALL "DIF3",Cum,Yy
16040 Yy=Yy/Xx
16050 Y=Yy
16090 GO TO 2110
18000 REM CALIBRATE ,FIND KD
18005 DIM Kda(Nrings),X(Nrings)
18010 REM                        NRINGS & CUM(I) SHOLD ALREADY BE IN MEMORY
18020 Sa=SIN(Alpha)
18030 Sb=SIN(Beta)
18040 Cb=COS(Beta)
18045 Ka000=Sa/(1-Sa)
18050 Kalpha=PI*(Ka000^2*Sb^2-Ka000^3*(1-Cb)^2)/3
18060 B=3*LO
18070 C=3*LO^2
18080 FOR I=1 TO Nrings
18090    Denom=Kalpha*(I^3+B*I^2+C*I)
18100    Kda(I)=Cum(I)/Denom
18110 NEXT I
18120 X=1
18130 CALL "INT",X,X
18140 X=X+1
18150 Kda=Kda*X
18160 Wt=Nrings*(Nrings-1)/2
18200 Kd=SUM(Kda)
18205 Kd=Kd/Wt
18210 PRINT " AVERAGED KD= ";Kd
18215 DELETE Akda
18220 RETURN
20000 REM GRAPH CUM SIGNAL STORED ON FILE
```

```
20010 PRINT "LENTER NAME OF FILE CUMULATED DATA IS STORED ON. ";
20020 INPUT Cumvsringstore$
20030 PRINT "ENTER NUMBER OF DATA POINTS. ";
20040 INPUT Nrings
20050 DIM Cumstore(Nrings),Cum(Nrings)
20060 CALL "OPEN",Cumvsringstore$,"LFN:1"
20070 INPUT #1:Cumstore
20075 CLOSE
20080 DIM Dummy(Nrings)
20100 Cum=Cumstore
20105 PRINT "THIS IS TITLE$. CHANGE IT IF YOU WANT, THEN <CR>."
20107 ALTER Title$,Title$
20110 GOSUB 2000
20120 END
21000 REM           DISK ERROR, PROBABLY DUPLICATE FILE
21010 DIM B$(1000)
21020 CALL "DSKERR",B$
21030 PRINT B$
21040 PRINT "JIF ERROR IS DUPLICATE FILE, (ERROR:25), YOU HAVE 2 OPTIONS
      ."
21050 PRINT "J1) ENTER <CR> AND OLD FILE, ";Cumvsring$;", WILL BE USED "
21060 PRINT "   AGAIN. <<<< OLD DATA WILL BE LOST! >>>>J"
21070 PRINT "                         -OR-J"
21080 PRINT "2) ENTER NEW FILE NAME TO BE CREATED IN ORDER FOR THE "
21090 PRINT "   CUMLATIVE SIGNAL TO BE STORED."
21100 PRINT "JJ         ENTER <CR>     -OR-      NAME &<CR>. "
21110 PRINT "                      J";
21120 INPUT Q$
21130 IF Q$="" THEN 21160
21140 Cumvsring$=Q$
21150 CALL "CREATE","A","D",Cumvsring$
21160 CALL "OFFERR"
21170 RETURN
60000 MOVE @Lun:Xmax*0.1,Vmax*0.75
60010 DASH 0
60020 PRINT @Lun:"EXPERIMENTAL ";
60025 GIN @Lun:Fx,Fy
60026 MOVE @Lun:Fx,Fy
60030 RDRAW @Lun:0.14*Xmax,0
60040 MOVE @Lun:0.1*Xmax,Vmax*0.75
60050 PRINT @Lun:"J";
60060 DASH 51
60070 PRINT @Lun:"CALCULATED   ";
60075 GIN @Lun:Fx,Fy
60076 MOVE @Lun:Fx,Fy
60080 RDRAW @Lun:0.14*Xmax,0
60085 DASH 0
60090 END
```

FIMSUPPLY

This program is used when IAP data are not to be collected. It primarily controls the Bertan model 205A-30R high voltage power supply. It is used to control the power supply in the FIM mode of operation. When the program is run to initialize parameters, several warnings are displayed. Foremost of these is to warn that the high voltage lead is connected and not the electrometer lead. Possible electric shock can occur if the open high voltage lead is touched. There is also possible damage to the electrometer if the high voltage pulser is used with the electrometer lead connected. The other warnings advise that all devices on the GPIB should be turned on (at least half of them should be on) and to protect the digitizer from voltage spikes when turning on the voltages to the chevron assembly. All controls are accomplished with the use of the user-definable keys.

This program is called-up when data collection is complete and the specimen is needed for other use, e.g. future use in the FIM/IAP or to be imaged in the TEM. The reason for this is that there is a routine in this program which will slowly ramp the voltage to zero. Samples have a lower mortality rate when this is done because they are not "shocked", going suddenly from a high stess state to zero.

```
1 ON SRQ THEN 50000  !FIMSUPPLY
2 GO TO 100
4 GO TO 1000
8 GO TO 2000
16 GO TO 4000
20 GO TO 5000
24 GO TO 6000
28 GO TO 7000
36 GO TO 9000
40 GO TO 10000
44 GO TO 50000
52 GO TO 13000
56 GO TO 14000
60 GO TO 15000
64 GO TO 16000
68 GO TO 17000
72 GO TO 18000
100 Meters$="12345678"
200 Vinc=0.015
300 PRINT "LJJJJJGGGGGGGGGGGGGGGGGGGGGGGGGGGGG"
305 PRINT "JJJJ                           D A N G E R"
306 PRINT "                           -----------JJJ"
308 PRINT "     ";
310 PRINT "C H E C K   H I G H   V O L T A G E   C O N N E C T I O N ! !"
330 PRINT USING 340:
340 IMAGE "__",72("*"),S
350 PRINT USING 360:
360 IMAGE "__",12("KK*",70X,"*_")
365 PRINT "KKKKKK"
370 PRINT USING 340:
410 PRINT "JJJJJJJJJJJJJJJJJJJJWARNING:"
420 PRINT "ALL DEVICES ON GPIB SHOULD BE ON!"
430 PRINT "PROTECT THE DIGITIZER FROM LARGE VOLTAGE SPIKES!"
500 END
1000   !READ V AND I
1010 ON SRQ THEN 50000
1020 Meter$="12345678"
1030 CALL "IOBCD",Meters$,I1,I2
1040 Met1$=SEG(Meters$,1,4)
1050 Voltage=VAL(Met1$)*0.01
1060 PRINT @4:"T2"
1070 INPUT @4:I$
1080 PRINT "LD.C. VOLTAGE IS ";Voltage;" KV._WITH ";I$
1090 RETURN
2000   !INCREASE VOLTAGE BY VINC
2010 ON SRQ THEN 50000
2020 SET NOKEY
2030 Meters$="12345678"
2040 CALL "IOBCD",Meters$,I1,I2
2050 Met1$=SEG(Meters$,1,4)
2060 V=VAL(Met1$)*0.01
2070 Vnew=V+Vinc
```

```
2080 Vprog=Vnew*1.06-0.012
2090 Vprog=INT(Vprog*1000)/1000
2100 PRINT @4:"P";Vprog;"KG"
2110 RETURN
4000   !INCREASE VOLTAGE
4001 ON SRQ THEN 50000
4006 Meters$="12345678"
4010 SET NOKEY
4020 CALL "IOBCD",Meters$,I1,I2
4030 Met1$=SEG(Meters$,1,4)
4040 V=VAL(Met1$)*0.01
4050 Vnew=V+0.1
4060 Vprog=Vnew*1.06-0.012
4070 Vprog=INT(Vprog*1000)/1000
4080 PRINT @4:"P";Vprog;"KG"
4090 RETURN
5000   !RESET
5001 ON SRQ THEN 50000
5010 SET NOKEY
5020 PRINT @4:"R"
5025 CALL "IFC"
5030 RETURN
6000   !incrase voltage increment by 10%
6010 SET NOKEY
6020 Vinc=INT(Vinc*1.1*1000)/1000
6030 PRINT @32,26:2
6040 PRINT "VOLTAGE INCREMENT= ";Vinc;" kV."
6050 PRINT @32,26:0
6060 RETURN
7000   !DECREASE VOLTAGE BY VINC
7010 ON SRQ THEN 50000
7020 SET NOKEY
7030 Meters$="12345678"
7040 CALL "IOBCD",Meters$,I1,I2
7050 Met1$=SEG(Meters$,1,4)
7060 V=VAL(Met1$)*0.01
7070 Vnew=V-Vinc
7080 Vprog=Vnew*1.059-0.012
7090 Vprog=INT(Vprog*1000)/1000 MAX 0
7100 PRINT @4:"P";Vprog;"KG"
7110 RETURN
9000   !DECREASE VOLTAGE
9001 ON SRQ THEN 50000
9006 Meters$="12345678"
9010 SET NOKEY
9020 CALL "IOBCD",Meters$,I1,I2
9030 Met1$=SEG(Meters$,1,4)
9040 V=VAL(Met1$)*0.01
9050 Vnew=V-0.1
9060 Vprog=Vnew*1.06-0.012
9070 Vprog=INT(Vprog*1000)/1000 MAX 0
9080 PRINT @4:"P";Vprog;"KG"
```

```
9090 RETURN
10000   !SHUTDOWN
10001 ON SRQ THEN 50000
10010 SET NOKEY
10020 PRINT @4:"S"
10030 RETURN
13000   !SET CURRENT LIMIT
13001 ON SRQ THEN 50000
13010 PRINT "LENTER CURRENT LIMIT AS  XXX.XX IN UAMPS"
13020 INPUT I$
13030 PRINT @4:"L";I$;"UG"
13040 RETURN
14000   !RAMP VOLTAGE TO ZERO
14010 ON SRQ THEN 50000
14020 Meters$="12345678"
14030 SET NOKEY
14040 CALL "IOBCD",Meters$,I1,I2
14050 Met1$=SEG(Meters$,1,4)
14060 V=VAL(Met1$)*0.01
14065 Vinc2=Vinc MAX 0.05
14070 Vnew=V-0.1
14080 Vprog=Vnew*1.06
14090 Vprog=INT(Vprog*1000)/1000 MAX 0
14100 PRINT @4:"P";Vprog;"KG"
14110 IF V<0.015 THEN 14140
14120 CALL "WAIT",1.5
14130 GO TO 14040
14140 RETURN
15000   !SET VOLTAGE TO ZERO
15001 ON SRQ THEN 50000
15010 SET NOKEY
15020 PRINT @4:"P";0;"KG"
15030 RETURN
16000   !decrease voltage increment by 10%
16010 SET NOKEY
16020 Vinc=INT(Vinc*0.9*1000)/1000
16030 PRINT @32,26:2
16040 PRINT "VOLTAGE INCREMENT= ";Vinc;" kV."
16050 PRINT @32,26:0
16060 RETURN
18000   !SET VOLTAGE LIMIT
18001 ON SRQ THEN 50000
18010 PRINT "LENTER VOLTAGE LIMIT AS XX.XXX IN KV"
18030 INPUT Vv
18035   !Vv=INT((1.0594*Vv-0.01276)*1000)/1000
18036 Vv=INT((1.0594*Vv-0.01276+0.073)*1000)/1000
18040 PRINT @4:"L";Vv;"KG"
18050 RETURN
50000   !SERIAL POLL
50005 SET NOKEY
50010 POLL X,P4;4
50020 POLL X,P1;1,0
```

```
50030 POLL X,P3;3
50040 POLL X,P2;2
50050 PRINT "JJ";"P1","P2","P3","P4"
50060 PRINT P1,P2,P3,P4
50065   !PRINT @4:"R"
50080 CALL "DECBIN",E$,E$,P1
50090 PRINT E$,"";
50130 CALL "DECBIN",E$,E$,P2
50140 PRINT E$,"";
50150 CALL "DECBIN",E$,E$,P3
50160 PRINT E$,"";
50170 CALL "DECBIN",E$,E$,P4
50180 PRINT E$
50190 RETURN
```

TIPREDUCER

This program utilizes the Tekronix 4662 Interactive Digital Plotter to digitize the critical parameters of the emitter from TEM micrographs. Explicit instructions are printed out to explain how to use the program when the "Run" command is executed. The sides of the tip are fitted with a least-squares straight line. The apex of the cone is found by the intersection of the two extended lines. The point on the surface along the centerline of the tip is also digitized, and l_0 is found by distance between the apex point and this point. The shank half-angle, α the radius of curvature, and the surface to apex distance are output values. It is important to note that the accuracy of the values, l_0 and R_0 are dependent on how well the magnification of the TEM is known. The digitized input information is also graphically displayed, showing the specimen's geometric parameters.

```
2 A$=""                                                    TIPREDUCER
4   !
39 GO TO 100
40 GO TO 910
64 Xpos=Xpos-1  !KEY16 MOVES TIP TO LEFT
65 RETURN
68 Xpos=Xpos+1  !KEY17 MOVES TIP TO RIGHT
69 RETURN
72 PRINT "INPUT NEW MAG. ";
73 INPUT Mag
74 RETURN
100 REM                                               TIP DATA REDUCER
105 Xpos=10
106 Mag=2
110 WINDOW 0,130,0,100
120 VIEWPORT 0,130,0,100
130 PAGE
```

```
140 DIM A$(80)
150 IF A$<>"" THEN 170
160 A$=""
170 PRINT "PLACE TEM PRINT OF FIM SPECIMEN ON 4662 PLOTTER SECURELY "
180 PRINT "ORIENTED HORIZONTALLY."
190 PRINT "JINSERT CROSS-HAIR VIEWER IN PEN HOLDER.J"
200 PRINT "THERE WILL BE AN AUDIO AND MESSAGE PROMPT FOR YOU TO "
210 PRINT "POSITION THE CROSS-HAIR AT AN APPROPRIATE LOCATION ON THE"
220 PRINT "MICROGRAPH. AFTER DOING SO, PRESS CALL BUTTON ON PLOTTER."
230 PRINT "JTO USE THE CALL FUNCTION ON PLOTTER, PRESS AND RELEASE
IT.JJJ"
240 PRINT "JJPLOTTER MUST BE SET UP FOR FULL PLATTEN. IF NOT, TURN OFF."
250 PRINT "JJHOW MANY POINTS ARE YOU GOING TO USE ?JJ"
260 INPUT N
270 DATA "PLACE PEN ON LOWER SIDE OF SHANK AND CALL TO DIGITIZE."
280 DATA "PLACE PEN FURTHER ALONG SHANK AND CALL TO DIGITIZE "
290 DATA "PLACE PEN APPROXIMATELY OPPOSITE TO FIRST POSITION AND CALL."
300 DATA "PLACE PEN FURTHER ALONG SHANK AND CALL TO DIGITIZE "
310 DATA "PLACE PEN AT THE EMITTER'S SURFACE ALONG CENTERLINE & CALL."
320 PRINT "GJJJALTER THE SAMPLE ID,";A$;" AND DESCRIPTION PLEASE"
330 ALTER A$,A$
340 SET DEGREES
350 RESTORE
360 DIM X1(N),X2(N),X3(2),X4(2),X5(2),V1(2),V2(2),W(2),A(2,3),B(2,3)
370 DIM Y1(N),Y2(N),X(N),Y(N),Xg1(N),Yg1(N),Xg2(N),Yg2(N)
380 DIM Apex(2),Vl(2)
390 PAGE
400 GOSUB 21000
410 FOR I=1 TO N
415    IF I<>N THEN 420
416    PRINT "GGGGGGGGGGGGGGGGGGGTHIS IS THE LAST ONE"
420      !
422    INPUT @3,27:X1(I),Y1(I)
430    IF I>1 THEN 470
440    GOSUB 21000
450    PRINT USING 460:N
460    IMAGE"FOR ",2D," DATA PAIRS"
470    PRINT I,X1(I),Y1(I)
480 NEXT I
490 X=X1
500 Y=Y1
502 Xg1=X1
504 Yg1=Y1
510 PAGE
520 GOSUB 29000
530 M1=M
540 B1=Bi
550 GOSUB 21000
560 FOR I=1 TO N
564    IF I<>N THEN 568
566    PRINT "GGGGGGGGGGGGGGGGGGGGGGGGGGGGGGGGGTHIS IS LAST ONE"
```

```
568      !
570    INPUT @3,27:X2(I),Y2(I)
580    IF I>1 THEN 620
590    GOSUB 21000
600    PRINT USING 610:N
610    IMAGE "FOR ",2D," DATA PAIRS "
620    PRINT I,X2(I),Y2(I)
630 NEXT I
640 X=X2
650 Y=Y2
652 Xg2=X2
654 Yg2=Y2
660 GOSUB 29000
670 M2=M
680 B2=Bi
690 GOSUB 21000
700 INPUT @3,27:X5
710 REM     ARANGEMENT OF THE DATA FOR THE REST OF THE PROGRAM
720 X1(2)=M1*X1(1)+B1  !  Y OF THE 1st DATA POINT ON THE LOWER SIDE
730 X2(2)=M1*X1(N)+B1  !  " "   "  2nd   "    "    "  "    "    "
740 X3(1)=X2(1)
750 X3(2)=M2*X2(1)+B2  !  " "   "  1st   "    "    "  "  UPPER  "
760 X4(2)=M2*X2(N)+B2  !  " "   "  2nd   "    "    "  "    "    "
770 X2(1)=X1(N)
780 X4(1)=X2(N)
790 DIM X1(2),X2(2)
800 REM X1-X2 = 1SIDE VECTOR, X3-X4 IS OTHER SIDE VECTOR
810 REM X5 IS POSITION VECTOR OF EMITTER'S LO
820 REM WILL CALCULATE 2 VECTORS, FIND THE ANGLE BETWEEN THEM AND THEIR
830 REM EQUATIONS. BY SOLVING SIMULTANEOUSLY THE APEX IS FOUND AND LO
840 REM CAN BE FOUND
850 V1=X1-X2
860 V2=X3-X4
870 W=V1*V2
880 Dp=SUM(W)
884 Ca=Dp/DISTANCE(V1(1),V1(2))/DISTANCE(V2(1),V2(2))   !ca=cos(alpha*2)
885   !Alpha=ACS(Ca)/2
900 Alpha=(ATN(M1)-ATN(M2))/2
910 PAGE
914 Mtermx=130/2/Mag
915 Mtermy=100/2/Mag
916 WINDOW X5(1)-Mtermx-Xpos,X5(1)+Mtermx-Xpos,X5(2)-Mtermy,X5(2)+Mtermy
920 MOVE @Lun:X1(1),X1(2)
930 DRAW @Lun:X2(1),X2(2)
940 MOVE @Lun:X3(1),X3(2)
950 DRAW @Lun:X4(1),X4(2)
960 MOVE @Lun:X5(1),X5(2)
970 RDRAW @Lun:0,0
980 A(1,1)=-V1(2)/V1(1)
990 A(2,1)=-V2(2)/V2(1)
1000 A(1,2)=1
1010 A(2,2)=1
```

```
1020 A(1,3)=X1(2)-V1(2)/V1(1)*X1(1)
1030 A(2,3)=X3(2)-V2(2)/V2(1)*X3(1)
1040 B=INV(A)
1050 Apex(1)=B(1,3)
1060 Apex(2)=B(2,3)
1070 Vl=Apex-X5
1080 LO=DISTANCE(Vl(1),Vl(2))
1090 LO=LO*0.1*25.4
1100 RO=LO*SIN(Alpha)/(1-SIN(Alpha))
1105   !PRINT@LUN:USING 1106:N
1106 IMAGE"JNUMBER POINTS USED = ",2D
1110   !PRINT "JJ",A$
1120   !PRINT USING 1130:Alpha,LO,RO
1130 IMAGE "ALPHA= ",3D.2D,"_LO= ",3D.2D,"mm_RO= ",3D.2D,"mm"
1135   !PRINT USING 1106:N
1140 MOVE @Lun:Apex(1),Apex(2)
1150 RDRAW @Lun:0,0
1160 MOVE @Lun:X5(1),X5(2)
1170 RMOVE @Lun:-RO*10/25.4,0
1180 Phi=90-Alpha
1190 ROTATE Phi
1200 RMOVE @Lun:RO*10/25.4,0
1210 FOR I=Phi TO -Phi STEP -5
1220    ROTATE I
1230    RDRAW @Lun:0,-RO*10/25.4*SIN(5)
1240 NEXT I
1250 ROTATE 0
1260 MOVE @Lun:X5(1),X5(2)
1270 PRINT "¯              DIGITIZED TIP GEOMETRY"
1275 PRINT "J";A$
1276 PRINT USING 1106:N
1278 PRINT USING 1130:Alpha,LO,RO
1280 MOVE @Lun:X5(1),X5(2)
1290 RMOVE @Lun:0,4*RO*10/25.4
1300 RDRAW @Lun:LO*10/25.4,0
1310 RMOVE @Lun:-LO*10/25.4/2,0
1320 PRINT @Lun:"KHLO"
1330 MOVE @Lun:Apex(1),Apex(2)
1340 RDRAW @Lun:0,RO*10/25.4
1350 RDRAW @Lun:0,-2*RO*10/25.4
1360 MOVE @Lun:Apex(1),Apex(2)
1370 DASH 85
1380 RDRAW @Lun:-4*Vl(1),-4*Vl(2)
1390 DASH 0
1400 GOSUB 40000
1410 END
21000 READ B$
21010 PRINT B$,"GG"
21020 CALL "WAIT",0.5
21030 PRINT "GG"
21040 RETURN
29000 PRINT "GGGGG     THANK YOU !  NOW, JJ"
```

```
30000 REM                                                     SUBROUTINE REGRETION
30010 DIM P(N),T(N)
30020 P=X*Y
30030 Ps=SUM(P)
30040 Q=SUM(X)
30050 R=SUM(Y)
30060 T=X*X
30070 Ts=SUM(T)
30080 M=(Ps-Q*R/N)/(Ts-Q^2/N)
30090 Bi=(R-M*Q)/N
30100 RETURN
40000 REM POINTS AND SCALE
40010 FOR I=1 TO N
40020    MOVE @Lun:Xg1(I),Yg1(I)
40030    RDRAW @Lun:0,0
40040 NEXT I
40050 FOR I=1 TO N
40060    MOVE @Lun:Xg2(I),Yg2(I)
40070    RDRAW @Lun:0,0
40080 NEXT I
40500 RETURN
```

PROFILER

This program will control the functions of the Scientific Instruments 5500. The program will input parameters into the 5500 and will program the 5500 for the temperature profile "RUN" mode. It will also graphically display the program put in the 5500, and actual temperature profile data from the program when it is run. Temperature profiles can also be taken in the Manual and STOP modes. Temperature set points can be put into the 5500 from the computer. Temperature profile programs can be stored on files which the program will create and retrieve them for future use.

```
1   !                                                                   PROFILER
2 GO TO 100
4 GO TO 1000  !!!INPUT DATA INTO 5500
8 GO TO 2000  !!!PROFILE OF INPUT DATA
12 GO TO 3000  !!RUN PROGRAM AND OUTPUT DATA TO PRINTER IN M OR R MODE
16 GO TO 4000  !!CREATES AND NAMES A FILE FOR PROGRAM FOR 5500
20 GO TO 5000  !!GRAPHIC PROFILE OF OUTPUT ON SCREEN
24 GO TO 6000  !!WILL PUT IN SET PT. & RUN SCAN IF DESIRED
32 GO TO 8000
36 GO TO 9000  !!REPEAT PREVIOUS SCAN W/ NO GRID DRAWN
40 GO TO 10000  !WILL OVERLAY 2ND PLOT ON FIRST & ALLOWS FOR PEN CHANGE
48 GO TO 12000  !GRAPHIC DISPLAY OF INPUT DATA ON PLOTTER
56 GO TO 14000  !READ PROGRAM FROM FILE. MUST KNOW NAME OF FILE
60 GO TO 15000  !GRAPHIC DISPLAY OF TEMP PROFILE ON PLOTTER
64 GO TO 16000  !READ SET POINT FROM 5500
100 CALL "RATE",9600,0,2
110 CALL "CMFLAG",4
120 Tint=0.5
130 Lun=32
140 STOP   !EXECUTION OF PROGRAM IS ENTIRELY FROM KEYS, 8 IS MENU KEY
1000 REM                                INPUT OF DATA INTO 5500 FROM KEYBOARD
1002 Tint=0.5
1010 PRINT "Enter numberof points __HH";
1020 INPUT Npt$
1030 Npt=VAL(Npt$)
```

```
1040 IF Npt<10 THEN
1050    Npt$=REP("0",1,1)
1060 END IF
1070 DIM Pt$(2),Temp$(5),Ttime$(5),Tprofile$(11*Npt)
1080 DIM Tempdata(Npt),Ttimedata(Npt)
1090 Tprofile$=""
1100 Profile$=Npt$&","
1110 PRINT @2:"#7";Profile$
1120 PRINT "Pt#","Temp","Time"
1130 PRINT "xx","xxx.x","xxx.x"
1140 FOR I=1 TO Npt
1150    PRINT I,"    HHHH";
1160    INPUT Temp$
1170    Tempdata(I)=VAL(Temp$)*0.1
1180    Temp$=Temp$&","
1190    PRINT "K  ","  ","    HHHH";
1200    INPUT Ttime$
1210    Ttimedata(I)=VAL(Ttime$)*0.1
1220    Ttime$=Ttime$&","
1230    Profile$=Temp$&Ttime$
1240    PRINT @2:Profile$
1250    Tprofile$=Tprofile$&Profile$
1260 NEXT I
1270 PAGE
1280 N=1
1290 PRINT "Number of points in profile is ";Npt$;"."
1295 PRINT "JJPt#","HHTemp*10","HHTime*10"
1300 FOR I=1 TO Npt
1310    L1$=SEG(Tprofile$,N,4)
1320    L2$=SEG(Tprofile$,N+5,4)
1330    PRINT I,L1$,L2$
1340    N=N+10
1350 NEXT I
1360 PRINT "JAre these values correct (y/n)? ";
1370 INPUT Q$
1380 IF Q$="n" THEN
1390    PRINT "Then put in the correct ones, dummy! "
1395    PRINT @2:"S"
1400    GO TO 1000
1420 END IF
1430 PRINT @2:"*"
1440 CALL "MAX",Tempdata,Tempmax,J
1450 CALL "MIN",Tempdata,Tempmin,J
1460 Tempmin=INT(Tempmin)
1470 Ttimetotal=SUM(Ttimedata)
1999 RETURN
2000 REM                                    PROFILE OF INPUT DATA @ SCREEN
2005 PAGE
2010 Lun=32
2020 CALL "MAX",Tempdata,Tempmax,J
2030 CALL "MIN",Tempdata,Tempmin,J
2040 GOSUB 2200
```

```
2050 Tempmin=INT(Tempmin)
2060 Ttimetotal=SUM(Ttimedata)
2070 GOSUB 31000
2080   !MOVE @Lun:Ttimedata(1)*60/Tint,Tempdata(1)
2090 MOVE @Lun:0,Tempcurrent
2100 DASH 85
2110 Ttimesum=0
2120 FOR I=1 TO Npt
2130    Ttimesum=Ttimesum+Ttimedata(I)*60/Tint
2140    DRAW @Lun:Ttimesum,Tempdata(I)
2150    DASH 0
2160 NEXT I
2170 HOME @Lun:
2180 PRINT @Lun:"               PROFILE OF TEMPERATURE INPUT DATA"
2182 MOVE @Lun:Ttimetotal*60/Tint*0.55,Tempmax
2185 PRINT @Lun:"KThe current temp is ";Tempcurrent;"K_"
2190 RETURN
2200 PRINT @2:"#41"  !INPUT CURRENT TEMP
2210 INPUT @2:S,S
2220 INPUT @2:S,Tempcurrent
2230 IF Tempcurrent<Tempmin THEN
2240    Tempmin=Tempcurrent
2250 END IF
2260 IF Tempcurrent>Tempmax THEN
2270    Tempmax=Tempcurrent
2280 END IF
2990 RETURN
3000 REM                                  DATA OUTPUTTED TO PRINTER
3005 SET NOKEY
3010 Ktr=0
3020 PAGE
3030 PRINT "What time interval in seconds between outputs? ";
3040 INPUT Tintprint
3050 PRINT "How long in minutes do you want data collected? ";
3060 INPUT Tlength
3070 Tlength=60*Tlength
3080 DIM Line$(73)
3090 PRINT @2:"#40"  !selects all variables
3100 PRINT "What mode do you want, ""M"" or ""R""? ";
3110 INPUT Mmode$
3119 DIM Ttile$(100)
3120 Title$=" N  K:N  K:N+1  M:N  M:REM  K:SET  K:DT  HT  K:ACT "
3130 Title$=Title$&"K2:ACT  TIME  MOD"
3140 PRINT @40:Title$;"   SEC."
3150 PRINT @2:Mmode$
3155 INPUT @2:A$
3160 INPUT @2:Line$
3170 P1=POS(Line$,"J",1)
3180 IF P1<>0 THEN 3160
3190 P1$=SEG(Line$,2,1)
3200 IF P1$=" " THEN   ! CHECKS FOR BLANK IN 2ND POSITION
3210    Line$=REP("",2,1)  !REPLACES BLANK WITH NULL
```

```
3220 END IF
3230 PRINT @40:Line$;"     ";Ktr*Tintprint
3240 Ktr=Ktr+1
3250 IF Ktr*Tintprint>Tlength THEN 3280
3260 CALL "WAIT",Tintprint
3270 GO TO 3160
3280 PRINT @2:"S"
3285 SET KEY
3290 RETURN
4000 REM                                    CREATE A FILE & STORE TPROFILE$
4010 PAGE
4020 PRINT "What is name of file to be created? ";
4030 INPUT Filename$
4040 Flength=11*Npt+28  !byte length of string
4050 CREATE Filename$,"a";Flength,0
4060 DIM A$(300)
4070 OPEN Filename$;1,"F",A$
4080 PRINT #1:Npt$
4085 PRINT #1:Tprofile$
4090 CLOSE 1
4100 RETURN
5000 REM         GRAPHIC DISPLAY OF DATA FROM 5500 & PLOTTED IN REAL TIME
5005 SET NOKEY
5010   !
5020   !TTIMETOTAL MUST BE DEFINED AND BE TOTAL OF TIME IN
5030   !MINUTES OF PROFILE PROGRAMMED.  OTHERWISE, TRUNCATION
5040   !OF PROFILE(i.e. the plot) WILL OCCUR.
5050   !Tempmax and Tempmin must also be known.
5060   !
5070 PAGE
5080 PRINT "ttimetotal,  tempmax, tempmin must be known!"
5090 CALL "wait",2
5100 Mmode$="R"
5111 PAGE   !    ALSO, ENTER POINT FOR MANUAL MODE
5120 Tint=0.5
5130 Num=60/Tint*Ttimetotal
5140 DIM Temp(Num)
5150 GOSUB 31000
5160 PRINT @2:"#43,3"  !SELECTS SET POINT FOR INPUT
5162 INPUT @2:S,S  !DUMMY STATEMENT NEEDED
5163 PRINT @2:"#43,3"  !NEEDED
5164 INPUT @2:S,S  !NEEDED
5170 INPUT @2:S,Spoint  !SET POINT
5180 PRINT @2:"#41,1"  ! SELECTS T1
5185 INPUT @2:J
5190 AXIS @Lun:0,0,Num,Spoint
5200 MOVE @Lun:Num,Spoint
5225 PRINT @Lun:" Set Pt.JHHHHHHH";Spoint
5226 MOVE @Lun:0,Spoint
5230 PRINT @2:Mmode$
5240 FOR I=1 TO Num
5250    INPUT @2:J,Temp(I)
```

```
5260    DRAW @Lun:I,Temp(I)
5270    CALL "WAIT",Tint
5274 END IF
5280 NEXT I
5290 PRINT @2:"S"
5292 MOVE @Lun:0,Tempmin
5294 PRINT @Lun:"JJJHHHHMODE: ";Mmode$;"_"
5300 HOME @Lun:
5310 SET KEY
5560 RETURN
6000 REM                                        ENTER A SET POINT INTO 5500
6001 SET NOKEY
6005   !PRINT @2:"MMMMMMMMMM"
6010 PRINT "ENTER A SET POINT FOR MANUAL MODE____HHHH";
6020 INPUT Spoint$
6025   !PRINT @2:"MMMMMMMMMM"
6030 PRINT @2:"M*3";Spoint$;",,,,,,,,,,,"
6040 PRINT @2:"S"
6050 PRINT "Do you want to see a Temp vs time curve for this"
6060 PRINT "set point (y/n)? ";
6070 INPUT Q$
6080 IF Q$="Y" THEN
6090    Mmode$="M"
6100    PRINT "Enter anticipated tempmin,tempmax(K) and total"
6110    PRINT "time in minutes for scan. ";
6120    INPUT Tempmin,Tempmax,Ttimetotal
6130    GOSUB 5111
6140 END IF
6200 SET KEY
6999 RETURN
8000 REM                                                       MENU ROUTINE
8005 RESTORE 8010
8010 DATA "KEY#            FUNCTION"
8020 DATA "____            ________J"
8030 DATA "   1 *********** INPUT DATA INTO 5500"
8040 DATA "   2 *********** GRAPHIC DISPLAY OF PROGRAM"
8050 DATA "   3 *********** OUTPUT DATA TO PRINTER IN <M> OR <R> MODE"
8060 DATA "   4 *********** CREATE FILE AND STORE 5500 PROGRAM IN E.MEM."
8070 DATA "   5 *********** GRAPHIC DISPLAY OF TEMP. PROFILE AT SCEEN"
8080 DATA "   6 *********** ENTER SET PT. AND RUN PROFILE IN <M> MODE"
8090 DATA "   7 *********** N/A"
8100 DATA "   8 *********** MENU"
8110 DATA "   9 *********** REPEAT SCAN W/ NO GRID REDRAWN"
8120 DATA "  10 *********** OVERLAY 2ND PLOT ON PLOTTER AND PEN CHANGE"
8130 DATA "  11 *********** N/A"
8140 DATA "  12 *********** GRAPHIC DISPLAY OF PROGRAM ON PLOTTER"
8150 DATA "  13 *********** N/A"
8160 DATA "  14 *********** RETRIEVE PROGRAM STORED IN EX. MEM."
8170 DATA "  15 *********** GRAPHIC DISPLAY OF TEMP PROFILE ON PLOTTER"
8180 DATA "  16 *********** READ SET POINT FROM 5500"
8190 DATA "  17 *********** N/A"
8200 DATA "  18 *********** N/A"
```

```
8210 DATA " 19 *********** N/A"
8220 DATA " 20 *********** N/A"
8230 PAGE
8240 FOR I=1 TO 22
8250    READ A$
8260    PRINT A$
8270 NEXT I
8280 RETURN
9000 REM REPEAT SACN IN <R> OR <M> MODE ALREADY CHOSEN
9005 SET NOKEY
9010 REM NO GRID PLOTTED, SET POINT MAY CHANGE
9020 MOVE @Lun:0,Tempmin
9030 GOSUB 5230
9035 SET KEY
9040 RETURN
10000 REM                         OVERLAY ACTUAL PROFILE ON INPUT PROFILE
10005 SET NOKEY
10010 REM                    ASSUMES INITIAL PLOT OF INPUT DATA @ PLOTTER
10020 Lun=3
10030 PRINT "Change pens now if you like, then press return."
10040 INPUT Q$
10050 GOSUB 15040
10055 SET KEY
10060 RETURN
12000 REM                                  PROFILE OF INPUT DATA @ PLOTTER
12010 PAGE
12020 Lun=3
12030 CALL "MAX",Tempdata,Tempmax,J
12040 CALL "MIN",Tempdata,Tempmin,J
12050 GOSUB 12230
12060 Tempmin=INT(Tempmin)
12070 Ttimetotal=SUM(Ttimedata)
12080 GOSUB 31000
12090   !MOVE @Lun:Ttimedata(1)*60/Tint,Tempdata(1)
12100 MOVE @Lun:0,Tempcurrent
12110 DASH 85
12120 Ttimesum=0
12130 FOR I=1 TO Npt
12140    Ttimesum=Ttimesum+Ttimedata(I)*60/Tint
12150    DRAW @Lun:Ttimesum,Tempdata(I)
12160    DASH 0
12170 NEXT I
12180 HOME @Lun:
12190 PRINT @Lun:"                  PROFILE OF TEMPERATURE INPUT DATA"
12200 MOVE @Lun:Ttimetotal*60/Tint*0.55,Tempmax
12210 PRINT @Lun:"KThe current temp is ";Tempcurrent;"K_"
12215 Lun=32
12220 RETURN
12230 PRINT @2:"#41"  !INPUT CURRENT TEMP
12240 INPUT @2:S,S
12250 INPUT @2:S,Tempcurrent
12260 IF Tempcurrent<Tempmin THEN
```

```
12270    Tempmin=Tempcurrent
12280 END IF
12290 IF Tempcurrent>Tempmax THEN
12300    Tempmax=Tempcurrent
12310 END IF
12320 RETURN
14000 REM                                         READ PROGRAM FROM FILE
14010 PRINT "LWhat is filename,please? ";
14020 INPUT Filename$
14030 OPEN Filename$;1,"R",A$
14040 INPUT #1:Npt$
14045 Npt=VAL(Npt$)
14050 DIM Tprofile$(11*Npt)
14070 INPUT #1:Tprofile$
14075 PRINT @2:"#7";Npt$;","
14080 N=1
14082 PRINT "JJJJPt#      Temp(K)      Time(min)"
14083 PRINT "---       -------       ---------"
14085 DIM Tempdata(Npt),Ttimedata(Npt)
14090 FOR I=1 TO Npt
14100    L1$=SEG(Tprofile$,N,4)
14101    Tempdata(I)=VAL(L1$)*0.1
14110    L2$=SEG(Tprofile$,N+5,4)
14114    Ttimedata(I)=VAL(L2$)*0.1
14120    PRINT USING "2D,2(8X,3D.1D)":I,Tempdata(I),Ttimedata(I)
14140    PRINT @2:L1$;",";L2$;","
14145    N=N+10
14150 NEXT I
14160 PRINT @2:"*"
14170 CLOSE 1
14175 GOSUB 1440  !GO DEFINE TEMPMIN,TEMPMAX,TTIMETOTAL
14180 RETURN
15000 REM                    PLOT ON PLOTTER THE RESULTS OF KEY 5 OR 6
15010 Lun=3
15020 WINDOW 0,Num,Tempmin,Tempmax
15030 GOSUB 31000
15040 AXIS @Lun:60/Tint,0,0,Spoint
15050 MOVE @Lun:Num,Spoint
15060 PRINT @Lun:" Set Pt.JHHHHHHH";Spoint
15070 MOVE @Lun:0,Spoint
15080 FOR I=1 TO Num
15090    DRAW @Lun:I,Temp(I)
15100 NEXT I
15102 MOVE @Lun:0,Tempmin
15104 PRINT @Lun:"JJJHHHHMODE: ";Mmode$
15110 HOME @Lun:
15120 Lun=32
15130 RETURN
16000 REM                                                 READ SET POINT
16010 PRINT @2:"#43"
16020 INPUT @2:S,S
16030 INPUT @2:S,Spoint
```

```
16040 PRINT @2:"#41"  !SELECTS T1
16050 INPUT @2:S,S
16060 PRINT "LThe current set point is ";Spoint;"K."
16070 RETURN
31000 REM                          SUBROUTINE FOR PLOT AND GRID LABELING
31001   !
31002   !***warning: Tempmax,Tempmin,Ttimetotal(min) must be defined.
31003   !
31010 Tempdif=Tempmax-Tempmin
31020 IF Tempdif>20 THEN 31060
31030 Lineint=2
31040 Ticint=0.5
31050 GO TO 31120
31060 IF Tempdif>100 THEN 31100
31070 Lineint=5
31080 Ticint=1
31090 GO TO 31120
31100 Lineint=10
31110 Ticint=2
31120 Ylinenum=Tempdif/Lineint
31130 R=Ylinenum-INT(Ylinenum)
31140 IF R<>0 THEN
31150    Tempmax=INT(Tempmax)+1
31160    GO TO 31000
31170 END IF
31180 IF Ttimetotal>30 THEN 31220
31190 Xlineint=2
31200 Xtic=60/Tint
31210 GO TO 31280
31220 IF Ttimetotal>100 THEN 31260
31230 Xlineint=5
31240 Xtic=60/Tint
31250 GO TO 31280
31260 Xlineint=10
31270 Xtic=5*60/Tint
31280 Xlinenum=Ttimetotal/Xlineint
31290 WINDOW 0,Ttimetotal*60/Tint,Tempmin,Tempmax
31300 VIEWPORT 10,110,10,90
31310 AXIS @Lun:Xtic,Ticint,0,Tempmin
31320 AXIS @Lun:Xtic,Ticint,Ttimetotal*120,Tempmax
31330 IF Ylinenum-Xlinenum=>0 THEN
31340    Linenum=Ylinenum
31350 ELSE
31360    Linenum=Xlinenum
31370 END IF
31380 FOR I=0 TO Linenum
31390    X=60/Tint*Xlineint*I
31400    Y=Tempmin+Lineint*I
31410    AXIS @Lun:0,0,X,Y
31420 NEXT I
31430 REM LABEL X AXIS
31440 FOR I=0 TO Xlinenum
```

```
31450    X=60/Tint*Xlineint*I
31460    MOVE @Lun:X,Tempmin
31470    PRINT @Lun:"JH";X/(60/Tint)
31480 NEXT I
31490 REM LABEL Y AXIS
31500 FOR I=0 TO Ylinenum
31510    Y=Tempmin+Lineint*I
31520    MOVE @Lun:0,Y
31530    PRINT @Lun:"HHHH";Y
31540 NEXT I
31550 MOVE @Lun:Ttimetotal/2*(60/Tint),Tempmin
31555 PRINT @Lun:"JJJHHHHHHHHHHTime of Profile(min)_"
31570 MOVE @Lun:0,Tempmax
31580 PRINT @Lun:"KHHHHHTemp(K)"
31585 HOME
31590 RETURN
```

APPENDIX E
INDEXED FIM MICROGRAPH MONTAGE

Figure E-1 shows an indexed FIM micrograph montage of a nickel emitter. The imaging voltage was 15.7 kV with Ne at a pressure of 6×10^{-6} Torr.

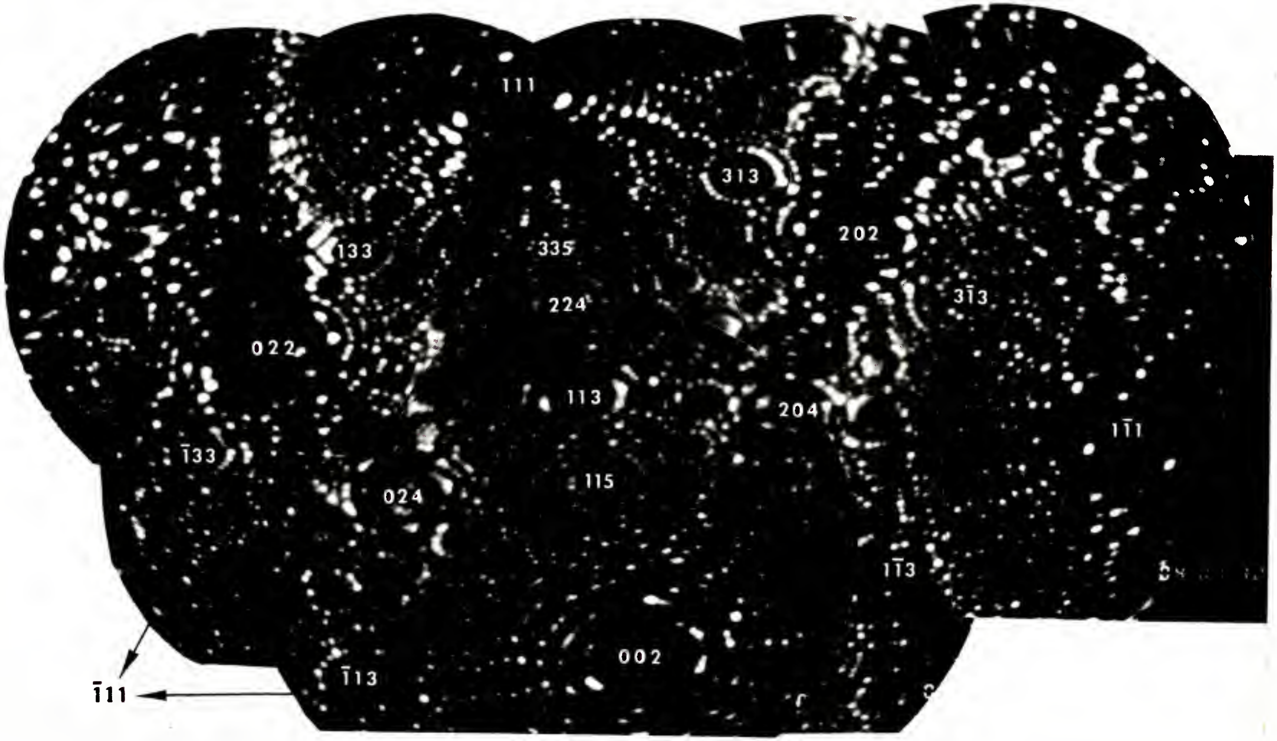

Figure E-1 Indexed FIM micrograph montage of Ni. The imaging voltage was 15.7 kV using a Ne pressure of $6x10^{-6}$ Torr.

RFERENCES

1. Wagner, A., and Seidman, D. N., 1979, Phys. Rev. Lett., 42, p. 515.

2. Seidman, D. N., Amano, J., and Wagner, A., 1982, Advanced Techniques for Characterizing Materials, TMS-AIME, Warrendale, PA, p. 125.

3. Hren, J. J., and Ranganathan, S., eds., 1968, Field Ion Microscopy, Plenum Press, New York.

4. Müller, E. W., and Tsong, T. T., 1969, Field Ion Microscopy, Principles and Applications, Elsevier Publ. Co., New York.

5. Wagner, R., 1982, Crystals, Growth, Properties, and Applications, 6, "Field-Ion Microscopy in Materials Science", Springer-Verlag, Berlin.

6. Müller, E. W., and Krishnaswamy, S. V., 1974, Rev. Sci. Instr., 45, p. 1053.

7. Poschenrieder, W. P., 1972, Int. J. Mass Spectrom. Ion Phys., 9, p. 357.

8. Waugh, A. R., 1977, Proc. of 24th Int. Field Emission Symp., Oxford, England.

9. Brinkman, A., 1956, Am. J. Phys., 24, p. 246.

10. Seeger, A., 1958, Proc. of the 2nd Geneva Conf. on Peaceful Use Atomic Energy, 6, p. 250.

11. van Jan, R., 1964, Phys. Stat., Sol., 6, p.925.

12. van Jan, R., 1965, Phys. Stat., Sol., 8, p. 331.

13. Wilkens, M., 1968, Vacancies and Interstials in Metals, Proc. of Int. Conf. on Vacancies and Interstials, Jülich, Germany, Seeger, A., Schumacher, D., Schilling, W., and Diehl. J., eds., North Holland, Amsterdam, p. 485.

14. Robertson, A. H., and Seidman, D. N., 1968, J. Phys. E: Sci. Instr., 1, p. 1244.

15. Seidman, D. N., Wilson, K. L., and Nielsen, C. H., 1975, Fundamental Aspects of Radiation Damage in Metals, Robinson, M. T., Yiung, Jr., F. W., eds., Nat. Tecn. Information Service, U. S. Dept. of Commerce, Springfield, p. 373.

16. Seidman, D. N., 1976, Radiation Damage in Metals, Peterson, N. L., Harkness, S. D., eds., ASM, Metals Park, OH, p. 28.

17. Seidman, D. N., 1978, Surf. Sci., 70, p. 532.

18. Wei., C. Y., and Seidman, D. N., 1977, Appl. Phys. Lett., 34, p. 622.

19. Wilson, K. L., and Seidman, D. N., Rad. Effects, 33, p. 149.

20. Scanlan, R. M., Styris, D. L., and Seidman, D. N., 1971, Phil. Mag., 23, p. 1459.

21. Wilson, K. L., Baskes, M. I., and Seidman, D. N., 1980, Acta. Met., 28, p. 89.

22. Wei, C. Y., and Seidman, D. N., 1978, Phil. Mag., A37, p. 257.

23. Wei, C. Y., and Seidman, D. N., 1977, Rad. Effects, 32, p. 229.

24. Pramanik, D., and Seidman, D. N., 1983, J. Appl. Phys., 54 (11), p. 6352.

25. Sykes, L. J., 1980, Ph.D. Dissertation, Univ. of Florida.

26. Sykes, L. J., Cooper, W. D., and Hren, J. J., 1981, Catalog of Computer Simulated TEM Images of Small FCC and BCC Dislocation Loops, Report No. ORNL/TM-7619, Oak Ridge National Laboratory, Oak Ridge.

27. Rühle, M. R., 1972, Radiation-Induced Voids in Metals, Proc. of Int. Conf. on Radiation-Induced Voids in Metals, Albany, 1971, Corbett, J. W., and Ianniello, L. C., eds., Nat. Techn. Information Service, U. S. Dept. of Commerce, Springfield, VA, p. 255.

28. Venables, J. A., and Thomas, G. J., 1968, Vacancies and Interstials in Metals, Proc. of Int. Conf. on Vacancies and Interstials, Jülich, Germany, Seeger, A., Schumacher, D., Schilling, W., and Diehl, J., eds., North Holland, Amsterdam, p. 531.

29. Zapffe, C., and Sims, C., 1941, Trans. AIME, 145, p. 325.

30. Petch, N. J., and Sables, P., 1952, Nature, 169, p. 842.

31. Petch, N. J., 1956, Phil. Mag., p. 331.

32. Lynch, S. P. 1979, Metals Forum, 2, p. 189.

33. Chornet, E., and Coughlin, R. W., 1972, J. Catalysis, 27, p. 245.

34. Oriani, R. A., 1977, Acta Metall., 25, p. 979.

35. Oriani, R. A., 1978, Ann. Rev. Mater. Sci., 8, p. 327.

36. Troiano, A. R., 1974, Hydrogen in Metals, Bernstein, I. M., and Thompson, A. W., eds., ASM, Metals Park, OH, p. 3.

37. Bernstein, I. M., and Thompson, A. W., 1960, Trans. ASM, 52, p. 54.

38. Oriani, R. A., and Josephic, P. H., 1979, Environment Sensitive Fracture of Engineering Materials, Foroulis, A. Z., ed., TMS-AIME, Warrendale, PA, p. 232.

39. Westlake, P. G., 1969, Trans. ASM, 62, p. 1000.

40. Gahr, S., Grossbeck, M. L., and Birnbaum, H. K., 1977, Acta Met., 25, p. 125.

41. Baranowski, B., 1972, Berchte der Bunsen Gessellschaft fur Physikalische Chemie, 76, p. 714.

42. Louthan, M. R., Jr., and McNitt, R. P., 1976, Effects of Hydrogen on Behavior of Materials, Thompson, A. W., and Bernstein, I. M., eds., ASM, Metals Park, OH, p. 496.

43. Hirth, J. P., and Carnahan, B., 1978, Acta Met., p. 1795.

44. Baskes, M. I., Melius, C. F., and Wilson W. D., 1981, TMS-AIME Symposium on Interatomic Potentials and Computer Simulation Defects in Metals, Sandia Laboratories, SAND80-8626, Unlimited Release.

45. Kellogg, G. L., and Panitz, J. K. G., 1980, Appl. Phys. Lett., 37, p. 625.

46. Macrander, A. T., and Seidman, D. N., 1984, J. Appl. Phys., 56 (6), p. 1623.

47. Panitz, J. A., 1977, J. Vac. Sci. Technol., 14, p. 502.

48. Hren, J. J., 1983, DOE proposal entitled, "Implantation Studies of Hydrogen by Field Ion Microscopy and Spectrscopy", Dept. of Energy contract number, DE-FG05-84ER45172.

49. Hirvonen, J. K., 1985, J. Vac. Sci. Techn., 3 (6), p. 2691.

50. Fromson R. E., and Kossowsky, R., 1982, Proc. of Mat. Res. Soc. Symp., Elsevier, New York p. 355.

51. Hirvonen, J. K., 1984, Proc. of Mat. Res. Soc. Symp., 27, Elsevier, New York, p. 621.

52. Sioshansi, P., 1984, Thin Solid Films, 118, p. 61.

53. Hartley, N. E. W., 1976, Applications of Ion Beams to Materials, Carter, G., Colligen, J. S., and Grant, W. A., eds., Inst. of Physics, London, p. 123.

54. Oliver, W. C., Hutchings, R., Pethica, J. B., Singer, G. K., and Hubler, G. K., 1984, Proc. of Mat. Res. Soc. Symp., 27, p. 603.

55. Pope, L. E., Yost, F. G., Follstedt, D. M., Picraux, S. T., and Knapp, J. A., 1984, Proc. of Mat. Res. Soc. Symp., 27, p. 661.

56. Longworth, G., and Hartley, N. E. W., 1977, Thin Solid Films, 48, p. 95.

57. Scott, D., Seifert, W. W., and Westcott, V. C., 1975, Wear, 34, p. 251.

58. Hutchings, R., and Oliver, W. C., 1983, Wear, 92, p. 143.

59. Williams, J. J., Beardsley, G. M.. Buchaman, and Bacon, R. K., 1984, Proc. of Mat. Res. Soc. Symp., 27, Elsevier, New York, p. 735.

60. Sioshansi, P, Oliver, R. W., and Matthews, F. D., 1985, J. Vac. Sci, Techn. A, 3 (6), p. 2670.

61. Oblas, D. W., 1984, Proc. of Mat. Res. Soc. Symp., 27, Elsevier, New York, p. 631.

62. Greggi, J., 1983, Scripta Metallurgica, 17, p. 765.

63. Kolitsch, A., and Richter, E., 1983, Crystal Res. and Techn., 18, pp. K5-K7.

64. Spalvins, T., 1985, J. Vac. Sci. Techn. A, 3, (6), p. 2329.

65. Dose Santos, C. A., Behar, M., De Souze, J. P., and Baumvol, I. J. R., 1983, Nucl. Inst. and Meth., 209/210, p. 907.

66. Dearnaley, G., and Hartley, N. E. W., 1978, Thin Solid Films, 54, p. 215.

67. Drako, V. M., and Gumanskij, G. A., 1982, Rad. Effects, 61, p. 111.

68. Dearnaley, G., 1982, Rad. Effects, 63, p. 1.

69. Panitz, J. A., 1978, Prog. in Surf. Sci., 8, p. 219.

70. Wiza, J. L., 1979, Nuc. Instrum. and Meth., 162, p. 587.

71. Müller, E. W., Panitz, J. A., and McLane, S. B., 1968, Rev. Sci. Instr., 39, p. 83.

72. Gipson, G. S., Yannitell, D. W., and Eaton, H. C., 1978, 25th Int. Field Emission Symp., Albuquerque, NM.

73. Waugh, A. R., and Southon, M. J., 1977, Surf. Sci., 68, p. 79.

74. Brenner, S. S., and Walck, S. D., 1980, Proc. 27th Intl. Field Emission Symp., Tokyo.

75. Wahlin, L., 1964, Nuc. Instrum. and Meth., 27, p. 55.

76. Newkirk, J. W., Walck, S. D., Hren, J. J., and Jones, R., 1984, Proc. of 42nd Ann. Meeting of EMSA, Bailey, F. W., ed., San Francisco Press.

77. Walck, S. D., Hren, J. J., 1984, Proc. Intl. Field Emission Symp., J. De Phys., 45 (12 Supplément), Paris, p. 355.

78. Henjered, A., and Nordén, H., 1983 J. Phys. E: Sci. Instrum., 16, p. 617.

79. Nordén, H., Andren, H.-O., Henjered, A., and Stiller, K., 1981, Proc. 28th Intl. Field Emission Symp., Portland, OR.

80. Newman, R. W., Sanwald, R. C., and Hren J. J., 1967, J. Sci. Instrum., 44, p. 828.

81. Nishikawa, O., and Müller, E. W., 1964, J. Appl. Phys., 35, p. 2806.

82. Walck, S. D., and Hren, J. J., 1984, Mat. Res. Soc. Symp., 41, Boston, Mass., p. 325.

83. Kellogg, G. L., and Tsong, T. T., 1980, J. Appl. Phys., 51 (2), p. 1184.

84. Kellogg, G. L., 1981, J. Appl. Phys., 74 (2), p. 1479.

85. Hren, J. J., and Kellogg, G. L., 1984, Surf. Sci., 147, p. 349.

86. Hren, J. J., 1968, "Interpretation of Field-Ion Microscope Images of Point and Line Defects", Field-Ion Microscopy, Hren J. J., and Ranganathan, S., eds., Plenum, New York, p. 102.

87. Sanwald, R. C., Ranganathan, S., and Hren, J. J., 1966, Appl. Phys. Lets., 9, p. 393.

88. Sanwald, R. C., and Hren, J. J., 1968, Surf. Sci, 9, p. 257.

89. J.P. Biersack, and L.G. Haggmark, 1980, Nucl. Instr. and Methods, 174, p. 257.

90. Andersen, H. H., and Ziegler, J. F., 1977, Hydrogen Stopping Powers and Ranges in All Elements, Pergamon, Elmsford, NY.

91. Hren, J. J., 1979, "Barriers To AEM: Contamination And Etching", Introduction To Analytical Electron Microscopy, Hren, J. J., Goldstein, J. I., and Joy, D. C., eds., Plenum, New York, p. 481.

92. Everett, K. G., Walck, S. D., Schmid, G. W., and Hren, J. J., 1983, Proc. of 30th Intl. Field Emission Symp., Philadelphia.

93. Everett, K. G., Walck, S. D., Schmid, G. W., and Hren, J. J., 1984, Surf. Sci. Let., 145, p. 475.

94. Hunter, P. T., Finlayson, B., Hirko, R. J., Voreck, W. C., Walker, R., Walck, S. D., and Nasr, M., 1985, "Measurement of Shock Wave Pressures Used for Lithotripsy", submitted to Investigative Urology.

95. Hunter, P. T., Finlayson, B., Hirko, R. J., Voreck, W. C., Walker, R., Walck, S. D., and Nasr, M., 1985, "Direct Pressure Measurements of Dornier Lithotripter and Electrode Longevity", Proc. of Symposium on ESWL, Inianapolis, IN.

96. Myers, S. M., Picraux, S. T., and Stoltz, R. E., 1979, J. Appl Phys., 50, p. 5710.

97. Myers, S. M., Picraux, S. T., and Stoltz, R. E., 1980, Appl. Phys. Lett., 37, p. 168.

98. Besenbacher, F., Bottiger, J., and Myers, S. M., 1982, J. Appl. Phys., 53 (6), p. 3536.

99. Besenbacher, F., Bottiger, J., and Myers, S. M., 1982, J. Appl. Phys., 53 (6), p. 3547.

100. Myers, S. M., Follstaedt, D. M., Besenbacher, F., and Bottiger, J., 1982, J. Appl. Phys., 53 (12), p. 8734.

101. Myers, S. M., Amos, D. E., and Brice, D. K., 1976, J. Appl. Phys., 47 (5), p. 1812.

102. Eaton, H. C., and Bayuzick, R. J., 1978, Surf. Sci., 70, p. 408.

103. Picraux, S. T., EerNisse, E. P., and Vook, F. L., eds., 1974, Applications of Ion Beams to Metals, Plenum, New York, p. 760.

104. Myers, S. M., 1977, Ion Implantation in Semi-Conductors, 1976, New York, Plenum, p. 167.

105. Borders, J. A., 1979, Ann. Rev. Mater. Sci., p. 313.

106. Loberg, B., and Nordén, H., 1970, Proc. Septieme Congress Int. de Microscopie Electronique, Grenoble.

BIOGRAPHICAL SKETCH

Scott Douglas Walck was born April 3, 1954, in Harrisburg, Pennsylvania. In 1972 he graduated from Susquehanna Township Senior High School where he was captain of the football team in his senior year. He then entered Gettysburg College where he double-majored in physics and mathematics. During this period of time he was an active member of the International Brotherhood of Teamsters, Local 776, and worked part-time or weekends and in the summers for Eastern Express, Inc., as a dockworker, earning his college tuition money. He received his Bachelor of Arts degree, cum laude, in 1976 and was admitted to the graduate program in physics at the University of Michigan. He was a teaching assistant for nine months, and a research assistant for three months. Searching for a more applied physics field of study and a slightly warmer climate, he transferred to the Materials Science and Engineering program at the University of Florida in the autumn of 1977. He first studied under Professor Rolf E. Hummel for six months until he started his research in Field Ion Microscopy under his Ph.D. advisor, Professor John J. Hren. In the summer of 1979 he worked at the U. S. Steel Research Center in Monroeville, Pennsylvania, under Dr. Sidney S. Brenner. The report on this work won the AIME graduate student paper contest for 1980. While studying at the University of Florida, he met and subsequently married his wife, Karen, on their birthday, 1980. In 1982 he received his Master of Science degree from the University of Florida while pursuing his doctorate in materials the University of Florida while pursuing his doctorate in materials science. In June of 1984, his pride and joy was born, a son named Adam. At the time of this writing, he is anxiously awaiting the arrival of his second child, currently nicknamed, "the frog", in late August of 1986.

He is a member of American Vacuum Society (AVS), Electron Microscopy Society of America (EMSA), American Metallurgy, Mining and Petroleum Engineering (AIME), Florida Society of Electron Microscopy (FSEM) and Alpha Sigma Mu.

I certify that I have read this study and that in my opinion it conforms to acceptable standards of scholarly presentation and is fully adequate, in scope and quality, as a dissertation for the degree of Doctor of Philosophy.

Gary G. Ihas

Gary G. Ihas
Professor of Physics

This dissertation was submitted to the Graduate Faculty of the College of Engineering and to the Graduate School and was accepted as partial fulfillment of the requirements for the degree of Doctor of Philosophy.

August, 1986

Hubert A. Bevis

Dean, College of Engineering

Dean, Graduate School

I certify that I have read this study and that in my opinion it conforms to acceptable standards of scholarly presentation and is fully adequate, in scope and quality, as a dissertation for the degree of Doctor of Philosophy.

John J. Hren, Chairman
Professor of Materials Science
and Engineering

I certify that I have read this study and that in my opinion it conforms to acceptable standards of scholarly presentation and is fully adequate, in scope and quality, as a dissertation for the degree of Doctor of Philosophy.

Christopher D. Batich
Associate Professor of Materials
Science and Engineering

I certify that I have read this study and that in my opinion it conforms to acceptable standards of scholarly presentation and is fully adequate, in scope and quality, as a dissertation for the degree of Doctor of Philosophy.

Robert T. DeHoff

Robert T. DeHoff
Professor of Materials Science
and Engineering

I certify that I have read this study and that in my opinion it conforms to acceptable standards of scholarly presentation and is fully adequate, in scope and quality, as a dissertation for the degree of Doctor of Philosophy.

Paul H Holloway

Paul H. Holloway
Professor of Materials Science
and Engineering

UNIVERSITY OF FLORIDA
3 1262 08553 5499